Novel Aspects of
Cyclotron Resonance Maser Theory

Gordon R. M. Robb

(B. Sc. University of Strathclyde)

Department of Physics and Applied Physics

University of Strathclyde

Thesis Submitted for the Degree of Ph.D.

October 1994

I would like to dedicate this piece of work to Catriona, Mum, Dad and Katherine.

Contents

Acknowledgements

I would like to thank my supervisors, Professor A. D. R. Phelps and Dr. B. W. J. M^{c}Neil for their constant help and support during the development of this work.

Thanks are also due to the SERC and AEA Technology for providing funding for this research by means of an SERC/CASE studentship.

I would also like to thank Dr S. N. Spark, Dr A. W. Cross, Dr S. Cooke, Dr M. Garven, Mr W. He, Mr K. Ronald and Mrs H. He for their support and their part in creating such a good working environment.

Finally, I would like to thank Catriona, my family and my friends for their support and encouragement over the course of the last three years.

Abstract

Cyclotron resonance masers (CRMs) are important devices for the generation of high power electromagnetic radiation in the millimetre and sub-millimetre region of the electromagnetic spectrum. In these devices, an electromagnetic wave is amplified by its interaction with a beam of relativistic electrons gyrating in a magnetostatic field. This thesis presents the results of novel theoretical investigations into the physical processes which occur in a CRM amplifier.

The basis of these investigations was a system of universally scaled evolution equations which describe the linear and nonlinear evolution of the CRM interaction. These equations involve a minimum number of free parameters and allow a general analysis of the interaction. By considering various limits of the free parameters, the physical processes which occur in the steady-state limit were identified and studied using numerical analysis and an extensive linear analysis based on the method of collective variables.

Neglecting the recoil of the electrons, it was shown that the universally scaled evolution equations could be written as a set of Hamilton's equations. The behaviour of this Hamiltonian system was investigated via a phase space analysis for some specific cases of the free parameters. In addition, it was shown that it is possible to approximately describe the evolution of the electromagnetic field up to saturation in a CRM amplifier by an analytically solveable Landau-Ginzburg equation.

Including slippage effects, it was shown that for electron beams with relativistic axial velocities, in addition to the steady-state evolution of the electromagnetic

field, superradiant field evolution could also occur. Superradiant phenomena were studied using an heuristic dissipative model, an extensive linear analysis and a nonlinear numerical analysis. The existence of weak superradiance, involving short electron pulses and low radiation intensities, and strong superradiance, involving long electron pulses and high intensity spikes of radiation, was demonstrated.

List of Figures

Chapter 1

The Cyclotron Resonance Maser

1.1 Introduction

The cyclotron resonance maser (CRM) is a class of device based on the interaction of electromagnetic waves with electrons oscillating in static magnetic fields, that is, on stimulated emission. A typical trajectory of an electron moving in a static magnetic field is shown schematically in figure 1.1. The electrons behave as excited classical oscillators, so the CRM is a type of 'classical' electron maser. As a classical electron maser, the CRM is distantly related to quantum mechanical devices such as masers and lasers and to conventional microwave electron beam tubes such as the klystron and the travelling wave tube (TWT). Since the CRM possesses the merits of both quantum and conventional devices, the natural frequency range of the CRM is, not surprisingly, located between the natural ranges of both related classes i.e. the domain of the CRM is expected to be found in the millimetre and sub-millimetre wave region of the electromagnetic spectrum.

The electromagnetic waves in a CRM will interact strongly with electrons

which satisfy the resonance condition

$$\omega - k_{||} v_{||} \approx s\frac{\omega_c}{\gamma} \quad s = 1, 2, ... \tag{1.1}$$

where ω_c/γ is the oscillation frequency of the electrons, ω_c being the nonrelativistic cyclotron frequency

$$\omega_c = \frac{eB_0}{m_e} \tag{1.2}$$

γ the relativistic factor, s the cyclotron harmonic and $v_{||}$ the drift velocity of the electrons. ω and $k_{||}$ are the frequency and longitudinal wavevector component of the electromagnetic wave. Unlike conventional microwave devices, where the phase velocity, v_p, of the electromagnetic wave is made to match the drift velocity of the electrons using a slow wave structure, the phase velocity of the electromagnetic wave required for cyclotron resonance to occur is arbitrary. This allows the use of fast waves with $v_p > c$ so the interaction can take place in a smooth walled waveguide. The great advantage of this over conventional microwave devices is that the shortest attainable radiation wavelength of, for example, a TWT is determined by the period of the slow-wave structure. As this period is decreased, the manufacture of the slow-wave structure becomes more difficult and the power handling capabilities of the device are severely limited. The use of a smooth walled waveguide allows high power generation of radiation at millimetre and sub-millimetre wavelengths.

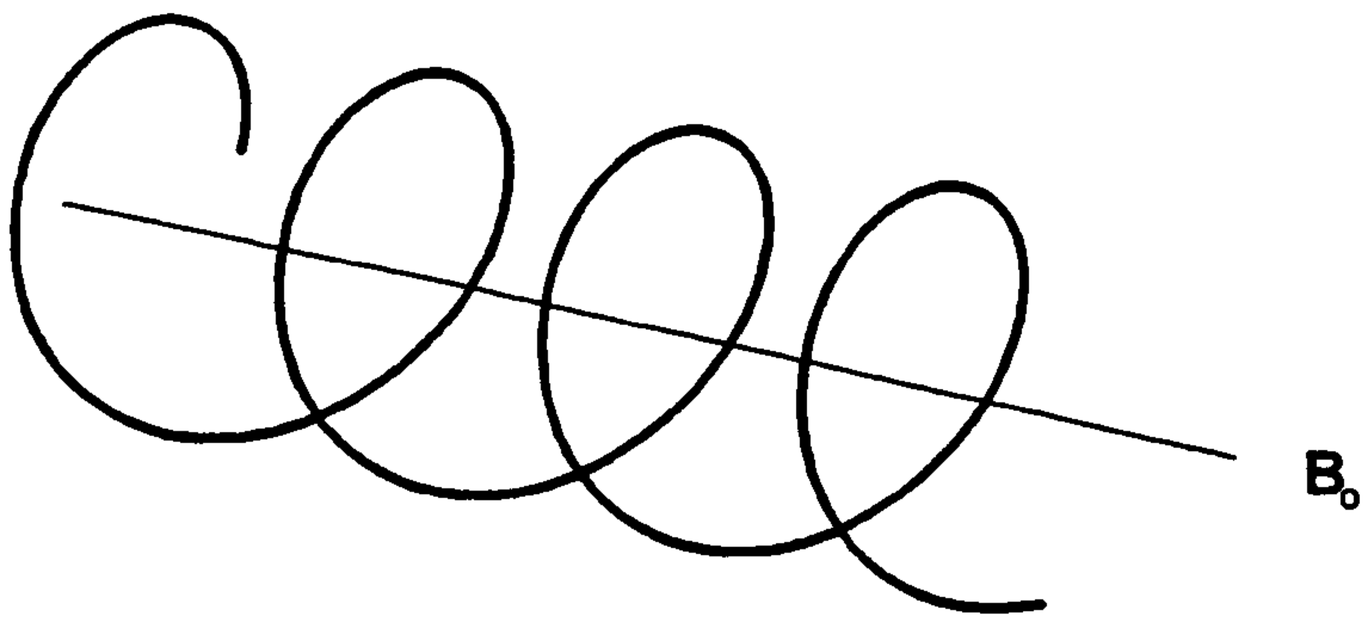

Figure 1.1: Electron gyrating in a static magnetic field.

1.2 Spontaneous Cyclotron Radiation

Consider a relativistic electron gyrating in a static magnetic field with velocity $\mathbf{v} = \mathbf{v}_\perp + \mathbf{v}_\parallel$, as shown in figure 1.1, but with no stimulating radiation present. In order to calculate the spontaneous emission spectral intensity, a known standard formula for radiation from a moving point charge will be used [1]. The energy emitted per electron per unit frequency per steradian is

$$\frac{d^2I}{d\Omega d\omega} = \frac{e^2\omega^2}{16\pi^3}\left|\int dt\, \hat{\mathbf{k}} \times \left(\frac{\hat{\mathbf{k}} \times \hat{\mathbf{v}}}{c}\right) \frac{|\mathbf{v}|}{c} \exp\left[i\omega(t - \hat{\mathbf{k}}.\mathbf{r}(t)/c)\right]\right|^2 \tag{1.3}$$

where $\hat{\mathbf{k}} = \mathbf{k}/|\mathbf{k}|$ and $\hat{\mathbf{v}} = \mathbf{v}/|\mathbf{v}|$ are unit vectors in the direction of the radiation wavevector and the electron velocity respectively. It is assumed here that only the components of the electron velocity that are perpendicular to the axial magnetic field contribute to the radiation. If the integration variable is changed from t to

z using

$$t = t_0 + \frac{z}{v_{||}}$$

then

$$\frac{d^2I}{d\Omega d\omega} = \frac{e^2}{4\pi\lambda^2}\left(\frac{\mu_0}{\epsilon_0}\right)^{1/2} \times \sin^2\Theta_k \left|\int_0^L dz \frac{v_\perp}{v_{||}} \exp\left[i(\omega/v_{||})z - i(\omega/c)\hat{\mathbf{k}}.\mathbf{r}_\perp(z) - i(\omega_c/\gamma_0)\hat{\mathbf{k}}.\hat{\mathbf{z}}z\right]\right|^2 \tag{1.4}$$

where Θ_k is the angle between the radiation wavevector, $\mathbf{k}$, and the transverse velocity of the electron, $\mathbf{v}_\perp$, L is the distance travelled by the electron and $\hat{\mathbf{z}}$ is a unit vector in the direction of the magnetic field. The transverse velocity can be represented as

$$\mathbf{v}_\perp = \frac{1}{2}\left(\tilde{\mathbf{v}}_\omega e^{-i(\omega_c/\gamma_0)t} + \tilde{\mathbf{v}}_\omega^* e^{i(\omega_c/\gamma_0)t}\right)$$

so substituting this result into (1.4) and multiplying by the electron injection rate I/e in order to obtain the spectral radiation intensity of a beam of electrons results in the equation [2]

$$\frac{d^2I}{d\Omega d\omega} = \frac{e^2}{4\pi\lambda^2}\frac{I}{e}\left(\frac{\mu_0}{\epsilon_0}\right)^{1/2}\frac{L^2}{4}\sin^2\Theta_k\left|\frac{\tilde{v}_\omega}{v_{||}}\right|\mathrm{sinc}^2\left(\frac{\bar{\theta}}{2}\right) \tag{1.5}$$

where $\bar{\theta}$ is

$$\bar{\theta} = \left(\frac{\omega - \omega_c/\gamma_0}{v_{||}} - k_{||}\right)L \tag{1.6}$$

The spectral intensity as a function of both detuning ($\Delta\omega = (\omega - \omega_c/\gamma_0 - k_{||}v_{||})/v_{||}$) and the distance travelled by the electrons, L, is shown in figure 1.2.

This spontaneous emission is due to the oscillation of the electrons in a static field. The presence of an electromagnetic wave in this system will induce stimulated emission and absorption processes. In a CRM, the stimulated emission

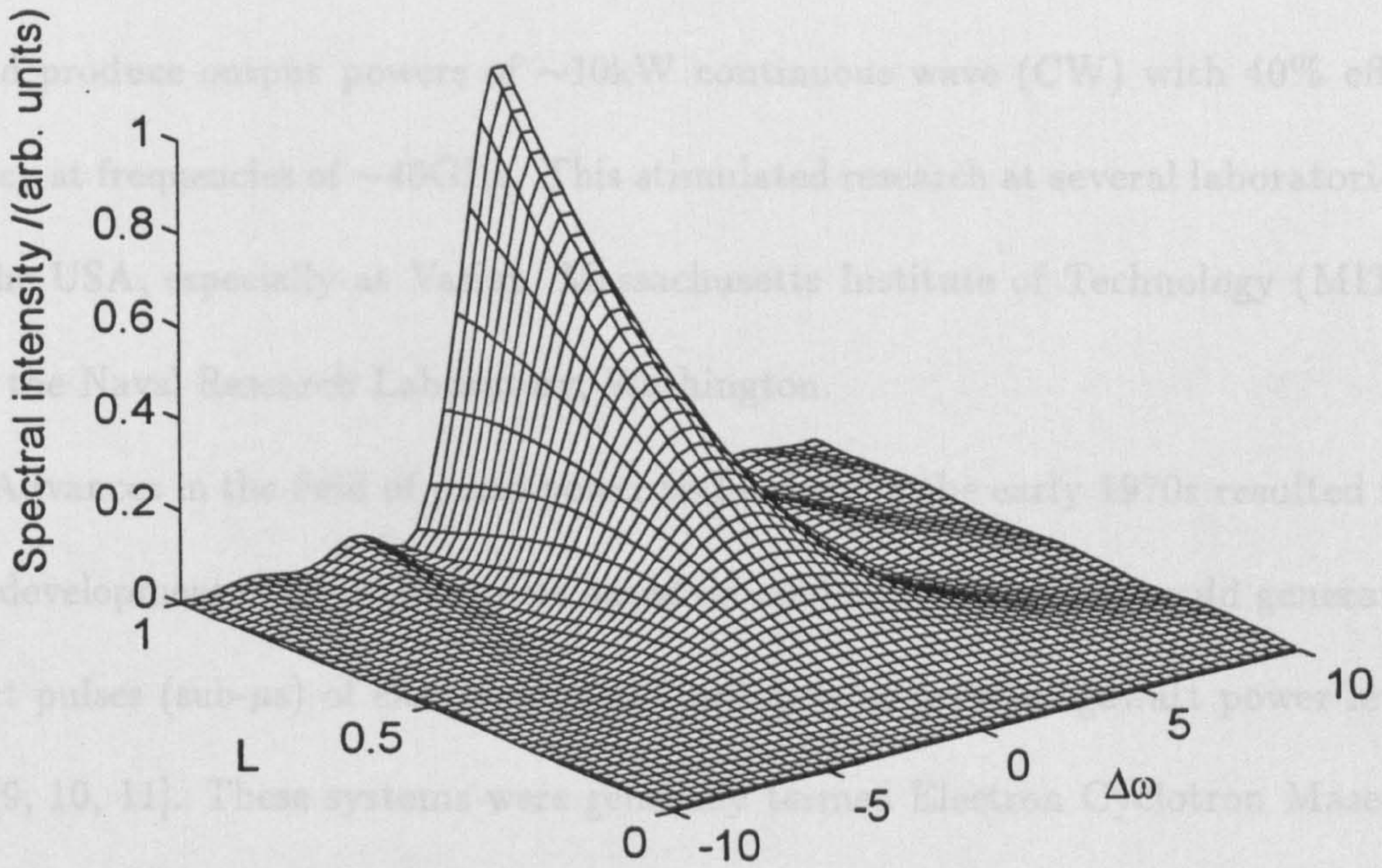

Figure 1.2: Spontaneous spectral intensity (arbitrary units) as a function of detuning $\Delta\omega$ and L.

may exceed the stimulated absorption, resulting in amplification of the electromagnetic wave. Various methods of analysing this gain process are described in chapter 2.

1.3 Evolution of the CRM

Early experimental studies of the interaction of electromagnetic radiation with gyrating electrons in a static magnetic field were a natural outgrowth in the development of the TWT. The first experimental results were produced by Pantell [3], Chow and Pantell [4], Bott [5, 6] and Feinstein [7]. All these devices were steady-state oscillators, utilising low voltage (~10kV), low current (~1mA) electron beams with total millimetre-wave power output of $\ll$ 1W. Following the

theoretical investigations of Gaponov [8], a substantial experimental and theoretical research effort was developed in the former USSR, resulting in devices which could produce output powers of ~10kW continuous wave (CW) with 40% efficiency at frequencies of ~40GHz. This stimulated research at several laboratories in the USA, especially at Varian, Massachusetts Institute of Technology (MIT) and the Naval Research Laboratory, Washington.

Advances in the field of pulse-power technology in the early 1970s resulted in the development of several systems based on cold cathodes which could generate short pulses (sub-μs) of electromagnetic radiation at multi-megawatt power levels [9, 10, 11]. These systems were generally termed Electron Cyclotron Masers (ECMs). The next significant step was the development of the three electrode, thermionic cathode magnetron injection gun (MIG) in the former USSR [22], which allowed the generation of high current electron beams with substantial transverse energies. This stimulated research into long pulse ($\gg 1\mu$s) and continuous wave (CW) high power ($\gtrsim$100kW) systems. Such systems, which have usually been oscillators utilising a single cavity, have been termed gyromonotrons or gyrotrons [28]. Initial experiments using the MIG were at conventional microwave frequencies ($\ll$ 30GHz) [12, 13, 14]. Subsequent experiments by Voronkov [15] and Gold [16], involving radiation generation at frequencies of $\sim$ 30GHz at power levels of $\sim$ 20MW moved the operating regime of the gyrotron outwith the boundaries of conventional microwave devices.

At short wavelengths (< 1mm), it is necessary to operate gyrotrons at harmonics of the cyclotron frequency (i.e. $s > 1$ in (1.1)) due to the difficulties involved

in generating large static magnetic fields [17, 18]. To increase the operation frequency without operating at harmonics of the cyclotron frquency, Bratman *et al.* suggested the concept of the cyclotron autoresonance maser (CARM) [19], the principles behind which will be discussed in the next section and chapters 3 and 4. Experimental studies of the CARM are still on a proof of principle basis, with the main centres of activity being at Nizhny Novgorod in the former USSR and MIT in the USA. Recent results from Nizhny Novgorod include the development of a CARM oscillator using a Bragg resonator which can generate power levels of 50MW at a wavelength of 4.4mm (frequency of 68.1GHz), or 30MW at a wavelength of 6mm (frequency of 50GHz) [21]. Recent developments at MIT include the operation of a long pulse CARM oscillator producing 1.9MW of output power at a frequency of 28GHz [20].

The possible applications of CRM devices span a wide range of technologies. The plasma-physics community has already taken advantage of recent advances in producing high power micro- and millimetre waves in the areas of RF plasma heating, for magnetic confinement fusion studies, as lower hybrid heating (1-8 GHz) and electron cyclotron resonance heating (28-140GHz), plasma production for numerous different processes and plasma diagnostic measurements as collective Thomson scattering or heat pulse propagation experiments [22, 23]. Recently, gyrotron oscillators were also successfully utilised in material processing (e.g. advanced ceramic sintering, surface hardening or dielectric coating of metals and alloys) as well as in plasma chemistry [24]. Other applications which await the development of novel high power sources include deep space communication, high

resolution radar, radar ranging in planetary science, drivers for next-generation high-gradient linear accelerators and technological applications.

1.4 Classification of CRM Devices

The basic principles of CRM devices are discussed in several books and review articles [25, 26, 27, 28, 29, 30]. This section will contain an outline description of these principles for several types of CRM devices most relevant to the aims of this thesis. The simple descriptions of the interactions given here will be elaborated on in a full general description in chapter 3.

1.4.1 The Gyromonotron or Gyrotron

The gyrotron is essentially the simplest type of CRM in terms of both theory and experiment. The electromagnetic waves propagate almost perpendicular to the direction of the magnetic field i.e. $k_\perp \gg k_{||}$, so the Doppler shift is small and the resonance condition (1.1) reduces to

$$\omega \approx s\frac{\omega_c}{\gamma}$$

which is shown schematically on a dispersion diagram in figure 1.3 for the case of fundamental resonance ($s = 1$). The gain mechanism is due to bunching in phase due to the relativistic mass dependence of the cyclotron frequency, which will be discussed in detail in chapters 2, 3 and 4. The neglect of the Doppler shift means that axial velocity spread, which can be as much as 10% depending on the type of beam formation system being used, does not affect the interaction,

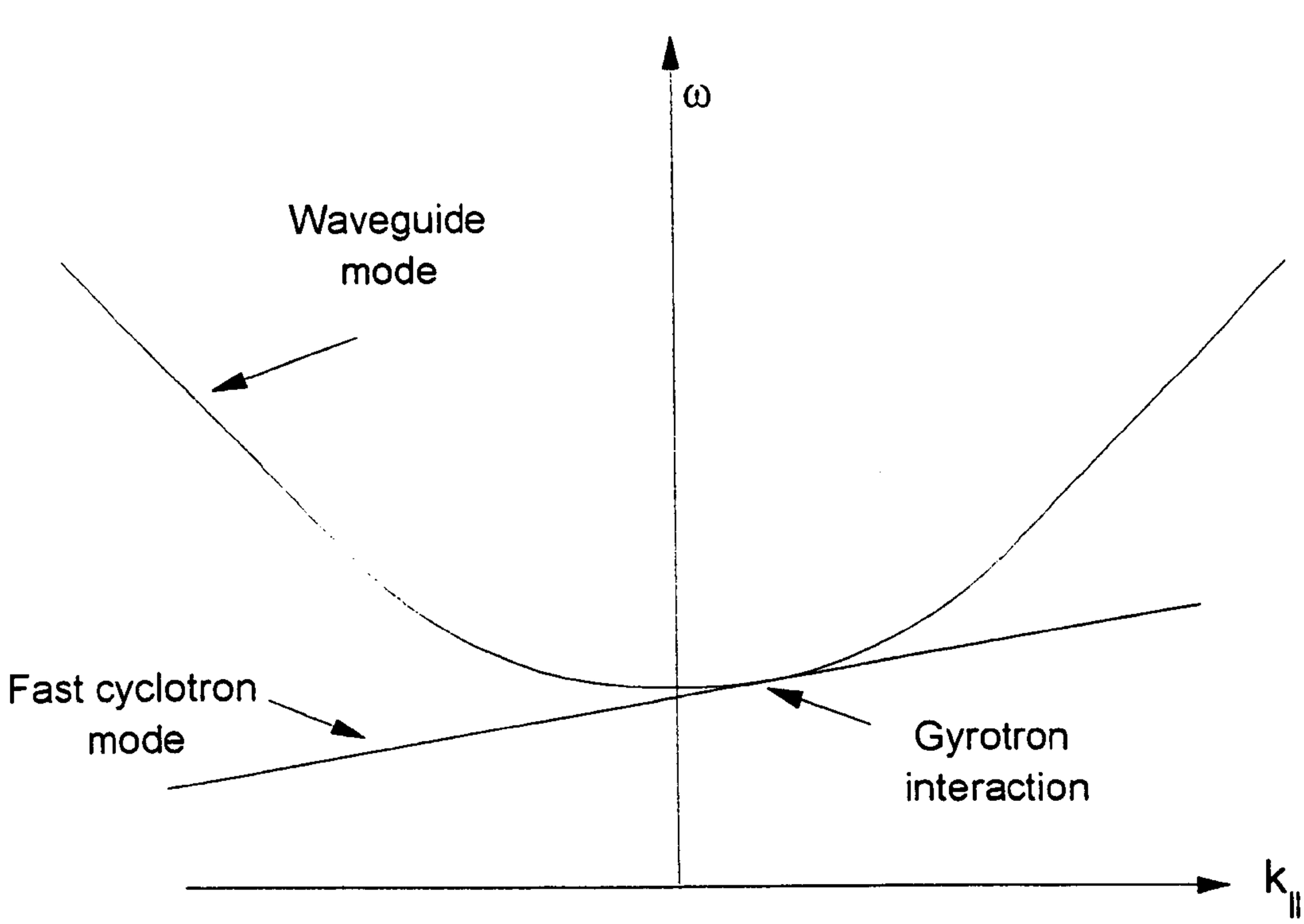

Figure 1.3: Dispersion relation for the gyrotron interaction.

so fairly poor quality electron beams may be used. Normally, gyrotrons utilise only weakly relativistic electron beams (< 100kV), with large transverse energies i.e. $v_\perp/v_\parallel > 1$. Cyclotron harmonic operation reduces the required magnetic field for a given frequency by a factor s. Gyrotrons are almost always operated as oscillators, using either a cylindrical open resonator or a quasi-optical mirror resonator [31], as shown in figure 1.4.

1.4.2 The Cyclotron Autoresonance Maser

In a gyrotron with a highly relativistic beam, the dependence of the cyclotron frequency on the electron energy is very strong. An efficient interaction will cause large variations in γ and consequently larger changes in the cyclotron frequency ω_c/γ than in the mildly relativistic case. It is therefore desirable to identify

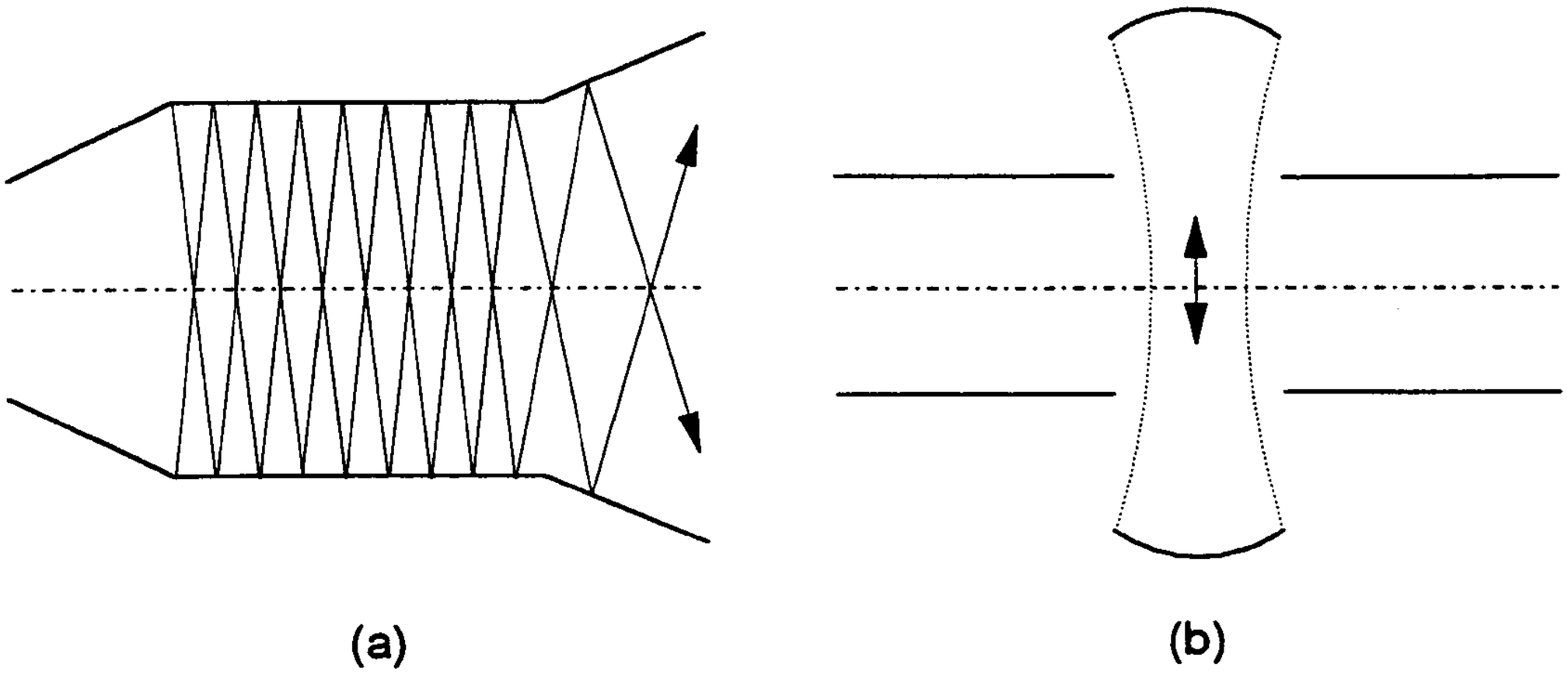

Figure 1.4: Diagram showng (a) a conventional open resonator and (b) a quasi-optical mirror resonator.

the condition under which an electron that loses energy remains in synchronism with the electromagnetic wave. A possibility for achieving such synchronism is to utilise the interaction of electrons with electromagnetic waves propagating at a phase velocity close to the speed of light i.e. almost parallel to the axis of the cylindrical waveguide. In this case, the Doppler shift is large and the appropriate resonance condition is (1.1). This is illustrated on a dispersion diagram in figure 1.5. If $v_p \approx c$, the increase in cyclotron frequency due to extraction of beam energy (decrease of γ) nearly compensates the decrease in the Doppler shifted term, as will be demonstrated in section 3.4. Therefore, if the resonance condition is initially fulfilled, it will continue to be satisfied during the interaction. This phenomenon is called *autoresonance* and CRM devices operating in

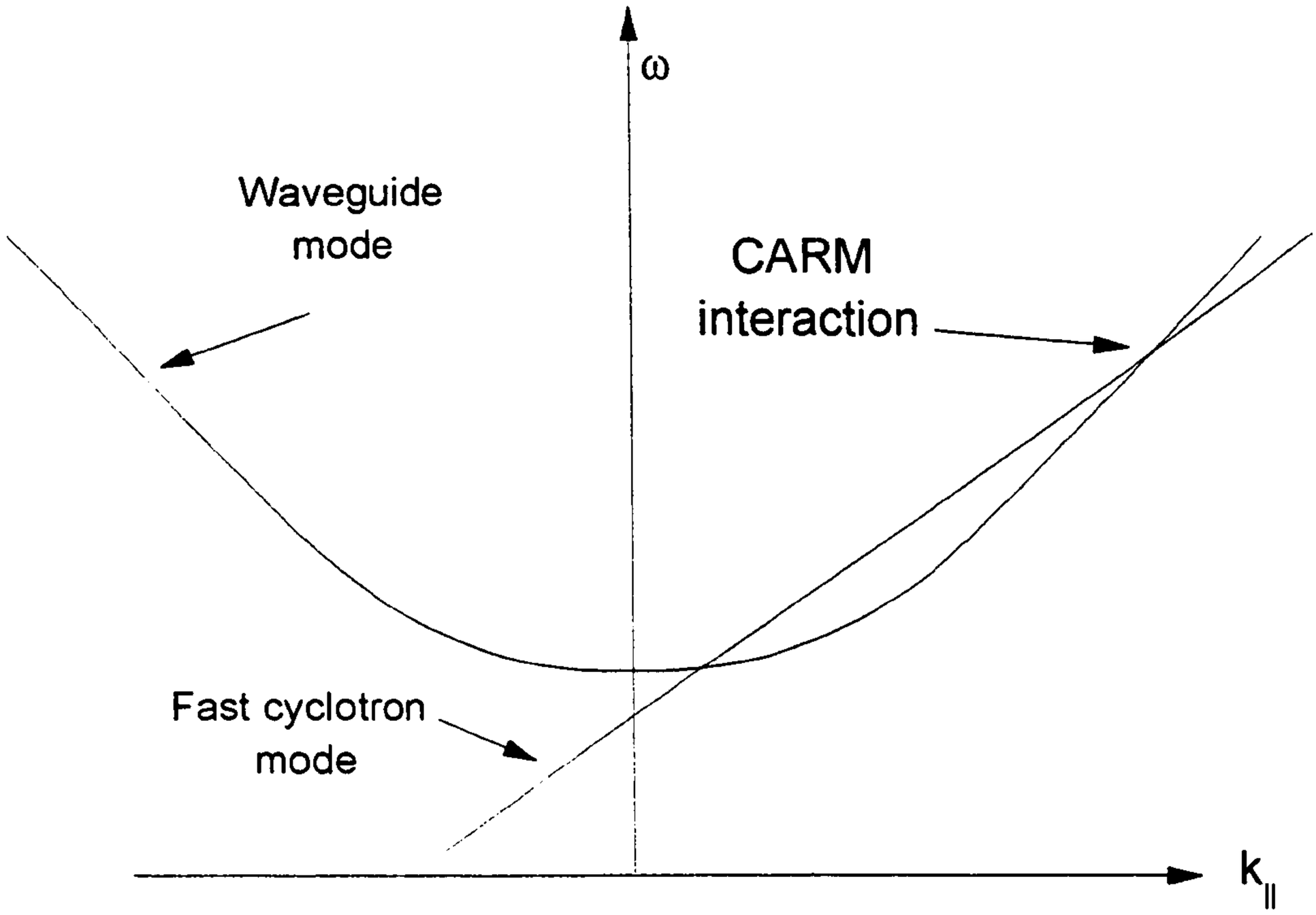

Figure 1.5: Dispersion relation for a CARM interaction.

the relativistic Doppler-shifted regime are called cyclotron autoresonance masers (CARMs). The CARM is an extremely attractive device because of its high frequency operation and because of the fact that it extracts energy from both the transverse and axial motion of the electron beam, making efficient interaction a possibility.

Experimentally, CARMs are much more complex devices than gyrotrons, for a number of reasons. Firstly, the strong dependence of the interaction on the Doppler shift means that high quality electrons beams must be used, with axial velocity spreads of $\Delta v_{||}/v_{||} \lesssim 2\%$ in order to come close to realising the potential efficiency of the interaction. In addition, the second intersection of the beam line with the waveguide mode gives rise to a relativistic gyrotron interaction or a backward wave interaction, which can grow parasitically and disrupt the

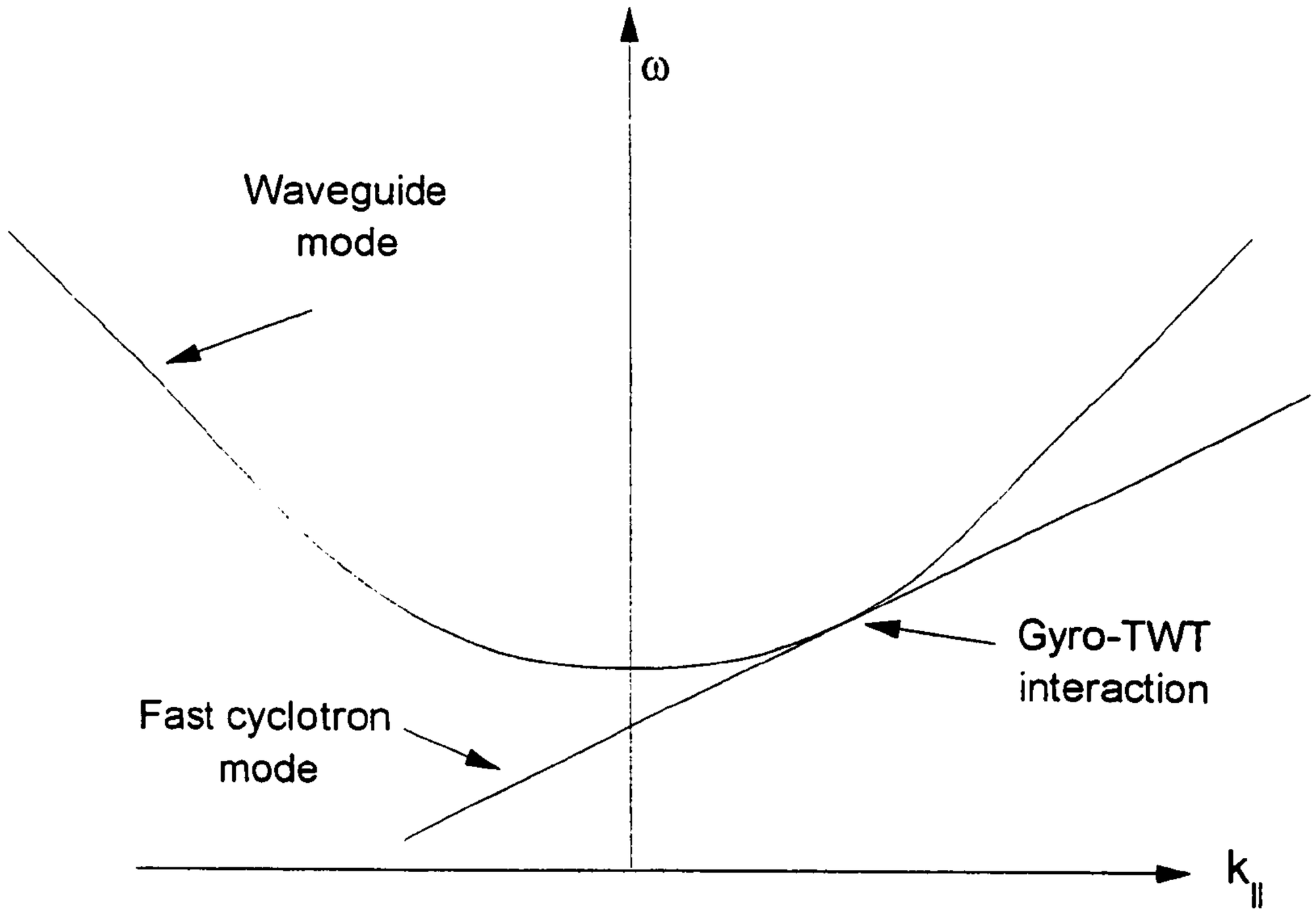

Figure 1.6: Dispersion relation for a gyro-TWT interaction.

CARM interaction with the wave. In order to avoid this, careful mode selection is necessary to allow the CARM interaction to progress while suppressing the other interactions. The CARM interaction is convective in nature, so it can be used in an amplifier configuration or, using external feedback e.g sandwiching the interaction region between Bragg reflectors, in an oscillator configuration.

1.4.3 The Gyro-TWT Amplifier

From a theoretical point of view, the gyro-TWT differs from the CARM only in regimes of operation. The gyro-TWT utilises a moderately relativistic electron beam to interact with a fast waveguide mode near the grazing interaction of the dispersion diagram, as shown in figure 1.6. In the gyro-TWT regime, $v_p \gg c$, so the axial bunching mechanism is too weak to be of any significance.

The general theory described in the following chapters is concerned only with interactions which give rise to convective instabilities i.e. instabilities which propagate in space (in the laboratory frame of reference) and consequently is most relevant to the gyro-TWT and CARM amplifier configurations. The absolute nature of the gyrotron instability makes it unsuitable for such an analysis.

1.5 CRM Research at Strathclyde University

CRM research has taken place at Strathclyde University since around 1980, when relativistic electron beam experiments were first performed [32]. Initial CRM experiments developed at Strathclyde operated at relatively low frequencies ($\approx$ 12GHz), with further development to higher frequencies resulting in a step-tunable CRM capable of operating in the range 35-200GHz [33, 34]. Much of this work owed its success to the development of a CRM electron beam source based on a field emission, field immersed, cold cathode configured within a two electrode diode. An electron beam of duration $\approx$ 400 ns was produced via plasma flare emission at the cathode tip. Due to the pulsed nature of the plasma flare cold cathode, initial devices used conventional, water cooled copper wound coils driven by RC networks to generate the intra-cavity magnetic field. These could produce quasi-static intra-cavity fields of up to 4T, with rise times of $\approx$ 120μs. Later designs utilized a superconducting magnet which could generate static magnetic fields of up to 11T.

The main thrust of research through the 1980s was concerned with increasing output powers and the frequency tunability of the device. In order to achieve this,

a great deal of work was done on the focussing of the electron beam around the cathode region and the design of the cavity [33]. This resulted in the generation of peak powers of $\approx$ 1MW at frequencies of $\approx$ 100GHz with step-tunable operation via discrete mode excitation [34].

Around 1990, work began on the first of several projects concerned with electron beam formation in the CRM. Until this time, all the experiments at Strathclyde had utilized a stainless steel cold cathode, emitting electrons due to plasma flare emission [33]. Development of a thermionic cathode opened up the possibility of eventual CW operation and resulted in the construction of a fully operational gyrotron using a MIG-type cathode operating at frequencies of 20-45GHz at power levels $>$ 1MW [35, 36]. In addition, a novel type of gyrotron cathode using field emission arrays (FEAs) was developed and successfully used as an electron source in a working gyrotron to generate microwave radiation. This type of cathode allows much greater control over the electron beam than conventional gyrotron cathodes and could be used to generate very short electron pulses at high repetition frequencies of $\approx$ 1kHz [37, 38].

The experiments described above all involve CRM oscillator/gyrotron devices. At the time of writing, a CARM oscillator experiment is under construction which when operational will be the first CARM of any type to be built outside the former USSR or the USA. The aim of the project is to generate output powers of $\approx$ 5MW at frequencies of 12-20GHz, with a Doppler upshift factor of around 4-7 [39]. As the quality of the electron beam is so important for CARM devices, electron beam diagnostics are also currently an active area of research.

1.6 Novel Aspects of CRM Theory

The new developments in the theory of the CRM which form the major part of the work in this thesis can be summarised as follows :

1. Starting from the Lorentz equation of motion for a relativistic electron and Maxwell's equations, a set of nonlinear, coupled differential equations was derived to describe both the linear and nonlinear evolution of the interaction between a beam of electrons and a single TE or TM waveguide mode in a CRM amplifier such as a gyro-TWT or CARM, chapter 3. These equations were universally scaled, which simplified both the analysis of the interaction and the interpretation of the results produced. The number of free parameters involved in the universally scaled set was just three : ρ, the fundamental CRM parameter, ν, the free energy parameter and δ, the detuning between the electrons and the wave. Using this universally scaled set of equations, the CRM interaction was studied far into the nonlinear regime over a wide range of the parameter space and the different saturation mechanisms were identified.

2. Using a rigorous linear analysis, the linear growth of the instability was studied using a linearised set of universally scaled evolution equations, chapter 4. The method of collective variables, which has not previously been applied to CRM-type devices, was used to derive a dispersion relation which determines the linear behaviour of the system. Using this dispersion relation, a threshold condition for linear instability to occur was derived. Above this threshold, an expression for the growth rate of the electromagnetic field was

found and compared with the results of other linear theories. The linear growth of the instability was found to consist of two distinct regimes : the low-gain regime, where the 'partial waves' which correspond to the roots of the dispersion relation interfere, and the high-gain regime, where the amplitude of the electromagnetic field grows exponentially. In the low-gain regime, it was found that Madey's relations between the stimulated emission (gain), spontaneous emission and the energy spread of the electrons, originally derived for the FEL, could be reproduced.

Using the linear analysis, it was also possible to identify the different bunching mechanisms responsible for wave amplification and the condition for autoresonance to occur. The condition for instability to occur at autoresonance was derived and the resulting growth rate of the instability was evaluated.

3. When the fundamental cyclotron parameter is very small i.e. $\rho \ll 1$, the resulting set of universally scaled equations are found to have a number of interesting properties. Firstly, it was found possible to state the equations of motion for the electrons *and* the electromagnetic field as a system of Hamilton's equations. This enabled a phase space analysis of the CRM to be carried out, chapter 5. Such an analysis was performed for the case where the evolution of the field is negligible and also for the case where the field evolution evolves self-consistently with a single particle. The former is representative of the situation in a low-gain oscillator close to saturation while the latter has relevance to experiments involving pre-bunched electron

beams.

The second feature of the universally scaled equations when $\rho \ll 1$ is that it was found possible to describe the linear and nonlinear evolution of the electromagnetic field using collective variables which are a generalisation of those variables used in the linear analysis of the interaction, chapter 5. This greatly reduced the number of equations to be solved and describes the interaction in a similar way to the equations which are used to describe the polarisation, population difference and field amplitude and phase in atomic lasers. Using this collective variable description, it was shown that it is possible to describe approximately the evolution of the electromagnetic field up to saturation by an analytically solveable Landau-Ginzburg equation, chapter 5. This allows quantities such as the saturation intensity, which usually have to be evaluated via the numerical solution of a large set of coupled differential equations, to be evaluated analytically.

4. The analysis of the CRM interaction in an amplifier has almost always been carried out in the steady-state limit, sometimes referred to as the limit of stationary oscillations. This is equivalent to assuming that an electron pulse of infinite extent is taking part in the interaction, with each part of the electron pulse evolving identically. In contrast, if finite length electron and radiation pulses are assumed, and the propagation velocity of the radiation pulse is not equal to the electron axial velocity, it can be shown that there is another gain mechanism which can occur : superradiance, chapter 6. It was shown that this superradiant emission is due to a spontaneous emission

process which results in intensities scaling as n_e^2, in contrast to the steady-state regime, where intensities scale as $n_e^{4/3}$, where n_e is the electron density.

The existence of two types of superradiance was demonstrated for a CRM utilising a highly relativistic electron beam : weak superradiance, which occurs when the electron pulse length is shorter than a pre-defined cooperation length, and strong superradiance, which can occur for electron pulses much longer than a cooperation length due to a portion of the electron pulse emitting superradiantly. Peak intensities for weak/strong superradiant pulses are less/greater than the peak intensity which occurs in the steady-state regime.

The superradiant instability in a CRM system was initially predicted using a dissipative model which heuristically described the effect of radiation escaping from the electron pulse. This analysis allowed the identification of a cooperation length, the size of which relative to the electron pulse length determines the importance of superradiant effects on the radiation field evolution. A more rigorous linear analysis was then used to identify the conditions for a superradiant instability to occur, and the resulting growth rates of such an instability. The nonlinear evolution was analysed using a set of coupled nonlinear partial differential equations. It was shown that under certain conditions, this set could be reduced to a self-similar set of ordinary differential equations. A condition for the effect of free energy depletion effects to be negligible during superradiant evolution was derived. Numerical simulation of superradiant phenomena produced evidence that

strong superradiance could occur in CRM devices. The effect of free-energy depletion effects on this strong superradiance was analysed and discussed.

Chapter 2

Cyclotron Resonance Maser Theory - A Review

2.1 Introduction

This chapter contains a brief description of some of the methods which have been used to investigate the CRM interaction, ranging from the very first theoretical analyses at the end of the 1950s to those those still in use at the present day.

2.2 Quantum Mechanical Analysis

The first theoretical papers to demonstrate the existence of an amplifying mechanism for free-electron gyro-radiation were those by Twiss [40] in 1958 and both Schneider [41] and Gaponov [8] in 1959. The approach used by Twiss and Schneider was quantum mechanical whereas that of Gaponov was classical.

The starting point of the quantum-mechanical analysis is an expression de-

scribing the energy levels of a relativistic electron in a uniform magnetic field. The derivation of this expression, which was not given in either [40] or [41], will be described below.

Consider the classical Hamiltonian for a relativistic electron with charge $e = |e|$ and rest mass m_e in a static magnetic field, given by

$$H = -e\Phi + \left(m_e^2c^4 + c^2(\mathbf{P} + e\mathbf{A})^2\right)^{1/2} \tag{2.1}$$

where c is the speed of light in vacuo, $\mathbf{P}$ is the canonical electron momentum, $\mathbf{A}$ is the vector potential and Φ is the scalar potential. Defining

$$\mathbf{u} = \frac{\mathbf{P} + e\mathbf{A}}{m_e} \tag{2.2}$$

and letting $\Phi = 0$, then the Hamiltonian becomes

$$H = (m^2c^4 + m^2c^2\mathbf{u}^2)^{1/2}. \tag{2.3}$$

It will be assumed for simplicity that the electron only has transverse momentum, i.e. $\mathbf{u} = \mathbf{u}_\perp$ and the vector potential has only transverse components i.e. $\mathbf{A} = \mathbf{A}_\perp$, consistent with an electron in a uniform magnetic field.

The operators which represent space and momentum are [42]

$$\hat{X}, \hat{Y}, \hat{Z}$$

$$\hat{P}_x, \hat{P}_y, \hat{P}_z$$

respectively, so the following commutation relations can be applied, using the notation $[\hat{A}, \hat{B}] \equiv \hat{A}\hat{B} - \hat{B}\hat{A}$:

$$[\hat{X}, \hat{P}_x] = [\hat{Y}, \hat{P}_y] = [\hat{Z}, \hat{P}_z] = i\hbar$$

$$[\hat{P}_x, \hat{P}_y] = [\hat{P}_x, \hat{P}_z] = [\hat{P}_y, \hat{P}_z] = 0$$

$$[\hat{A}_x, \hat{A}_y] = [\hat{A}_x, \hat{A}_z] = [\hat{A}_y, \hat{A}_z] = 0$$

as the vector potential is a function of space only i.e. $\hat{A}_{x,y,z} = \hat{A}_{x,y,z}(\hat{X}, \hat{Y}, \hat{Z})$.

The operator equivalent of (2.2) can be written as

$$\hat{U}_x = \frac{\hat{P}_x + e\hat{A}_x}{m_e} \tag{2.4}$$

$$\hat{U}_y = \frac{\hat{P}_y + e\hat{A}_y}{m_e} \tag{2.5}$$

$$\hat{U}_z = 0 \tag{2.6}$$

so the commutation relation $[\hat{U}_x, \hat{U}_y]$ becomes

$$\begin{aligned}[\hat{U}_x, \hat{U}_y] &= \frac{1}{m_e^2}\Big((\hat{P}_x - e\hat{A}_x)(\hat{P}_y - e\hat{A}_y) - (\hat{P}_y - e\hat{A}_y)(\hat{P}_x - e\hat{A}_x)\Big) \\ &= -\frac{e}{m_e^2}\Big([\hat{A}_y, \hat{P}_x] + [\hat{P}_y, \hat{A}_x]\Big) \end{aligned} \tag{2.7}$$

This expression can be further reduced using the rules [42]

$$[\hat{P}_x, \hat{F}(\hat{X})] = -i\hbar\frac{d\hat{F}(\hat{X})}{d\hat{X}}$$

$$[\hat{P}_y, \hat{G}(\hat{Y})] = -i\hbar\frac{d\hat{G}(\hat{Y})}{d\hat{Y}}$$

where $\hat{F}(\hat{X})$ and $\hat{G}(\hat{Y})$ are arbitrary operators, resulting in

$$\begin{aligned}[\hat{U}_x, \hat{U}_y] &= -\frac{i\hbar e}{m_e^2}\left(\frac{\partial\hat{A}_y}{\partial\hat{X}} - \frac{\partial\hat{A}_x}{\partial\hat{Y}}\right) \\ &= \frac{-i\hbar e}{m_e^2}\hat{B}_z \end{aligned} \tag{2.8}$$

where $\hat{B}_z = (\partial\hat{A}_y/\partial\hat{X} - \partial\hat{A}_x/\partial\hat{Y})$ is the operator representing the axial magnetic field. If the the magnetic field vector is written as

$$\mathbf{B} = (0, 0, B_0)$$

then (2.8) can be written as

$$[\hat{U}_x, \hat{U}_y] = -\frac{i\hbar e}{m_e^2} B_0$$

$$[\hat{U}_y, \hat{U}_z] = 0$$

$$[\hat{U}_z, \hat{U}_x] = 0.$$

The definition of the non-relativistic cyclotron frequency is

$$\omega_c = \frac{eB_0}{m_e}$$

so (2.8) can be rewritten as

$$[\hat{U}_x, \hat{U}_y] = -\frac{i\hbar\omega_c}{m_e}. \tag{2.9}$$

The Hamiltonian (2.3) written in terms of operators is

$$\hat{H} = \left(m_e^2c^4 + m_e^2c^2\left(\hat{U}_x^2 + \hat{U}_y^2\right)\right)^{1/2} \tag{2.10}$$

which can be written in a form related to that of a one-dimensional harmonic oscillator using the operators

$$\hat{Q} = \sqrt{\frac{m_e}{\hbar\omega_c}}\hat{U}_y \qquad \hat{S} = \sqrt{\frac{m_e}{\hbar\omega_c}}\hat{U}_x \tag{2.11}$$

such that

$$[\hat{Q}, \hat{S}] = -\frac{m}{\hbar\omega_c}[\hat{U}_x, \hat{U}_y] = i.$$

Substituting for $\hat{U}_x$ and $\hat{U}_y$ in $\hat{H}$ using (2.11) produces

$$\hat{H} = \left(m_e^2c^4 + m_ec^2\hbar\omega_c(\hat{S}^2 + \hat{Q}^2)\right)^{1/2} \tag{2.12}$$

so if the so-called destruction operator, $\hat{a}$, and creation operator, $\hat{a}^\dagger$, are defined as

$$\hat{a} = \frac{1}{\sqrt{2}}(\hat{Q} + i\hat{S}) \qquad \hat{a}^\dagger = \frac{1}{\sqrt{2}}(\hat{Q} - i\hat{S}) \tag{2.13}$$

then

$$\begin{aligned}\hat{a}^\dagger\hat{a} &= \frac{1}{2}(\hat{Q}-i\hat{S})(\hat{Q}+i\hat{S}) \\ &= \frac{1}{2}\left(\hat{Q}^2+\hat{S}^2+i[\hat{Q},\hat{S}]\right) \\ &= \frac{1}{2}\left(\hat{Q}^2+\hat{S}^2-1\right)\end{aligned}$$

so

so

$$\hat{Q}^2+\hat{S}^2 = 2\hat{a}^\dagger\hat{a}+1. \tag{2.14}$$

Substitution of this result in (2.12) results in

$$\hat{H} = \left(m_e^2c^4+m_ec^2\hbar\omega_c(2\hat{a}^\dagger\hat{a}+1)\right)^{1/2}$$

which can be further reduced to

$$\hat{H} = \left(m_e^2c^4+2m_ec^2\hbar\omega_c\left(\hat{N}+\frac{1}{2}\right)\right)^{1/2}$$

due to the fact that [42]

$$\hat{a}^\dagger\hat{a} = \hat{N}$$

where $\hat{N}$ is the number operator. It can be shown that that this operator has integral eigenvalues which are greater than or equal to zero [42].

The eigenvalue equation

$$\hat{H}|\Psi\rangle = E_n|\Psi\rangle$$

where $|\Psi\rangle$ is an eigenvector of H, results in the expression for the energy of the nth quantum level i.e.

$$E_n = m_ec^2\left(1+\frac{2\hbar\omega_c}{m_ec^2}\left(n+\frac{1}{2}\right)\right)^{1/2} \tag{2.15}$$

so the energy spacing between the nth and the $(n+1)$th levels is

$$E_{n+1} - E_n \approx \hbar\omega_c \left(1 - n\frac{\hbar\omega_c}{m_e c^2}\right) \tag{2.16}$$

to first order of $\hbar\omega_c/m_e c^2$. This means that as the electron energy is increased, the spacing of adjacent levels becomes smaller, as shown schematically in figure 2.1. This unequal level spacing allows the probability for stimulated emission to exceed that for absorption and consequently gain can occur [41]. For non-relativistic electrons, (2.15) reduces to the famous expression derived by Landau [43],

$$E_n = \hbar\omega_c \left(n + \frac{1}{2}\right).$$

In this case, the levels are equally spaced and no gain can occur. This gain mechanism is therefore a purely relativistic effect. In addition to a change in its mass, the electron will also undergo recoil, as it emits a photon of momentum $\hbar\mathbf{k}$ i.e. its longitudinal momentum will decrease by an amount $\hbar k_{\|}$. This recoil lies behind the gain mechanism in conventional travelling-wave tubes (TWTs).

Although the quantum mechanical approach is of historical interest, having proved extremely useful in demonstrating the existence of the gain mechanism, it is of little use in the design of physical devices. As the frequencies involved are in the microwave region of the electromagnetic spectrum, an electron will emit many ($\sim 10^8$) photons before its interaction with the stimulating radiation becomes negligible, in contrast to devices such as atomic lasers, where the atom can emit only a single photon before its interaction with the stimulating radiation effectively ceases. This means that the levels can be assumed to form a continuum and the gain mechanism in CRMs can be described classically. The

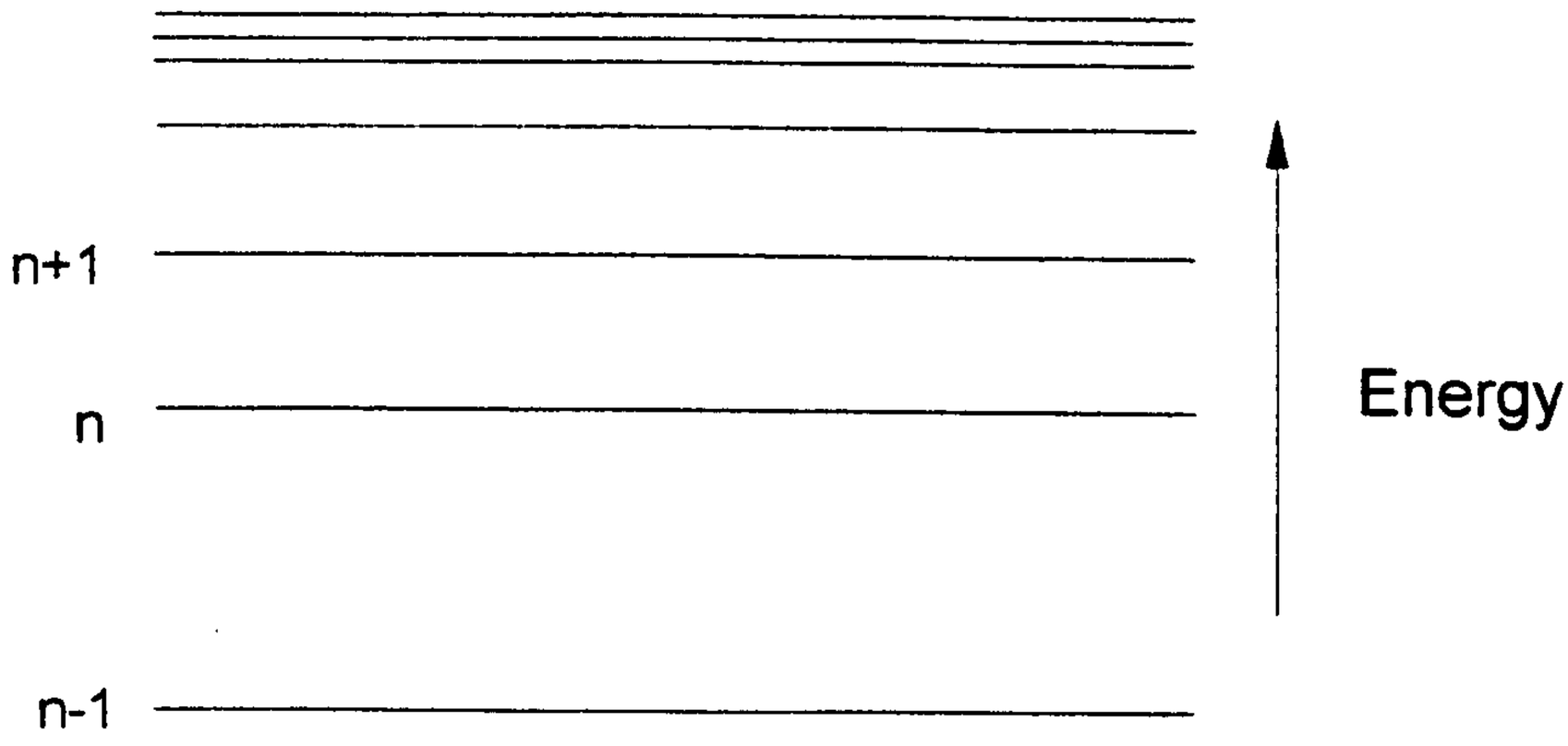

Figure 2.1: Schematic diagram of the energy levels for a relativistic electron in a static magnetic field.

gain mechanism due to the relativistic mass change manifests itself classically as azimuthal bunching i.e. bunching in the gyro-angle $\phi_g \approx \omega_c/\gamma\ t$ whereas the electron recoil results in longitudinal or axial bunching. Some classical approaches are described in the following sections.

2.3 Fluid Theory

One of the most fruitful methods of analysing the CRM interaction in the linear regime has been the use of fluid theory, where the electron beam is treated as a charged relativistic fluid. The procedure is basically to calculate the response of the fluid to temporal and spatial perturbations, and work out the conditions under which the perturbed system becomes unstable. The origins of this method

lie in analyses of travelling wave tube devices by Pierce [44].

One of the first applications of fluid theory to CRM devices was performed by Lau [45], in which the CRM system was represented as a rotating annular electron fluid enclosed in a metallic waveguide, as shown in figure 2.2. By perturbing the electron beam, and self-consistently calculating the electromagnetic fields generated via Maxwell's equations, Lau was able to show that the system was unstable and that this CRM instability was of negative-mass type. The negative-mass nature of the instability is easily shown by considering the rate of change of the cyclotron frequency

$$\frac{d}{dt}\left(\frac{\omega_c}{\gamma}\right) = -\omega_c \frac{d\gamma}{dt}$$

so as the electron mass (γm_e) increases, its angular velocity decreases and vice-versa. Lau also showed that for electron beams of finite thickness, the cyclotron maser instability could be interpreted as an instability of the shear flow of the relativistic electron fluid. i.e. instability due to the angular velocity of the electron beam changing in the radial direction.

One of the main advantages of using fluid theory in an analysis of the CRM instability is that it is entirely self-consistent, and an analysis resulting in a single dispersion relation can simultaneously describe a number of different phenomena, which can then be isolated by taking specific limits. In this respect it is similar to plasma kinetic theory but as fluid theory is macroscopic i.e. it is not concerned with the distribution function of the electrons in momentum space, it is often simpler to apply and interpret. Examples of such 'unified' fluid theories describing several effects are those by Lau [46] and Lashmore-Davies [47] which between

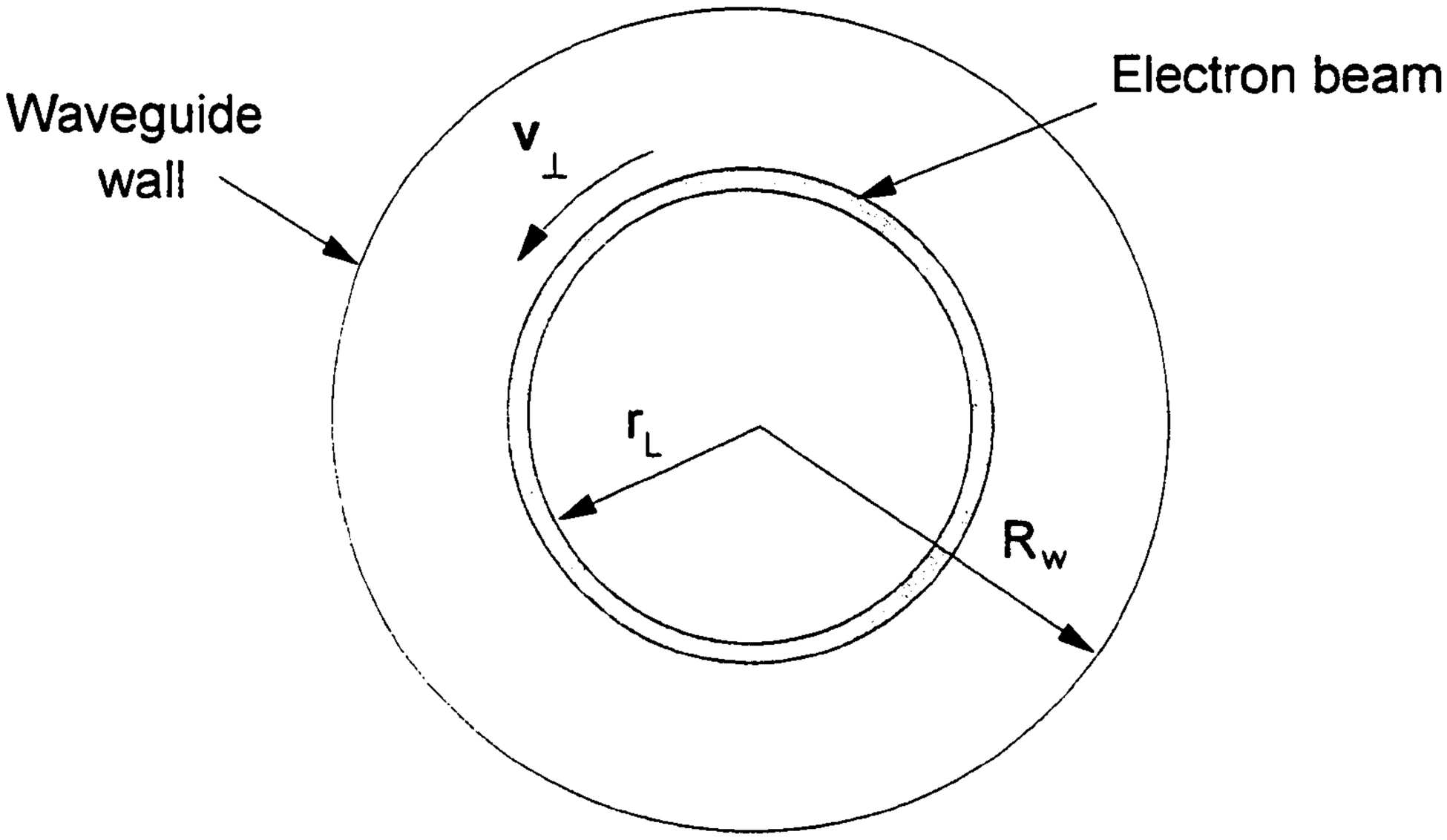

Figure 2.2: Fluid model of CRM interaction

them describe the gyrotron, diocotron, peniotron, CARM and harmonic auto-resonant peniotron (HARP) instabilities including coupling between TE and TM waveguide modes. The results of Lashmore-Davies for the Doppler-shifted CRM interaction for both TE and TM modes in the limit of weak space charge are most relevant to the analysis which will be described in the following chapters. The spatial growth rates for TE_{1n} and TM_{1n} waveguide modes involved in such an interaction are

$$g_{TE} = \frac{\sqrt{3}}{2}\left(\frac{k_\perp^2}{8k_{||}}\frac{v_{\perp 0}^2}{\gamma_0 v_{||0}^2}\frac{\omega_p^2}{c^2}\frac{1}{\left(1-1/\chi_{1n}'^2\right)J_1^2(\chi_{1n}')}\right)^{1/3} \tag{2.17}$$

$$g_{TM} = \frac{\sqrt{3}}{2}\left(\frac{\omega^2\omega_c^2}{8k_{||}c^4}\omega_p^2 v_{\perp 0}^2\gamma_0\left(\frac{v_g}{v_{||}}-1\right)^2\frac{1}{J_1'^2(\chi_{1n})}\right)^{1/3} \tag{2.18}$$

where ω_p is the plasma frequency, χ_{1n} satisfies $J_1(\chi_{1n}) = 0$ and χ_{1n}' satisfies $J_1'(\chi_{1n}) = 0$. These growth rates are valid for the case of an axis encircling beam

when stabilising terms are neglected, the beam and the waveguide mode are close to resonance ($\omega \approx \omega_c/\gamma_0 + k_{||}v_{||0}$) and $k_\perp r_L \ll 1$, so that the transverse mode profile is approximately uniform over the electron gyro-orbit.

The self-consistent nature of the fluid theory makes it ideal for studying effects which occur when the beam density is large. It has been shown by several authors [46, 47, 48], that for a fully self-consistent analysis of these effects in Doppler-shifted CRM type devices, it is necessary to include both TE and TM modes and the coupling between them. The reason for this can be deduced from geometical considerations. The aximuthal bunching effects characteristic of the gyrotron instability provide a source for an azimuthal and hence transverse or TE type electric field. In contrast, axial bunching effects provide a source for a longitudinal or TM type electric field. As both types of bunching occur simultaneously in Doppler-shifted CRM devices, both types of mode will also be simultaneously generated. In this respect, the CRM is a more complicated device than, for example, the FEL, which at the fundamental level is inherently one-dimensional, with its gain mechanism due to an axial bunching effect only.

2.4 Kinetic Theory

The other method which has been used most predominantly for the study of the CRM ineraction in the linear regime is that of plasma kinetic theory [49, 50, 51, 52]. This is a microscopic theory which involves the simultaneous solution of the

Vlasov equation

$$\frac{\partial f}{\partial t} + \frac{\mathbf{u}}{\gamma}.\underline{\nabla} f - \frac{e}{m_e}\left(\mathbf{E} + \frac{\mathbf{u}\times\mathbf{B}}{\gamma}\right).\frac{\partial f}{\partial \mathbf{u}} = 0 \qquad (2.19)$$

where $f = f(\mathbf{r}, \mathbf{u}, t)$ is the electron distribution function, with Maxwell's equations usually via transform techniques to form a dispersion relation.

Although this method usually requires more algebraic manipulation than fluid theory, it has an advantage in that it can be used to study the effect of different electron momentum distributions in the beam. This is particularly useful when analysing the effect of velocity spread on the growth of the interaction, as this can often have a dramatic effect on the growth rate of the instability, possibly stabilising it altogether. Among the first to use this method to analyse the CRM instability were Ott and Manheimer [49], who studied the interaction in a planar geometry, where the electron beam is sandwiched between two conducting surfaces, all of which are assumed infinite in one dimension (figure 2.3). As they assumed a cold electron beam, their result agreed with that for the TE mode (2.17) obtained from fluid theory to within a geometrical factor. Later papers extended the theory to include the effects of cylindrical geometry [50], guiding centre motion [53], TE-TM mode coupling [54] and ohmic losses in the waveguide walls [55].

The dispersion relation describing the CRM instability for the geometry shown in figure 2.2 and for the case of a cold electron beam interacting with a TE_{mn} waveguide mode is [56]

$$(\omega^2 - k_{||}^2 c^2 - k_{\perp}^2 c^2)\left(\omega - s\frac{\omega_c}{\gamma_0} - k_{||}v_{||0}\right)^2 =$$

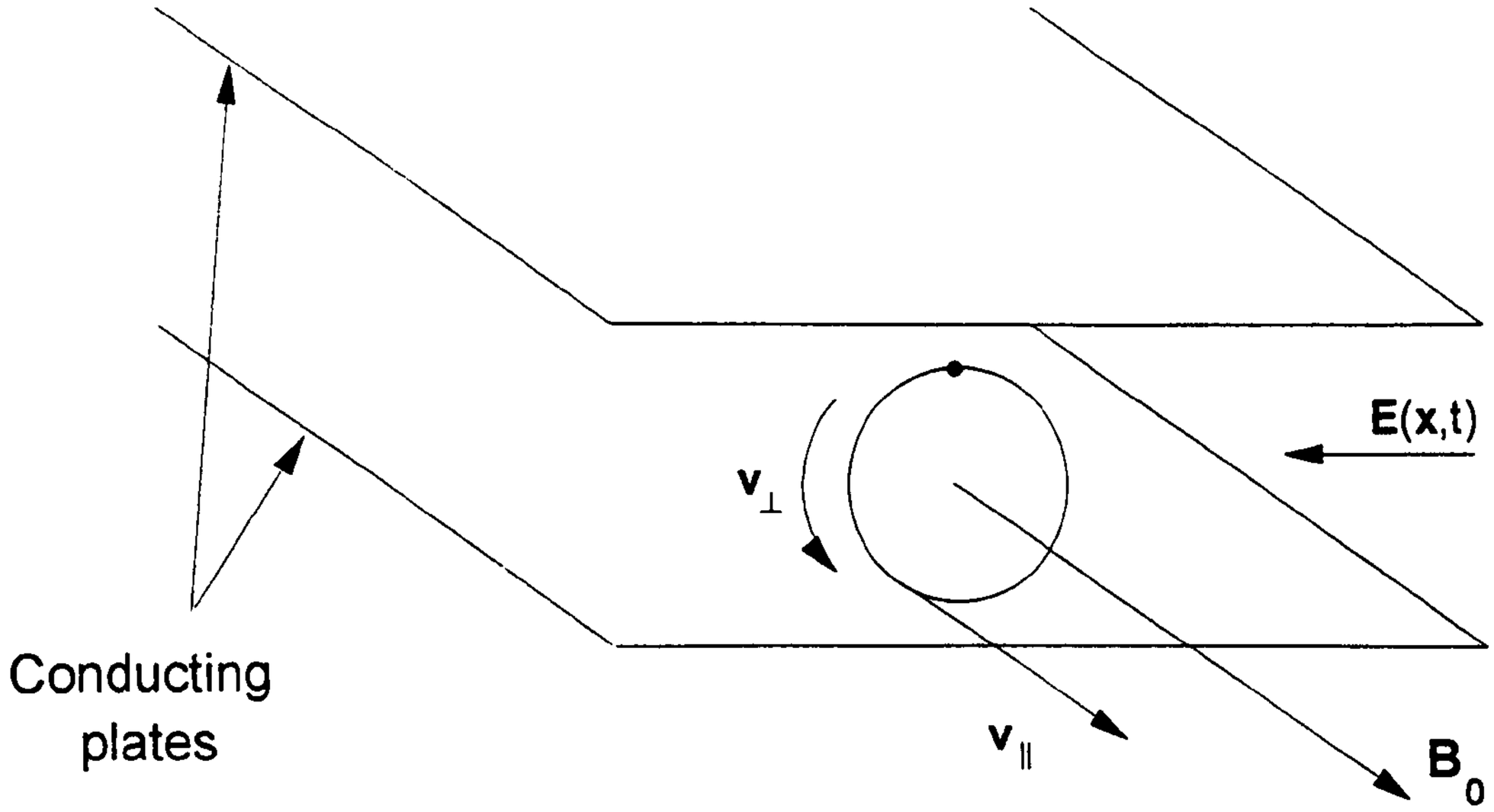

Figure 2.3: CRM interaction in planar geometry

$$-\frac{\omega_p^2 k_\perp^2 v_{\perp 0}^2}{\gamma_0 K_{mn}} \left[H_{sm} - \left(\omega - s\frac{\omega_c}{\gamma_0} - k_{||} v_{||0} \right) \frac{s\omega_c}{\gamma_0 v_{\perp 0}^2 k_\perp^2} Q_{sm} \right] \qquad (2.20)$$

where $K_{mn} = J_m^2(k_\perp R_w)\left(1 - \dfrac{m^2}{k_\perp^2 R_w^2}\right)$

$$H_{sm} = \left(J_{s-m}(k_\perp R_0) J_s'(k_\perp r_L)\right)^2$$

$$Q_{sm} = 2H_{sm} + k_\perp r_L \left[\begin{array}{ll} & J_{s-m}^2(k_\perp R_0) J_s'(k_\perp r_L) J_s''(k_\perp r_L) \\ + & \frac{1}{2} J_{s-m-1}^2(k_\perp R_0) J_s'(k_\perp r_L) J_{s-1}'(k_\perp r_L) \\ - & \frac{1}{2} J_{s-m}^2(k_\perp R_0) J_s'(k_\perp r_L) J_s''(k_\perp r_L) \\ + & \frac{1}{2} J_{s-m+1}^2(k_\perp R_0) J_s'(k_\perp r_L) J_{s+1}'(k_\perp r_L) \end{array} \right].$$

where R_0 is the guiding centre radius and r_L is the Larmor radius of the electrons.

The first term on the RHS of (2.20) has a destabilising effect and the second has a stabilising effect. This stabilising term places a lower limit on the transverse energy of the beam below which no instability will occur. If it assumed that the interaction takes place at the fundamental cyclotron harmonic ($s = 1$) and

$k_\perp r_L \ll 1$, the constants H_{sm} and Q_{sm} simplify considerably to

$$H_{1m} \approx \frac{1}{4} J_{m-1}^2(k_\perp R_0)$$

$$Q_{1m} \approx \frac{1}{2} J_{m-1}^2(k_\perp R_0)$$

and the threshold condition can be written as

$$v_{\perp 0}^4 > \frac{4}{27} \frac{\omega_p^2 \omega_c^3 v_{\|0} J_{m-1}^2(k_\perp R_0)}{k_\perp^4 k_\| \gamma_0^4 c^2 J_m^2(k_\perp R_w) \left(1 - \frac{m^2}{k_\perp^2 R_w^2}\right)} \tag{2.21}$$

It will be shown in chapters 3 and 4 that this threshold is due to depletion of the transverse momentum of the electron beam. Far from this threshold, the spatial growth rate of the interaction is just that obtained from fluid theory (2.17).

2.5 Nonlinear Theory

Although a linear theory is sufficient to ascertain whether instability will occur and what the growth rate of the instability will be, in order to calculate or estimate accurately quantities such as the maximum electromagnetic power which can be produced by the system, a nonlinear theory is required.

Among the first nonlinear analyses of the CRM interaction was that of Sprangle and Drobot [51], which studied the temporal evolution of the interaction between electrons in a sheet electron beam and an electromagnetic wave in a planar waveguide in a reference frame moving at the electron longitudinal velocity. After analysing the linear regime of the interaction using a plasma kinetic approach, the nonlinear evolution of the interaction was studied. The saturation of the interaction was found to depend critically on how far the unstable system was above the threshold (2.21), resulting in two different types of saturation. Close to the

threshold, the electromagnetic field intensity would increase at the expense of the transverse electron energy until the instability threshold was no longer satisfied, and wave growth was halted. Far above the threshold, however, the saturation of the instability was found to be due to the electrons bunching in phase until no further bunching was possible. The electrons then began to debunch, absorbing energy from the radiation field and saturating the instability. These saturation mechanisms will be discussed in more detail in section 3.4.

Most of the nonlinear analyses of CRM-type devices involve the simultaneous solution of the Lorentz equation of motion with Maxwell's equations. Depending on the particular system being studied, certain approximations can be made to simplify the equations, but the result is always a set of coupled nonlinear differential equations which are then numerically integrated. In a full three-dimensional analysis, it is necessary to simultaneously solve five equations for each (macro)electron involved in the integration, one each for the phase difference between the electron and the wave, transverse momentum, axial momentum, and the co-ordinates of the guiding centre (R_0, θ_0) [57, 58]. Although a full three-dimensional analysis is useful, it requires a large amount of computation and does not readily lend itself to a basic understanding of the physical processes occurring in the interaction. Full three dimensional analyses are usually used in the design of specific devices with a given set of design parameters.

In order to obtain a general understanding of the physics involved in the nonlinear regime of the interaction, the large number of equations used in a three-dimensional analysis has to be reduced using various assumptions, e.g. that the

guiding centres of the electrons remain approximately stationary. This approach has been used by Bratman *et al.* [19] resulting in a set of $2N$ differential equations, which describe the evolution of the energy and the phase difference between the electron and the wave, for N particles undergoing an interaction with a mode of a high diffraction-Q cavity. The high-Q factor of the cavity means that the axial structure of the mode will be determined by the shape of the cavity rather than the motion of the electrons, removing the need to solve Maxwell's wave equation i.e. the electron and field evolution equations are not solved self-consistently. The power output from the cavity is found by calculating the power lost by the electrons at the end of the interaction region. The CRM amplifier has also been studied in this way [59], but Maxwell's wave equation must also be solved for this case, as the motion of the electrons acts as the source term for the generation of the electromagnetic field i.e. a self-consistent calculation is required. This results in the number of differential equations to be solved being increased by two (field amplitude and phase) if the field is assumed to be evolving slowly or four (field amplitude, phase and first derivatives) if not.

A slightly different approach to the nonlinear analysis of the CRM interaction which has been applied to the case of a high-Q oscillator operating close to cutoff is that employed by Nusinovich [60] [62], which involves assuming that the evolution of the mode amplitude and phase in the cavity is small in the time taken for the electrons to cross the interaction region. A set of 'slow' equations can then be derived describing the evolution of the mode amplitude and phase on a time scale much longer than the transit time. This method has been used to describe

multimode effects, such as the growth of parasitic modes [60, 61] and parametric effects [62].

2.6 Conclusions

A brief description of some of the theoretical methods used to study the CRM interaction has been given in this chapter. Some, such as the quantum mechanical analysis, are now only of historical interest, while others, such as three-dimensional numerical simulation, are tailored towards an engineering approach to device design rather than physical investigation. It will be shown in the following chapters however, that there is scope for further theoretical investigation of the physical processes involved in the CRM interaction.

Chapter 3

Universally Scaled Evolution Equations

3.1 Introduction

Starting from the Lorentz equation of motion for an electron in an electromagnetic field and Maxwell's equations, it is possible to derive a set of universally scaled equations which describe the linear and nonlinear interaction of a beam of relativistic electrons with a TE or TM waveguide mode. A universal scaling of the evolution equations reduces the number of free parameters and hence the number of solutions to a minimum. In addition, a truly universal scaling should be based on *physically significant* quantities e.g. growth rates etc. The universally scaled set of equations considerably simplify both the analysis of the interaction and the physical interpretation of results.

3.2 TE Mode Interaction

The cylindrical components of the electric (**E**) and magnetic (**B**) field of a TE_{mn} cold cylindrical waveguide mode are

$$E_r = -\frac{m}{2r}F(z)D_{TE}J_m(k_\perp r)e^{i(\omega t-m\theta)} + c.c. \quad (3.1)$$

$$E_\theta = \frac{ik_\perp}{2}F(z)D_{TE}J'_m(k_\perp r)e^{i(\omega t-m\theta)} + c.c. \quad (3.2)$$

$$E_z = 0 \quad (3.3)$$

$$B_r = \frac{k_\perp}{2\omega}\frac{dF(z)}{dz}D_{TE}J'_m(k_\perp r)e^{i(\omega t-m\theta)} + c.c. \quad (3.4)$$

$$B_\theta = -\frac{im}{2r\omega}\frac{dF(z)}{dz}D_{TE}J_m(k_\perp r)e^{i(\omega t-m\theta)} + c.c. \quad (3.5)$$

$$B_z = \frac{k_\perp^2}{2\omega}F(z)D_{TE}J_m(k_\perp r)e^{i(\omega t-m\theta)} + c.c. \quad (3.6)$$

where: $D_{TE} = \left(J_m\left(\chi'_{mn}\right)\sqrt{\pi(\chi'^2_{mn}-m^2)}\right)^{-1}$ is a mode dependent constant, χ'_{mn} is the nth root of $J'_m(k_\perp R_w) = 0$, ω is the radiation frequency, $k_\perp$ is the component of the wavevector perpendicular to the waveguide axis and (r,θ) are polar co-ordinates with respect to the waveguide axis as shown in figure 3.1. F(z) is a complex field amplitude with the dimensions of voltage and is of the form

$$F(z) = |F(z)|e^{-i(k_\parallel z-\xi(z))}$$

where $|F(z)|$ and $\xi(z)$ are slowly varying functions of z and $k_\parallel$ is the component of the wavevector parallel to the waveguide axis. The fact that $|F(z)|$ and $\xi(z)$ are slowly varying means that

$$\left|\frac{d\xi}{dz}\right| << k_\parallel \qquad \left|\frac{d|F|}{dz}\right| << k_\parallel|F|$$

with the result that

$$\frac{dF(z)}{dz} \approx -ik_\parallel F_s(z)e^{-ik_\parallel z}$$

where $F_s(z) = |F(z)|e^{i\xi(z)}$ is a slowly varying function of z. Substituting for F and dF/dz in terms of F_s in (3.1..3.6) gives

$$E_r = -\frac{m}{2r}F_s(z)D_{TE}J_m(k_\perp r)e^{i\Psi} + c.c. \quad (3.7)$$

$$E_\theta = \frac{ik_\perp}{2}F_s(z)D_{TE}J'_m(k_\perp r)e^{i\Psi} + c.c. \quad (3.8)$$

$$E_z = 0 \quad (3.9)$$

$$B_r = -\frac{k_\parallel}{\omega}E_\theta \quad (3.10)$$

$$B_\theta = \frac{k_\parallel}{\omega}E_r \quad (3.11)$$

$$B_z = \frac{k_\perp^2}{2\omega}F_s(z)D_{TE}J_m(k_\perp r)e^{i\Psi} + c.c. \quad (3.12)$$

where

$$\Psi = \omega t - m\theta - k_\parallel z \quad (3.13)$$

3.2.1 Electron Equations of Motion

Figure 3.1 shows the model used to describe the motion of an electron. The electron gyrates about the guiding centre (R_0, θ_0) with momentum both perpendicular and parallel to the waveguide axis. Note that in the absence of any interaction of the electron with an electromagnetic wave, the guiding centre position, momentum and cyclotron frequency of the electron will all be constant. It is assumed that when an electromagnetic wave is also present, these quantities vary slowly i.e. they vary on a timescale large compared to the cyclotron period $2\pi\gamma/\omega_c$. Using complex notation, the transverse position of the electron

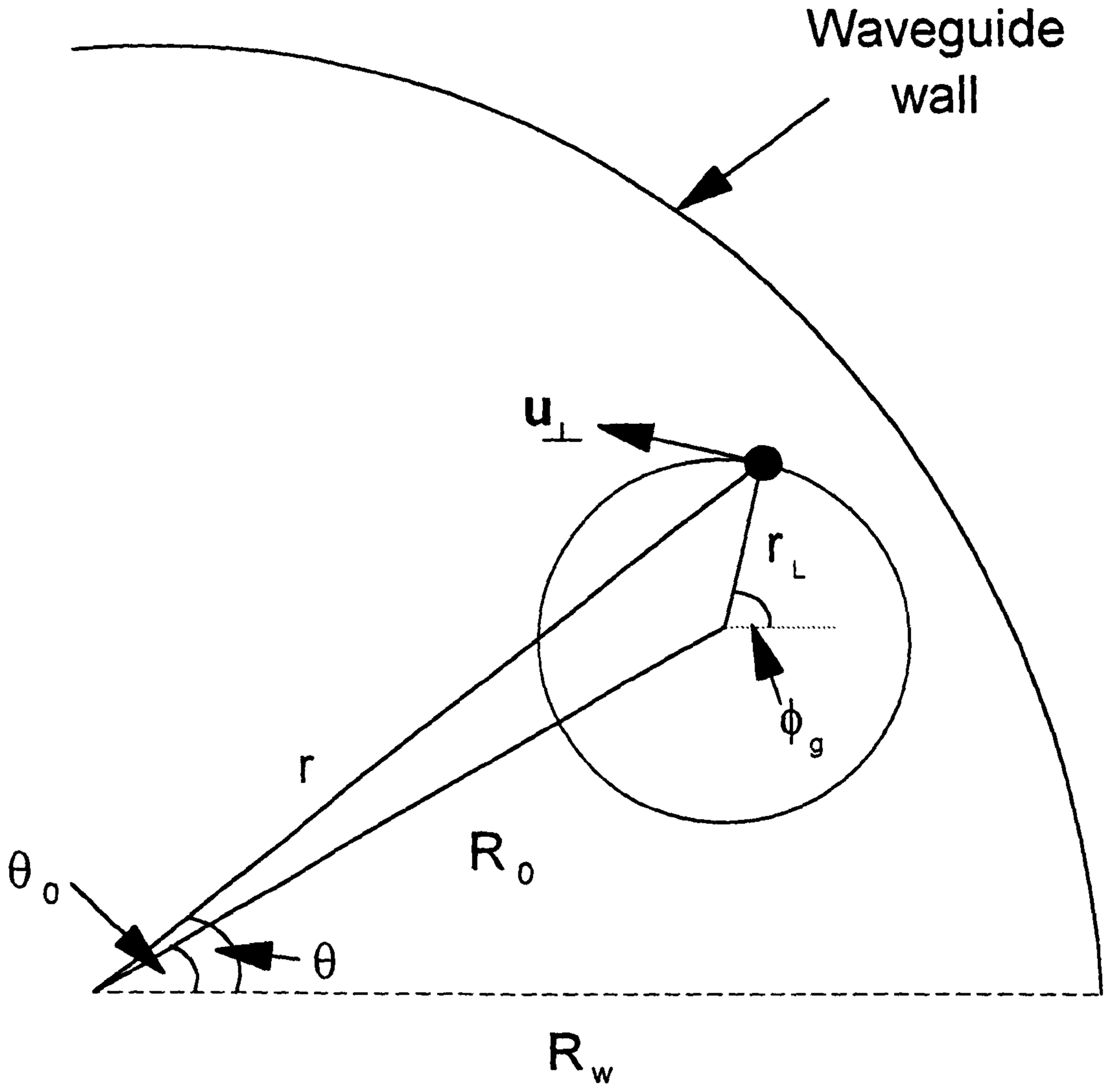

Figure 3.1: Diagram of an electron orbit

is represented by

$$\mathbf{r}_\perp = re^{i\theta} = R_0 e^{i\theta_0} + r_L e^{i\phi_g}$$

where r_L is the Larmor radius of the electron orbit, and ϕ_g is the electron gyro-angle which is defined as

$$\phi_g = \frac{\pi}{2} - \tan^{-1}\left(\frac{u_x}{u_y}\right) \tag{3.14}$$

where $\mathbf{u} = (\mathbf{u}_\perp, u_\parallel) = \gamma\mathbf{v}$, $\mathbf{v}$ is the electron velocity and γ is the relativistic factor. The perpendicular component $\mathbf{u}_\perp$ can be written in complex notation as

$$\mathbf{u}_\perp = u_x + iu_y = iu_\perp e^{i\phi_g} \tag{3.15}$$

where (3.14) has been used and $u_\perp = |\mathbf{u}_\perp|$. It is assumed from here on that the guiding centre co-ordinates remain approximately constant for any given electron, as they play no significant role in the CRM interaction. Motion of the guiding centre in a radially non-uniform electromagnetic field can itself cause amplification of an electromagnetic wave. An example of a device which employs this gain mechanism is the peniotron [47].

The Lorentz equation of motion for an electron in both electric and magnetic fields is

$$\frac{d\mathbf{u}}{dt} = \frac{u_\parallel}{\gamma}\frac{d\mathbf{u}}{dz} = -\frac{e}{m_e}\left(\mathbf{E} + \frac{\mathbf{u}\times\mathbf{B}}{\gamma}\right) \tag{3.16}$$

where e is the magnitude of the electron charge and m_e is the rest mass of the electron. The interaction length z is used here as the independent variable. Splitting this equation into perpendicular and parallel components gives

$$\frac{d\mathbf{u}_\perp}{dz} = -\frac{e}{m_e}\frac{\gamma}{u_\parallel}\left(\mathbf{E}_\perp + \frac{1}{\gamma}(\mathbf{u}\times\mathbf{B})_\perp\right) \tag{3.17}$$

$$\frac{du_\parallel}{dz} = -\frac{e}{m_e}\frac{1}{u_\parallel}(\mathbf{u}\times\mathbf{B})_\parallel \tag{3.18}$$

as $E_{||} = E_z = 0$ for a TE_{mn} waveguide mode.

Analagous with (3.15),

$$\mathbf{E}_\perp = E_x + iE_y \quad , E_{||} = 0 \tag{3.19}$$

$$\mathbf{B}_\perp = B_x + iB_y \quad , B_{||} = B_0 + B_z \tag{3.20}$$

where B_0 is the static magnetic field. It is now possible to write the perpendicular component of the Lorentz equation as two equations

$$u_\perp \frac{d\phi_g}{dz} = \frac{e\gamma}{u_{||} m_e} \left(\begin{array}{l} E_x \cos\phi_g + E_y \sin\phi_g + \frac{u_\perp}{\gamma}(B_0 + B_z) \\ + \quad \frac{u_{||}}{\gamma}(B_x \sin\phi_g - B_y \cos\phi_g) \end{array} \right) \tag{3.21}$$

$$\frac{du_\perp}{dz} = -\frac{e\gamma}{u_{||} m_e} \left(\begin{array}{l} -E_x \sin\phi_g + E_y \cos\phi_g \\ + \quad \frac{u_{||}}{\gamma}(B_x \cos\phi_g + B_y \sin\phi_g) \end{array} \right) \tag{3.22}$$

and the parallel component of the Lorentz equation as

$$\frac{du_{||}}{dz} = \frac{e}{m_e} \frac{u_\perp}{u_{||}} (B_y \sin\phi_g + B_x \cos\phi_g) \tag{3.23}$$

where (3.15) has been used and E_x, E_y, B_x and B_y are found using the relations

$$\left\{ \begin{array}{c} E_x \\ B_x \end{array} \right\} = \left\{ \begin{array}{c} E_r \\ B_r \end{array} \right\} \cos\theta - \left\{ \begin{array}{c} E_\theta \\ B_\theta \end{array} \right\} \sin\theta \tag{3.24}$$

$$\left\{ \begin{array}{c} E_y \\ B_y \end{array} \right\} = \left\{ \begin{array}{c} E_r \\ B_r \end{array} \right\} \sin\theta + \left\{ \begin{array}{c} E_\theta \\ B_\theta \end{array} \right\} \cos\theta. \tag{3.25}$$

which lead to

$$E_x = -k_\perp |F(z)| D_{TE} \times$$

$$\left(\frac{m}{k_\perp r} J_m(k_\perp r) \cos(\Psi + \xi) \cos\theta - J'_m(k_\perp r) \sin(\Psi + \xi) \sin\theta \right)$$

$$E_y = -k_\perp |F(z)| D_{TE} \times$$

$$\left(\frac{m}{k_\perp r}J_m(k_\perp r)\cos(\Psi+\xi)\sin\theta + J'_m(k_\perp r)\sin(\Psi+\xi)\cos\theta\right)$$

$$B_x = \frac{k_\perp k_\parallel}{\omega}|F(z)|D_{TE}\times$$

$$\left(\frac{m}{k_\perp r}J_m(k_\perp r)\cos(\Psi+\xi)\sin\theta + J'_m(k_\perp r)\sin(\Psi+\xi)\cos\theta\right)$$

$$B_y = -\frac{k_\perp k_\parallel}{\omega}|F(z)|D_{TE}\times$$

$$\left(\frac{m}{k_\perp r}J_m(k_\perp r)\cos(\Psi+\xi)\cos\theta - J'_m(k_\perp r)\sin(\Psi+\xi)\sin\theta\right).$$

Using the Bessel function relations

$$\frac{m}{x}J_m(x) = \frac{1}{2}(J_{m-1}(x)+J_{m+1}(x)) \tag{3.26}$$

$$J'_m(x) = \frac{1}{2}(J_{m-1}(x)-J_{m+1}(x)) \tag{3.27}$$

then these equations can be further reduced to

$$E_x = \frac{k_\perp|F(z)|D_{TE}}{2}\times$$

$$(J_{m-1}(k_\perp r)\cos(\Psi+\theta+\xi)+J_{m+1}(k_\perp r)\cos(\Psi-\theta+\xi))$$

$$E_y = \frac{k_\perp|F(z)|D_{TE}}{2}\times$$

$$(J_{m-1}(k_\perp r)\sin(\Psi+\theta+\xi)-J_{m+1}(k_\perp r)\sin(\Psi-\theta+\xi))$$

$$B_x = \frac{k_\perp k_\parallel}{2\omega}|F(z)|D_{TE}\times$$

$$(J_{m-1}(k_\perp r)\sin(\Psi+\theta+\xi)-J_{m+1}(k_\perp r)\sin(\Psi-\theta+\xi))$$

$$B_y = -\frac{k_\perp k_\parallel}{2\omega}|F(z)|D_{TE}\times$$

$$(J_{m-1}(k_\perp r)\cos(\Psi+\theta+\xi)+J_{m+1}(k_\perp r)\cos(\Psi-\theta+\xi))$$

The equation for B_z is

$$B_z = \frac{k_\perp^2}{\omega}|F(z)|D_{TE}J_m(k_\perp r)\cos(\Psi+\xi)$$

Substituting for E_x,E_y,B_x,B_y and B_z in the equations of motion (3.21),(3.22) and (3.23) results in the following equations of motion :

$$\frac{d\phi_g}{dz} = \frac{e\gamma}{u_\perp u_{||} m_e} \times \tag{3.28}$$

$$\left[\begin{array}{l} \frac{k_\perp D_{TE}|F(z)|}{2}\left(\frac{k_{||}u_{||}}{\omega\gamma}-1\right)\left(\begin{array}{rl} & J_{m-1}(k_\perp r)\cos(\Psi+\theta-\phi_g+\xi) \\ + & J_{m+1}(k_\perp r)\cos(\Psi-\theta+\phi_g+\xi) \end{array} \right) \\ + \frac{u_\perp}{\gamma}\frac{k_\perp^2}{\omega}|F(z)|D_{TE}J_m(k_\perp r)\cos(\Psi+\xi) \\ + \frac{u_\perp B_0}{\gamma} \end{array} \right]$$

$$\frac{du_\perp}{dz} = -\frac{e\gamma}{u_{||}m_e}\frac{k_\perp D_{TE}|F(z)|}{2}\left(\frac{k_{||}u_{||}}{\omega\gamma}-1\right)\times \tag{3.29}$$

$$\left(\begin{array}{rl} & J_{m-1}(k_\perp r)\sin(\Psi+\theta-\phi_g+\xi) \\ - & J_{m+1}(k_\perp r)\sin(\Psi-\theta+\phi_g+\xi) \end{array} \right)$$

$$\frac{du_{||}}{dz} = \frac{eu_\perp}{m_e u_{||}}\frac{k_\perp k_{||}}{2\omega}|F(z)|D_{TE}\left(\begin{array}{rl} & J_{m-1}(k_\perp r)\sin(\Psi+\theta-\phi_g+\xi) \\ - & J_{m+1}(k_\perp r)\sin(\Psi-\theta+\phi_g+\xi) \end{array} \right) \tag{3.30}$$

$$\frac{dt}{dz} = \frac{\gamma}{u_{||}} \tag{3.31}$$

where the evolution equation for t has also been given. The next stage in the analysis involves the use of Graf's addition theorem [63], which in its general form states that

$$J_m(w)\left\{ \begin{array}{l} \cos m\chi \\ \\ \sin m\chi \end{array} \right\} = \sum_{n=-\infty}^{\infty} J_{m+n}(u)J_n(v)\left\{ \begin{array}{l} \cos n\alpha \\ \\ \sin n\alpha \end{array} \right\} \tag{3.32}$$

where

$$w^2 = u^2+v^2-2uv\cos\alpha$$

$$u - v\cos\alpha = w\cos\alpha$$

$$v\sin\alpha = w\sin\chi$$

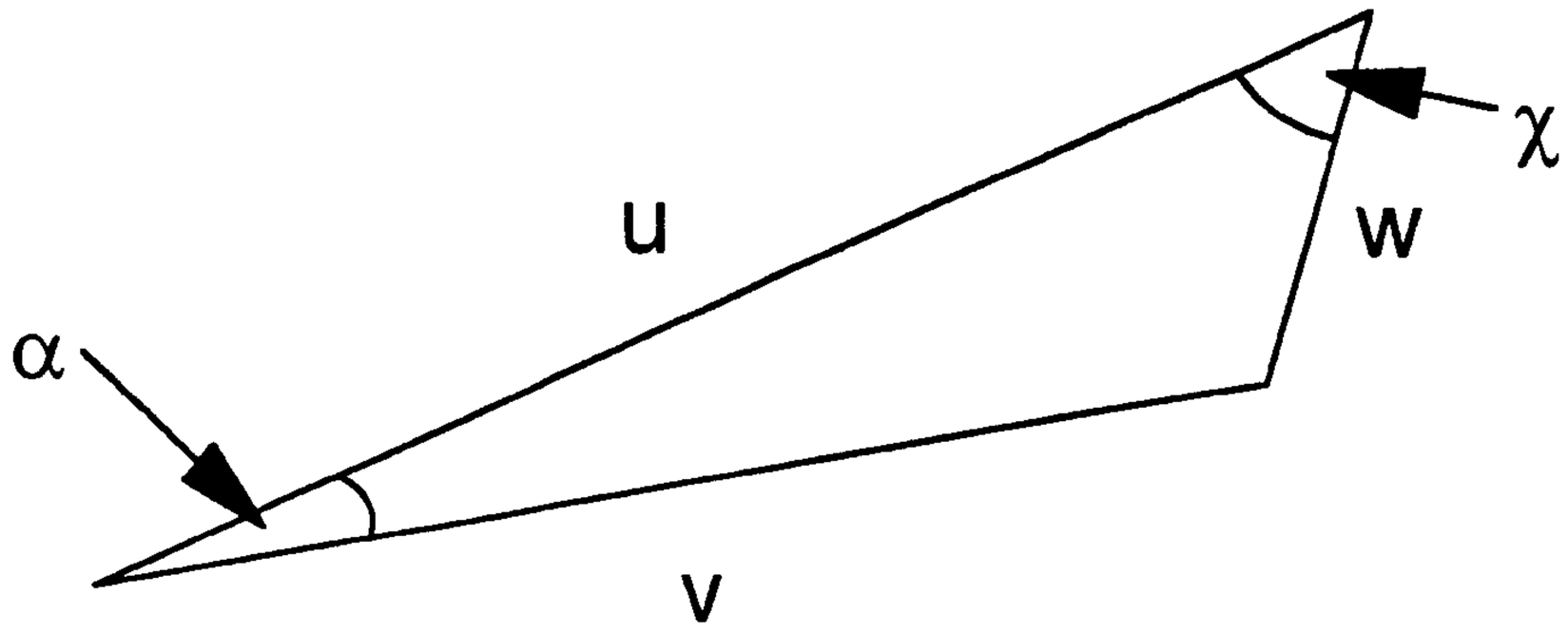

Figure 3.2: Graf's addition theorem

and w,u,v,α and χ are defined in figure 3.2. From a comparison of figure 3.2 and figure 3.1, it can be seen that

$$w = k_\perp r, \quad u = k_\perp R_0, \quad v = k_\perp r_L$$

$$\alpha = \pi - \phi_g + \theta_0$$

$$\chi = \theta - \theta_0$$

Equation (3.32), written in complex form, becomes

$$J_m(k_\perp r)e^{im\chi} = \sum_{n=-\infty}^{\infty} J_{m+n}(k_\perp R_0)J_n(k_\perp r_L)e^{in\alpha}$$

Expanding α and χ, the complex conjugate of this is

$$\begin{aligned} J_m(k_\perp r)e^{-im\theta} &= \sum_{n=-\infty}^{\infty} J_{m+n}(k_\perp R_0)J_n(k_\perp r_L)e^{-in\pi}e^{in\phi_g}e^{-i(m+n)\theta_0} \\ &= \sum_{n=-\infty}^{\infty} (-1)^n J_{m+n}(k_\perp R_0)J_n(k_\perp r_L)e^{in\phi_g}e^{-i(m+n)\theta_0} \end{aligned} \quad (3.33)$$

Similarly,

$$\begin{aligned} J_{m-1}(k_\perp r)e^{-i(m-1)\theta} &= \sum_{n=-\infty}^{\infty} (-1)^n J_{m+n-1}(k_\perp R_0)J_n(k_\perp r_L)e^{in\phi_g}e^{-i(m+n-1)\theta_0} \\ J_{m+1}(k_\perp r)e^{-i(m+1)\theta} &= \sum_{n=-\infty}^{\infty} (-1)^n J_{m+n+1}(k_\perp R_0)J_n(k_\perp r_L)e^{in\phi_g}e^{-i(m+n+1)\theta_0} \end{aligned}$$

so

$$\begin{aligned} J_{m-1}(k_\perp r)e^{i(\Psi+\theta-\phi_g+\xi)} &= J_{m-1}(k_\perp r)e^{i(\omega t-(m-1)\theta-k_\parallel z-\phi_g+\xi)} \\ &= \sum_{n=-\infty}^{\infty} (-1)^n J_{m+n-1}(k_\perp R_0)J_n(k_\perp r_L)e^{i\Omega_-} \\ J_{m+1}(k_\perp r)e^{i(\Psi-\theta+\phi_g+\xi)} &= J_{m+1}(k_\perp r)e^{i(\omega t-(m+1)\theta-k_\parallel z+\phi_g+\xi)} \\ &= \sum_{n=-\infty}^{\infty} (-1)^n J_{m+n+1}(k_\perp R_0)J_n(k_\perp r_L)e^{i\Omega_+} \end{aligned}$$

where

$$\Omega_- = \omega t + (n-1)\phi_g - k_\parallel z - (m+n-1)\theta_0 + \xi \quad (3.34)$$

$$\Omega_+ = \omega t + (n+1)\phi_g - k_\parallel z - (m+n+1)\theta_0 + \xi \quad (3.35)$$

The real and imaginary parts of this pair of equations provide the terms used in the equations of motion (3.28..3.30) i.e.

$$\begin{aligned} J_{m-1}(k_\perp r)\cos(\Psi+\theta-\phi_g+\xi) &= \sum_{n=-\infty}^{\infty} (-1)^n J_{m+n-1}(k_\perp R_0)J_n(k_\perp r_L)\cos\Omega_- \\ J_{m-1}(k_\perp r)\sin(\Psi+\theta-\phi_g+\xi) &= \sum_{n=-\infty}^{\infty} (-1)^n J_{m+n-1}(k_\perp R_0)J_n(k_\perp r_L)\sin\Omega_- \end{aligned}$$

$$J_{m+1}(k_\perp r)\cos(\Psi-\theta+\phi_g+\xi) = \sum_{n=-\infty}^{\infty}(-1)^n J_{m+n+1}(k_\perp R_0)J_n(k_\perp r_L)\cos\Omega_+$$

$$J_{m+1}(k_\perp r)\sin(\Psi-\theta+\phi_g+\xi) = \sum_{n=-\infty}^{\infty}(-1)^n J_{m+n+1}(k_\perp R_0)J_n(k_\perp r_L)\sin\Omega_+$$

Substituting these terms in (3.28..3.30) gives

$$\frac{d\phi_g}{dz} = \frac{e\gamma}{u_\perp u_\parallel m_e}\times \tag{3.36}$$

$$\left[\begin{array}{l} \frac{k_\perp D_{TE}|F(z)|}{2}\left(\frac{k_\parallel u_\parallel}{\omega\gamma}-1\right)\left(\begin{array}{l}\sum_{n=-\infty}^{\infty}(-1)^n J_{m+n-1}(k_\perp R_0)J_n(k_\perp r_L)\cos\Omega_- \\ +\sum_{n=-\infty}^{\infty}(-1)^n J_{m+n+1}(k_\perp R_0)J_n(k_\perp r_L)\cos\Omega_+\end{array}\right) \\ +\frac{u_\perp}{\gamma}\frac{k_\perp^2}{\omega}|F(z)|D_{TE}\sum_{n=-\infty}^{\infty}(-1)^n J_{m+n}(k_\perp R_0)J_n(k_\perp r_L)\cos\Omega_0 \\ +\frac{u_\perp B_0}{\gamma}\end{array}\right]$$

$$\frac{du_\perp}{dz} = -\frac{e\gamma}{u_\parallel m_e}\frac{k_\perp D_{TE}|F(z)|}{2}\left(\frac{k_\parallel u_\parallel}{\omega\gamma}-1\right)\times \tag{3.37}$$

$$\left(\begin{array}{l}\sum_{n=-\infty}^{\infty}(-1)^n J_{m+n-1}(k_\perp R_0)J_n(k_\perp r_L)\sin\Omega_- \\ -\sum_{n=-\infty}^{\infty}(-1)^n J_{m+n+1}(k_\perp R_0)J_n(k_\perp r_L)\sin\Omega_+\end{array}\right)$$

$$\frac{du_\parallel}{dz} = \frac{eu_\perp}{m_e u_\parallel}\frac{k_\perp k_\parallel}{2\omega}|F(z)|D_{TE}\times$$

$$\left(\begin{array}{l}\sum_{n=-\infty}^{\infty}(-1)^n J_{m+n-1}(k_\perp R_0)J_n(k_\perp r_L)\sin\Omega_- \\ -\sum_{n=-\infty}^{\infty}(-1)^n J_{m+n+1}(k_\perp R_0)J_n(k_\perp r_L)\sin\Omega_+\end{array}\right) \tag{3.38}$$

where

$$\Omega_0 = \omega t + n\phi_g - k_\parallel z - (m+n)\theta_0 + \xi \tag{3.39}$$

As this analysis is concerned with evolution over a large number of cyclotron periods, these equations will now be averaged over a cyclotron period. In order to do this, the gyro-angle ϕ_g is split into a quickly varying part $\phi_g^{(f)}$ and a slowly

varying part $\phi_g^{(s)}$ i.e.

$$\phi_g = \phi_g^{(f)} + \phi_g^{(s)} \tag{3.40}$$

where $\phi_g^{(f)} = \omega_c t/\gamma_0$ and $\omega_c = eB_0/m_e$ is the nonrelativistic electron cyclotron frequency. Averaging over a cyclotron period involves integrating the equations of motion with respect to $\phi_g^{(f)}$ over the interval 0 to 2π. The slowly varying variables and their derivatives are assumed to remain approximately constant over this interval.

Consider equation (3.36) for $d\phi_g/dz$. Using the relation (3.40) this can be written as

$$\begin{aligned}
\frac{d\phi_g^{(s)}}{dz} &= \frac{\omega_c}{u_{||}}\left(1-\frac{\gamma}{\gamma_0}\right) + \frac{e\gamma}{u_\perp u_{||} m_e} \times \\
&\left[\frac{k_\perp D_{TE}|F(z)|}{2}\left(\frac{k_{||}u_{||}}{\omega\gamma}-1\right)\left(\sum_{n=-\infty}^{\infty} (-1)^n J_{m+n-1}(k_\perp R_0) J_n(k_\perp r_L)\cos\Omega_- \right.\right. \\
&\left.\left. + \sum_{n=-\infty}^{\infty} (-1)^n J_{m+n+1}(k_\perp R_0) J_n(k_\perp r_L)\cos\Omega_+ \right) \right. \\
&\left. + \frac{u_\perp}{\gamma}\frac{k_\perp^2}{\omega}|F(z)| D_{TE} \sum_{n=-\infty}^{\infty} (-1)^n J_{m+n}(k_\perp R_0) J_n(k_\perp r_L)\cos\Omega_0 \right]
\end{aligned}$$

where (3.34), (3.35) and (3.39) are now given by

$$\begin{aligned}
\Omega_- &= (\omega + (n-1)\frac{\omega_c}{\gamma_0})t - k_{||}z + (n-1)\phi_g^{(s)} - (m+n-1)\theta_0 + \xi \\
\Omega_+ &= (\omega + (n+1)\frac{\omega_c}{\gamma_0})t - k_{||}z + (n+1)\phi_g^{(s)} - (m+n+1)\theta_0 + \xi \\
\text{and } \Omega_0 &= (\omega + n\frac{\omega_c}{\gamma_0})t - k_{||}z + n\phi_g^{(s)} - (m+n)\theta_0 + \xi
\end{aligned}$$

When averaging this equation over a cyclotron period, it must be remembered that $u_\perp$, $u_{||}$, γ, $\phi_g^{(s)}$, $|F|$ and ξ are slowly varying by definition. In addition, it is assumed that the electrons and the wave are close to resonance at the sth

cyclotron harmonic i.e.

$$\omega - s\frac{\omega_c}{\gamma_0} - k_{||}v_{||} \approx 0 \tag{3.41}$$

This means that the quantity

$$(\omega - s\frac{\omega_c}{\gamma_0})t - k_{||}z = (\omega - s\frac{\omega_c}{\gamma_0} - k_{||}\frac{u_{||}}{\gamma})t$$

is also slowly varying. Therefore on averaging over a cyclotron period only the terms in the summation which have trigonometric arguments containing (3.41) will remain as the other terms will give rise to quickly varying terms which average to zero. Consequently, averaging the equations of motion (3.36..3.38) over a cyclotron period produces

$$\begin{aligned}
\frac{d\phi_g^{(s)}}{dz} &= \frac{\omega_c}{u_{||}}\left(1 - \frac{\gamma}{\gamma_0}\right) + \frac{e\gamma}{u_\perp u_{||} m_e} \times \\
&\left[- \frac{k_\perp D_{TE}|F(z)|}{2}\left(\frac{k_{||}u_{||}}{\omega\gamma} - 1\right)(-1)^{-s} J_{m-s}(k_\perp R_0) \times \right. \\
&\quad (J_{-s+1}(k_\perp r_L) + J_{-s-1}(k_\perp r_L))\cos(\phi + \xi) \\
&\left. + \frac{u_\perp}{\gamma}\frac{k_\perp^2}{\omega}|F(z)|D_{TE}(-1)^{-s} J_{m-s}(k_\perp R_0) J_{-s}(k_\perp r_L)\cos(\phi + \xi) \right]
\end{aligned} \tag{3.42}$$

$$\begin{aligned}
\frac{du_\perp}{dz} &= \frac{e\gamma}{u_{||}m_e}\frac{k_\perp D_{TE}|F(z)|}{2}\left(\frac{k_{||}u_{||}}{\omega\gamma} - 1\right)(-1)^{-s} J_{m-s}(k_\perp R_0) \times \\
&\quad (J_{-s+1}(k_\perp r_L) - J_{-s-1}(k_\perp r_L))\sin(\phi + \xi)
\end{aligned} \tag{3.43}$$

$$\begin{aligned}
\frac{du_{||}}{dz} &= -\frac{eu_\perp}{u_{||}m_e}\frac{k_\perp k_{||}}{2\omega} D_{TE}|F(z)|(-1)^{-s} J_{m-s}(k_\perp R_0) \times \\
&\quad (J_{-s+1}(k_\perp r_L) - J_{-s-1}(k_\perp r_L))\sin(\phi + \xi)
\end{aligned} \tag{3.44}$$

where the variable ϕ has been defined to be

$$\phi = (\omega - s\frac{\omega_c}{\gamma_0})t - k_{||}z - s\phi_g^{(s)} - (m - s)\theta_0 \tag{3.45}$$

Using the Bessel function relations (3.26) and (3.27), and the fact that

$$\frac{d\phi}{dz} = \frac{\gamma}{u_{||}}\left(\omega - \frac{\omega_c}{\gamma_0}\right) - k_{||} - s\frac{d\phi_g^{(s)}}{dz}$$

equations (3.42..3.44) can be further reduced to

$$\begin{aligned}
\frac{d\phi}{dz} &= \frac{\gamma}{u_{\|}}\left(\omega - s\frac{\omega_c}{\gamma} - \frac{k_{\|}u_{\|}}{\gamma}\right) \\
&- s\frac{e\gamma}{u_{\|}u_{\perp}m_e}J_{m-s}(k_{\perp}R_0)J_{-s}(k_{\perp}r_L)(-1)^s k_{\perp}D_{TE}|F(z)|\cos(\phi+\xi)\times \\
&\left[\frac{s}{k_{\perp}r_L}\left(\frac{k_{\|}u_{\|}}{\omega\gamma}-1\right)+\frac{u_{\perp}}{\gamma}\frac{k_{\perp}}{\omega}\right] \qquad (3.46)\\
\frac{du_{\perp}}{dz} &= -\frac{e\gamma}{u_{\|}m_e}k_{\perp}D_{TE}|F(z)|\left(\frac{k_{\|}u_{\|}}{\omega\gamma}-1\right)\times \\
&J_{m-s}(k_{\perp}R_0)J'_{-s}(k_{\perp}r_L)(-1)^s\sin(\phi+\xi) \qquad (3.47)\\
\frac{du_{\|}}{dz} &= \frac{eu_{\perp}}{u_{\|}m_e}\frac{k_{\perp}k_{\|}}{\omega}D_{TE}|F(z)|J_{m-s}(k_{\perp}R_0)J'_{-s}(k_{\perp}r_L)(-1)^s\sin(\phi+\xi) \qquad (3.48)
\end{aligned}$$

It is now assumed that the interaction is occuring close to the fundamental cyclotron resonance i.e. $s = 1$. Therefore

$$\begin{aligned}
\omega &\approx \frac{\omega_c}{\gamma} + k_{\|}\frac{u_{\|}}{\gamma} \\
\Rightarrow \frac{k_{\|}u_{\|}}{\omega\gamma} - 1 &\approx -\frac{\omega_c}{\gamma}.
\end{aligned}$$

In addition, it is assumed that the transverse variation of the electromagnetic mode amplitude is negligible over the electron gyro-orbit i.e.

$$k_{\perp}r_L << 1 \qquad (3.49)$$

This is an experimentally desirable condition as it allows the electron beam to be positioned on a maximum of the transverse mode profile, maximising the beam-wave coupling. This is more easily achieved for low order modes e.g. TE_{01} than high-order modes e.g.$TE_{22,6}$, where the transverse mode profile is highly complicated. The use of (3.49) allows the Bessel functions in (3.46..3.48), with $k_{\perp}r_L$ as their argument, to be replaced by the corresponding small argument expansions

$$J_{-1}(k_{\perp}r_L) \approx -\frac{1}{2}k_{\perp}r_L \qquad J'_{-1}(k_{\perp}r_L) \approx -\frac{1}{2}$$

The above approximations and the relation $u_\perp = \omega_c r_L$ allow the equations of motion (3.46..3.48) to be written as

$$\begin{aligned}
\frac{d\phi}{dz} &= \frac{\gamma}{u_\parallel}\left(\omega - \frac{\omega_c}{\gamma} - k_\parallel \frac{u_\parallel}{\gamma}\right) \\
&+ \frac{e\omega_c}{2u_\perp u_\parallel m_e \omega} k_\perp D_{TE} |F(z)| J_{m-1}(k_\perp R_0) \cos(\phi + \xi) \qquad (3.50) \\
\frac{du_\perp}{dz} &= \frac{e\omega_c}{2m_e u_\parallel \omega} k_\perp |F(z)| D_{TE} J_{m-1}(k_\perp R_0) \sin(\phi + \xi) \qquad (3.51) \\
\frac{du_\parallel}{dz} &= \frac{eu_\perp}{2m_e u_\parallel \omega} k_\perp k_\parallel |F(z)| D_{TE} J_{m-1}(k_\perp R_0) \sin(\phi + \xi) \qquad (3.52)
\end{aligned}$$

These equations constitute the electron equations of motion for a slowly varying interaction between a relativistic electron gyrating in a static magnetic field and a TE_{mn} waveguide mode at the fundamental cyclotron harmonic in the limit $k_\perp r_L << 1$.

3.2.2 The Electromagnetic Field Evolution Equation

The electromagnetic field evolution equation is derived here for the case of a single TE_{mn} waveguide mode. The field evolution is described by Maxwell's wave equation

$$\left(\nabla^2 - \frac{1}{c^2}\frac{\partial^2}{\partial t^2}\right)\mathbf{E}(\mathbf{r},t) = \mu_0 \frac{\partial \mathbf{J}(\mathbf{r},t)}{\partial t} + \nabla\left(\nabla.\mathbf{E}(\mathbf{r},t)\right)$$

For a TE_{mn} mode, $E_z = 0$, so

$$\left(\nabla^2 - \frac{1}{c^2}\frac{\partial^2}{\partial t^2}\right)\mathbf{E}_\perp(\mathbf{r},t) = \mu_0 \frac{\partial \mathbf{J}_\perp(\mathbf{r},t)}{\partial t} - e\nabla_\perp\left(\frac{n_e}{\epsilon_0}\right) \qquad (3.53)$$

where n_e is the electron number density.

It can be seen from (3.7) and (3.8) that the electric field can be expressed as

$$\mathbf{E}_\perp(\mathbf{r},t) = \Re\left(\tilde{\mathbf{E}}_\perp(\mathbf{r})e^{i(\omega t - k_\parallel z)}\right) = \frac{1}{2}\left(\tilde{\mathbf{E}}_\perp(\mathbf{r})e^{i(\omega t - k_\parallel z)} + c.c.\right) \qquad (3.54)$$

where $\tilde{\mathbf{E}}_\perp = F_s(z,t)\mathbf{e}_{mn}$, $\mathbf{e}_{mn} = e_r\hat{\mathbf{i}}_r + e_\theta\hat{\mathbf{i}}_\theta$ and

$$e_r = -\frac{m}{r}D_{TE}J_m(k_\perp r)e^{-im\theta} \tag{3.55}$$

$$e_\theta = ik_\perp D_{TE}J'_m(k_\perp r)e^{-im\theta} \tag{3.56}$$

where $\hat{\mathbf{i}}_r$ and $\hat{\mathbf{i}}_\theta$ are unit vectors in the radial and azimuthal direction respectively such that $\hat{\mathbf{i}}_r$, $\hat{\mathbf{i}}_\theta$ and $\hat{\mathbf{i}}_z$ form a right hand set. The complex field amplitude $F_s(z,t)$ describes a slowly varying pulse envelope such that

$$\left|\frac{\partial F_s(z,t)}{\partial t}\right| \ll |\omega F_s(z,t)| \tag{3.57}$$

$$\left|\frac{\partial F_s(z,t)}{\partial z}\right| \ll |k_\parallel F_s(z,t)| \tag{3.58}$$

$$\tag{3.59}$$

and the quantities $\mathbf{e}_{mn}$ are orthogonal mode vectors i.e.

$$\int \mathbf{e}_{mn}.\mathbf{e}^*_{m'n'}dA = \delta_{mm'}\delta_{nn'}$$

where the integration is over the cross-sectional area of the waveguide and δ_{pq} is a Kronecker delta. In addition, the transverse mode vectors satisfy the Helmholtz equation

$$\left(\nabla_\perp^2 + k_\perp^2\right)\mathbf{e}_{mn}(r,\theta) = 0. \tag{3.60}$$

If (3.53) is multiplied by $e^{-i\omega t}$ and integrated over ωt from $0 \rightarrow 2\pi$ then

$$\pi\left(\nabla^2 - \frac{1}{c^2}\frac{\partial^2}{\partial t^2}\right)F_s(z,t)e^{-ik_\parallel z}\mathbf{e}_{mn} \approx \mu_0\int_0^{2\pi}\frac{\partial \mathbf{J}_\perp(\mathbf{r},t)}{\partial t}e^{-i\omega t}\,d(\omega t)$$

where the transverse derivative of the electron density has been neglected. The RHS of this expression can be simplified by integrating by parts, assuming that $\mathbf{J}_\perp(\mathbf{r},t)$ is periodic in ωt with period 2π. The resulting equation is

$$\left(\nabla^2 - \frac{1}{c^2}\frac{\partial^2}{\partial t^2}\right)F_s(z,t)e^{-ik_\parallel z}\mathbf{e}_{mn} \approx i\mu_0\omega\int_0^{2\pi}\mathbf{J}_\perp(\mathbf{r},t)e^{-i\omega t}\,d(\omega t). \tag{3.61}$$

The LHS of (3.61) can be simplified using the fact that $F_s(z,t)$ is a slowly varying function. This means that

$$\left(\frac{\partial^2}{\partial z^2} - \frac{1}{c^2}\frac{\partial^2}{\partial t^2}\right) F_s(z,t)e^{i(\omega t - k_\parallel z)} \approx$$
$$\left[-2ik_\parallel\left(\frac{\partial}{\partial z} + \frac{\omega}{k_\parallel c^2}\frac{\partial}{\partial t}\right) + \left(\frac{\omega^2}{c^2} - k_\parallel^2\right)\right] F_s(z,t)e^{i(\omega t - k_\parallel z)} \qquad (3.62)$$

so using (3.60) and the fact that the dispersion relation for a cold cavity waveguide mode is

$$\frac{\omega^2}{c^2} = k_\perp^2 + k_\parallel^2 \qquad (3.63)$$

the LHS of (3.61) can be written as

$$\pi\left(\nabla^2 - \frac{1}{c^2}\frac{\partial^2}{\partial t^2}\right) F_s(z,t)e^{-ik_\parallel z}\mathbf{e}_{mn} \approx -2\pi ik_\parallel\left(\frac{\partial}{\partial z} + \frac{1}{v_g}\frac{\partial}{\partial t}\right) F_s(z,t)e^{-ik_\parallel z}\mathbf{e}_{mn} \qquad (3.64)$$

where $v_g = k_\parallel c^2/\omega$ is the group velocity of the waveguide mode. If the independent variables are now transformed using

$$z' = z \quad , \quad t' = t - \frac{z}{v_\parallel} \qquad (3.65)$$

then the differential operator in the wave equation becomes

$$\left(\frac{\partial}{\partial z} + \frac{1}{v_g}\frac{\partial}{\partial t}\right) \rightarrow \frac{\partial}{\partial z'} - \frac{1}{v_g\beta}(1-\beta)\frac{\partial}{\partial t'} \qquad (3.66)$$

where $\beta = v_\parallel/v_g$.

The second term in (3.66), which gives rise to effects due to the relative propagation of the radiation with respect to the electrons, can be neglected if the velocity difference between the radiation and the electrons is not appreciable during the interaction. In this limit, only the space dependence is left in the

differential operator in (3.64) i.e.

$$\left(\frac{\partial}{\partial z}+\frac{1}{v_g}\frac{\partial}{\partial t}\right)\approx\frac{d}{dz} \tag{3.67}$$

so it is possible to follow the 'steady-state' evolution of the system as it moves through the interaction region. For now, and for the analysis of chapters 4 and 5, only the steady-state limit will be considered. The inclusion of propagation or slippage effects in the analysis of the CRM interaction will be described in chapter 6.

Performing scalar multiplication of (3.61) with $\mathbf{e}^*_{mn}$ after (3.62) and (3.67) have been applied, and integrating over the cross-sectional area gives

$$-2\pi i k_{\|}\frac{dF_s(z,t)}{dz}e^{-ik_{\|}z}=\frac{i\omega\mu_0}{\pi}\int_A\int_0^{2\pi}\mathbf{J}_\perp(\mathbf{r},t).\mathbf{e}^*(r,\theta)\,dA\,d(\omega t)$$

where the mode subscript has been dropped as only a single mode interaction is considered. The current density $\mathbf{J}_\perp(\mathbf{r},t)$ is represented by a collection of N electrons i.e.

$$\mathbf{J}_\perp(\mathbf{r},t)=-e\sum_{j=1}^{N}\mathbf{v}_{\perp j}(\mathbf{r},t)\delta(\mathbf{r}-\mathbf{r}_j)$$

so

$$\int_A\mathbf{J}_\perp(\mathbf{r},t).\mathbf{e}^*(r,\theta)\,dA=-e\sum_{j=1}^{N}\mathbf{v}_{\perp j}.\mathbf{e}^*(r_j,\theta_j)\delta(z-z_j).$$

The delta function in z can be rewritten as

$$\delta(z-z_j)=\frac{\delta(t-t_j)}{|\frac{dz}{dt_j}|}=\frac{\delta(t-t_j)}{v_{\|j}}=\frac{\omega}{v_{\|j}}\delta(\omega t-\omega t_j)$$

so multiplying both sides of (3.61) by $e^{ik_{\|}z}$ and rearranging reduces the full wave equation to a single differential equation for the slowly varying complex field amplitude $F_s(z,t)$,

$$\frac{dF_s}{dz}=\frac{\omega^2\mu_0 e}{2\pi k_{\|}}\sum_{j=1}^{N}\frac{\mathbf{v}_{\perp j}.\mathbf{e}^*(r_j,\theta_j)}{v_{\|j}}e^{-i(\omega t_j-k_{\|}z)}. \tag{3.68}$$

Each electron is considered to carry a partial current of

$$I_j = \frac{e\omega}{2\pi}$$

so the total current is represented by

$$I = \sum_{j=1}^{N} I_j = \frac{Ne\omega}{2\pi}$$

therefore (3.68) can be written as

$$\frac{dF_s}{dz} = \frac{\omega\mu_0 I}{k_{\|}} \left\langle \frac{\mathbf{v}_\perp . \mathbf{e}^*}{v_{\|}} e^{-i(\omega t - k_{\|} z)} \right\rangle \tag{3.69}$$

where $\langle ... \rangle \equiv \frac{1}{N} \sum_{j=1}^{N} (...)$.

All that remains now is to evaluate the $\mathbf{v}_\perp . \mathbf{e}^*$ term. Expressing $\mathbf{v}_\perp$ and $\mathbf{e}^*$ as

$$\mathbf{v}_\perp = v_r \hat{\mathbf{i}}_r + v_\theta \hat{\mathbf{i}}_\theta \qquad \mathbf{e} = e_r \hat{\mathbf{i}}_r + e_\theta \hat{\mathbf{i}}_\theta$$

where

$$v_r = v_x \cos\theta + v_y \sin\theta \quad , \quad v_\theta = -v_x \sin\theta + v_y \cos\theta$$

and e_r, e_θ are given by (3.55) and (3.56) respectively, the product $\mathbf{v}_\perp . \mathbf{e}^*$ becomes

$$\mathbf{v}_\perp . \mathbf{e}^* = k_\perp D_{TE} e^{im\theta} \left[\begin{array}{rl} & (v_x \cos\theta + v_y \sin\theta) \left(-\frac{m}{k_\perp r} J_m(k_\perp r) \right) \\ + & (-v_x \sin\theta + v_y \cos\theta) \left(-i J'_m(k_\perp r) \right) \end{array} \right] .$$

Using the fact that the velocity components can be written as

$$v_x = -|\mathbf{v}_\perp| \sin\phi_g \qquad v_y = |\mathbf{v}_\perp| \cos\phi_g$$

and the Bessel function relations (3.26) and (3.27) then

$$\mathbf{v}_\perp . \mathbf{e}^* e^{-i(\omega t - k_{\|} z)} = -\frac{i k_\perp D_{TE} |v_\perp|}{2} \left(J_{m-1} e^{-i(\Psi + \theta - \phi_g)} - J_{m+1} e^{-i(\Psi - \theta + \phi_g)} \right)$$

The application of Graf's theorem (3.32) to this expression results in the field evolution equation (3.69) becoming

$$\frac{dF_s(z)}{dz} = -\frac{i\omega\mu_0 I k_\perp D_{TE}}{2k_{||}} \times \left\langle \frac{|\mathbf{v}_\perp|}{v_{||}} \left(\begin{array}{l} \displaystyle\sum_{n=-\infty}^{\infty} (-1)^n J_{m+n-1}(k_\perp R_0) J_n(k_\perp r_L) e^{-i\Omega_-} \\ - \displaystyle\sum_{n=-\infty}^{\infty} (-1)^n J_{m+n+1}(k_\perp R_0) J_n(k_\perp r_L) e^{-i\Omega_+} \end{array} \right) \right\rangle \tag{3.70}$$

where Ω_- and Ω_+ are defined in (3.34) and (3.35). After averaging over a cyclotron period, and making use of (3.27) then (3.70) becomes

$$\frac{dF_s(z)}{dz} = -\frac{i\omega\mu_0 k_\perp D_{TE} J_{m-s}(k_\perp R_0)}{k_{||}} (-1)^{-s+1} \left\langle \frac{u_\perp}{u_{||}} J_s'(k_\perp r_L) e^{-i\phi} \right\rangle$$

where ϕ has been defined in (3.45). Using the conditions that $s = 1$ and $k_\perp r_L << 1$, the evolution equation for the complex field amplitude finally reduces to

$$\frac{dF_s(z)}{dz} = -\frac{i\omega\mu_0 k_\perp D_{TE} J_{m-1}(k_\perp R_0)}{2k_{||}} \left\langle \frac{u_\perp}{u_{||}} e^{-i\phi} \right\rangle$$

This is the steady-state evolution equation for the slowly varying complex amplitude of a TE_{mn} waveguide mode due to its interaction with a beam of relativistic electrons gyrating in a static magnetic field. The interaction is assumed to occur at the fundamental cyclotron harmonic and the transverse variation of the mode profile is assumed to be negligible over the gyro-orbit of the electrons.

3.2.3 Scaling the Evolution Equations

From the results of the two previous sections, the full set of electron and field evolution equations are

$$\frac{d\phi_j}{dz} = p_j + \frac{e\omega_c}{2u_{\perp j} u_{||j} m_e \omega} k_\perp D_{TE} |F(z)| J_{m-1}(k_\perp R_0) \cos(\phi_j + \xi) \tag{3.71}$$

$$\frac{du_{\perp j}}{dz} = \frac{e\omega_c}{2m_e u_{\|j}\omega} k_\perp |F(z)| D_{TE} J_{m-1}(k_\perp R_0) \sin(\phi_j + \xi) \quad (3.72)$$

$$\frac{du_{\|j}}{dz} = \frac{eu_{\perp j}}{2m_e u_{\|j}\omega} k_\perp k_\| |F(z)| D_{TE} J_{m-1}(k_\perp R_0) \sin(\phi_j + \xi) \quad (3.73)$$

$$\frac{dF_s(z)}{dz} = -\frac{i\omega\mu_0 k_\perp D_{TE} J_{m-1}(k_\perp R_0)}{2k_\|} \left\langle \frac{u_\perp}{u_\|} e^{-i\phi} \right\rangle \quad (3.74)$$

where

$$\phi_j = \omega t_j - k_\| z + \tan^{-1}\left(\frac{u_y}{u_x}\right) - (m-1)\theta_0 - \frac{\pi}{2} \quad (3.75)$$

$$p_j = \frac{\gamma_j \omega}{u_{\|j}} - \frac{\omega_c}{u_{\|j}} - k_\| \quad (3.76)$$

$$\text{and } j = 1..N \quad (3.77)$$

In order to find dp/dz, it is necessary to find $d\gamma/dz$. This is achieved using the relation

$$\gamma = \sqrt{1 + \frac{u_\perp^2}{c^2} + \frac{u_\|^2}{c^2}}$$

and the equations (3.51) and (3.52). The result is

$$\frac{d\gamma}{dz} = \frac{ek_\perp u_\perp}{2m_e c^2} \frac{u_\perp}{u_\|} |F(z)| D_{TE} J_{m-1}(k_\perp R_0) \sin(\phi_j + \xi) \quad (3.78)$$

It is immediately obvious on comparing (3.78) with (3.52) that

$$\frac{d\gamma}{du_\|} = \frac{\omega}{k_\| c^2}$$

This interesting relation can be explained physically by considering an electron emitting a photon of energy $\hbar\omega$ and axial momentum $\hbar k_\|$. Consequently the energy and axial momentum of the electron will also change by these amounts i.e.

$$m_e c^2 \Delta\gamma = \hbar\omega \qquad m_e \Delta u_\| = \hbar k_\|$$

$$\Rightarrow \frac{\Delta\gamma}{\Delta u_\|} = \frac{\omega}{k_\| c^2}$$

From the definition (3.76), the rate of change of p can now be shown to be

$$\frac{dp}{dz} = +\frac{c^2 k_{||} \omega_c}{\omega u_{||}^2} \frac{d\gamma}{dz} - \frac{\omega}{v_{||}^2} \frac{dv_{||}}{dz} \tag{3.79}$$

Note that if the rate of change of γ and $v_{||}$ are of the same sign, the two terms in (3.79) are of opposite sign. This expression can be rearranged to give

$$\frac{dp}{dz} = \frac{1}{u_{||}} \left(\frac{k_\perp^2}{k_{||}} - p \right) \frac{du_{||}}{dz} \tag{3.80}$$

where (3.73) and (3.78) have been used. Note that on comparing terms in (3.79) and (3.80), the $k_\perp^2/k_{||}$ term in the bracket of (3.80) arises from the change in γ, whereas the p term in the bracket of (3.80) arises from the change in $v_{||}$. This is an important point which will be returned to in section 3.4 and chapter 4.

Defining the variables

$$z' = 2k_{c0} z \quad , \quad p' = \frac{p}{2k_{c0}}$$

$$u'_\perp = \frac{u_\perp}{u_{\perp 0}} \quad , \quad u'_{||} = \frac{u_{||}}{u_{||0}}$$

$$A' = \frac{e k_{||} k_{c0}}{8 m_e c k_\perp \omega} D_{TE} J_{m-1}(k_\perp R_0) i F_s(z)$$

where $k_{c0} = \omega_c / u_{||0}$ is the 'cyclotron wavenumber' and the subscripts 0 indicate initial values at $z = 0$ then the evolution equations (3.71..3.74) and (3.80) can be written as

$$\frac{d\phi_j}{dz'} = p'_j - i \frac{k_\perp^2 c}{k_{||} k_{c0} u_{\perp 0}} \frac{1}{u'_{\perp j} u'_{||j}} \left(A' e^{i\phi_j} - c.c. \right) \tag{3.81}$$

$$\frac{dp'_j}{dz'} = -\frac{k_\perp^2 c u_{\perp 0}}{k_{c0}^2 u_{||0}^2} \frac{u'_{\perp j}}{{u'_{||j}}^2} \left(\frac{k_\perp^2}{2k_{||} k_{c0}} - p'_j \right) \left(A' e^{i\phi_j} + c.c. \right) \tag{3.82}$$

$$\frac{du'_{\perp j}}{dz'} = -\frac{k_\perp^2 c}{k_{||} k_{c0} u_{\perp 0}} \frac{1}{u'_{||j}} \left(A' e^{i\phi_j} + c.c. \right) \tag{3.83}$$

$$\frac{du'_{||j}}{dz'} = -\frac{k_\perp^2 c u_{\perp 0}}{k_{c0}^2 u_{||0}^2} \frac{u'_{\perp j}}{u'_{||j}} \left(A' e^{i\phi_j} + c.c. \right) \tag{3.84}$$

$$\frac{dA'}{dz'} = \frac{e}{32m_e c}\mu_0 D_{TE}^2 J_{m-1}^2(k_\perp R_0)\frac{u_{\perp 0}}{u_{\|0}}\left\langle \frac{u'_\perp}{u'_\|}e^{-i\phi}\right\rangle \tag{3.85}$$

It has been assumed here that there are no spreads in the electron's perpendicular or parallel momenta i.e. $u_{\perp 0}$ and $u_{\|0}$ are the same for all electrons. These equations will now be rescaled so that all coefficients are equal to one. To do this, the following set of variables are used

$$\hat{z} = c_1 z' \quad \hat{p} = c_2 p' \quad \hat{u}_\perp = c_3 u'_\perp \quad \hat{u}_\| = c_4 u'_\| \quad \hat{A} = c_5 A'$$

where the c_i, $i = 1..5$ are constants which will be defined so as to leave the evolution equations in the simplest scaled form possible. Writing the equations (3.81..3.85) in terms of these variables produces

$$\begin{aligned}
\frac{d\phi_j}{d\hat{z}} &= \left(\frac{1}{c_1 c_2}\right)\hat{p}_j - i\left(\frac{k_\perp^2 c}{k_\| k_{c0} u_{\perp 0}}\frac{c_3 c_4}{c_1 c_5}\right)\frac{1}{\hat{u}_{\perp j}\hat{u}_{\|j}}\left(\hat{A}e^{i\phi_j} - c.c.\right)\\
\frac{d\hat{p}_j}{d\hat{z}} &= -\left(\frac{k_\perp^4 c u_{\perp 0}}{2k_\| k_{c0}^3 u_{\|0}^2}\frac{c_2 c_4^2}{c_1 c_3 c_5}\right)\frac{\hat{u}_{\perp j}}{\hat{u}_{\|j}^2}\left(\hat{A}e^{i\phi_j} + c.c.\right)\\
&+ \left(\frac{k_\perp^2 c u_{\perp 0}}{k_{c0}^2 u_{\|0}^2}\frac{c_4^2}{c_1 c_3 c_5}\right)\frac{\hat{p}_j\hat{u}_{\perp j}}{\hat{u}_{\|j}^2}\left(\hat{A}e^{i\phi_j} + c.c.\right)\\
\frac{d\hat{u}_{\perp j}}{d\hat{z}} &= -\left(\frac{k_\perp^2 c}{k_\| k_{c0} u_{\perp 0}}\frac{c_3 c_4}{c_1 c_5}\right)\frac{1}{\hat{u}_{\|j}}\left(\hat{A}e^{i\phi_j} + c.c.\right)\\
\frac{d\hat{u}_{\|j}}{d\hat{z}} &= -\left(\frac{k_\perp^2 c u_{\perp 0}}{k_{c0}^2 u_{\|0}^2}\frac{c_4^2}{c_1 c_3 c_5}\right)\frac{\hat{u}_{\perp j}}{\hat{u}_{\|j}}\left(\hat{A}e^{i\phi_j} + c.c.\right)\\
\frac{d\hat{A}}{d\hat{z}} &= \left(\frac{c_5 c_4}{c_1 c_3}J\right)\left\langle\frac{\hat{u}_\perp}{\hat{u}_\|}e^{-i\phi}\right\rangle
\end{aligned}$$

where $J = \frac{e}{32m_e c}\mu_0 D_{TE}^2 J_{m-1}^2(k_\perp R_0)\frac{u_{\perp 0}}{u_{\|0}}$.

The sets of coefficients are now chosen to be equal to 1, which produces the following set of simultaneous equations

$$\begin{aligned}
c_1 c_2 &= 1\\
\frac{k_\perp^2 c}{k_\| k_{c0} u_{\perp 0}}\frac{c_3 c_4}{c_1 c_5} &= 1
\end{aligned}$$

$$\frac{k_\perp^4 c u_{\perp 0}}{2k_\parallel k_{c0}^3 u_{\parallel 0}^2}\frac{c_2 c_4^2}{c_1 c_3 c_5} = 1$$

$$\frac{k_\perp^2 c u_{\perp 0}}{k_{c0}^2 u_{\parallel 0}^2}\frac{c_4^2}{c_1 c_3 c_5} = 1$$

$$\frac{k_\perp^2 c}{k_\parallel k_{c0} u_{\perp 0}}\frac{c_3 c_4}{c_1 c_5} = 1$$

$$\frac{k_\perp^2 c u_{\perp 0}}{k_{c0}^2 u_{\parallel 0}^2}\frac{c_4^2}{c_1 c_3 c_5} = 1$$

$$\frac{c_5 c_4}{c_1 c_3} J = 1$$

which have the solutions

$$c_1 = \frac{k_\perp^2}{2k_\parallel k_{c0}} \qquad c_2 = \frac{2k_\parallel k_{c0}}{k_\perp^2}$$

$$c_3 = \frac{1}{u_{\parallel 0}}\left(\frac{k_\parallel k_\perp^2 u_{\perp 0}^5}{4k_{c0}^3 c}\frac{1}{J}\right)^{\frac{1}{4}} \qquad c_4 = \frac{1}{2}\left(\frac{u_{\perp 0} k_\perp^2}{c k_\parallel k_{c0}}\frac{1}{J}\right)^{\frac{1}{2}}$$

$$c_5 = \frac{1}{u_{\parallel 0}}\left(\frac{k_\perp^6 c u_{\perp 0}}{4k_\parallel k_{c0}^5}\frac{1}{J^3}\right)^{\frac{1}{4}}$$

Therefore the set of evolution equations becomes

$$\frac{d\phi_j}{d\hat{z}} = \hat{p}_j - i\frac{1}{\hat{u}_{\perp j}\hat{u}_{\parallel j}}\left(\hat{A}e^{i\phi_j} - c.c.\right) \tag{3.86}$$

$$\frac{d\hat{p}_j}{d\hat{z}} = (\hat{p}_j - 1)\frac{\hat{u}_{\perp j}}{\hat{u}_{\parallel j}^2}\left(\hat{A}e^{i\phi_j} + c.c.\right) \tag{3.87}$$

$$\frac{d\hat{u}_{\perp j}}{d\hat{z}} = -\frac{1}{\hat{u}_{\parallel j}}\left(\hat{A}e^{i\phi_j} + c.c.\right) \tag{3.88}$$

$$\frac{d\hat{u}_{\parallel j}}{d\hat{z}} = -\frac{\hat{u}_{\perp j}}{\hat{u}_{\parallel j}}\left(\hat{A}e^{i\phi_j} + c.c.\right) \tag{3.89}$$

$$\frac{d\hat{A}}{d\hat{z}} = \left\langle \frac{\hat{u}_\perp}{\hat{u}_\parallel} e^{-i\phi} \right\rangle \tag{3.90}$$

where

$$\hat{z} = \frac{k_\perp^2}{k_\parallel} z \qquad \hat{p} = \frac{k_\parallel}{k_\perp^2} p$$

$$\hat{u}_\perp = \frac{1}{u_{\parallel 0}}\left(\frac{k_\parallel k_\perp^2 u_{\perp 0}^5}{4k_{c0}^3 c}\frac{1}{J}\right)^{\frac{1}{4}} u'_\perp \qquad \hat{u}_\parallel = \frac{1}{2}\left(\frac{u_{\perp 0} k_\perp^2}{c k_\parallel k_{c0}}\frac{1}{J}\right)^{\frac{1}{2}} u'_\parallel \tag{3.91}$$

$$\hat{A} = \frac{1}{u_{\parallel 0}}\left(\frac{k_\perp^6 c u_{\perp 0}}{4k_\parallel k_{c0}^5}\frac{1}{J^3}\right)^{\frac{1}{4}} A'$$

Notice from (3.87..3.89) that there is a functional relationship between the variables $\hat{p}$, $\hat{u}_\perp$ and $\hat{u}_\parallel$ i.e.

$$\frac{\hat{u}_\parallel^2}{\hat{u}_\perp}\frac{d\hat{p}}{(\hat{p}-1)} = -\hat{u}_\parallel d\hat{u}_\perp = -\frac{\hat{u}_\parallel}{\hat{u}_\perp}d\hat{u}_\parallel \tag{3.92}$$

Integrating produces the following :

$$\begin{aligned}\hat{u}_\perp &= \sqrt{\hat{u}_{\perp 0}^2 + 2\hat{u}_{\parallel 0}\left(\frac{(1-\hat{\delta})}{(1-\hat{p})} - 1\right)} \\ \hat{u}_\parallel &= \frac{(1-\hat{\delta})}{(1-\hat{p})}\hat{u}_{\parallel 0}\end{aligned}$$

where $\hat{\delta}$, $\hat{u}_{\perp 0}$ and $\hat{u}_{\parallel 0}$ are the values at $z = 0$ of $\hat{p}$, $\hat{u}_\perp$ and $\hat{u}_\parallel$ respectively. At first glance, it would appear that the set of equations (3.86..3.90) is universally scaled as it contains no free parameters. The solution to these equations therefore depends only on the values of the dependent variables at $\hat{z} = 0$. However, it will be shown that this set of equations is related to another set with a different scaling which is much more physically significant. A number of approximations will now be used to simplify (3.86..3.90) in order to deduce the nature of this true universal scaling. The approximations will be justified using physical arguments in section 3.4.

Consider the case where $|\hat{p}|, |\hat{\delta}| << 1$. This means that

$$\hat{u}_\perp \approx \hat{u}_{\perp 0}\sqrt{1 + 2\frac{\hat{u}_{\parallel 0}}{\hat{u}_{\perp 0}^2}(\hat{p} - \hat{\delta})} \tag{3.93}$$

$$\hat{u}_\parallel \approx \hat{u}_{\parallel 0} \tag{3.94}$$

Assume that the term under the square root is ≈ 1 i.e. $\hat{u}_\perp \approx \hat{u}_{\perp 0}$. Under these conditions, the set of five equations (3.86..3.90) reduces to the set of three which

are

$$\begin{aligned}
\frac{d\phi_j}{d\hat{z}} &= \hat{p}_j - i\frac{1}{\hat{u}_{\perp 0}\hat{u}_{\|0}}\left(\hat{A}e^{i\phi_j} - c.c.\right) \\
\frac{d\hat{p}_j}{d\hat{z}} &= -\frac{\hat{u}_{\perp 0}}{\hat{u}_{\|0}^2}\left(\hat{A}e^{i\phi_j} + c.c.\right) \\
\frac{d\hat{A}}{d\hat{z}} &= \frac{\hat{u}_{\perp 0}}{\hat{u}_{\|0}}\left\langle e^{-i\phi_j}\right\rangle
\end{aligned}$$

Assuming for the moment that the second term in $d\phi_j/d\hat{z}$ is negligibly small, and introducing the variables

$$\bar{z} = K_1\hat{z} \qquad \bar{p} = \frac{\hat{p}}{K_1} \qquad \bar{A} = K_2\hat{A}$$

then the three equations become

$$\begin{aligned}
\frac{d\phi_j}{d\bar{z}} &= \bar{p}_j \\
\frac{d\bar{p}_j}{d\bar{z}} &= -\left(\frac{\hat{u}_{\perp 0}}{\hat{u}_{\|0}^2}\frac{1}{K_1^2K_2}\right)\left(\bar{A}e^{i\phi_j} + c.c.\right) \qquad (3.95) \\
\frac{d\bar{A}}{d\bar{z}} &= \left(\frac{\hat{u}_{\perp 0}}{\hat{u}_{\|0}}\frac{K_2}{K_1}\right)\left\langle e^{-i\phi}\right\rangle
\end{aligned}$$

Setting

$$\left.\begin{aligned}
\tfrac{\hat{u}_{\perp 0}}{\hat{u}_{\|0}^2}\tfrac{1}{K_1^2K_2} &= 1 \\
\tfrac{\hat{u}_{\perp 0}}{\hat{u}_{\|0}}\tfrac{K_2}{K_1} &= 1
\end{aligned}\right\} \quad \Rightarrow \quad \begin{aligned}
K_1 &= \tfrac{\hat{u}_{\perp 0}^{2/3}}{\hat{u}_{\|0}} \\
K_2 &= \tfrac{1}{\hat{u}_{\perp 0}^{1/3}}
\end{aligned}$$

Substituting for $\hat{u}_{\perp 0}$ and $\hat{u}_{\|0}$ from (3.91) gives

$$K_1 = \left(\frac{4k_{\|}^2u_{\perp 0}c}{k_{\perp}^2u_{\|0}^2}J\right)^{\frac{1}{3}} \qquad K_2 = \left(2\frac{k_{c0}^{3/2}u_{\|0}^2c^{1/2}}{k_{\|}^{1/2}k_{\perp}u_{\perp 0}^{5/2}}J^{1/2}\right)^{\frac{1}{6}} \qquad (3.96)$$

and the set of equations (3.95) is

$$\begin{aligned}
\frac{d\phi_j}{d\bar{z}} &= \bar{p}_j \\
\frac{d\bar{p}_j}{d\bar{z}} &= -\left(\bar{A}e^{i\phi_j} + c.c.\right) \qquad (3.97) \\
\frac{d\bar{A}}{d\bar{z}} &= \left\langle e^{-i\phi}\right\rangle
\end{aligned}$$

which are exactly the same equations used to describe the high gain Compton FEL [64]. From a linear analysis of these equations, such as the one which will be performed in chapter 4, it can be shown that the exponential growth rate, g, of the wave field is

$$g = \frac{\sqrt{3}}{2}\bar{z} = \frac{\sqrt{3}}{2}K_1\hat{z} = \frac{\sqrt{3}}{2}\frac{k_\perp^2}{k_{||}}K_1 z$$

The constant K_1 will now be renamed ρ, and termed the 'Fundamental CRM Parameter' analagously to the 'Fundamental FEL Parameter' [64]. Therefore, using (3.96),

$$\rho = \left(\frac{e}{8m_e}\frac{k_{||}^2}{k_\perp^2}\frac{u_{\perp 0}^2}{u_{||0}^3}\mu_0 I D_{TE}^2 J_{m-1}^2(k_\perp R_0)\right)^{\frac{1}{3}} \tag{3.98}$$

The constant K_2 is

$$K_2 = \rho^{\frac{1}{4}}\left(\frac{k_{||}}{k_{c0}}\frac{u_{\perp 0}^2}{u_{||0}^3}\right)^{-\frac{1}{4}} = \left(\frac{\rho}{\nu}\right)^{\frac{1}{4}} \tag{3.99}$$

where ν has been defined as

$$\nu = \frac{k_{||}}{k_{c0}}\frac{u_{\perp 0}^2}{u_{||0}^2} \tag{3.100}$$

It is now possible to write the 'hat' variables ($\hat{}$) defined in (3.91) solely in terms of ρ and ν i.e.

$$\hat{z} = \frac{\bar{z}}{\rho} \qquad \hat{p} = \rho\bar{p}$$

$$\hat{u}_\perp = \left(\frac{\nu}{\rho}\right)^{\frac{3}{4}} u'_\perp \qquad \hat{u}_{||} = \frac{1}{\rho}\left(\frac{\nu}{\rho}\right)^{\frac{1}{2}} u'_{||} \tag{3.101}$$

$$\hat{A} = \left(\frac{\nu}{\rho}\right)^{\frac{3}{4}} \bar{A} \tag{3.102}$$

Using these definitions, the set of five equations (3.86..3.90) can be written in terms of the universal scaling parameters ρ and ν :

$$\frac{d\phi_j}{d\bar{z}} = \bar{p}_j - i\frac{\mu}{\bar{u}_{\perp j}\bar{u}_{||j}}\left(\bar{A}e^{i\phi_j} - c.c.\right)$$

$$
\begin{aligned}
\frac{d\bar{p}_j}{d\bar{z}} &= (\rho\bar{p}_j - 1)\frac{\bar{u}_{\perp j}}{\bar{u}_{\parallel j}^2}\left(\bar{A}e^{i\phi_j} + c.c.\right) \\
\frac{d\bar{u}_{\perp j}}{d\bar{z}} &= -\frac{\mu}{\bar{u}_{\parallel j}}\left(\bar{A}e^{i\phi_j} + c.c.\right) \\
\frac{d\bar{u}_{\parallel j}}{d\bar{z}} &= -\rho\frac{\bar{u}_{\perp j}}{\bar{u}_{\parallel j}}\left(\bar{A}e^{i\phi_j} + c.c.\right) \\
\frac{d\bar{A}}{d\bar{z}} &= \left\langle \frac{\bar{u}_\perp}{\bar{u}_\parallel} e^{-i\phi} \right\rangle
\end{aligned}
$$

where for consistency, $u'_\perp$ and $u'_\parallel$ have been redefined as $\bar{u}_\perp$ and $\bar{u}_\parallel$ respectively i.e.

$$\bar{u}_\perp = \frac{u_\perp}{u_{\perp 0}} \qquad \bar{u}_\parallel = \frac{u_\parallel}{u_{\parallel 0}}$$

and $\mu = \rho/\nu$. Note that $\bar{u}_\perp$ and $\bar{u}_\parallel$ are no longer scaled with respect to any beam or mode parameters such as I or D_{TE}. It is this which has brought ρ and μ out explicitly in the equations. An analysis of these equations and a description of the physical significance of the universal scaling parameters ρ, μ and so ν will be performed in section 3.4.

3.3 TM Mode Interaction

The cylindrical components of the electric (**E**) and magnetic (**B**) field of a TM_{mn} cold cylindrical waveguide mode are

$$E_r = -i\frac{k_\perp k_\parallel c^2}{2\omega} G_s(z) D_{TM} J'_m(k_\perp r) e^{i\Psi} + c.c. \tag{3.103}$$

$$E_\theta = -\frac{m k_\parallel c^2}{2r\omega} G_s(z) D_{TM} J_m(k_\perp r) e^{i\Psi} + c.c. \tag{3.104}$$

$$E_z = \frac{k_\perp^2 c^2}{2\omega} G_s(z) D_{TM} J_m(k_\perp r) e^{i\Psi} + c.c. \tag{3.105}$$

$$B_r = -\frac{\omega}{k_\parallel c^2} E_\theta \tag{3.106}$$

$$B_\theta = \frac{\omega}{k_\parallel c^2} E_r \tag{3.107}$$

$$B_z = 0 \tag{3.108}$$

where:

$$D_{TM} = \left(\sqrt{\pi}\chi_{mn}J'_m(\chi_{mn})\right)^{-1} \tag{3.109}$$

is a mode dependent constant, χ_{mn} is the nth root of $J_m(k_\perp R_w) = 0$ and $G_s(z)$ is a slowly varying complex field amplitude with the dimensions of current which has the form

$$G_s(z) = |G_s(z)|e^{i\xi(z))} \tag{3.110}$$

where $|G_s(z)|$ and $\xi(z)$ are slowly varying functions of z. All other symbols have the same meaning as for the TE mode.

Equations (3.103..3.108) are analogous to (3.7..3.12) of the TE mode analysis of section 3.2. The derivation of the electron equations of motion and the electromagnetic field evolution equation for a TM_{mn} mode follows that for TE_{mn} mode almost identically.

3.3.1 Electron Equations of motion

The components of the Lorentz equation in this case are

$$\frac{d\mathbf{u}_\perp}{dz} = -\frac{e}{m_e}\frac{\gamma}{u_\parallel}\left(\mathbf{E}_\perp + \frac{1}{\gamma}(\mathbf{u}\times\mathbf{B})_\perp\right) \tag{3.111}$$

$$\frac{du_\parallel}{dz} = -\frac{e}{m_e}\frac{\gamma}{u_\parallel}\left(E_\parallel + \frac{(\mathbf{u}\times\mathbf{B})_\parallel}{\gamma}\right) \tag{3.112}$$

Writing the components of the Lorentz equations in terms of ϕ_g, $u_\perp$ and $u_\parallel$, and using the vector relations (3.19), (3.20),(3.24) and (3.25), the equations of motion can be found to be

$$\frac{d\phi_g}{dz} = \frac{e\gamma}{u_\perp u_\parallel m_e}\times \tag{3.113}$$

$$+\frac{u_\perp B_0}{\gamma}\left[\frac{k_\perp k_\| c^2 D_{TM}|G_s(z)|}{2\omega}\left(1-\frac{u_\| \omega}{\gamma k_\| c^2}\right)\left(\begin{array}{rl} & J_{m-1}(k_\perp r)\sin(\Psi+\theta-\phi_g+\xi) \\ - & J_{m+1}(k_\perp r)\sin(\Psi-\theta+\phi_g+\xi)\end{array}\right)\right]$$

$$\frac{du_\perp}{dz} = \frac{e\gamma}{u_\| m_e}\frac{k_\perp k_\| c^2 D_{TM}|G_s(z)|}{2\omega}\left(1-\frac{u_\| \omega}{\gamma k_\| c^2}\right)\times$$

$$\left(\begin{array}{rl} & J_{m-1}(k_\perp r)\cos(\Psi+\theta-\phi_g+\xi) \\ + & J_{m+1}(k_\perp r)\cos(\Psi-\theta+\phi_g+\xi)\end{array}\right) \tag{3.114}$$

$$\frac{du_\|}{dz} = \frac{e\gamma}{m_e u_\|}k_\perp|G_s(z)|D_{TM}\times$$

$$\left[\begin{array}{rl} & \frac{u_\perp}{2\gamma}\left(\begin{array}{rl} & J_{m-1}(k_\perp r)\cos(\Psi+\theta-\phi_g+\xi) \\ + & J_{m+1}(k_\perp r)\cos(\Psi-\theta+\phi_g+\xi)\end{array}\right) \\ - & \frac{k_\perp c^2}{\omega}J_m(k_\perp r)\cos(\Psi+\xi)\end{array}\right] \tag{3.115}$$

$$\frac{dt}{dz} = \frac{\gamma}{u_\|} \tag{3.116}$$

Graf's theorem can now be used to simplify these equations, as

$$J_m(k_\perp r)\cos(\Psi+\xi) = \sum_{n=-\infty}^{\infty}(-1)^n J_{m+n}(k_\perp R_0)J_n(k_\perp r_L)\cos\Omega_0$$

$$J_{m-1}(k_\perp r)\cos(\Psi+\theta-\phi_g+\xi) = \sum_{n=-\infty}^{\infty}(-1)^n J_{m+n-1}(k_\perp R_0)J_n(k_\perp r_L)\cos\Omega_-$$

$$J_{m-1}(k_\perp r)\sin(\Psi+\theta-\phi_g+\xi) = \sum_{n=-\infty}^{\infty}(-1)^n J_{m+n-1}(k_\perp R_0)J_n(k_\perp r_L)\sin\Omega_-$$

$$J_{m+1}(k_\perp r)\cos(\Psi-\theta+\phi_g+\xi) = \sum_{n=-\infty}^{\infty}(-1)^n J_{m+n+1}(k_\perp R_0)J_n(k_\perp r_L)\cos\Omega_+$$

$$J_{m+1}(k_\perp r)\sin(\Psi-\theta+\phi_g+\xi) = \sum_{n=-\infty}^{\infty}(-1)^n J_{m+n+1}(k_\perp R_0)J_n(k_\perp r_L)\sin\Omega_+$$

where, as for the TE mode interaction,

$$\Omega_0 = \omega t + n\phi_g - k_\| z - (m+n)\theta_0 + \xi$$

$$\Omega_- = \omega t + (n-1)\phi_g - k_\| z - (m+n-1)\theta_0 + \xi$$

$$\Omega_+ \;=\; \omega t + (n+1)\phi_g - k_{\|} z - (m+n+1)\theta_0 + \xi.$$

Again, the gyro-angle is split into quickly and slowly varying parts and the equations of motion are averaged over a cyclotron period. Using the Bessel function relations (3.26) and (3.27), and making the same assumptions as for the TE mode case i.e.

$$k_\perp r_L << 1 \quad , \quad s = 1$$

where s is the cyclotron harmonic, then

$$\begin{aligned}
\frac{d\phi_g^{(s)}}{dz} &= \frac{\omega_c}{u_{\|}}\left(1 - \frac{\gamma}{\gamma_0}\right) \\
&+ \frac{e k_\perp D_{TM}}{2 u_\perp m_e} |G_s(z)| J_{m-1}(k_\perp R_0)\left(\frac{k_{\|} c^2 \gamma}{\omega u_{\|}} - 1\right) \sin(\phi + \xi) \\
\frac{du_\perp}{dz} &= \frac{e}{2m_e} k_\perp D_{TM} |G_s(z)| J_{m-1}(k_\perp R_0)\left(\frac{k_{\|} c^2 \gamma}{\omega u_{\|}} - 1\right) \cos(\phi + \xi) \\
\frac{du_{\|}}{dz} &= -\frac{e\gamma u_\perp}{2 u_{\|} m_e} \frac{k_\perp}{\omega_c} D_{TM} |G_s(z)| J_{m-1}(k_\perp R_0)\left(\frac{k_\perp^2 c^2}{\omega} - \frac{\omega_c}{\gamma}\right) \cos(\phi + \xi)
\end{aligned}$$

where

$$\phi = (\omega - \frac{\omega_c}{\gamma_0})t - k_{\|} z - \phi_g^{(s)} - (m-1)\theta_0$$

as before. The bracketed term in $du_{\|}/dz$ can be altered using the dispersion relation for the waveguide mode and the condition for operation close to resonance as follows

$$\frac{k_\perp^2 c^2}{\omega} - \frac{\omega_c}{\gamma} = \omega - \frac{\omega_c}{\gamma} - \frac{k_{\|}^2 c^2}{\omega} \approx -\frac{k_{\|} u_{\|}}{\gamma}\left(\frac{k_{\|} c^2 \gamma}{\omega u_{\|}} - 1\right)$$

Using this relation and the fact that

$$\frac{d\phi}{dz} = \frac{\gamma}{u_{\|}}\left(\omega - \frac{\omega_c}{\gamma_0}\right) - k_{\|} - \frac{d\phi_g^{(s)}}{dz}$$

then the equations of motion become

$$\frac{d\phi}{dz} \;=\; \frac{\gamma\omega}{u_{\|}} - \frac{\omega_c}{u_{\|}} - k_{\|}$$

$$- \frac{ek_\perp D_{TM}}{2u_\perp m_e}|G_s(z)|J_{m-1}(k_\perp R_0)\left(\frac{k_{||}c^2\gamma}{\omega u_{||}}-1\right)\sin(\phi+\xi) \quad (3.117)$$

$$\frac{du_\perp}{dz} = \frac{e}{2m_e}k_\perp D_{TM}|G_s(z)|J_{m-1}(k_\perp R_0)\left(\frac{k_{||}c^2\gamma}{\omega u_{||}}-1\right)\cos(\phi+\xi) \quad (3.118)$$

$$\frac{du_{||}}{dz} = \frac{eu_\perp}{2m_e}\frac{k_\perp k_{||}}{\omega_c}D_{TM}|G_s(z)|J_{m-1}(k_\perp R_0)\times \left(\frac{k_{||}c^2\gamma}{\omega u_{||}}-1\right)\cos(\phi+\xi) \quad (3.119)$$

Evaluating $d\gamma/dz$ using (3.118) and (3.119), it is found that

$$\frac{d\gamma}{dz} = \frac{eu_\perp}{2m_e}\frac{k_\perp\omega}{c^2\omega_c}D_{TM}|G_s(z)|J_{m-1}(k_\perp R_0)\left(\frac{k_{||}c^2\gamma}{\omega u_{||}}-1\right)\cos(\phi+\xi)$$

so that on comparison with (3.119), it is clear that

$$\frac{d\gamma}{dz} = \frac{\omega}{k_{||}c^2}\frac{du_{||}}{dz}$$

as expected. The consequence of this relation is that on integrating each side,

$$\gamma - \gamma_0 = \frac{\omega}{k_{||}c^2}(u_{||}-u_{||0}) \quad (3.120)$$

which can be rearranged to give

$$\frac{k_{||}c^2\gamma}{\omega u_{||}} - 1 = \frac{1}{u_{||}}\left(\frac{k_{||}c^2}{\omega}\gamma_0 - u_{||0}\right) \quad (3.121)$$

Defining p as

$$p = \frac{\gamma\omega}{u_{||}} - \frac{\omega_c}{u_{||}} - k_{||}$$

then

$$\frac{dp}{dz} = \frac{1}{u_{||}}\left(\frac{k_\perp^2}{k_{||}} - p\right)\frac{du_{||}}{dz}$$

so the final form of the equations of motion is therefore

$$\frac{d\phi}{dz} = p \quad (3.122)$$
$$- \frac{ek_\perp D_{TM}}{2m_e u_\perp u_{||}}\left(\frac{k_{||}c^2}{\omega}\gamma_0 - u_{||0}\right)|G_s(z)|J_{m-1}(k_\perp R_0)\sin(\phi+\xi)$$

$$\frac{dp}{dz} = \frac{ek_\perp k_\parallel D_{TM}}{2m_e\omega_c}\left(\frac{k_\parallel c^2}{\omega}\gamma_0 - u_{\parallel 0}\right) \times$$
$$J_{m-1}(k_\perp R_0)\frac{u_\perp}{u_\parallel^2}|G_s(z)|\left(\frac{k_\perp^2}{k_\parallel} - p\right)\cos(\phi+\xi) \quad (3.123)$$

$$\frac{du_\perp}{dz} = \frac{e}{2m_e}k_\perp D_{TM}\left(\frac{k_\parallel c^2}{\omega}\gamma_0 - u_{\parallel 0}\right) \times$$
$$\frac{1}{u_\parallel}|G_s(z)|J_{m-1}(k_\perp R_0)\cos(\phi+\xi) \quad (3.124)$$

$$\frac{du_\parallel}{dz} = \frac{e}{2m_e}\frac{k_\perp k_\parallel}{\omega_c}D_{TM}\left(\frac{k_\parallel c^2}{\omega}\gamma_0 - u_{\parallel 0}\right) \times$$
$$|G_s(z)|J_{m-1}(k_\perp R_0)\frac{u_\perp}{u_\parallel}\cos(\phi+\xi). \quad (3.125)$$

These equations constitute the slowly varying electron equations of motion for a relativistic electron gyrating in a static magnetic field interacting with a TM_{mn} waveguide mode at the fundamental cyclotron harmonic. The transverse variation of the mode profile is assumed to be negligible over the electron gyro-orbit.

3.3.2 The Electromagnetic Field Evolution Equation

As for the TE mode interaction, the electromagnetic field equation is derived for the case of steady-state evolution. The starting point of the derivation is Maxwell's wave equation

$$\left(\nabla^2 - \frac{1}{c^2}\frac{\partial^2}{\partial t^2}\right)\mathbf{E}(\mathbf{r},t) = \mu_0\frac{\partial \mathbf{J}(\mathbf{r},t)}{\partial t} - e\nabla\left(\frac{n_e(\mathbf{r},t)}{\epsilon_0}\right)$$

where n_e here represents the number density of the electrons. Consider the component of the wave equation parallel to the waveguide axis

$$\left(\nabla^2 - \frac{1}{c^2}\frac{\partial^2}{\partial t^2}\right)E_z(\mathbf{r},t) = \mu_0\frac{\partial J_z(\mathbf{r},t)}{\partial t} - \frac{e}{\epsilon_0}\frac{\partial n_e(\mathbf{r},t)}{\partial z} \quad (3.126)$$

From (3.105), it is clear that E_z can be represented by

$$E_z(\mathbf{r},t) = \frac{1}{2}\left(G_s(z)e_z(r,\theta)e^{i(\omega t - k_\parallel z)} + c.c.\right)$$

where

$$e_z(r,\theta) = \frac{k_\perp^2 c^2}{\omega} D_{TM} J_m(k_\perp r) e^{-im\theta} \tag{3.127}$$

which satisfies the Helmholtz equation

$$\left(\nabla_\perp^2 + k_\perp^2\right) e_z(r,\theta) = 0$$

. This means that (3.126) becomes

$$\left(\nabla^2 - \frac{1}{c^2}\frac{\partial^2}{\partial t^2}\right) \frac{1}{2}\left(G_s(z) e^{i(\omega t - k_\parallel z)} + c.c.\right) e_z(r,\theta) = \mu_0 \frac{\partial J_\parallel(\mathbf{r},t)}{\partial t} - \frac{e}{\epsilon_0}\frac{\partial n_e(\mathbf{r},t)}{\partial z} \tag{3.128}$$

Performing a scalar product of this equation with e_z^* and integrating over the cross-sectional area of the waveguide, the LHS of (3.128) can be simplified using Lommel's integral [65]

$$\begin{aligned}\int_0^{R_w} r J_m^2(k_\perp r) dr &= \frac{R_w^2}{2}\left[J'^2_m(k_\perp R_w) + \left(1 - \frac{m^2}{k_\perp^2 R_w^2}\right) J_m^2(k_\perp R_w)\right] \\ &= \frac{R_w^2}{2} J'^2_m(\chi_{mn})\end{aligned}$$

as $\chi_{mn} = k_\perp R_w$ for a TM_{mn} mode and $J_m(\chi_{mn}) = 0$. As the complex field amplitude $G_s(z)$ is slowly varying, (3.128) can be further simplified using the approximation (3.62) and its complex conjugate. This means that (3.128) can be written as

$$\begin{aligned}2\pi\left(\frac{k_\perp^2 c^2}{\omega} D_{TM}\right)^2 \left(-ik_\parallel \frac{dG_s(z)}{dz} e^{i(\omega t - k_\parallel z)} + \mathrm{c.c}\right) \frac{R_w^2}{2} J'^2_m(\chi_{mn}) = \\ \int_A \left(\mu_0 \frac{\partial J_\parallel(\mathbf{r},t)}{\partial t} - \frac{e}{\epsilon_0}\frac{\partial n_e(\mathbf{r},t)}{\partial z}\right) e_z^*(r,\theta) dA\end{aligned} \tag{3.129}$$

where the steady-state limit has been assumed.

If the current density $J_\parallel(\mathbf{r},t)$ and the electron number density $n_e(\mathbf{r},t)$ are assumed to be of the same form as the electric field i.e.

$$J_\parallel(\mathbf{r},t) = \frac{1}{2}\left(J_{\parallel s}(\mathbf{r},t) e^{i(\omega t - k_\parallel z)} + c.c.\right) \tag{3.130}$$

$$n_e(\mathbf{r},t) = \frac{1}{2}\left(n_{es}(\mathbf{r},t)e^{i(\omega t - k_\parallel z)} + c.c.\right) \tag{3.131}$$

where $J_{\parallel s}(\mathbf{r},t)$ and $n_{es}(\mathbf{r},t)$ are slowly varying functions of z and t such that

$$\left|\frac{\partial J_{\parallel s}(\mathbf{r},t)}{\partial t}\right| \ll \left|\omega J_{\parallel s}(\mathbf{r},t)\right| \quad , \quad \left|\frac{\partial J_{\parallel s}(\mathbf{r},t)}{\partial z}\right| \ll \left|k_\parallel J_{\parallel s}(\mathbf{r},t)\right|$$
$$\left|\frac{\partial n_{es}(\mathbf{r},t)}{\partial t}\right| \ll \left|\omega n_{es}(\mathbf{r},t)\right| \quad , \quad \left|\frac{\partial n_{es}(\mathbf{r},t)}{\partial z}\right| \ll \left|k_\parallel n_{es}(\mathbf{r},t)\right|$$

then the partial derivatives on the RHS of (3.129) can be approximated by

$$\frac{\partial J_{\parallel s}(\mathbf{r},t)}{\partial t} \approx i\omega J_{\parallel s}(\mathbf{r},t) \tag{3.132}$$
$$\frac{\partial n_{es}(\mathbf{r},t)}{\partial z} \approx -ik_\parallel n_{es}(\mathbf{r},t) \tag{3.133}$$

so

$$\mu_0\frac{\partial J_\parallel(\mathbf{r},t)}{\partial t} - \frac{e}{\epsilon_0}\frac{\partial \rho(\mathbf{r},t)}{\partial z} = \omega\mu_0\frac{dJ_\parallel(\psi)}{d\psi} + \frac{ek_\parallel}{\epsilon_0}\frac{d\rho(\psi)}{d\psi}$$
$$= \omega\mu_0\frac{1}{2}\left(1 - \frac{k_\parallel c^2\gamma}{\omega u_\parallel}\right)\left(iJ_{\parallel s}(\mathbf{r},t)e^{i(\omega t - k_\parallel z)} + c.c.\right)$$

where $\psi = \omega t - k_\parallel z$ and the relations $n_e = -J_\parallel/(ev_\parallel)$ and $1/(\mu_0\epsilon_0) = c^2$ have been used. Using (3.121), equation (3.129) can be written as

$$2\pi\left(\frac{k_\perp^2 c^2}{\omega}D_{TM}\right)^2\left(-ik_\parallel\frac{dG_s(z)}{dz}e^{i(\omega t - k_\parallel z)} + c.c\right)\frac{R_w^2}{2}J'^2(\chi_{mn}) = \tag{3.134}$$
$$-\omega\mu_0\int_A\frac{1}{u_\parallel}\left(\frac{k_\parallel c^2}{\omega}\gamma_0 - u_{\parallel 0}\right)\left(iJ_{\parallel s}(\mathbf{r},t)e^{i(\omega t - k_\parallel z)} + c.c.\right)e_z^*(r,\theta)dA$$

Multiplying both sides of (3.135) by $e^{-i\omega t}$ and integrating with respect to ωt over the interval 0 to 2π, leads to

$$-4\pi^2 ik_\parallel\left(\frac{k_\perp^2 c^2}{\omega}D_{TM}\right)^2\frac{R_w^2}{2}J'^2(\chi_{mn})\frac{dG_s(z)}{dz} =$$
$$i\omega\mu_0\left(\frac{k_\parallel c^2}{\omega}\gamma_0 - u_{\parallel 0}\right)J_{\parallel s}(\mathbf{r},t)e^{ik_\parallel z}$$

To evaluate the slowly varying compoment of the current density, it is necessary to multiply both sides of (3.130) by $e^{-i\omega t}$ and integrate over ωt in the range $0 \rightarrow 2\pi$. Rearranging then gives

$$J_{\|s}(\mathbf{r},t) = \frac{1}{\pi}\int_0^{2\pi} J_{\|}(\mathbf{r},t)e^{-i\omega t}\, d(\omega t). \tag{3.135}$$

As for the TE mode interaction, the current density $\mathbf{J}_\perp(\mathbf{r},t)$ is represented by a collection of N electrons i.e.

$$J_{\|}(\mathbf{r},t) = -e\sum_{j=1}^{N} v_{\|j}(\mathbf{r},t)\delta(\mathbf{r}-\mathbf{r}_j)$$

Expressing the delta function as

$$\delta(\mathbf{r}-\mathbf{r}_j) = \frac{\delta(r-r_j)}{r}\delta(\theta-\theta_j)\delta(z-z_j)$$

and using the fact that

$$\delta(z-z_j) = \frac{\omega}{v_{\|j}}\delta(\omega t-\omega t_j)$$

then the integral (3.135) becomes

$$\frac{1}{\pi}\int_0^{2\pi} J_{\|}(\mathbf{r},t)e^{-i\omega t}\, d(\omega t) = -\frac{e\omega}{\pi}\sum_{j=1}^{N}\frac{\delta(r-r_j)}{r}\delta(\theta-\theta_j)e^{-i\omega t_j}.$$

Using (3.127) for e_z, the definition of the current

$$I = \sum_{j=1}^{N} I_j = \frac{Ne\omega}{2\pi}$$

and the definition of D_{TM}, (3.109), then the differential equation for the slowly varying complex amplitude $G_s(z,t)$ is

$$\frac{dG_s}{dz} = \frac{-\mu_0 I\omega^2}{c^2 k_{\|}} D_{TM}\left(\frac{k_{\|}c^2}{\omega}\gamma_0 - u_{\|0}\right)\left\langle \frac{J_m(k_\perp r)}{u_{\|}} e^{-i(\omega t - k_{\|}z)}\right\rangle. \tag{3.136}$$

From Graf's theorem,

$$J_m(k_\perp r)e^{-i\Psi_j} = \sum_{n=-\infty}^{\infty}(-1)^n J_{m+n}(k_\perp R_0)J_n(k_\perp r_L)e^{-i(\omega t - k_\parallel z - n\phi_g - (m+n)\theta_0)}$$

so splitting ϕ_g into quickly and slowly varying parts, averaging (3.136) over a cyclotron period and specifying that

$$s = 1 \qquad k_\perp r_L << 1$$

allows (3.136) to be written as

$$\frac{dG_s(z)}{dz} = \frac{-\mu_0 I k_\perp \omega^2}{2c^2 k_{||} k_{c0} u_{||0}} \left(\frac{k_{||}c^2}{\omega}\gamma_0 - u_{||0}\right) D_{TM} J_{m-1}(k_\perp R_0) \left\langle \frac{u_\perp}{u_{||}} e^{-i\phi} \right\rangle \qquad (3.137)$$

This is the steady-state evolution equation for the slowly varying complex amplitude of a TM_{mn} waveguide mode due to its interaction with a beam of relativistic electrons gyrating in a static magnetic field. The interaction is assumed to occur at the fundamental cyclotron harmonic and the transverse variation of the mode profile is assumed to be negligible over the gyro-orbit of the electrons.

3.3.3 Wave Group Velocity and Electron Axial Velocity

It is immediately noticeable that all the equations of motion and the wave equation for the TM mode interaction contain the term $v_g\gamma_0 - u_{||0}$, where $v_g = c^2 k_{||}/\omega$ is the radiation group velocity. This implies that if the electron axial velocity is equal to the radiation group velocity, then the electrons and the radiation do not interact. The physical reason for this can be deduced by considering a frame of reference, K′, in which the electron has only transverse momentum i.e. one which travels at a speed of $v_{||}$ parallel to the waveguide axis relative to the laboratory

frame, K. The electric and magnetic fields of the wave in K are $\mathbf{E} = (E_r, E_\theta, E_z)$ and $\mathbf{B} = (B_r, B_\theta, B_z)$ respectively. Similarly in K′, the electric and magnetic fields are $\mathbf{E}' = (E'_r, E'_\theta, E'_z)$ and $\mathbf{B}' = (B'_r, B'_\theta, B'_z)$ respectively. The relations between the electric field components in the two frames are given by

$$E'_r = \gamma(E_r - v_{||}B_\theta) \ , \ E'_\theta = \gamma(E_\theta + v_{||}B_r) \ , \ E'_z = E_z$$

Using (3.103..3.107), the components of $\mathbf{E}'$ are therefore

$$\begin{aligned} E'_r &= (1 - \frac{v_{||}}{v_g})E_r \\ E'_\theta &= (1 - \frac{v_{||}}{v_g})E_\theta \\ E'_z &= E_z \end{aligned}$$

Therefore if $v_{||} = v_g$, there is no transverse electric field in K′. Consequently, the rate of energy exchange is zero because

$$\frac{d\gamma}{dt} \propto \mathbf{E}'.\mathbf{v}' = E'_x v'_x + E'_y v'_y + E'_z v'_z = 0$$

as E'_x, E'_y and v'_z are all zero. Therefore no interaction occurs between the electron and the radiation field when $v_{||} = v_g$.

3.3.4 Scaling the TM Mode Evolution Equations

The full set of electron and field evolution equations are

$$\begin{aligned} \frac{d\phi_j}{dz} &= p_j \qquad (3.138) \\ &\quad + i\frac{ek_\perp D_{TM}}{4m_e u_{\perp_j} u_{||_j}} \left(\frac{k_{||}c^2}{\omega}\gamma_0 - u_{||0}\right) J_{m-1}(k_\perp R_0)\left(G_s e^{i\phi_j} - c.c.\right) \\ \frac{dp_j}{dz} &= \frac{ek_\perp k_{||} D_{TM}}{4m_e\omega_c}\left(\frac{k_{||}c^2}{\omega}\gamma_0 - u_{||0}\right) \times \end{aligned}$$

$$J_{m-1}(k_\perp R_0)\frac{u_{\perp_j}}{u_{\|_j}^2}\left(\frac{k_\perp^2}{k_\|}-p_j\right)\left(G_s e^{i\phi_j}+c.c.\right) \tag{3.139}$$

$$\frac{du_{\perp_j}}{dz} = \frac{e}{4m_e}k_\perp D_{TM}\left(\frac{k_\| c^2}{\omega}\gamma_0 - u_{\|0}\right)\times$$

$$\frac{1}{u_{\|_j}}J_{m-1}(k_\perp R_0)\left(G_s e^{i\phi_j}+c.c.\right) \tag{3.140}$$

$$\frac{du_{\|_j}}{dz} = \frac{e}{4m_e}\frac{k_\perp k_\|}{\omega_c}D_{TM}\left(\frac{k_\| c^2}{\omega}\gamma_0 - u_{\|0}\right)\times$$

$$J_{m-1}(k_\perp R_0)\frac{u_{\perp_j}}{u_{\|_j}}\left(G_s e^{i\phi_j}+c.c.\right) \tag{3.141}$$

$$\frac{dG_s(z)}{dz} = \frac{-\mu_0 I k_\perp \omega^2}{2c^2 k_\| k_{c0} u_{\|0}}\left(\frac{k_\| c^2}{\omega}\gamma_0 - u_{\|0}\right)\times$$

$$D_{TM}J_{m-1}(k_\perp R_0)\left\langle\frac{u_\perp}{u_\|}e^{-i\phi}\right\rangle \tag{3.142}$$

where ϕ_j and p_j have the same definition as for the TE mode interaction and $j = 1..N$. It has again been assumed that there is no spread in the perpendicular or parallel momenta of the electrons i.e. $u_{\perp 0}$ and $u_{\|0}$ are the same for all electrons. From this point on, the procedure for scaling the evolution equations is identical to that which was performed for the TE mode interaction in section 3.2.3. Defining

$$z' = 2k_{c0}z \quad , \quad p' = \frac{p}{2k_{c0}}$$

$$u'_\perp = \frac{u_\perp}{u_{\perp 0}} \quad , \quad u'_\| = \frac{u_\|}{u_{\|0}}$$

$$A' = -\frac{ek_\|}{8m_e c k_\perp}\frac{1}{u_{\|0}}\left(\frac{k_\| c^2}{\omega}\gamma_0 - u_{\|0}\right)D_{TM}J_{m-1}(k_\perp R_0)G_s(z)$$

then (3.138..3.142) become

$$\frac{d\phi_j}{dz'} = p'_j - \frac{k_\perp^2 c}{k_\| k_{c0} u_{\|0}}\frac{1}{u'_{\perp j}u'_{\|j}}\left(A'e^{i\phi_j}-c.c.\right) \tag{3.143}$$

$$\frac{dp'_j}{dz'} = -\frac{k_\perp^2 c u_{\perp 0}}{k_{c0}^2 u_{\|0}^2}\left(\frac{k_\perp^2}{2k_\| k_{c0}}-p'_j\right)\frac{u'_{\perp j}}{u'^2_{\|j}}\left(A'e^{i\phi_j}+c.c.\right) \tag{3.144}$$

$$\frac{du'_{\perp j}}{dz'} = -\frac{k_\perp^2 c}{k_\| k_{c0} u_{\perp 0}}\frac{1}{u'_{\|j}}\left(A'e^{i\phi_j}+c.c.\right) \tag{3.145}$$

$$\frac{du'_{\|j}}{dz'} = -\frac{k_\perp^2 c u_{\perp 0}}{k_{c0}^2 u_{\|0}^2}\frac{u'_{\perp j}}{u'_{\|j}}\left(A'e^{i\phi_j}+c.c.\right) \tag{3.146}$$

$$\frac{dA'}{dz'} = \frac{e\mu_0 I\omega^2}{32m_e c^3 k_{c0}^2}\frac{u_{\perp 0}}{u_{\|0}}\left(\frac{k_\| c^2}{\omega}\gamma_0 - u_{\|0}\right)^2 \times D_{TM}^2 J_{m-1}^2(k_\perp R_0)\left\langle \frac{u'_\perp}{u'_\|}e^{-i\phi}\right\rangle \quad (3.147)$$

Note that (3.143..3.146) are identical in form to (3.81..3.84). Therefore, from the scaling process used for the TE mode interaction, the following variables can be used

$$\hat{z} = c_1 z' \quad , \quad \hat{p} = c_2 p' \quad , \quad \hat{u_\perp} = c_3 u'_\perp \quad , \quad \hat{u_\|} = c_4 u'_\| \quad , \quad \hat{A} = c_5 A'$$

and the constants c_i, $i = 1..5$ can be defined by setting the coefficients in the resulting set of equations to 1. Therefore, as for the TE mode interaction, the set of equations is

$$\begin{aligned}
\frac{d\phi_j}{d\hat{z}} &= \hat{p}_j - i\frac{1}{\hat{u}_{\perp j}\hat{u}_{\|j}}\left(\hat{A}e^{i\phi_j} - c.c.\right)\\
\frac{d\hat{p}_j}{d\hat{z}} &= (\hat{p}_j - 1)\frac{\hat{u}_{\perp j}}{\hat{u}_{\|j}^2}\left(\hat{A}e^{i\phi_j} + c.c.\right)\\
\frac{d\hat{u}_{\perp j}}{d\hat{z}} &= -\frac{1}{\hat{u}_{\|j}}\left(\hat{A}e^{i\phi_j} + c.c.\right)\\
\frac{d\hat{u}_{\|j}}{d\hat{z}} &= -\frac{\hat{u}_{\perp j}}{\hat{u}_{\|j}}\left(\hat{A}e^{i\phi_j} + c.c.\right)\\
\frac{d\hat{A}}{d\hat{z}} &= \left\langle \frac{\hat{u}_\perp}{\hat{u}_\|}e^{-i\phi}\right\rangle
\end{aligned}$$

where

$$\begin{aligned}
\hat{z} &= \tfrac{k_\perp^2}{k_\|}z \quad , \quad \hat{p} = \tfrac{k_\|}{k_\perp^2}p\\
\hat{u_\perp} &= \tfrac{1}{u_{\|0}}\left(\tfrac{k_\| k_\perp^2 u_{\perp 0}^5}{4k_{c0}^3 c}\tfrac{1}{J}\right)^{\frac{1}{4}}u'_\perp \quad , \quad \hat{u_\|} = \tfrac{1}{2}\left(\tfrac{u_{\perp 0}k_\perp^2}{ck_\| k_{c0}}\tfrac{1}{J}\right)^{\frac{1}{2}}u'_\| \qquad (3.148)\\
\hat{A} &= \tfrac{1}{u_{\|0}}\left(\tfrac{k_\perp^6 c u_{\perp 0}}{4k_\| k_{c0}^5}\tfrac{1}{J^3}\right)^{\frac{1}{4}}A'
\end{aligned}$$

and the only difference from the TE mode case is in the definition of J which in this case is

$$J = \frac{e\mu_0 I\omega^2}{32m_e c^3 k_{c0}^2}\frac{u_{\perp 0}}{u_{\|0}}\left(\frac{k_\| c^2}{\omega}\gamma_0 - u_{\|0}\right)^2 D_{TM}^2 J_{m-1}^2(k_\perp R_0). \quad (3.149)$$

Following the analysis of the TE mode interaction, these equations can be rewritten in terms of the variables

$$\bar{z} = K_1 \hat{z} \quad , \quad \bar{p} = \frac{\hat{p}}{K_1}$$

$$\bar{u}_\perp = u'_\perp = \frac{u_\perp}{u_{\perp 0}} \quad , \quad \bar{u}_\parallel = u'_\parallel = \frac{u_\parallel}{u_{\parallel 0}}$$

$$\bar{A} = K_2 \hat{A}$$

where K_1 and K_2 have been defined in (3.96). Consequently, the constant K_1 will be renamed ρ_{TM}, which is found to be

$$\rho_{TM} = \left(\frac{e}{8 m_e c^2} \frac{\omega^2 k_\parallel^2}{k_\perp^2 k_{c0}^2} \mu_0 I \frac{u_{\perp 0}^2}{u_{\parallel 0}^3} \left(\frac{k_\parallel c^2 \gamma_0}{\omega u_{\parallel 0}} - 1 \right)^2 D_{TM}^2 J_{m-1}^2 (k_\perp R_0) \right)^{\frac{1}{3}} \tag{3.150}$$

using (3.149). The constant K_2 then becomes

$$K_2 = \left(\frac{\rho_{TM}}{\nu} \right)^{\frac{1}{4}}$$

where ν is given by (3.100). Note that unlike ρ, the definition of ν is independent of the mode type. As for TE modes, the 'hat' variables ($\hat{}$) can be written in terms of ρ and ν i.e.

$$\hat{z} = \frac{\bar{z}}{\rho} \quad , \quad \hat{p} = \rho \bar{p}$$

$$\hat{u}_\perp = \left(\frac{\nu}{\rho} \right)^{\frac{3}{4}} u'_\perp \quad , \quad \hat{u}_\parallel = \frac{1}{\rho} \left(\frac{\nu}{\rho} \right)^{\frac{1}{2}} u'_\parallel$$

$$\hat{A} = \left(\frac{\nu}{\rho} \right)^{\frac{3}{4}} \bar{A}$$

The set of evolution equations for both TE and TM modes is therefore

$$\frac{d\phi_j}{d\bar{z}} = \bar{p}_j - i \frac{\mu}{\bar{u}_\perp \bar{u}_\parallel} \left(\bar{A} e^{i\phi_j} - c.c. \right) \tag{3.151}$$

$$\frac{d\bar{p}_j}{d\bar{z}} = (\rho \bar{p}_j - 1) \frac{\bar{u}_{\perp j}}{\bar{u}_{\parallel j}^2} \left(\bar{A} e^{i\phi_j} + c.c. \right) \tag{3.152}$$

$$\frac{d\bar{u}_{\perp j}}{d\bar{z}} = -\frac{\mu}{\bar{u}_{\|j}}\left(\bar{A}e^{i\phi_j} + c.c.\right) \tag{3.153}$$

$$\frac{d\bar{u}_{\|j}}{d\bar{z}} = -\rho\frac{\bar{u}_{\perp j}}{\bar{u}_{\|j}}\left(\bar{A}e^{i\phi_j} + c.c.\right) \tag{3.154}$$

$$\frac{d\bar{A}}{d\bar{z}} = \left\langle \frac{\bar{u}_{\perp}}{\bar{u}_{\|}} e^{-i\phi} \right\rangle \tag{3.155}$$

where $\mu = \rho/\nu$, $\rho = \rho_{TE}$ for a TE mode interaction and $\rho = \rho_{TM}$ for a TM mode interaction.

It has been shown that the interaction between a relativistic beam of electrons gyrating and drifting in a uniform magnetic field and a TE_{mn} or TM_{mn} waveguide mode can be described by the same set of universally scaled evolution equations. The difference between the two interactions is incorporated into the analysis by using different definitions of the ρ parameter for each case.

3.4 Analysis of the Scaled Equations

In this section, the universally scaled equations derived in the previous sections will be used to investigate the physical processes which occur during the CRM interaction in the steady-state regime.

3.4.1 Constants of the Motion

It is possible to obtain a constant of the motion relating the scaled electromagnetic field intensity to the axial momenta of the electrons by averaging (3.154) over a range of ϕ from 0 to 2π, which results in

$$\frac{d\langle\bar{u}_{\|}\rangle}{d\bar{z}} = -\rho\left(\bar{A}\langle\frac{\bar{u}_{\perp}}{\bar{u}_{\|}}e^{i\phi}\rangle + \bar{A}^{*}\langle\frac{\bar{u}_{\perp}}{\bar{u}_{\|}}e^{-i\phi}\rangle\right)$$

$$= -\rho\left(\bar{A}\frac{d\bar{A}^*}{d\bar{z}} + \bar{A}^*\frac{d\bar{A}}{d\bar{z}}\right)$$
$$= -\rho\frac{d|\bar{A}|^2}{d\bar{z}}$$

where (3.155) has also been used. Consequently,

$$\frac{d}{d\bar{z}}\left(\rho|\bar{A}|^2 + \langle\bar{u}_{\|}\rangle\right) = 0$$

so the constant of motion relating the scaled axial momentum of the electrons to the electromagnetic field intensity is

$$\rho|\bar{A}|^2 + \langle\bar{u}_{\|}\rangle = \rho|\bar{A}_0|^2 + 1 \tag{3.156}$$

as $\bar{A} = \bar{A}_0$ and $\bar{u}_{\|} = 1$ at $\bar{z} = 0$. Using (3.121), (3.156) can be rearranged to give

$$\rho\left(|\bar{A}|^2 - |\bar{A}_0|^2\right) = \frac{v_g}{v_{\|0}}\frac{(\gamma_0 - 1)}{\gamma_0}\eta \tag{3.157}$$

where η is the interaction efficiency, defined as

$$\eta = \left(\frac{\gamma_0 - \langle\gamma\rangle}{\gamma_0 - 1}\right)$$

and $v_g = c^2 k_{\|}/\omega$ is the group velocity of the radiation.

From (3.152..3.154), there is a functional relationship between the variables $\bar{p}$, $\bar{u}_{\perp}$ and $\bar{u}_{\|}$ which is just (3.92) written in the new scaling i.e.

$$\frac{1}{\rho\bar{p} - 1}\frac{\bar{u}_{\|}^2}{\bar{u}_{\perp}}d\bar{p} = -\frac{1}{\mu}\bar{u}_{\|}d\bar{u}_{\perp} = -\frac{1}{\rho}\frac{\bar{u}_{\|}}{\bar{u}_{\perp}}d\bar{u}_{\|} \tag{3.158}$$

This means that $\bar{u}_{\perp}$ and $\bar{p}$ can be written in terms of the axial momentum $\bar{u}_{\|}$, and two of the five evolution equations become redundant. The interaction can therefore be described by the three evolution equations

$$\frac{d\phi_j}{d\bar{z}} = \frac{1}{\bar{u}_{\|j}}\left(\delta - \frac{1}{\rho}\right) + \frac{1}{\rho} - i\frac{\mu}{\bar{u}_{\|j}\sqrt{1 + \frac{2\mu}{\rho}\left(\bar{u}_{\|j} - 1\right)}}\left(\bar{A}e^{i\phi_j} - c.c.\right) \tag{3.159}$$

$$\frac{d\bar{u}_{\|_j}}{d\bar{z}} = -\rho\frac{\sqrt{1+\frac{2\mu}{\rho}\left(\bar{u}_{\|_j}-1\right)}}{\bar{u}_{\|_j}}\left(\bar{A}e^{i\phi_j}+c.c.\right) \tag{3.160}$$

$$\frac{d\bar{A}}{d\bar{z}} = \left\langle\frac{\sqrt{1+\frac{2\mu}{\rho}\left(\bar{u}_{\|}-1\right)}}{\bar{u}_{\|}}e^{-i\phi}\right\rangle \tag{3.161}$$

Note that $\bar{u}_{\|}$ can be expressed in terms of $\bar{u}_{\perp}$ i.e.

$$\bar{u}_{\|} = \frac{\nu}{2}(\bar{u}_{\perp}^2-1)+1 \tag{3.162}$$

The parameter $\nu \equiv \rho/\mu$ therefore determines the amount of axial momentum change relative to the perpendicular energy change of the electron.

Substituting for $\bar{u}_{\|}$ in (3.156) produces a constant of motion relating the perpendicular momenta of the electrons to the electromagnetic field intensity :

$$\rho\left(|\bar{A}|^2-|\bar{A}_0|^2\right) = -\frac{\nu}{2}\left(\langle\bar{u}_{\perp}^2\rangle-1\right) \tag{3.163}$$

From (3.157), it is clear that the efficiency will be maximised when $\langle\bar{u}_{\perp}^2\rangle = 0$ i.e. when the transverse energy of the electrons is exhausted. If this occurs, the efficiency will be

$$\eta_{max} = \frac{v_{\|0}}{v_g}\frac{\gamma_0}{(\gamma_0-1)}\frac{\nu}{2} \tag{3.164}$$

Consequently, sufficiently small values of ν will limit the energy of the electron beam available for transfer to the radiation field. For this reason, ν is termed the 'Free Energy Parameter'. It is now apparent why ν does not depend on whether a TE or TM mode is involved in the interaction. Note that, from the definition of ν,

$$\eta_{max} = \frac{v_{\perp 0}^2}{2c^2}\frac{\gamma_0}{(\gamma_0-1)}\frac{\omega}{(\omega_c/\gamma_0)}$$

This suggests that for a given set of beam parameters, if all the transverse electron energy is exhausted, interactions which involve a large Doppler shift (e.g. CARM,

where $\omega >> \omega_c/\gamma_0$) will be more efficient than those involving small Doppler shifts (e.g. gyrotron, where $\omega \approx \omega_c/\gamma_0$). As this is that which would occur if every particle gave up all its transverse energy to the field, it is sometimes termed the 'single particle efficiency' and denoted by η_{sp} [19]. The actual efficiency of the interaction is then

$$\eta = \eta_{sp}\left(1 - \langle \bar{u}_\perp^2 \rangle\right)$$

.

3.4.2 The Meaning of ρ

From (3.157), it can be seen that the limit $\rho << 1$ corresponds to the limit of low efficiency. The reason for this is apparent from (3.154), which when $\rho << 1$ implies

$$\bar{u}_\parallel \approx 1 \tag{3.165}$$

so clearly very little energy is being extracted from the axial motion of the electrons. i.e. the 'recoil' of the electrons is negligible. The energy extraction is therefore almost exclusively from the perpendicular energy of the electrons. A consequence of (3.165) is that the functional relation between $\bar{p}$ and $\bar{u}_\perp$ becomes

$$\bar{u}_\perp = \sqrt{1 + 2\mu(\bar{p} - \delta)} \tag{3.166}$$

where $\delta = \bar{p}(\bar{z} = 0)$ is the initial detuning from resonance. The set of equations (3.151..3.155) can then be reduced to

$$\frac{d\phi_j}{d\bar{z}} = \bar{p}_j - i\frac{\mu}{\sqrt{1 + 2\mu(\bar{p}_j - \delta)}}\left(\bar{A}e^{i\phi_j} - c.c.\right) \tag{3.167}$$

$$\frac{d\bar{p}_j}{d\bar{z}} = -\sqrt{1 + 2\mu(\bar{p}_j - \delta)}\left(\bar{A}e^{i\phi_j} + c.c.\right) \tag{3.168}$$

$$\frac{d\bar{A}}{d\bar{z}} = \left\langle \sqrt{1+2\mu(\bar{p}-\delta)}e^{-i\phi} \right\rangle \tag{3.169}$$

For the purposes of numerical integration, it is better to rewrite (3.167..3.169) in terms of $\bar{u}_\perp$ using (3.166) to give

$$\frac{d\phi_j}{d\bar{z}} = \frac{\bar{u}_{\perp j}^2 - 1}{2\mu} + \delta - i\frac{\mu}{\bar{u}_{\perp j}}\left(\bar{A}e^{i\phi_j} - c.c.\right) \tag{3.170}$$

$$\frac{d\bar{u}_{\perp j}}{d\bar{z}} = -\mu\left(\bar{A}e^{i\phi_j} + c.c.\right) \tag{3.171}$$

$$\frac{d\bar{A}}{d\bar{z}} = \langle \bar{u}_\perp e^{-i\phi} \rangle \tag{3.172}$$

Averaging (3.168) over ϕ, it is possible to find a constant of the motion for this set of equations as

$$\begin{aligned}\frac{d\langle\bar{p}\rangle}{d\bar{z}} &= -\left(\bar{A}\langle\sqrt{1+2\mu(\bar{p}-\delta)}e^{i\phi}\rangle + \bar{A}^*\langle\sqrt{1+2\mu(\bar{p}-\delta)}e^{-i\phi}\rangle\right) \\ &= -\left(\bar{A}\frac{d\bar{A}^*}{d\bar{z}} + \bar{A}^*\frac{d\bar{A}}{d\bar{z}}\right) \\ &= \frac{d|\bar{A}|^2}{d\bar{z}}\end{aligned}$$

where (3.169) has also been used. Consequently,

$$\frac{d}{d\bar{z}}\left(|\bar{A}|^2 + \langle\bar{p}\rangle\right) = 0$$

so that

$$|\bar{A}|^2 + \langle\bar{p}\rangle = |\bar{A}_0|^2 + \delta \tag{3.173}$$

as $\bar{A} = \bar{A}_0$ and $\bar{p} = \delta$ at $\bar{z} = 0$. Multiplying both sides of (3.173) by ρ and using (3.157) then it is easily shown that

$$\eta = \frac{v_{\|0}}{v_g}\frac{\gamma_0}{(\gamma_0 - 1)}\rho\left(\delta - \langle\bar{p}\rangle\right) \tag{3.174}$$

so the energy change of the jth electron is proportional to $\rho\left(\bar{p}_j - \delta_j\right)$ in the limit $\rho << 1$ i.e. in this limit, the change in the detuning of the electron $(\bar{p}_j - \delta_j)$ is directly proportional to the energy change of the electron.

In addition to the energy conservation relation, there is also a phase-dependent constant of motion. If b is used to represent the source term of the wave equation i.e.

$$b = \left\langle \sqrt{1 + 2\mu(\bar{p} - \delta)} e^{-i\phi} \right\rangle \tag{3.175}$$

then the evolution equations (3.167..3.169) can be used to show that

$$\frac{d}{d\bar{z}} (A^* b - A b^*) = i \left\langle \bar{p} \frac{d\bar{p}}{d\bar{z}} \right\rangle = \frac{i}{2} \frac{d \langle \bar{p}^2 \rangle}{d\bar{z}} \tag{3.176}$$

so the constant of the motion is

$$\frac{\langle \bar{p}^2 \rangle}{2} + i \left(\bar{A}^* b - \bar{A} b^* \right) = \text{constant} \tag{3.177}$$

This constant is actually the Hamiltonian of the system and will be discussed in more detail in section 5.1.

Consider now the effect of relaxing the limit $\rho << 1$. This implies that the axial momentum and hence the energy of the electrons can now vary appreciably, leading to higher efficiencies. One method of increasing ρ is to increase the beam current and consequently the electron density of the beam. However, when the electron density of the beam is large, it becomes necessary to include the effect of space charge forces on the interaction. Unfortunately, although the problem of space-charge effects can be tackled more readily in devices such as the FEL [66] where the space charge forces depend on the relative positions of the electrons in only one dimension (z), this is not the case for CRM-type devices where the space charge forces also depend on the transverse position of the electrons. For this reason, the analysis described here neglects high-beam density effects, as they require a full three-dimensional treatment.

When $\rho \ll 1$ and $\bar{p} > 0$, the sign of the factor $\rho\bar{p} - 1$ in (3.152) becomes important. Comparing (3.152) with its unscaled equivalent (3.80), and recalling the significance of each term in the bracket of (3.80), it is clear that the 1 in $\rho\bar{p} - 1$ arises from the change in the electron energy, whereas the $\rho\bar{p}$ arises from the change in the axial velocity of the electron. In chapter 2, it was shown that changes in γ resulted in azimuthal bunching, whereas changes in $v_{||}$ resulted in axial bunching. The sign of $\rho\delta - 1$ therefore determines which bunching mechanism is dominant. If $\rho\delta = 1$, $d\bar{p}/d\bar{z}$ will be zero. This means that $\bar{p}$ remains constant, even while the energy of the electron is changing. Note that for a significant energy exchange to occur, δ cannot be very large, so this effect cannot occur for small values of ρ. i.e. the variation of the axial momentum of the electron plays a crucial role. As $\bar{p}$ is a constant under these conditions, if the electron and the field are initially close to resonance, they will remain close to resonance for as long as free energy depletion effects remain small. The condition

$$\rho\delta = 1 \tag{3.178}$$

is therefore the condition for exact autoresonance to occur, where the change in the cyclotron frequency of the electron (ω_c/γ) due to the variation of the relativistic electron mass is exactly compensated by the change in the Doppler shift ($k_{||}u_{||}/\gamma$) due to the variation of the axial momentum of the electron. The product $\rho\delta = \delta$ so (3.178) can be written in unscaled variables using (3.91) as

$$\omega - \frac{\omega_c}{\gamma_0} - k_{||}v_{||0} = \frac{k_\perp^2}{k_{||}}v_{||0} \tag{3.179}$$

When averaging the evolution equations in sections 3.2 and 3.3 over a gyroperiod to make the resultant equations slowly varying, it was necessary to use

the condition

$$\omega - \frac{\omega_c}{\gamma_0} - k_{||} v_{||0} \approx 0 \tag{3.180}$$

so for consistency (3.178) can only be satified for waveguide modes which propagate close to the waveguide axis i.e. $k_\perp \ll k_{||}$. The axial electron velocity must remain finite as this analysis is concerned with convective instabilities only, i.e. those which propagate in space. Note that (3.179) implies that it is only possible for autoresonance to occur at exact resonance in free space ($k_\perp = 0$). Devices which operate using a relativistic electron beam gyrating in a uniform magnetic field in free space are termed 'nonwiggler FELs' [67, 68]. For autoresonance to occur in a system where the radiation field is contained within a waveguide, a positive detuning is necessary.

3.4.3 The Meaning of μ

When the limit $\mu << 1$ is applied, it can be seen from (3.153) that

$$\bar{u}_\perp \approx 1 \tag{3.181}$$

Therefore, the perpendicular momentum of the electrons remains approximately constant. The equations (3.167..3.169) in the limit $\mu << 1$ are

$$\frac{d\phi_j}{d\bar{z}} = \bar{p}_j \tag{3.182}$$

$$\frac{d\bar{p}_j}{d\bar{z}} = -(\bar{A} e^{i\phi_j} + c.c.) \tag{3.183}$$

$$\frac{d\bar{A}}{d\bar{z}} = \langle e^{-i\phi} \rangle \tag{3.184}$$

Note that these equations were derived in section 3.2.3, after several approximations were made. i.e.

$$|\hat{p}|, |\hat{\delta}| \ << 1 \tag{3.185}$$

$$2\frac{\hat{u}_{\|0}}{\hat{u}_{\perp 0}}(\hat{p} - \hat{\delta}) << 1 \quad , \quad \left|\frac{\hat{A}}{\hat{u}_{\|}\hat{u}_{\perp}}\right| << 1 \tag{3.186}$$

Writing the 'hat' variables ($\hat{}$) in terms of ρ and μ using (3.101), the conditions (3.185) and (3.186) correspond to the limits $\rho << 1$ and $\mu << 1$ respectively. On inspection of equations (3.182..3.183), it can be seen that the number of electron variables has been reduced to just two: the phase or position of the electrons in the ponderomotive potential due to the combined action of the electron motion in the guiding magnetic field and the wave field, and the energy change of the electron. It is possible under certain conditions to reduce the equations of motion for several other beam-wave devices e.g. Compton FELs, Cerenkov masers and Smith-Purcell lasers to exactly the form of (3.182..3.184) [69]. The gain-mechanism in all these devices is due to electrons bunching in phase due to the action of the electromagnetic field and collectively losing energy to the field. The special property of equations (3.182..3.184) is that there are no free parameters, so for the initial conditions of $\delta = 0$ and $|\bar{A}_0|^2 \ll 1$, there is only one solution, which is shown in figure 3.3. The value of the scaled electromagnetic field intensity at saturation is $|\bar{A}|^2 \approx 1.4$. It has already been shown in (3.157) that

$$\rho\left(|\bar{A}|^2 - |\bar{A}_0|^2\right) \propto \eta \propto \frac{U_F}{U_B}$$

where U_F and U_b are the energy densities of the electromagnetic field and the electron beam respectively. The beam energy density is proportional to the elec-

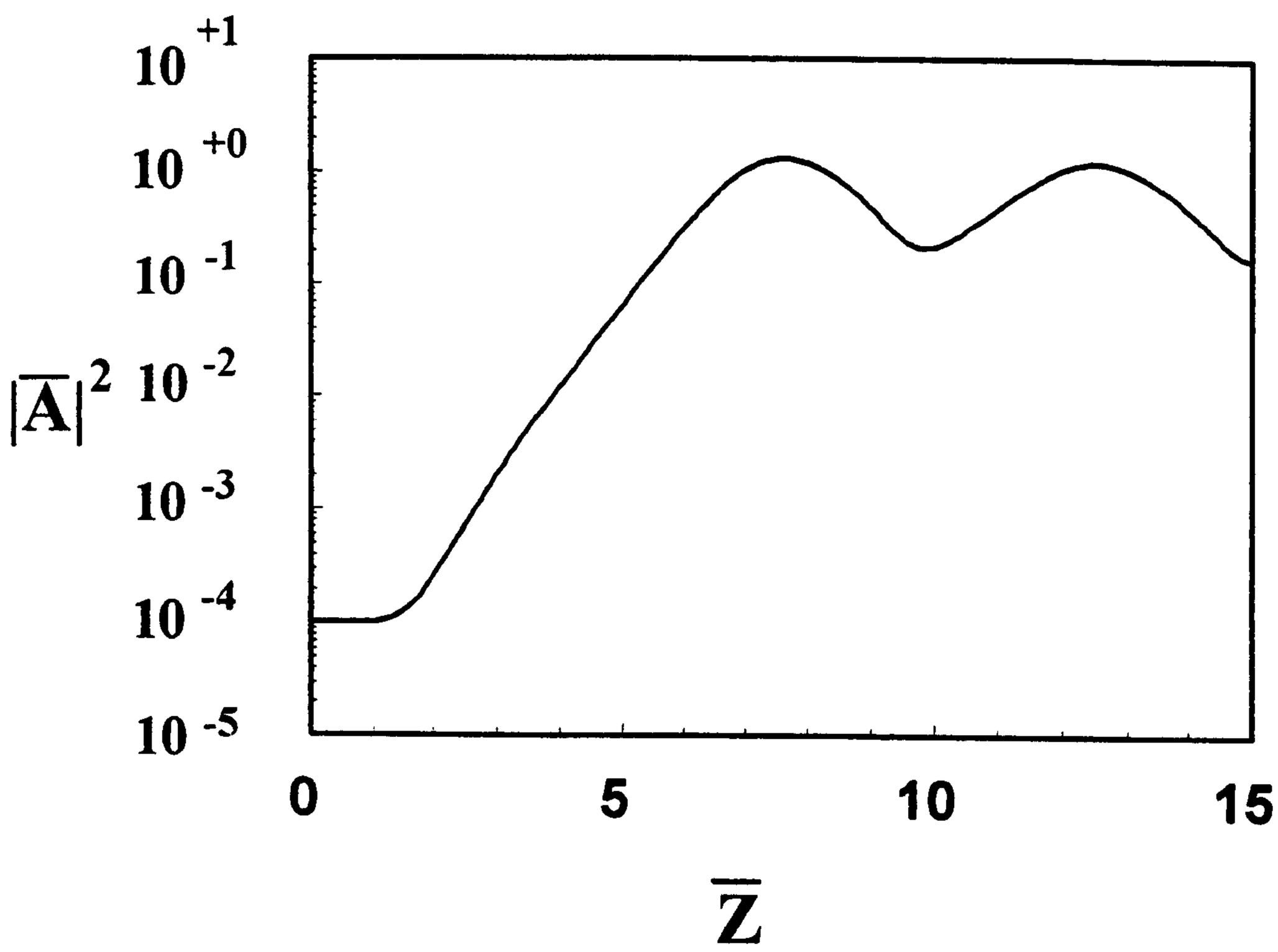

Figure 3.3: Solution to equations (3.182..3.184)

tron number density, n_e, which can be shown to be proportional to ρ^3 from (3.98) and (3.150). Consequently, at saturation, where $|\bar{A}|^2 \sim 1$ and $|\bar{A}_0|^2 \ll |\bar{A}|^2$, the electromagnetic field intensity I_{sat} varies as

$$I_{sat} \propto \rho^4 \propto {n_e}^{4/3} \tag{3.187}$$

This simple deduction demonstrates the usefulness of the universal scaling in determining the physical relationship between different quantities.

Consider now the effect of relaxing the limit on μ. Inspection of (3.153) shows that the perpendicular momentum of any electron may vary appreciably from its initial value. From equations (3.167) and (3.168) it can be seen that as the field amplitude grows then for an electron which is giving up its perpendicular energy to the field, as $\bar{u}_\perp$ decreases the second term in (3.167) will cause $d\phi_j/d\bar{z}$ to become large. The electrons losing transverse energy to the field therefore tend to fall out of resonance and their energy exchange with the field becomes small. This loss of resonance does not occur for electrons which are absorbing energy from the field. This effect is termed 'Free Energy Depletion' [51] as it is due to the exhaustion of the free energy of the beam which drives the interaction. From the simple arguments above, it is obvious that free energy depletion has a detrimental effect on the amplification of the radiation. As μ determines the importance of free energy depletion effects, it is named the 'Depletion Parameter'. The second term in (3.167) is sometimes called the 'force bunching' term as it is proportional to the field amplitude. The first term is called the 'inertial bunching' term as it is related to the variation of the relativistic mass change and the axial momentum variation of the electron.

Figure 3.4 shows the evolution of an initially monoenergetic, resonant ($\delta = 0$), unbunched electron beam for the case where free energy depletion effects are negligible ($\mu << 1$). The electrons can be seen to bunch in phase ($q = \phi + \xi$) as the interaction progresses. These bunched electrons then lose energy to the wave until saturation is reached when the bunched electrons reach the bottom of the potential well. After saturation, the electrons trapped in the potential well oscillate about the potential minimum. In the FEL literature, these oscillations are called 'synchrotron oscillations' [70]. Figure 3.5 shows the evolution of a beam of electrons for the same initial conditions as that of figure 3.4 with the exception that free energy depletion effects are not negligible ($\mu = 0.5$ in this case). It can be seen that although the electrons begin to bunch in phase and lose energy to the wave, they only lose a relatively small amount of energy before the free energy depletion effects cause the bunched electrons to disperse, effectively halting the energy exchange. From the relation between $\bar{u}_\perp$ and $\bar{p}$ in the limit $\rho \ll 1$, equation (3.166), it is clear that there is a lower limit on $\bar{p}$ of

$$\bar{p}_{min} = \delta - \frac{1}{2\mu} \tag{3.188}$$

which corresponds to the value of $\bar{p}$ when $\bar{u}_\perp = 0$. The limit is clearly seen in figure 3.5, where $\mu = 0.5$ and $\delta = 0$, so $\bar{p}_{min} = -1$.

The effect of different values of μ for the same ρ parameter on the radiation field evolution is seen from numerical solutions to equations (3.151..3.155) for a case where the electrons and the electromagnetic field are resonant ($\delta = 0$) in figure 3.6. To obtain these solutions, a collection of N particles, ($N = 50$ in the cases shown here), were spaced equally in ϕ over the range 0 to 2π and the field

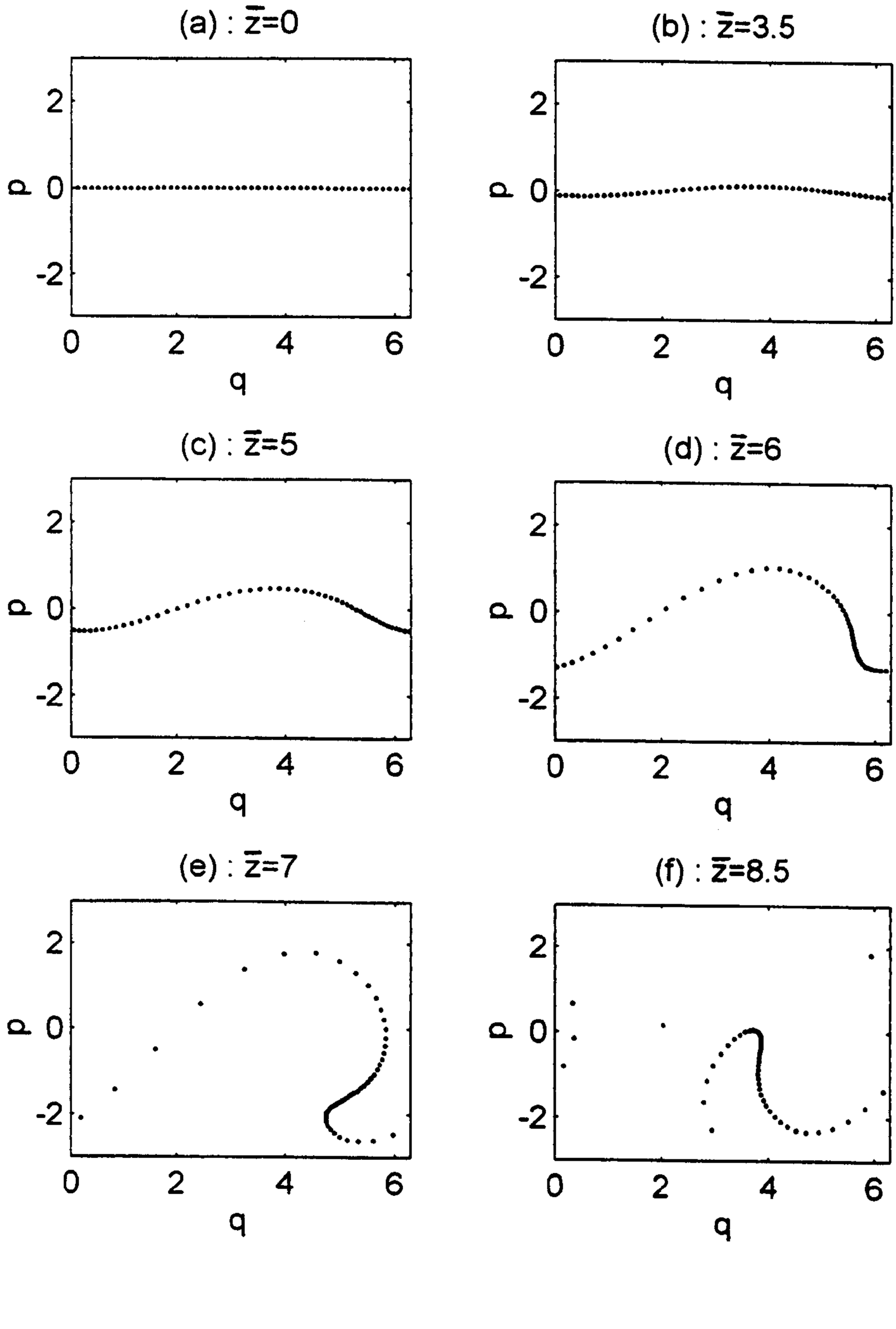

Figure 3.4: Electron evolution when free energy effects are negligible ($\mu \ll 1$).

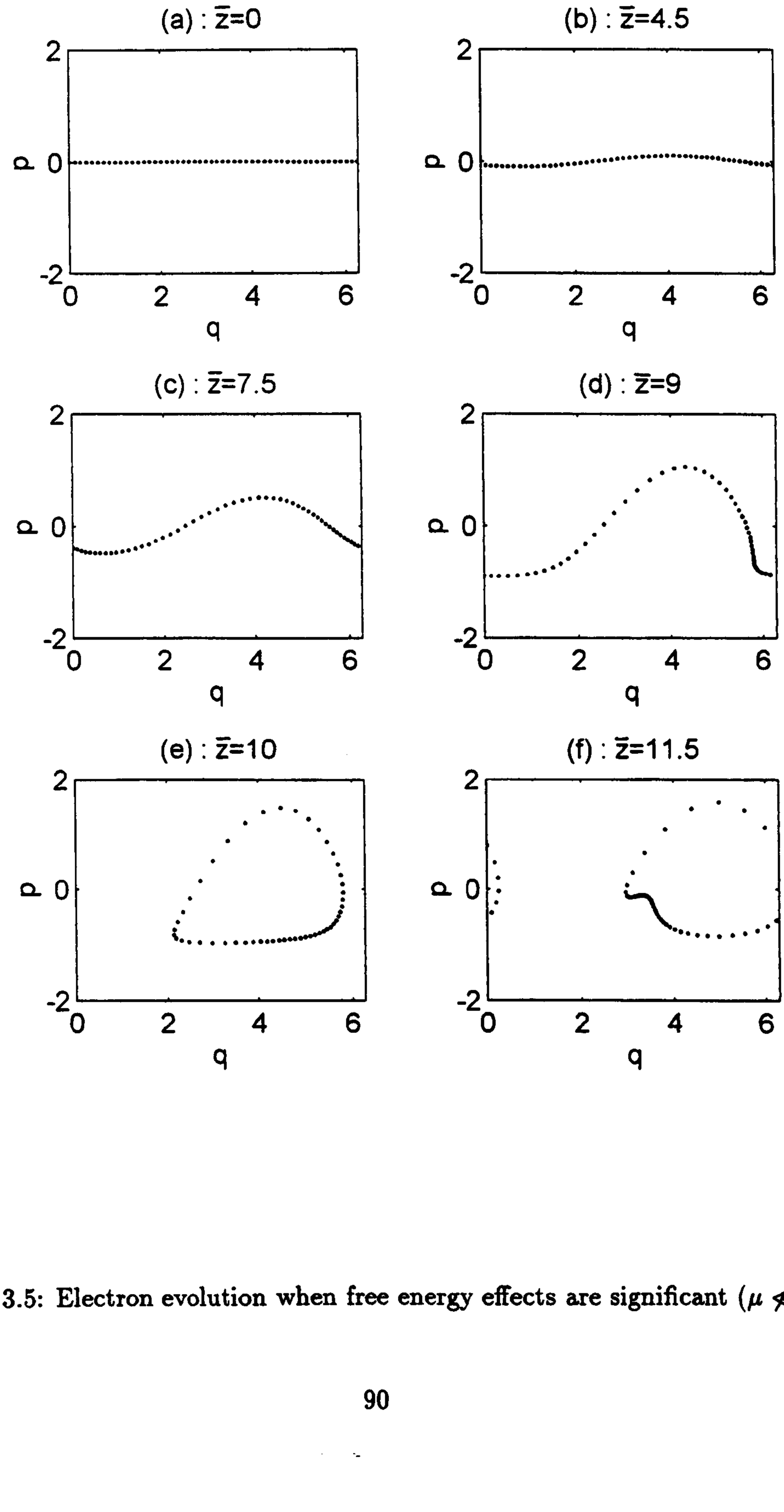

Figure 3.5: Electron evolution when free energy effects are significant ($\mu \not\ll 1$).

amplitude was set at a small value ($|\bar{A}| = 10^{-2}$ here) at $\bar{z} = 0$. As μ is increased, it can be seen that changes occur in several regions of the field evolution : At the beginning of the interaction, the field intensity remains approximately constant when $\bar{z} < 1$ for small values of μ. This phenomena is called 'lethargy' and will be treated in more detail in chapter 4. As μ is increased, the field intensity decreases in this region before increasing and entering the region of exponential growth. It can be seen from the graphs that another effect of increasing μ is to decrease the rate of exponential growth and the value of the field intensity at saturation. A plot of the saturation intensity against μ is shown in figure 3.7 for the conditions used to obtain graphs (a)..(c) in figure 3.6. The other main effect of increasing μ which can be seen from these graphs is that the synchrotron-type oscillations which occur after saturation for small values of μ become less pronounced, with both their amplitude and regularity decreasing. This is due to the fact that at saturation, the electrons which have lost energy to the field no longer oscillate about the bottom of a potential well as was the case for $\mu << 1$ as their phase 'velocity' $d\phi/d\bar{z}$ increases as they lose energy, making trapping impossible.

3.4.4 Axial Momentum Depletion

Consider the relation between the axial momentum change of an electron and the change in its perpendicular energy, which is found by rearranging (3.162) and states that

$$\frac{\bar{u}_{\parallel} - 1}{\bar{u}_{\perp}^2 - 1} = \frac{\rho}{2\mu} = \frac{\nu}{2}. \tag{3.189}$$

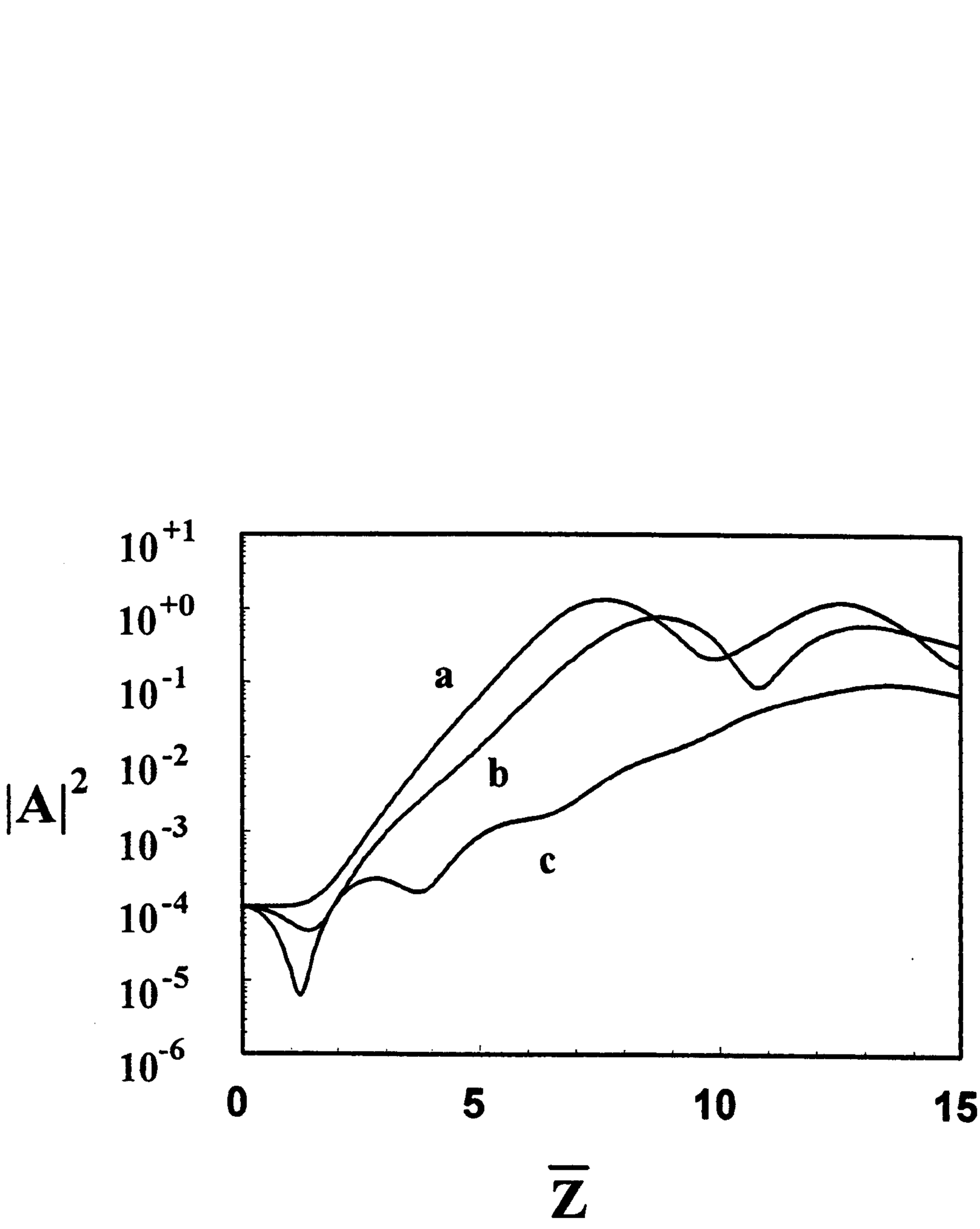

Figure 3.6: Field intensity evolution for different values of μ : (a) $\mu = 0.01$, (b) $\mu = 0.25$ (c) $\mu = 0.75$

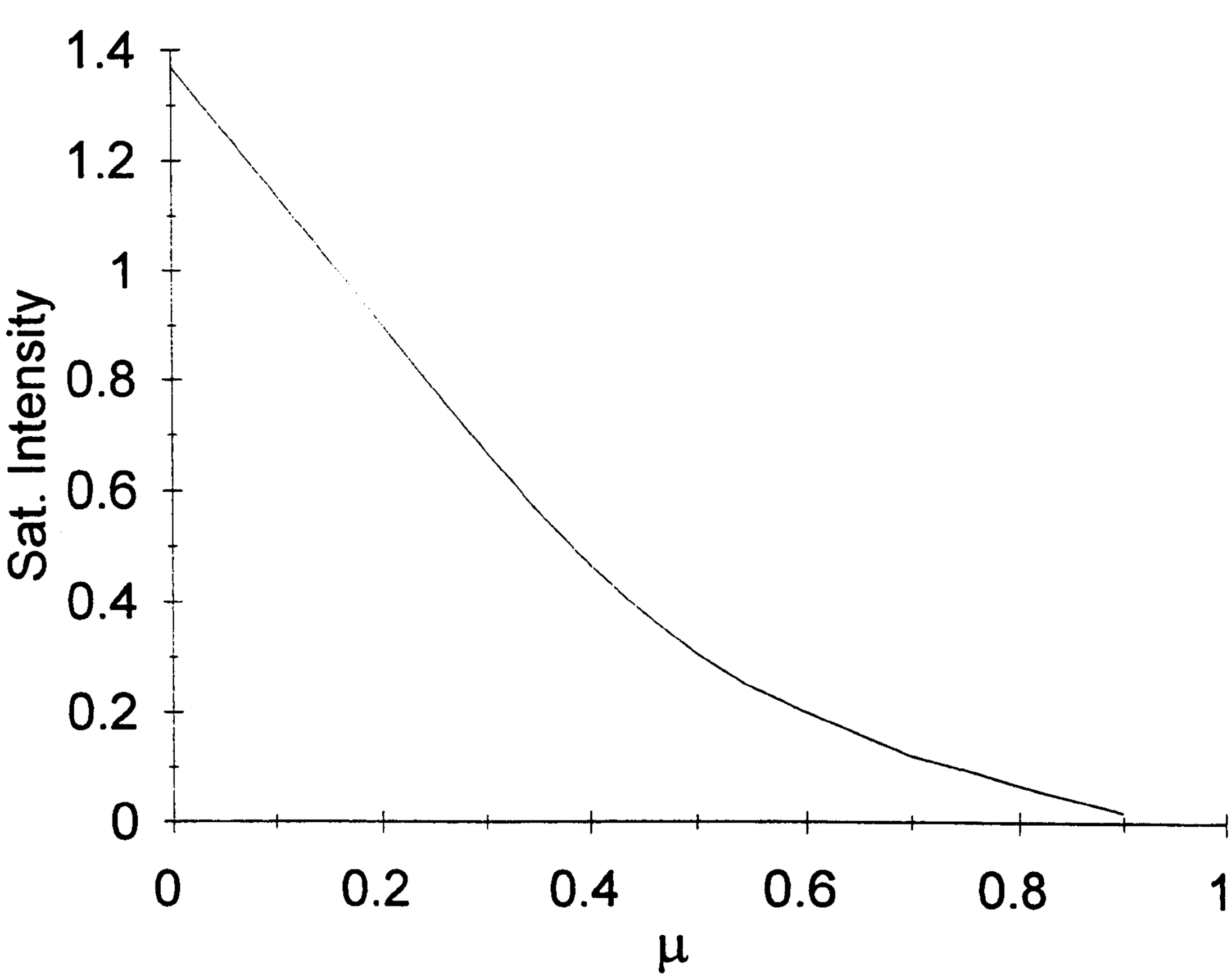

Figure 3.7: Plot of saturation intensity against μ for $\rho \ll 1$

If $\rho > 2\mu$, then $\bar{u}_{\|} < \bar{u}_{\perp}^2$ and it becomes possible for $\bar{u}_{\|} \rightarrow 0$ and become negative. i.e. the electron can slow down, stop and begin to move backwards. This causes the solution to the evolution equations to be numerically unstable as the integration is with carried out with respect to z. This was found to occur when $\rho \gtrsim 0.4$. In an attempt to avoid this problem in a numerical integration, any electrons whose axial momentum approaches sufficiently close to zero is 'switched off' and makes no further contribution to the evolution of the radiation field. This is justified physically because an electron travelling in the opposite direction to that of the field propagation will be massively out of resonance with the electromagnetic field.

3.4.5 Energy and Momentum Spreads

The derivation of equations (3.151..3.155) was carried out for the case of no spread in the electron energies or momenta. For the case where spreads in these quantities exist and the interaction involves a TE mode, these same equations can be used if a different definition of $\bar{u}_{\perp}$ and $\bar{u}_{\|}$ is used i.e.

$$\bar{u}_{\perp} = \frac{u_{\perp}}{\langle \bar{u}_{\perp 0} \rangle} \qquad \bar{u}_{\|} = \frac{u_{\|}}{\langle \bar{u}_{\|0} \rangle}$$

The definitions of ρ and ν then become

$$\rho = \left(\frac{e}{8m_e} \frac{k_{\|}^2}{k_{\perp}^2} \frac{\langle u_{\perp 0} \rangle^2}{\langle u_{\|0} \rangle^3} \mu_0 I D_{TE}^2 J_{m-1}^2(k_{\perp} R_0) \right)^{\frac{1}{3}} \tag{3.190}$$

$$\nu = \frac{k_{\|}}{k_{c0}} \frac{\langle u_{\perp 0} \rangle^2}{\langle u_{\|0} \rangle^2} \tag{3.191}$$

The constant of motion (3.156) is unchanged for the case of momentum spreads but (3.163) becomes

$$\rho\left(|\bar{A}|^2 - |\bar{A}_0|^2\right) = \frac{\nu}{2}\left(1 + \frac{\sigma_{\perp 0}^2 - \langle u_\perp^2 \rangle}{\langle u_{\perp 0} \rangle^2}\right) \tag{3.192}$$

where $\sigma_{\perp 0}^2$ is the variance of the initial distribution of transverse electron momenta. In addition, the relation between the scaled field intensity and the interaction efficiency, η, becomes

$$\rho\left(|\bar{A}|^2 - |\bar{A}_0|^2\right) = \frac{v_g}{\langle u_{\|0} \rangle}(\langle \gamma_0 \rangle - 1)\eta \tag{3.193}$$

where η is now defined as

$$\eta = \left(\frac{\gamma_0 - \langle \gamma \rangle}{\langle \gamma_0 \rangle - 1}\right)$$

An attempt was made to apply this type of scaling to interactions involving TM modes and electron beams with spreads in energy and momentum. However, due to the presence of the $(v_g \gamma_{0j} - u_{\|0j})$ terms in (3.138..3.142), the averaging over the initial distributions was found to be inhibitively complicated.

3.5 Conclusions

It has been shown in this chapter that starting from the Lorentz equation of motion for an electron in an electromagnetic field and Maxwell's equations, it is possible to derive a system of universally scaled equations which describe the processes which occur in a CRM amplifier in the steady-state regime. Using this universally scaled set, the number of parameters is reduced to just three, ρ, the fundamental cyclotron parameter, ν, the free energy parameter, and δ, the detuning parameter. ρ and ν are then combined to form the depletion parameter,

μ. By considering various limits of these parameters, the different phenomena which occur in CRM amplifiers were studied. In the limit where the variation of the transverse and axial momentum of the electron beam was very small, the set of evolution equations reduced to a set which had no free parameters. This set of equations can also be used to describe the gain mechanism in several other types of electron beam-wave devices such as the high-gain Compton FEL, the Cerenkov maser and the Smith-Purcell laser.

Chapter 4

Linear Analysis of the CRM Interaction

4.1 Introduction

In this chapter, the linear regime of the CRM interaction in the steady state limit is analysed using the scaled evolution equations derived in chapter 3. The linear analysis described in this chapter is performed using a different method from the conventional plasma theoretical approaches which were reviewed in chapter 2. The results of the differing analyses will be discussed and compared.

4.2 Linear Analysis

The linear analysis described here uses the method of 'Collective Variables' [71] and is performed for the case of no spread in the electron energy or momenta.

For convenience, the following variables are introduced :

$$\phi' = \phi - \delta\bar{z} \tag{4.1}$$

$$p' = \bar{p} - \delta \tag{4.2}$$

$$A' = \bar{A}e^{i\delta\bar{z}} \tag{4.3}$$

The evolution equations (3.151..3.155) are linearised about their equilibrium values

$$\left\langle e^{-i\phi'_0} \right\rangle = 0$$

$$p'_{j0} = 0, \quad \bar{u}_{\perp j0} = 1, \quad \bar{u}_{\|j0} = 1 \qquad \forall\ j$$

$$A'_0 = 0$$

which corresponds to a boundary condition of an unbunched beam with no field excitation at $\bar{z} = 0$. Linearising around their equilibrium values the dependent variables are

$$\phi'_j = \phi'_{j0} + \phi'_{j1} \tag{4.4}$$

$$p'_j = p'_{j1} \tag{4.5}$$

$$\bar{u}_{\perp j} = 1 + \bar{u}_{\perp j1} \tag{4.6}$$

$$\bar{u}_{\|j} = 1 + \bar{u}_{\|j1} \tag{4.7}$$

$$A' = A'_1 \tag{4.8}$$

where all subscripts '1' refer to small changes from equilibrium. The linearised evolution equations are obtained by substituting (4.4..4.8) in (3.151..3.155) and neglecting all terms of second order and above. The resultant linear equations

are

$$\frac{d\phi'_{j1}}{d\bar{z}} = p'_{j1} - i\mu(A'_1 e^{i\phi'_{j0}} - c.c.) \tag{4.9}$$

$$\frac{dp'_{j1}}{d\bar{z}} = (\rho\delta - 1)\left(A'_1 e^{i\phi'_{j0}} + c.c\right) \tag{4.10}$$

$$\frac{d\bar{u}_{\perp j1}}{d\bar{z}} = -\mu\left(A'_1 e^{i\phi'_{j0}} + c.c\right) \tag{4.11}$$

$$\frac{d\bar{u}_{\|j1}}{d\bar{z}} = -\rho\left(A'_1 e^{i\phi'_{j0}} + c.c\right) \tag{4.12}$$

$$\frac{dA'_1}{d\bar{z}} = -i\left\langle \phi'_1 e^{-i\phi'_0}\right\rangle + \left\langle \bar{u}_{\perp 1} e^{-i\phi'_0}\right\rangle - \left\langle \bar{u}_{\|1} e^{-i\phi'_0}\right\rangle + i\delta A'_1 \tag{4.13}$$

Defining the collective variables as

$$b = -i\left\langle \phi'_1 e^{-i\phi'_0}\right\rangle \tag{4.14}$$

$$P = \left\langle p'_1 e^{-i\phi'_0}\right\rangle \tag{4.15}$$

$$U_\perp = \left\langle \bar{u}_{\perp 1} e^{-i\phi'_0}\right\rangle \tag{4.16}$$

$$U_\| = \left\langle \bar{u}_{\|1} e^{-i\phi'_0}\right\rangle \tag{4.17}$$

$$\tag{4.18}$$

the following can be easily obtained from (4.9..4.13) :

$$\frac{db}{d\bar{z}} = -iP - \mu\mathcal{A} \tag{4.19}$$

$$\frac{dP}{d\bar{z}} = (\rho\delta - 1)\mathcal{A} \tag{4.20}$$

$$\frac{dU_\perp}{d\bar{z}} = -\mu\mathcal{A} \tag{4.21}$$

$$\frac{dU_\|}{d\bar{z}} = -\rho\mathcal{A} \tag{4.22}$$

$$\frac{d\mathcal{A}}{d\bar{z}} = b + U_\perp - U_\| + i\delta\mathcal{A} \tag{4.23}$$

where terms proportional to $\left\langle e^{-i2\phi_0}\right\rangle$ have been dropped and A'_1 has been written simply as $\mathcal{A}$. Laplace transforming this set of equations using the standard

Laplace transform :

$$\tilde{X}(s) = \int_0^\infty X(\bar{z}) e^{-s\bar{z}} d\bar{z} \tag{4.24}$$

gives

$$s\tilde{b} = -i\tilde{P} - \mu\tilde{\mathcal{A}} \tag{4.25}$$

$$s\tilde{P} = (\rho\delta - 1)\tilde{\mathcal{A}} \tag{4.26}$$

$$s\tilde{U}_\perp = -\mu\tilde{\mathcal{A}} \tag{4.27}$$

$$s\tilde{U}_\parallel = -\rho\tilde{\mathcal{A}} \tag{4.28}$$

$$s\tilde{\mathcal{A}} - \mathcal{A}_0 = \tilde{b} + \tilde{U}_\perp - \tilde{U}_\parallel + i\delta\tilde{\mathcal{A}} \tag{4.29}$$

where the boundary conditions $b_0 = P_0 = U_{\perp 0} = U_{\parallel 0} = 0$ and $\mathcal{A}(\bar{z} = 0) = \mathcal{A}_0$ have been utilised. Equations (4.25..4.29) can now be rearranged, reducing the system of equations to a single equation for $\tilde{\mathcal{A}}(s)$ i.e.

$$\tilde{\mathcal{A}}(s) = \frac{s^2\mathcal{A}_0}{s^3 - i\delta s^2 + (2\mu - \rho)s - i(1 - \rho\delta)} \tag{4.30}$$

When inverted, this expression describes the steady-state evolution of the electromagnetic field in the linear regime. The inverse Laplace transform of (4.24) is defined as

$$X(\bar{z}) = \frac{1}{2\pi i}\int_{\sigma-i\infty}^{\sigma+i\infty} \tilde{X}(s) e^{s\bar{z}} ds \quad (\bar{z} > 0) \tag{4.31}$$

where σ is greater than the real part of any of the singularities of the integrand. Introducing the change of variable

$$\lambda = -is \tag{4.32}$$

then the inverse Laplace transform of (4.30) becomes

$$\mathcal{A}(\bar{z}) = \frac{1}{2\pi}\int_{-\infty-i\sigma}^{\infty-i\sigma} \tilde{\mathcal{A}}(\lambda) e^{i\lambda\bar{z}} d\lambda \quad (\bar{z} > 0) \tag{4.33}$$

where the transformed field variable expressed in terms of λ is

$$\tilde{\mathcal{A}}(\lambda) = \frac{-i\lambda^2 \mathcal{A}_0}{\lambda^3 - \delta\lambda^2 + (\rho - 2\mu)\lambda + (1 - \rho\delta)} \tag{4.34}$$

As the denominator of $\tilde{\mathcal{A}}(\lambda)$ is a cubic, the integrand of (4.33) has three simple poles, so the integral becomes the sum of the residues multiplied by $2\pi i$ i.e.

$$\mathcal{A}(\bar{z}) = \mathcal{A}_0 \sum_{k=1}^{3} \frac{\lambda_k^2 e^{i\lambda_k \bar{z}}}{(\lambda_k - \lambda_l)(\lambda_k - \lambda_m)} \quad (k \neq l \neq m) \tag{4.35}$$

where $\lambda_{1,2,3}$ are the roots of the denominator of equation (4.34) which forms the dispersion relation

$$\lambda^3 - \delta\lambda^2 + (\rho - 2\mu)\lambda + (1 - \rho\delta) = 0 \tag{4.36}$$

The above analysis can be repeated for the alternative set of boundary conditions which correspond to a small initial bunching of the electron phases and zero initial field i.e. $\mathcal{A}_0 = P_0 = U_{\perp 0} = U_{\parallel 0} = 0$ and $b_0 = \langle e^{-i\phi_0} \rangle \neq 0$. The expression for the resultant field amplitude in this case is

$$\mathcal{A}(\bar{z}) = -ib_0 \sum_{k=1}^{3} \frac{\lambda_k e^{i\lambda_k \bar{z}}}{(\lambda_k - \lambda_l)(\lambda_k - \lambda_m)} \quad (k \neq l \neq m) \tag{4.37}$$

As $\mathcal{A} \propto e^{i\lambda_k \bar{z}}$ for both the above cases, the system will be unstable if the dispersion relation has complex roots. These roots will always occur as a complex conjugate pair. Complex roots will occur when

$$\begin{aligned} &\delta^4\rho - \delta^3 + 2\rho^2\delta^2 + 10\rho\delta^2\mu - 9\rho\delta - \\ &\delta^2\mu^2 - 9\delta\mu + \rho^3 - 6\rho^2\mu + 12\rho\mu^2 - 8\mu^3 + \frac{27}{4} > 0. \end{aligned} \tag{4.38}$$

The exponentially growing term will be

$$\mathcal{A}(\bar{z}) \propto \exp\left(|\Im(\lambda_3(\delta, \rho, \mu)|)\bar{z}\right) \tag{4.39}$$

where $\Im(\lambda_3(\delta,\rho,\mu))$ is the negative imaginary part of the complex conjugate pair of roots which occur when (4.38) is satisfied. At resonance ($\delta = 0$), and when both ρ and μ are $\ll 1$ i.e. when the variation of both the perpendicular and the axial momentum of the electrons is small then $|\Im(\lambda_3(\delta,\rho,\mu))| = \sqrt{3}/2$ and using the definition of $\bar{z}$ given in (3.101), (4.39) can be rewritten as

$$\mathcal{A}(z) \propto \exp\left(\frac{\sqrt{3}}{2}\frac{k_\perp^2}{k_{||}}\rho z\right)$$

so the spatial growth rate of the field amplitude is

$$g = \frac{\sqrt{3}}{2}\frac{k_\perp^2}{k_{||}}\rho. \tag{4.40}$$

The significance of the scaling of $\bar{z}$ is now apparent : the interaction distance has been scaled with respect to the growth rate of the exponential instability at resonance in the limit ρ and $\mu \ll 1$ i.e. $\bar{z} \propto gz$. Substituting for ρ using the definition (3.98) for a TE mode interaction or (3.150) for a TM mode interaction, the expressions for the spatial growth rate of the instability for an axis-encircling beam ($R_0 = 0$) in terms of unscaled variables, (2.17) and (2.18), are reproduced.

If it is assumed that the electrons and the field are resonant ($\delta = 0$), the condition for the system to be unstable, from (4.38) becomes

$$2\mu - \rho < \left(\frac{27}{4}\right)^{\frac{1}{3}}$$

This shows the different nature of ρ and μ with regard to the linear stability of the system: increasing μ has a stabilising effect on the interaction whereas increasing ρ has a destabilising effect. Whereas ρ represents the growth rate of the field amplitude, μ can be interpreted as the decay rate of the transverse energy of the

beam. A plot of $|\Im(\lambda_3(\delta,\rho,\mu))|$ at resonance for different values of ρ and μ is shown in figure 4.1.

4.2.1 The Low Efficiency Limit

When $\rho \longrightarrow 0$, the axial momentum of the electrons remains approximately constant. From (3.157), the efficiency η varies as $\eta \propto \rho|\bar{A}|^2$, this condition implies that the efficiency of the interaction will be small.

The full expression for the electromagnetic field amplitude in the linear regime (4.35) can be written in the more compact form

$$\mathcal{A}(\bar{z}) = \mathcal{A}_0 \sum_{k=1}^{3} c_k e^{i\lambda_k \bar{z}} \tag{4.41}$$

$$\text{where} \qquad c_k = \frac{\lambda_k^2}{(\lambda_k - \lambda_l)(\lambda_k - \lambda_m)} \qquad (k \neq l \neq m)$$

The scaled field intensity in the linear regime is therefore the product of (4.41) with its complex conjugate. In the low effeciency limit $\rho \approx 0$, where the recoil of the electrons is negligible, the dispersion relation (4.36) becomes

$$\lambda^3 - \delta\lambda^2 - 2\mu\lambda + 1 \approx 0 \tag{4.42}$$

where it has been assumed that we are close enough to resonance so that $\rho\delta \ll 1$. A plot of $|\Im(\lambda_3(\delta,\rho,\mu))|$ for various values of δ and μ is shown in figure 4.2. Note that the maximum occurs when $\mu = 0$ and $\delta = 0$. The threshold condition which δ and μ must satisfy for instability to occur is

$$\delta^3 + \delta^2\mu^2 + 9\delta\mu + 8\mu^3 < \frac{27}{4} \tag{4.43}$$

which has been obtained by taking the limit $\rho \longrightarrow 0$ in (4.38). From this, the value of μ above which the system is linearly stable at resonance is $\mu_T = \sqrt[3]{27/32}$.

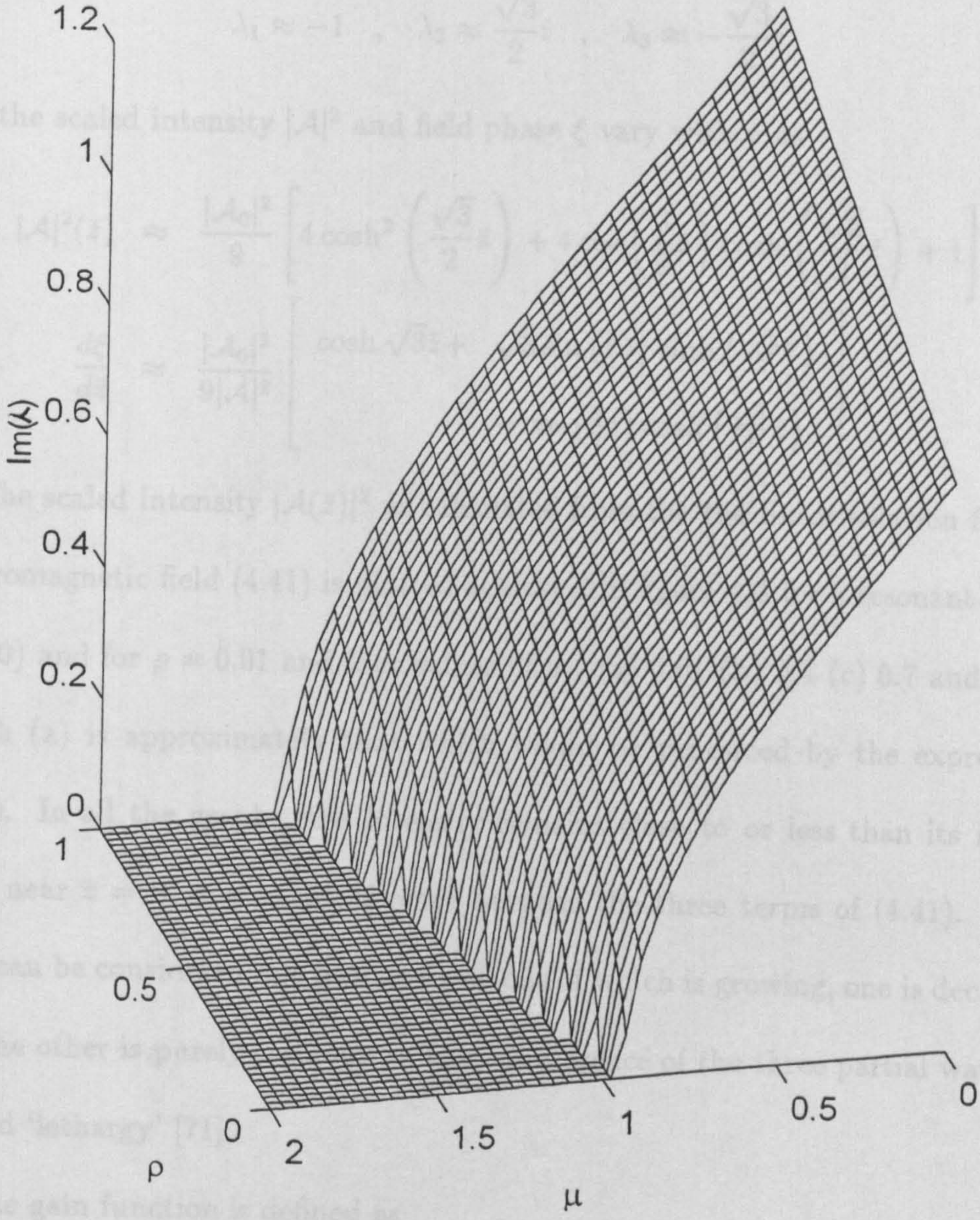

Figure 4.1: Plot of $|\Im(\lambda_3)|$ for different ρ and μ

Similarly, the threshold value of δ above which the system is linearly stable is $\delta_T = \sqrt[3]{27/4}$ at $\mu = 0$.

For the special case of resonance and $\mu \approx 0$, the three roots of the cubic (4.42) are

$$\lambda_1 \approx -1 \quad , \quad \lambda_2 \approx \frac{\sqrt{3}}{2}i \quad , \quad \lambda_3 \approx -\frac{\sqrt{3}}{2}i$$

and the scaled intensity $|\mathcal{A}|^2$ and field phase ξ vary with $\bar{z}$ as

$$|\mathcal{A}|^2(\bar{z}) \approx \frac{|\mathcal{A}_0|^2}{9}\left[4\cosh^2\left(\frac{\sqrt{3}}{2}\bar{z}\right) + 4\cos\left(\frac{3}{2}\bar{z}\right)\cosh\left(\frac{\sqrt{3}}{2}\bar{z}\right) + 1\right] \quad (4.44)$$

$$\frac{d\xi}{d\bar{z}} \approx \frac{|\mathcal{A}_0|^2}{9|\mathcal{A}|^2}\left[\begin{array}{ll} \cosh\sqrt{3}\bar{z} + & \sqrt{3}\sin\left(\frac{3}{2}\bar{z}\right)\sinh\left(\frac{\sqrt{3}}{2}\bar{z}\right) \\ & -\cos\left(\frac{3}{2}\bar{z}\right)\cosh\left(\frac{\sqrt{3}}{2}\bar{z}\right) \end{array}\right]. \quad (4.45)$$

The scaled intensity $|\mathcal{A}(\bar{z})|^2$ as calculated from the the linear solution for the electromagnetic field (4.41) is plotted against $\bar{z}$ in figure 4.3 for a resonant beam ($\delta = 0$) and for $\rho = 0.01$ and four values of μ : (a) 0.01 (b) 0.4 (c) 0.7 and (d)1. Graph (a) is approximately that which would be produced by the expression (4.44). In all the graphs, the intensity remains close to or less than its initial value near $\bar{z} = 0$, due to interference between the three terms of (4.41). Each term can be considered as a partial wave, one of which is growing, one is decaying and the other is purely oscillatory. This interference of the three partial waves is termed 'lethargy' [71].

The gain function is defined as

$$G(\bar{z}, \delta, \mu) = \frac{|\mathcal{A}|^2(\bar{z}) - |\mathcal{A}_0|^2}{|\mathcal{A}_0|^2}. \quad (4.46)$$

As $G \sim 1$ in the region where lethargy occurs, it is also called the 'low-gain regime' as opposed to the 'high-gain' regime where $G \gg 1$ and the field intensity

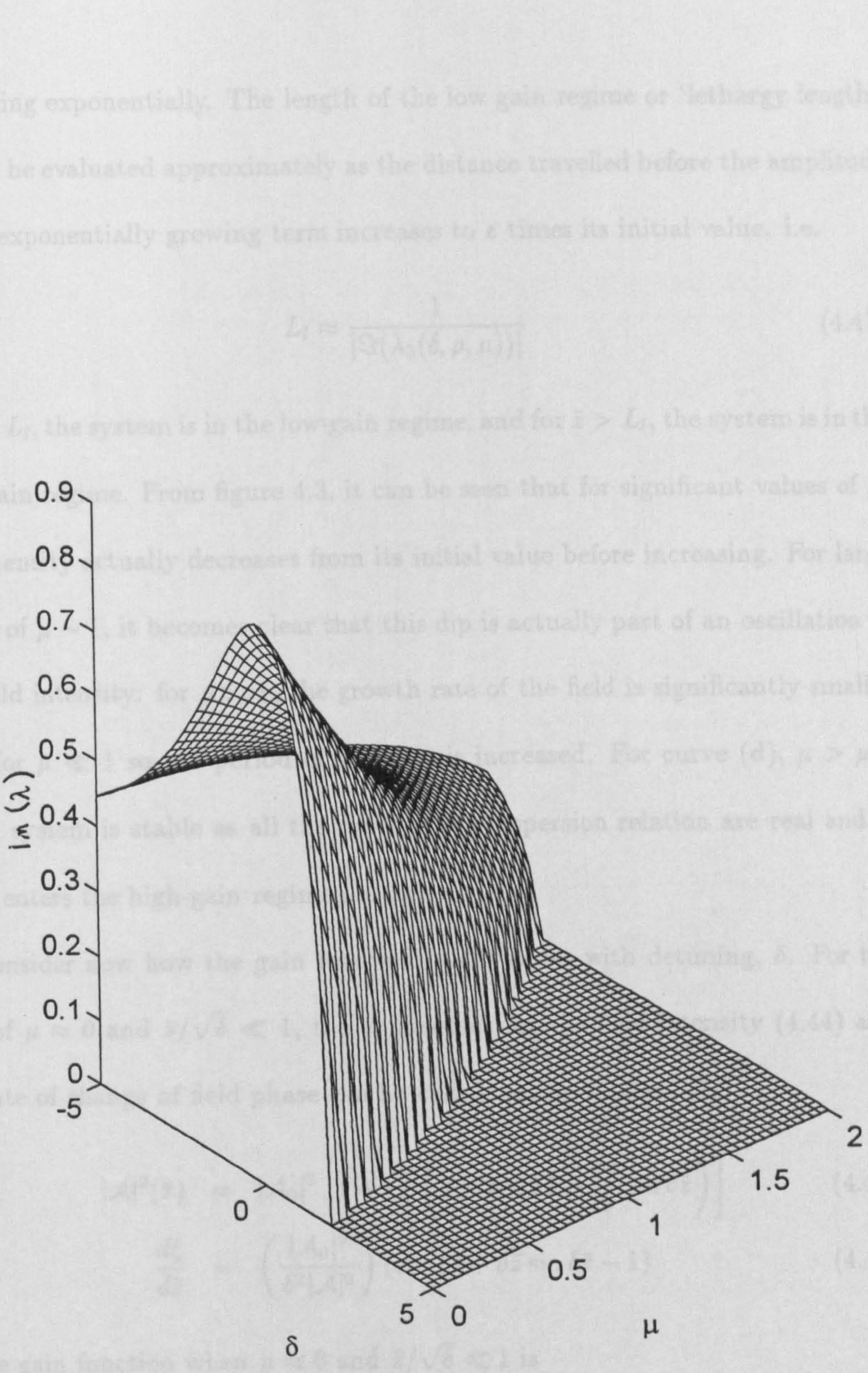

Figure 4.2: Plot of $|\Im(\lambda_3)|$ for different μ and δ when $\rho \ll 1$.

is growing exponentially. The length of the low gain regime or 'lethargy length', L_l, can be evaluated approximately as the distance travelled before the amplitude of the exponentially growing term increases to e times its initial value. i.e.

$$L_l \approx \frac{1}{|\Im(\lambda_3(\delta,\rho,\mu))|} \tag{4.47}$$

For $\bar{z} \lesssim L_l$, the system is in the low-gain regime, and for $\bar{z} > L_l$, the system is in the high-gain regime. From figure 4.3, it can be seen that for significant values of μ, the intensity actually decreases from its initial value before increasing. For large values of $\mu \sim 1$, it becomes clear that this dip is actually part of an oscillation in the field intensity: for $\mu \lesssim \mu_T$, the growth rate of the field is significantly smaller than for $\mu \ll 1$ so the period of lethargy is increased. For curve (d), $\mu > \mu_T$, so the system is stable as all the roots of the dispersion relation are real and it never enters the high-gain regime i.e. $L_l \to \infty$.

Consider now how the gain function (4.46) varies with detuning, δ. For the case of $\mu \approx 0$ and $\bar{z}/\sqrt{\delta} \ll 1$, the expressions for the field intensity (4.44) and the rate of change of field phase can be calculated from (4.44) [71]

$$|\mathcal{A}|^2(\bar{z}) = |\mathcal{A}_0|^2\left[1+\frac{4}{\delta^3}\left(1-\cos\delta\bar{z}-\frac{\delta\bar{z}}{2}\sin\delta\bar{z}\right)\right] \tag{4.48}$$

$$\frac{d\xi}{d\bar{z}} = \left(\frac{|\mathcal{A}_0|^2}{\delta^2|\mathcal{A}|^2}\right)(\cos\delta\bar{z}+\delta\bar{z}\sin\delta\bar{z}-1) \tag{4.49}$$

so the gain function when $\mu \approx 0$ and $\bar{z}/\sqrt{\delta} \ll 1$ is

$$G(\bar{z},\delta) = \frac{4}{\delta^3}\left(1-\cos\delta\bar{z}-\frac{\delta\bar{z}}{2}\sin\delta\bar{z}\right) \quad (\mu \approx 0\,,\ \frac{\bar{z}}{\sqrt{\delta}} \ll 1). \tag{4.50}$$

From (4.49) it is seen that the phase evolution is small i.e. $|d\xi/d\bar{z}| \ll 1$. Equation (4.50) is the expression for the small-signal or interference gain which was

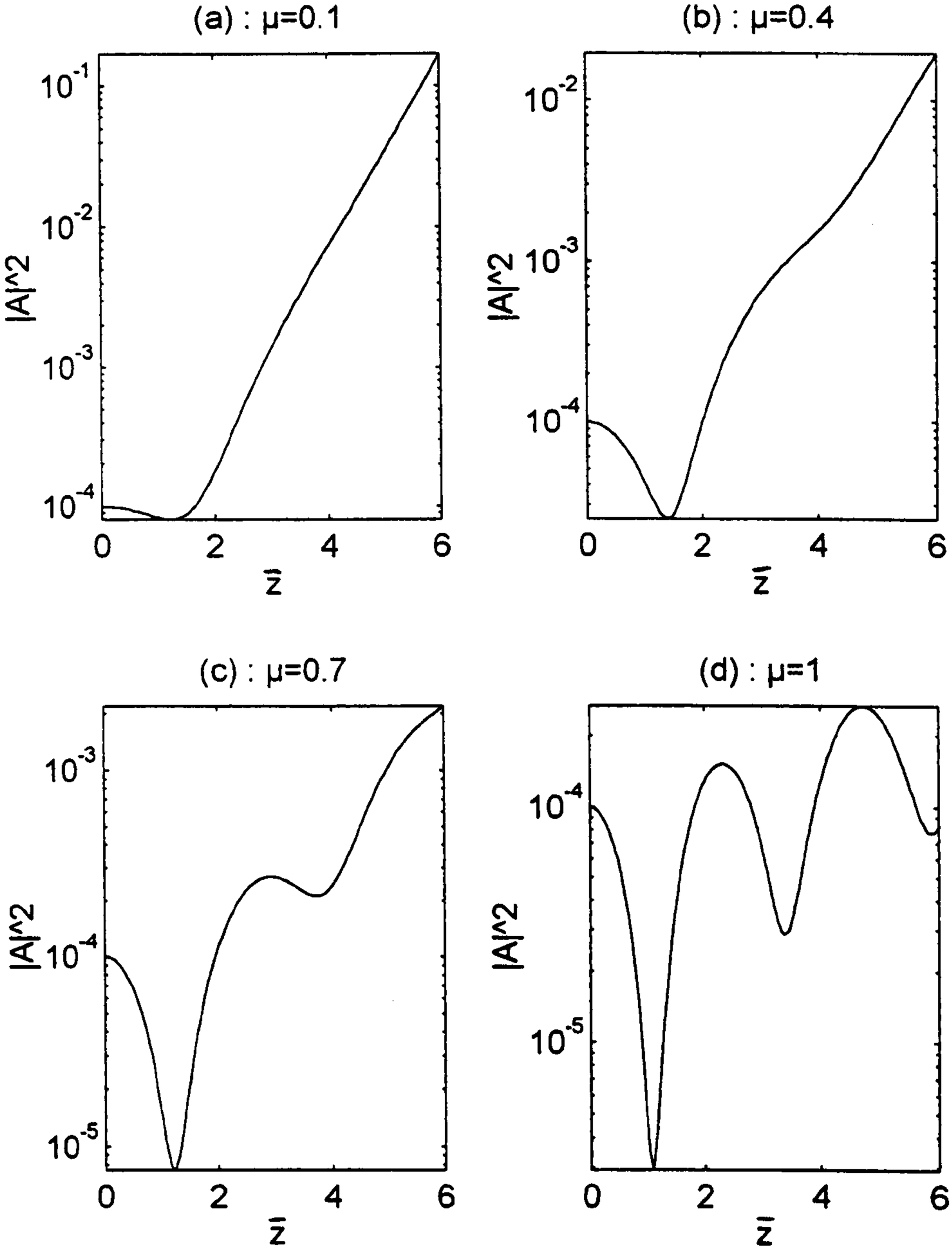

Figure 4.3: Plots of $|\mathcal{A}|^2$ against $\bar{z}$ for $\rho = 0.01$ and (a)$\mu = 0.1$, (b)$\mu = 0.4$ (c) $\mu = 0.7$ and (d)$\mu = 1$.

originally derived by Madey for FELs [72]. It can be rewritten as

$$G(\bar{z},\delta) = -\frac{\bar{z}^3}{2}\frac{d}{d(\Delta/2)}\mathrm{sinc}^2\left(\frac{\Delta}{2}\right) \tag{4.51}$$

where $\Delta = \delta\bar{z}$. Rewriting $\bar{z}$ and δ in unscaled variables

$$\bar{z} = \frac{k_\perp^2}{k_\parallel}\rho z \quad , \quad \delta = \frac{k_\parallel}{k_\perp^2}\frac{1}{\rho v_{\parallel 0}}\left(\omega - \frac{\omega_c}{\gamma_0} - k_\parallel v_{\parallel 0}\right)$$

then

$$\Delta = \left(\frac{\omega - \omega_c/\gamma_0}{v_{\parallel 0}} - k_\parallel\right) z$$

so, on comparison with (1.5), it can be seen that

$$G \propto \frac{d^2 I}{d\Omega d\omega} \tag{4.52}$$

which means that the small-signal gain is proportional to the derivative of the spontaneous emission spectrum. The gain function $G(\bar{z},\delta,\mu)$ from (4.46) and (4.41) is plotted against δ at various stages of the field evolution for a case where $\mu \ll 1$ in figure 4.4(a..d). Figure 4.4(a), where $\bar{z} < 1$, shows the asymmetric gain curve which is characteristic of a Madey-type gain process and is described by (4.50). Note that at $\delta = 0$, the gain is approximately zero. As $\bar{z}$ increases, the system undergoes a transition from the low-gain to the high-gain regime, and the value of δ at which maximum gain occurs approaches zero. Figures 4.5(a..d) and 4.6(a..d), show equivalent graphs to those in figure 4.4 for cases where $\mu = 0.2$ and $\mu = 0.8$ respectively. The effect of finite free-energy depletion on the low-gain regime can be seen from a comparision of figures 4.4(a),4.5(a) and 4.6(a). As μ is increased, the maximum of the gain curve is reduced and shifted to larger δ, so that the gain function is negative at $\delta = 0$. In addition, the magnitude

of the maximum positive gain for a given μ becomes less than the maximum negative gain. It is noticeable for all values of μ that in the low-gain regime, the maximum of the gain function occurs for positive δ whereas in the high gain regime, it has been shown that maximum gain occurs when $\delta \approx 0$. This is similar to the Compton FEL.

This contrast between the low and high-gain regimes can be explained using the constant of motion (3.177) and the wave equation (3.169). Combining these two expressions and using the definition of the gain function (4.46) produces

$$\langle p'^2 \rangle = 4\left(|\bar{A}|^2 \frac{d\xi}{d\bar{z}} - |\bar{A}_0|^2 \frac{d\xi_0}{d\bar{z}}\right) + 2\delta|\bar{A}_0|^2 G \tag{4.53}$$

where, as previously, $p' = \bar{p} - \delta \propto \gamma - \gamma_0$ and ξ is the slowly varying radiation phase i.e. $\bar{A} = |\bar{A}|e^{i\xi}$. The subscript '0' represents values at $\bar{z} = 0$. This expression relates the energy spread $\langle p'^2 \rangle$, the field intensity $|\bar{A}|^2$ and the field phase variation $d\xi/d\bar{z}$ and is valid in the linear and nonlinear regimes. The energy conservation relation (3.173) can now be used to obtain the variance

$$\begin{aligned} \sigma^2(p'^2) &\equiv \langle p'^2 \rangle - \langle p' \rangle^2 \\ &= 4\left(|\bar{A}|^2 \frac{d\xi}{d\bar{z}} - |\bar{A}_0|^2 \frac{d\xi_0}{d\bar{z}}\right) + 2\delta|\bar{A}_0|^2 G - |\bar{A}_0|^4 G^2 \end{aligned}$$

from which the inequality

$$\frac{d\xi}{d\bar{z}} \geq \frac{1}{4|\bar{A}^2|}\left(4|\bar{A}_0^2| - 2\delta|\bar{A}_0|^2 G + |\bar{A}_0|^4 G^2\right) \tag{4.54}$$

follows. For the case where there is no initial field excitation ($|\bar{A}_0|^2 = 0$) and no detuning ($\delta = 0$), (4.54) reduces to

$$\frac{d\xi}{d\bar{z}} \geq \frac{|\bar{A}^2|}{4} \tag{4.55}$$

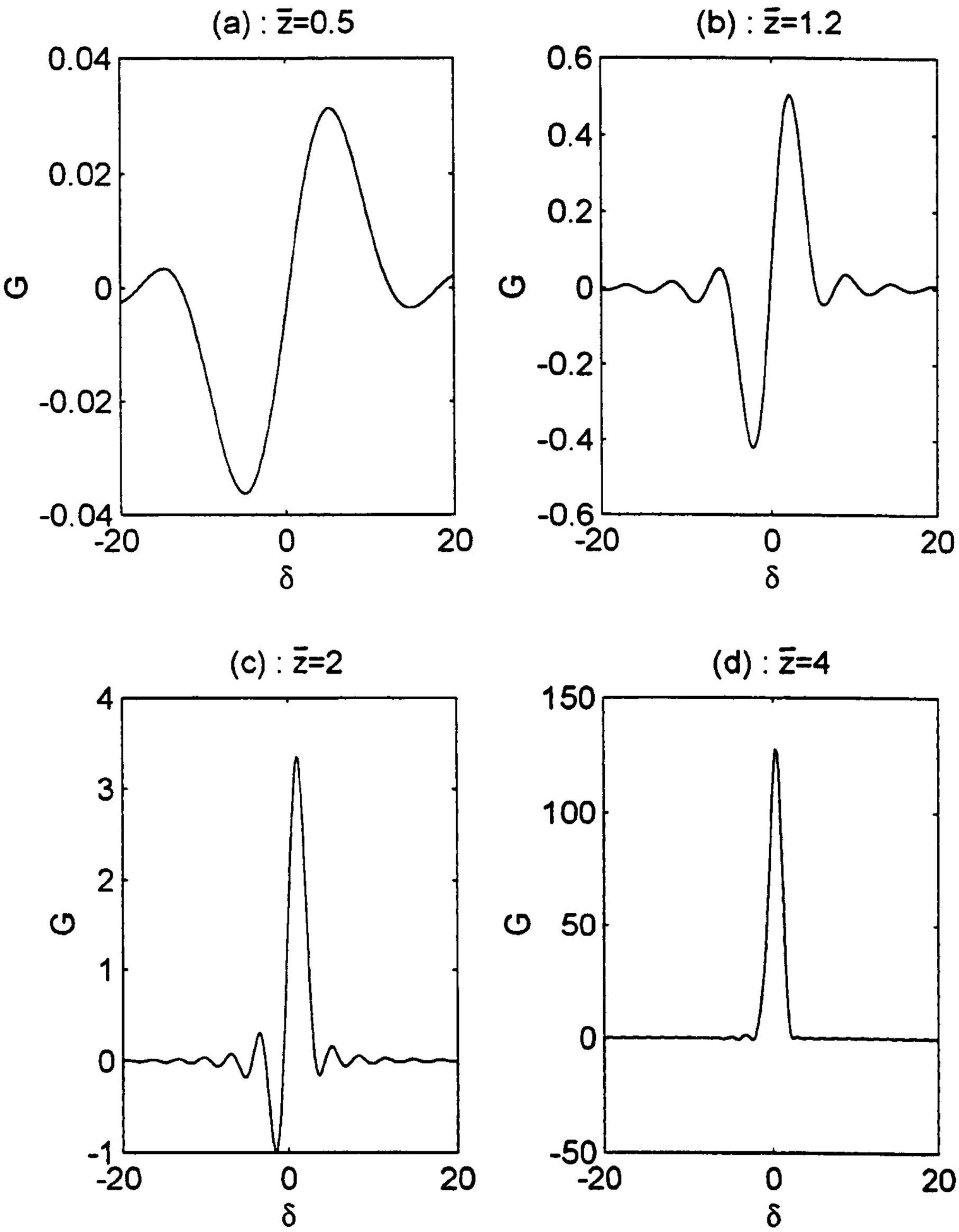

Figure 4.4: Plots of G against δ as the interaction evolves for $\mu = 0.01$: (a) $\bar{z} \ll L_l$, (b) $\bar{z} \approx L_l$, (c) $\bar{z} > L_l$, (d) $\bar{z} \gg L_l$.

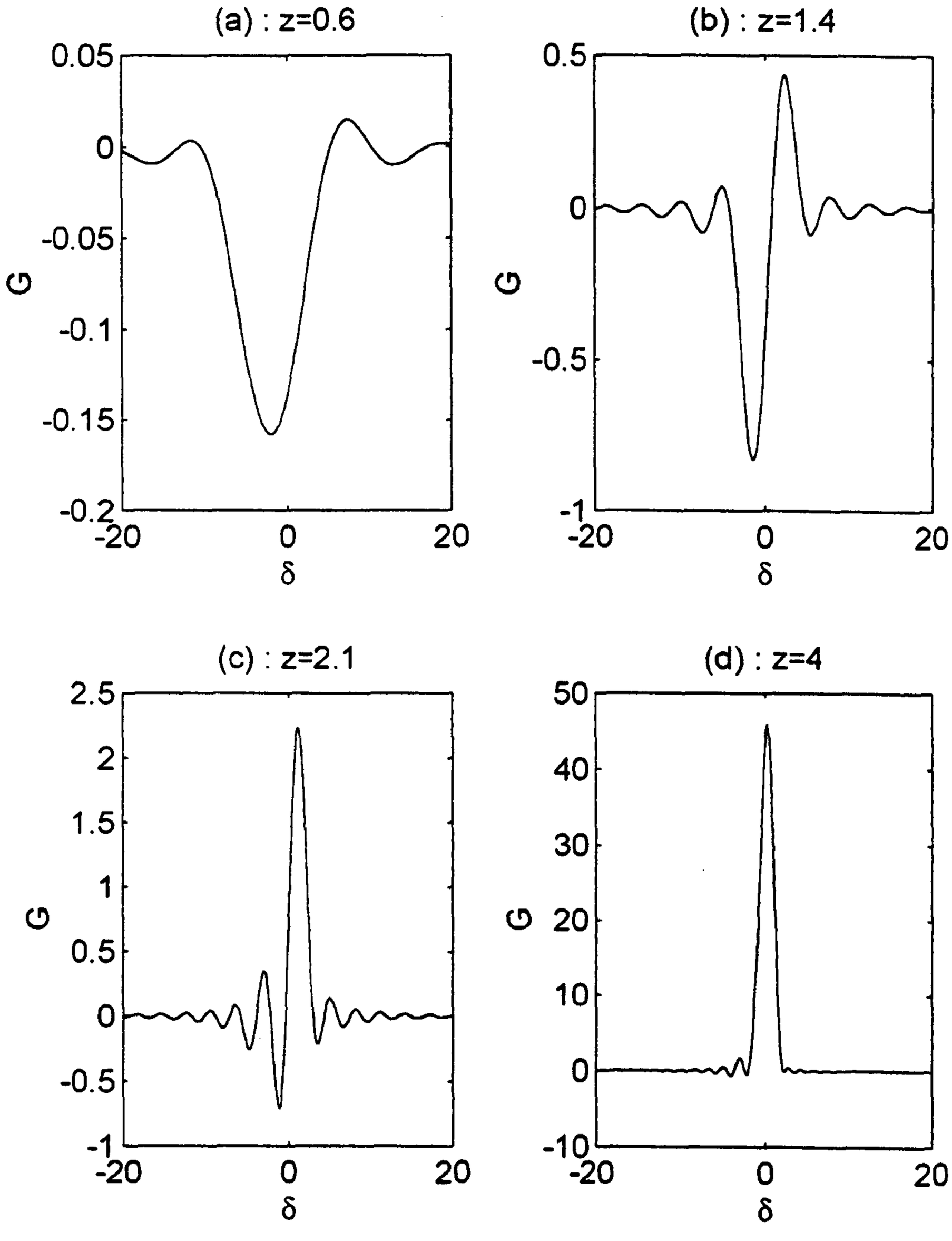

Figure 4.5: Plots of G against δ as the interaction evolves for $\mu = 0.2$: (a) $\bar{z} \ll L_l$, (b) $\bar{z} \approx L_l$, (c) $\bar{z} > L_l$, (d) $\bar{z} \gg L_l$.

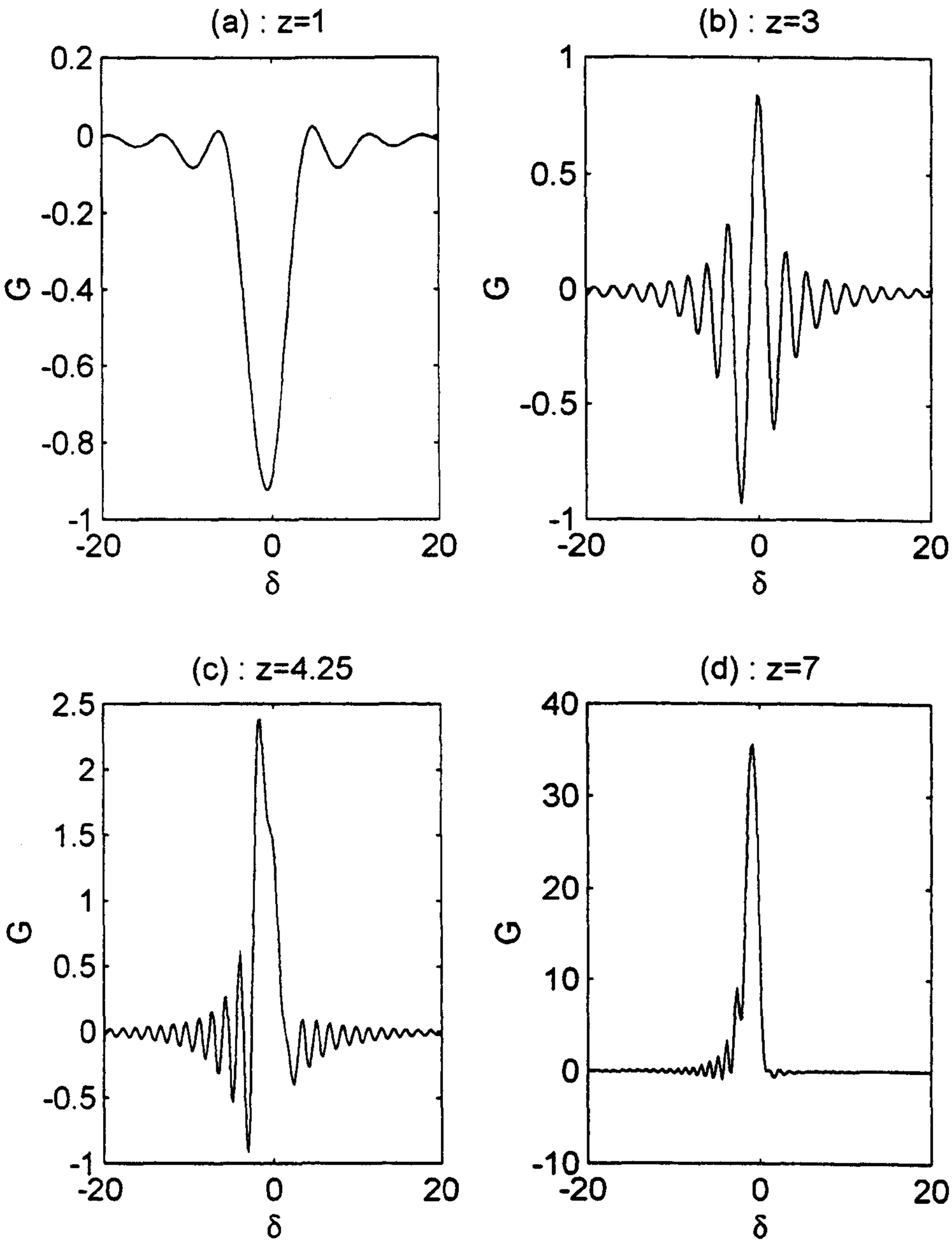

Figure 4.6: Plots of G against δ as the interaction evolves for $\mu = 0.8$: (a) $\bar{z} \ll L_l$, (b) $\bar{z} \approx L_l$, (c) $\bar{z} > L_l$, (d) $\bar{z} \gg L_l$.

which means $d\xi/d\bar{z}$ is always positive. In order to see the significance of this result, consider the phase of the electron with respect to the electromagnetic field, denoted by q. This is just the trigonometric argument in (3.167) and (3.168) i.e.

$$q \equiv \phi + \xi$$

From the definition of ϕ, (3.45), when free energy depletion is negligible ($\mu \ll 1$), it is possible to write

$$\dot{q} = \text{constant} \times \left(\omega - \frac{\omega_c}{\gamma} - k_{\|} v_{\|}\right) + \dot{\xi} \tag{4.56}$$

where $\dot{} \equiv d/d\bar{z}$. Consider first of all the case where the phase evolution of the electromagnetic field is negligible ($d\xi/dt \approx 0$). This is the case described by (4.48) and (4.49). From (3.168), in a resonant and randomly phased electron beam, approximately half of the electrons will absorb energy ($\pi/2 < q < 3\pi/2$) and half will lose energy ($0 \leq q < \pi/2$ and $3\pi/2 < q \leq 2\pi$), and the electrons will bunch slightly about a point where there is no energy exchange with the radiation field($q = 3\pi/2$), resulting in no net gain. When the evolution of the radiation phase is significant ($|\dot{\xi}| > 0$), then (4.56) shows that the effective frequency of the wave is $\omega + \dot{\xi}$. It has been shown in (4.55) that $\dot{\xi}$ is always positive, so $\dot{q}$ is increased by the field phase evolution. Consequently, resonant electrons will bunch around a phase corresponding to gain, resulting in instability. The crucial difference between the low and high gain regimes is therefore the significant evolution of the phase of the electromagnetic field in the high gain regime.

When free energy depletion effects are present ($\mu > 0$) the above scenario is complicated by the presence of the second term in (3.167), which makes an additional contribution to $\dot{q}$. This term disrupts the bunching mechanism by being

larger for those electrons which are losing energy to the field. The symmetry between the number of particles gaining and losing energy at resonance is therefore lost, and a net negative gain will occur even when the field phase evolution is negligible, as shown in figures 4.5(a) and 4.6(a). The field phase evolution will cause the electrons to bunch about a point corresponding to gain, but the size of this gain becomes smaller as free energy depletion effects increase.

Another interesting feature of the gain-spread relation (4.53) in the low-gain regime ($|d\xi/d\bar{z}| \ll 1$) becomes apparent when it is differentiated with respect to the detuning δ, producing the relation [71]

$$\frac{1}{2}\frac{\partial}{\partial\delta}\langle p'^2\rangle \approx -|\bar{A}_0|^2 G \tag{4.57}$$

This is Madey's gain-spread relation [72], which states that the system cannot undergo gain without the simultaneous introduction of an energy spread in the electron beam.

4.2.2 The High Efficiency Limit and Autoresonance

For values of $\rho \not\ll 1$, the variations in the axial momenta of the electrons are not negligible. The difficulty in investigating this regime as extensively as that where $\rho \ll 1$ is that the parameter space is now three-dimensional i.e. (ρ, μ, δ) so quantities such as growth rates cannot readily be plotted over the entire parameter space on one graph. It is still possible however to extract useful information from the results of the linear analysis in this regime, the most significant of which are described below.

The linear behaviour of the system when $\rho \not\ll 1$ must be investigated using

the full dispersion relation (4.36). Figures 4.7(a..d) show regions of instability ($|\Im(\lambda_3(\rho,\mu,\delta))| > 0$) in the (ρ,δ) plane for several values of μ. On examination of figure 4.7(a), where $\mu \ll 1$, it can be seen that for $\rho \approx 0$ there is only one region of instability, which occurs when $\delta < \delta_T = \sqrt[3]{27/4}$. As ρ increases however, another region of instability appears for values of $\delta > 1/\rho$. These two distinct regions of instability will be termed region 1 and region 2 respectively. As ρ increases further, the two regions of instability eventually merge. Figures 4.7(b..d) show the effects of increasing μ i.e. increasing the depletion rate of the beam's transverse energy. It can be seen from these figures that region 1 is significantly affected by the increase of μ, with the most obvious effect being a decrease in δ_T at $\rho = 0$. The value of $|\Im(\lambda_3(\rho,\mu,\delta))|$ is also reduced, particularly at small values of ρ. In contrast, the effect of changing μ appears less significant on region 2.

In order to explain the graphs shown in figure 4.7, it is necessary to recall the discussion of the $(\rho\delta - 1)$ term in section 3.4. It was shown there that the sign of this term determined the type of bunching mechanism which was occurring. When $\rho\delta < 1$, the azimuthal bunching mechanism due to changes in γ is dominant, whereas when $\rho\delta > 1$, the axial bunching mechanism due to changes in $v_{||}$ is dominant. Region 1, where $\rho\delta < 1$, is where the azimuthal bunching mechanism dominates the axial bunching mechanism, with most energy being extracted from the transverse motion of the electrons. Consequently, μ, which represents the depletion rate of the transverse energy of the electrons, will have a large effect on the interaction, as was seen in section 4.2.1. In contrast, region 2 in figures 4.7(a..d) occurs when $\rho\delta > 1$, so the axial bunching mechanism

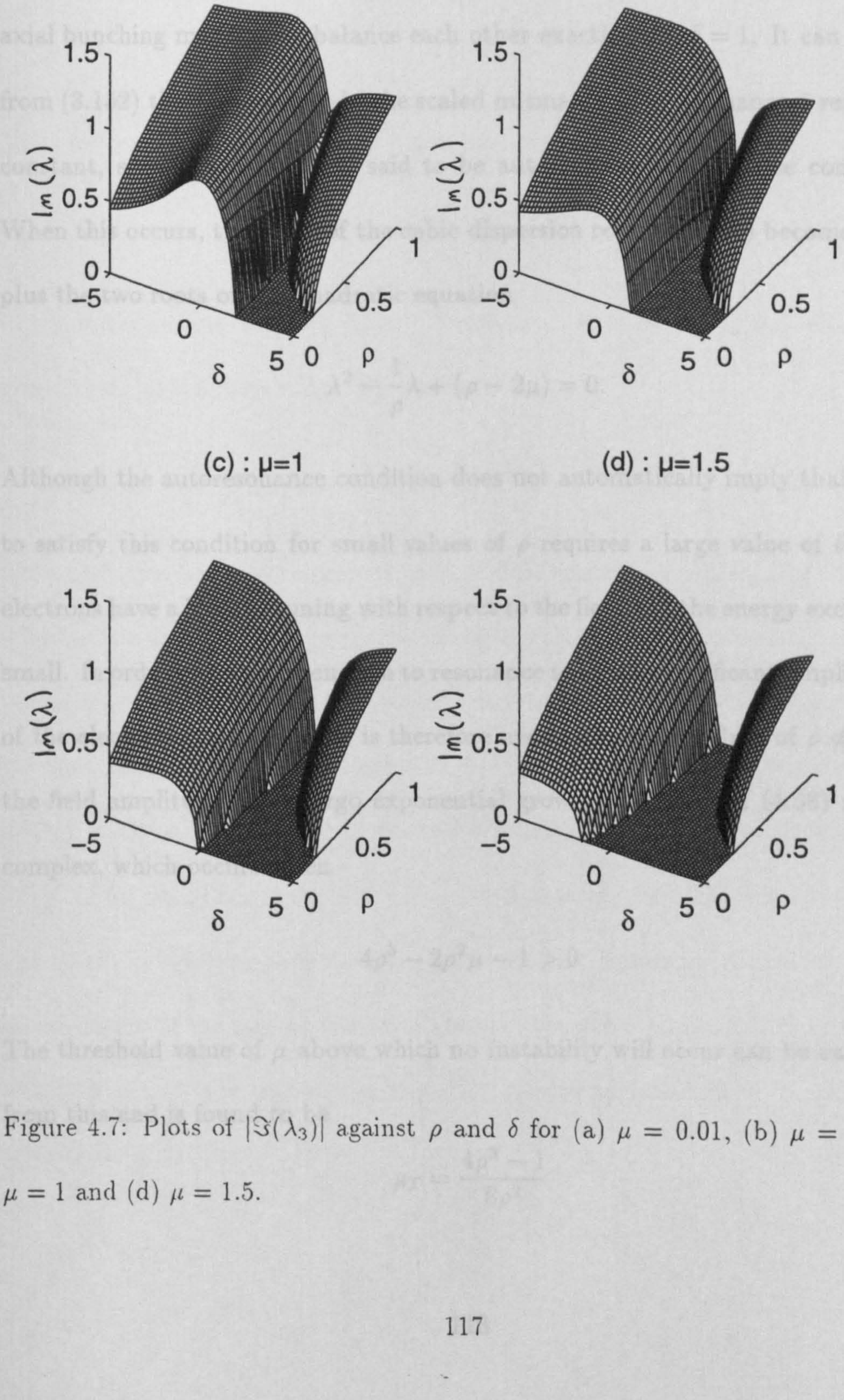

Figure 4.7: Plots of $|\Im(\lambda_3)|$ against ρ and δ for (a) $\mu = 0.01$, (b) $\mu = 0.5$, (c) $\mu = 1$ and (d) $\mu = 1.5$.

is dominant, with most energy being extracted from the axial motion of the electrons. Increasing the depletion rate of the transverse energy of the electrons will have less effect in this region.

Consider now what happens when the azimuthal bunching mechanism and the axial bunching mechanism balance each other exactly i.e. $\rho\delta = 1$. It can be seen from (3.152) that this results in the scaled mismatch from resonance $\bar{p}$ remaining constant, so the interaction is said to be autoresonant under these conditions. When this occurs, the roots of the cubic dispersion relation (4.36) become $\lambda_1 = 0$ plus the two roots of the quadratic equation

$$\lambda^2 - \frac{1}{\rho}\lambda + (\rho - 2\mu) = 0. \tag{4.58}$$

Although the autoresonance condition does not automatically imply that $\rho \ll 1$, to satisfy this condition for small values of ρ requires a large value of δ, so the electrons have a large detuning with respect to the field and the energy exchange is small. In order to get close enough to resonance to enable significant amplification of the electromagnetic field, it is therefore necessary to use values of $\rho \ll 1$. For the field amplitude to undergo exponential growth, the roots of (4.58) must be complex, which occurs when

$$4\rho^3 - 2\rho^2\mu - 1 > 0 \tag{4.59}$$

The threshold value of μ above which no instability will occur can be calculated from this and is found to be

$$\mu_T = \frac{4\rho^3 - 1}{8\rho^2} \tag{4.60}$$

For $\rho \gg \sqrt[3]{1/4}$, $\mu_T \approx \rho/2$. When $\rho \gg 2\mu$, (4.59) reduces to

$$\rho > 2^{-\frac{2}{3}} \approx 0.63 \tag{4.61}$$

Far above this threshold, the imaginary part of the complex root is

$$\lambda_i \approx \rho^{\frac{1}{2}}$$

Now, as the electromagnetic field varies as

$$\mathcal{A} \propto \exp |\Im(\lambda_3)| \bar{z}$$

in the linear regime, the definition of $\bar{z}$ can be used to obtain g, the exponential growth rate of the instability. The result is

$$g = \frac{k_\perp^2}{k_\parallel} \rho^{\frac{3}{2}} \tag{4.62}$$

Note that the exponential growth rate of this instability varies as $\rho^{3/2} \propto I^{1/2}$ whereas the exponential growth rate of the instability which occurs when $\rho \ll 1$ varies as $\rho \propto I^{1/3}$, where I is the beam current. The crucial difference between the two interactions is the evolution of $\bar{p}$. When $\rho\delta \neq 1$, $\bar{p}$ varies as the electron energy changes, which leads to phase bunching of the electrons. However, for $\rho\delta = 1$, no phase bunching will occur, even though the axial velocity and the energy of the electrons may be either increasing or decreasing. Equation (3.151), which describes the rate of change of phase of the jth electron, can be integrated simply if $\rho\delta = 1$ and free-energy depletion effects are small ($\mu \ll 1$), producing the result that

$$\phi_j = \phi_{j0} + \delta \bar{z} \quad \forall j$$

so phase bunching clearly cannot occur. The mechanism responsible for amplification of the electromagnetic field can be deduced from an examination of the source term in the wave equation (3.155) and the axial momentum equation (3.154). It is clear from these equations that an electron whose axial momentum is decreasing becomes more strongly coupled to the field whereas an electron gaining axial momentum becomes less strongly coupled to the field. If the electron phases do not change too rapidly, i.e. δ is small, then a large exchange of energy can occur between the electrons and the field. If $\mu \not\ll 1$, then the second term in the phase evolution equation (3.151) and the perpendicular momentum equation (3.153) can no longer be neglected. The effect of these terms increases as $\bar{u}_{||}$ decreases, causing the electron phase to change and its perpendicular momentum to decrease, resulting in a reduction of the coupling and hence the energy exchange between the electron and the field. It is therefore clear that terms which are proportional to μ act to stabilise the instability. This type of instability where no phase bunching occurs also arises when a beam of relativistic electrons in a uniform magnetic field interacts with an electromagnetic field in free space. This is the interaction which occurs in a 'non-wiggler FEL'. It has been studied previously using a single particle small signal analysis [67] and a Vlasov linear analysis [68]. The result obtained for the spatial growth rate, g of the field amplitude in [68] was

$$g = \frac{\omega_p}{\sqrt{2\gamma_0}} \frac{v_{\perp 0}}{c v_{||0}}$$

where ω_p is the plasma frequency. Note that

$$g \propto \omega_p \propto I^{1/2} \tag{4.63}$$

in agreement with (4.62). This scaling of the growth rate reflects the fact that the instability at exact autoresonance and the instability in a NWFEL do not arise from phase bunching, but from depletion of the axial momentum of the electron beam.

4.2.3 Conclusions

In this chapter, the scaled evolution equations derived in chapter 3 were linearised and analysed using the method of collective variables, which has not previously been used in the analysis of CRM-type devices. The analysis resulted in a dispersion relation which governs the linear behaviour of the system. From the dispersion relation, a threshold for instability to occur and growth rates of the electromagnetic field amplitude were derived. Neglecting the variation of the electron axial momentum, ($\rho \ll 1$), a detailed study of the linear growth of the electromagnetic field was performed in both the low and high gain regimes. In the low-gain regime, it was shown that Madey's relations relating the stimulated emission, the spontaneous emission and the energy spread of the electrons could be obtained. The role of the phase evolution of the electromagnetic field in the high-gain regime was also demonstrated.

When significant variations in the electron axial momentum were also considered ($\rho \not\ll 1$), it was shown that another region of instability appeared for $\rho\delta > 1$, and was due to the axial bunching mechanism dominating the azimuthal bunching mechanism. The effect of μ on this instability was found to be less significant than for the azimuthal bunching instability. The condition for instability

to occur at exact autoresonance ($\rho\delta = 1$) was found and the resulting growth rates showed a dependence of $I^{1/2}$ as opposed to $I^{1/3}$ when $\rho \ll 1$. This reflects the fact that the instability at exact autoresonance arises from depletion of the axial momentum of the electron beam as opposed to bunching of the electrons in phase.

Chapter 5

Further Aspects of the Steady - State CRM Interaction

5.1 Hamiltonian Theory of the CRM Interaction

5.1.1 Introduction

In a low-efficiency cyclotron resonance maser, the dynamics of the electrons and the electromagnetic field of a single TE_{mn} or TM_{mn} waveguide mode can be described using the scaled evolution equations (3.167..3.169) :

$$\frac{d\phi_j}{d\bar{z}} = \bar{p}_j - i\frac{\mu}{\sqrt{1+2\mu(\bar{p}_j-\delta_j)}}(\bar{A}e^{i\phi_j} - \text{c.c.}) \tag{5.1}$$

$$\frac{d\bar{p}_j}{d\bar{z}} = -\sqrt{1+2\mu(\bar{p}_j-\delta_j)}(\bar{A}e^{i\phi_j} + \text{c.c.}) \tag{5.2}$$

$$\frac{d\bar{A}}{d\bar{z}} = \left\langle \sqrt{1+2\mu(p-\delta)}e^{-i\phi} \right\rangle \tag{5.3}$$

where $j = 1..N$ and $\langle .. \rangle \equiv 1/N \sum_1^N$. The set of equations (5.1..5.3) are valid in the limit $\rho \ll 1$. An initially monoenergetic electron beam has been assumed.

The equations (5.1..5.3) can be written in Hamiltonian form :

$$\dot{\phi}_j = \frac{\partial H}{\partial \bar{p}_j} \ , \ \dot{\bar{p}}_j = -\frac{\partial H}{\partial \phi_j} \quad \text{where } j = 0..N \tag{5.4}$$

with respect to the Hamiltonian

$$\begin{aligned} H &= \sum_{j=1}^{N} \frac{{p'_j}^2}{2} + \sqrt{\frac{2}{N}} \left(p'_0 \sum_{j=1}^{N} \sqrt{1 + 2\mu p'_j} \cos \phi'_j + \phi'_0 \sum_{j=1}^{N} \sqrt{1 + 2\mu p'_j} \sin \phi'_j \right) \\ &- \frac{\delta}{2} ({\phi'_0}^2 + {p'}_0^2) \end{aligned} \tag{5.5}$$

where $\phi' = \phi - \delta \bar{z}$ and $p' = \bar{p} - \delta$ are the canonical position and momentum variables respectively and ' $\cdot$ ' indicates $\mathrm{d}/\mathrm{d}\bar{z}$. Note that the field has been defined in terms of the canonical variables ϕ'_0 and p'_0 where :

$$\phi'_0 = \sqrt{\frac{N}{2}} \left(\bar{A} e^{i\delta \bar{z}} + c.c. \right) \qquad p'_0 = -i \sqrt{\frac{N}{2}} \left(\bar{A} e^{i\delta \bar{z}} - c.c. \right) \tag{5.6}$$

Another constant of evolution of equations (5.1..5.3) is (3.173)

$$\langle \bar{p} \rangle + \left| \bar{A} \right|^2 = \delta + \left| \bar{A}_0 \right|^2 = \Delta \tag{5.7}$$

which corresponds to conservation of energy. For the remainder of this Hamiltonian analysis, the scaled energy variable $\bar{p}_j$ will just be written as p_j.

5.1.2 Electron Dynamics Neglecting Field Evolution

Consider first of all the dynamics of electron evolution in an electromagnetic field whose amplitude and phase are independent of $\bar{z}$. This corresponds to the case of a CRM operating in a high-Q cylindrical cavity, where the electromagnetic

field profile is determined primarily by the cavity structure alone and not by the interaction with the electron beam. The radiation power output from the cavity is assumed to be equal to that lost by the beam, this being a small proportion of the radiation power in the cavity. With no field evolution, there is no collective interaction between electrons via the field and each electron trajectory is independent of the others. It is then possible to drop the electron index subscript j and consider the evolution of a single representative particle. Consider the resonant case where there is no initial detuning between the wave and the particle ($\delta = 0$). Defining the canonical variable

$$q = \phi + \xi_0 \tag{5.8}$$

the Hamiltonian (5.5) transforms to

$$H = \frac{p^2}{2} + 2\left|\bar{A}_0\right|\sqrt{1+2\mu p}\sin q \tag{5.9}$$

and the evolution equations, from equations (5.4), (5.7) and (5.9), are

$$\dot{q} = p + \frac{2\mu\Delta^{1/2}}{\sqrt{1+2\mu p}}\sin q \tag{5.10}$$

$$\dot{p} = -2\Delta^{1/2}\sqrt{1+2\mu p}\cos q \tag{5.11}$$

As both p and q are real there is a lower bound on the value of p such that for any particle trajectory $p \geq -1/2\mu$. Physically this is because when $p = -1/2\mu$ the transverse momentum of the particle is zero, uncoupling it from the wave.

From (5.11), stationary points in phase space will occur at $q = \pi/2$ and $q = 3\pi/2$ for values of p which satisfy $\dot{q} = 0$. Using the variable

$$x = \sqrt{1+2\mu p} \tag{5.12}$$

and equation (5.10), stationary points will occur at values of p corresponding to real positive roots for x of

$$x^3 - x + 4\mu^2\Delta^{1/2} = 0 \qquad \text{for } q = \pi/2 \tag{5.13}$$

$$x^3 - x - 4\mu^2\Delta^{1/2} = 0 \qquad \text{for } q = 3\pi/2 \tag{5.14}$$

From an analysis of the discriminant of equations (5.13) and (5.14), it is possible to show that the topology of the phase space (q, p) depends upon the size of the depletion parameter μ relative to a critical value μ_c where

$$\mu_c = \left(\frac{1}{108\Delta}\right)^{1/4} \tag{5.15}$$

Note that when $\mu = 0$, the evolution equations (5.10) and (5.11) reduce to those of a simple pendulum (except for a constant phase factor).

At $q = 3\pi/2$ there is an elliptic stationary point for all values of μ. For $\mu < \mu_c$ this point is bounded between $p = 0$ in the limit $\mu \to 0$ and $p = 1/6\mu$ as $\mu \to \mu_c$. On increasing μ above its critical value then the elliptic point has a $p > 1/6\mu$.

At $q = \pi/2$ and for $\mu < \mu_c$ there are two stationary points. One is elliptic and bounded by the values $-1/2\mu \leq p < -1/3\mu$, the other hyperbolic and bounded by $0 \geq p > -1/3\mu$. The left hand values on the bounds of p are for the limit $\mu \to 0$ and the right hand for the limit $\mu \to \mu_c$.

As μ approaches its critical value from $\mu < \mu_c$, both stationary points converge to the value $p = -1/3\mu$ where they annihilate in a bifurcation at $\mu = \mu_c$.

At $q = \pi/2$ and for $\mu > \mu_c$ there are no stationary points.

Examples of these phase spaces for the constant field case are shown in figures 5.1(a..d). Note that for the case of $\mu \ll \mu_c$, figure 5.1(a), the elliptic stationary point at $q = \pi/2$ is outwith the scale of the figure.

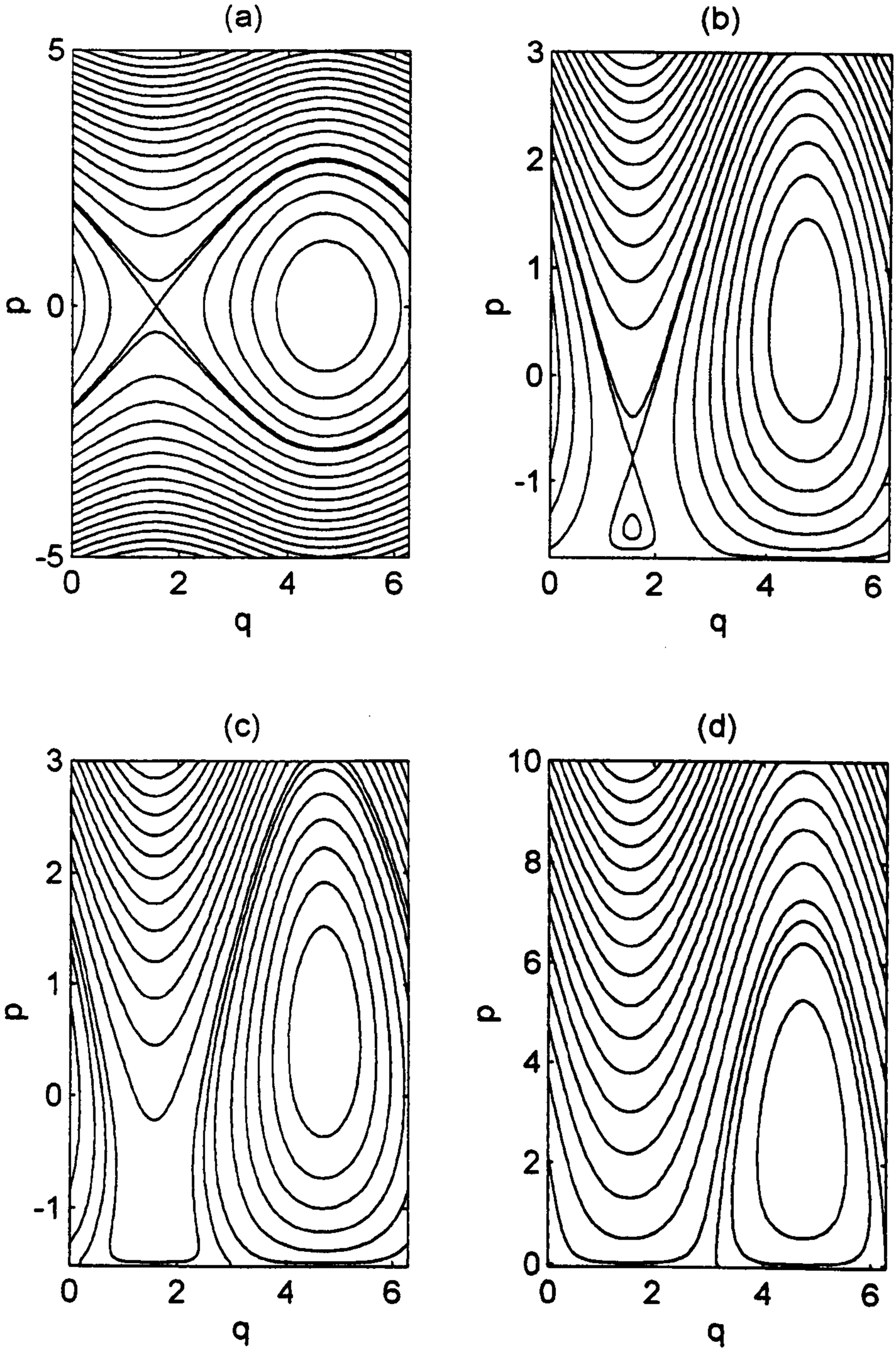

Figure 5.1: Particle phase space plots for a constant field: (a) $\Delta = 1$, $\mu = 10^{-3}$; (b) $\Delta = 1$, $\mu = \mu_c - 0.02$; (c) $\Delta = 1$, $\mu = \mu_c + 0.02$; (d) $\Delta = 1$, $\mu = 10$.

5.1.3 Self-Consistent Single Particle and Field Evolution

The phase space for the case of a single particle interacting self-consistently with the field will now be analysed. This case may be a useful first approximation to a CRM operating with a beam of pre-bunched electrons where the bunch length is less than the radiation field wavelength. These are sometimes referred to as compact electron bunches. Such pre-bunching of electron beams is becoming more feasible with the advent of fast-switching photo-cathodes [73] and field emission array (FEA) cathodes [37, 74], both of which are under development at Strathclyde University (see chapter 1).

A similar single particle analysis has been performed for the Compton FEL [75] where $\mu = 0$. By considering $\mu > 0$ a richer particle phase space topology results.

It is possible to eliminate the field variables using the constant of motion (5.7) i.e.

$$|A| = \sqrt{\Delta - p} \tag{5.16}$$

It is again assumed that the system is at resonance ($\delta = 0$), and the canonical variable is defined as

$$q = \phi + \xi \tag{5.17}$$

The Hamiltonian (5.5) then transforms to

$$H = \frac{p^2}{2} + 2\sqrt{1+2\mu p}\sqrt{\Delta - p}\sin q \tag{5.18}$$

Using (5.4) and (5.18), the evolution equations become

$$\dot{q} \;=\; p + 2\mu\frac{\sqrt{\Delta - p}}{\sqrt{1+2\mu p}}\sin q - \frac{\sqrt{1+2\mu p}}{\sqrt{\Delta - p}}\sin q \tag{5.19}$$

$$\dot{p} = -2\sqrt{1+2\mu p}\sqrt{\Delta - p}\cos q \tag{5.20}$$

As in the previous constant field case, $p = -1/2\mu$ is a lower bound corresponding to the zero of transverse electron momentum. There is now also an upper bound, $p = \Delta$, corresponding to zero field amplitude.

Stationary points will occur when $q = \pi/2$ and $q = 3\pi/2$ for $\dot{q} = 0$. Using the variable

$$y = \frac{\sqrt{1+2\mu p}}{\sqrt{\Delta - p}} \tag{5.21}$$

and equation (5.19), the stationary points will occur at values of p corresponding to real positive roots for y of:

$$y^4 - \Delta y^3 + y - 4\mu^2 = 0 \qquad \text{for } q = \pi/2 \tag{5.22}$$

$$y^4 + \Delta y^3 - y - 4\mu^2 = 0 \qquad \text{for } q = 3\pi/2 \tag{5.23}$$

The quartic nature of these equations indicates that the phase space may be more complex than that of the constant field case of the previous section.

An analysis of the discriminant of equation (5.23) shows that there can only be one elliptic stationary point at $q = 3\pi/2$ for any value of μ or Δ.

By performing a similar analysis of the discriminant of equation (5.22) for points with $q = \pi/2$, a map of regions of parameter space (Δ, μ), can be produced, as shown in figure 5.2. Each region of this map represents phase spaces with different characteristics: In region (a) three stationary points exist, one hyperbolic point situated at a value of p between two elliptic points, and in regions (b)..(d) there is only one elliptic point.

On moving from region (a) to (c) the upper elliptic and hyperbolic points annihilate in a bifurcation leaving only the lower elliptic point. On moving from

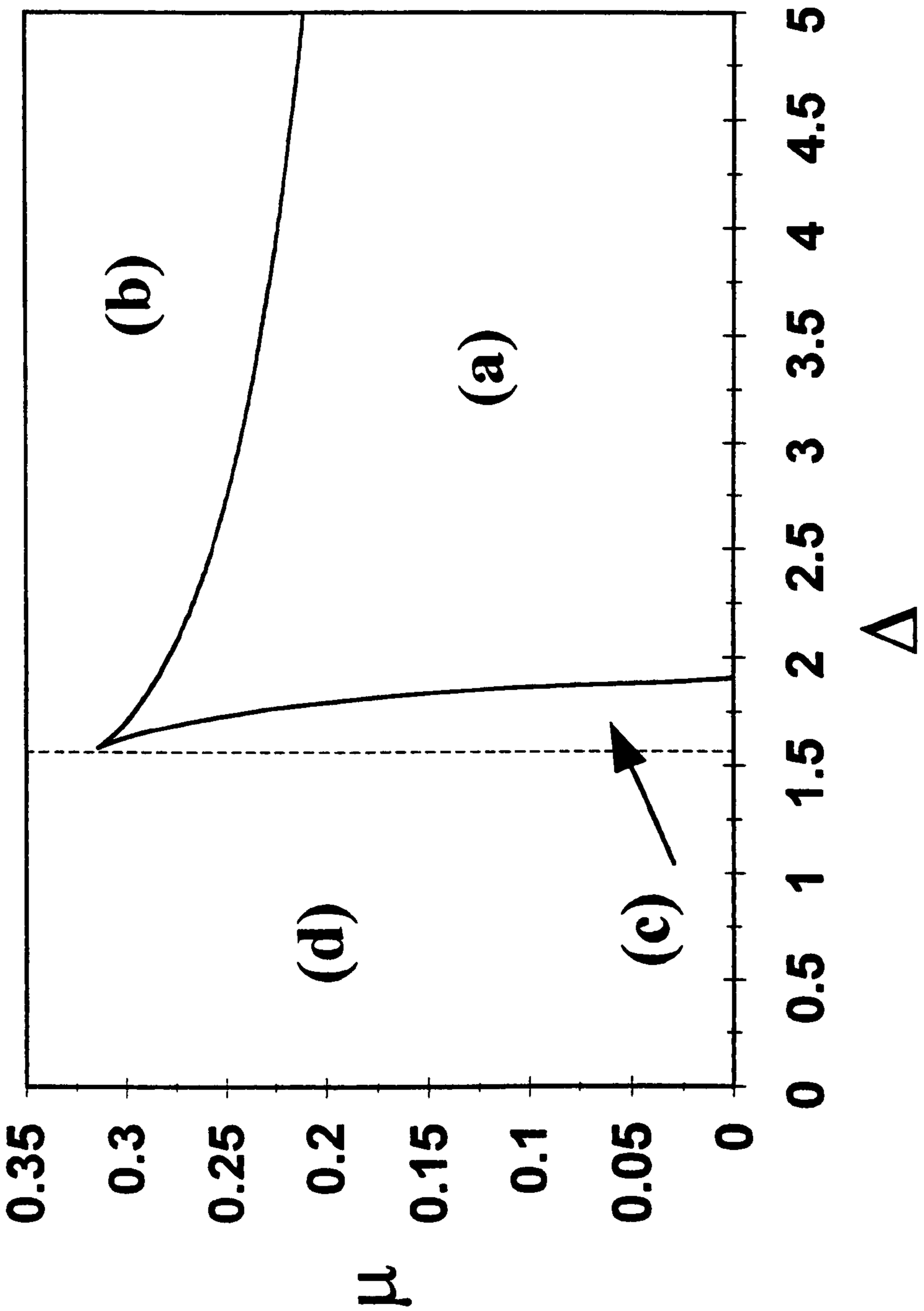

Figure 5.2: The regions of parameter space (Δ,μ) where particle phase space trajectories have different characteristics.

region (a) to (b) it is the lower elliptic and hyperbolic points which similarly annihilate leaving the upper elliptic point. The only difference between regions (c) and (d) is that in region (d) there is only the one (lower) elliptic point for *all* values of μ. The phase spaces for the different regions are shown in figure 5.3.

Also shown in figure 5.3 (d) is the point where $\Delta = 2^{2/3}$ and $\mu = 2^{-5/3}$, that is the point where all regions converge. It occurs when the quartic (5.22) has an inflexion point which is also a triple root. It can be seen that at both $q = \pi/2$ and $q = 3\pi/2$ there are elliptic points at $p = 0$. More generally when $\Delta = 1/2\mu$ the phase space has reflection symmetry about the line $p = 0$.

Also of interest is the case where $\mu = 0$, which corresponds to the case of the high gain Compton FEL. From figure 5.2, it can be seen that when $\Delta > (27/4)^{1/3}$, the system is in region (a), so the above analysis predicts that the region of phase space at $q = \pi/2$ should consist of an hyperbolic point situated between two elliptic points. However, from (5.22), it can be shown that in the limit $\mu \to 0$ the lower elliptic point has a $p \to -\infty$. For $\mu = 0$ and on decreasing Δ from a value of $\Delta > (27/4)^{1/3}$, the upper elliptic and hyperbolic points converge and annihilate in a bifurcation when $\Delta = (27/4)^{1/3}$. The phase space then shows no stationary points at $q = \pi/2$ for $\Delta < (27/4)^{1/3}$ except for the inaccessible elliptic point at $p = -\infty$. This concurs with previous studies of the single particle model of the high gain Compton FEL [75].

By finding the turning points of (5.22), it is possible to find the range of values of y that the stationary points at $q = \pi/2$ in regions (a), (b) or (c) will have as a function of Δ. This is shown in figure 5.4. For $\Delta > 2^{2/3}$ it is seen that there are

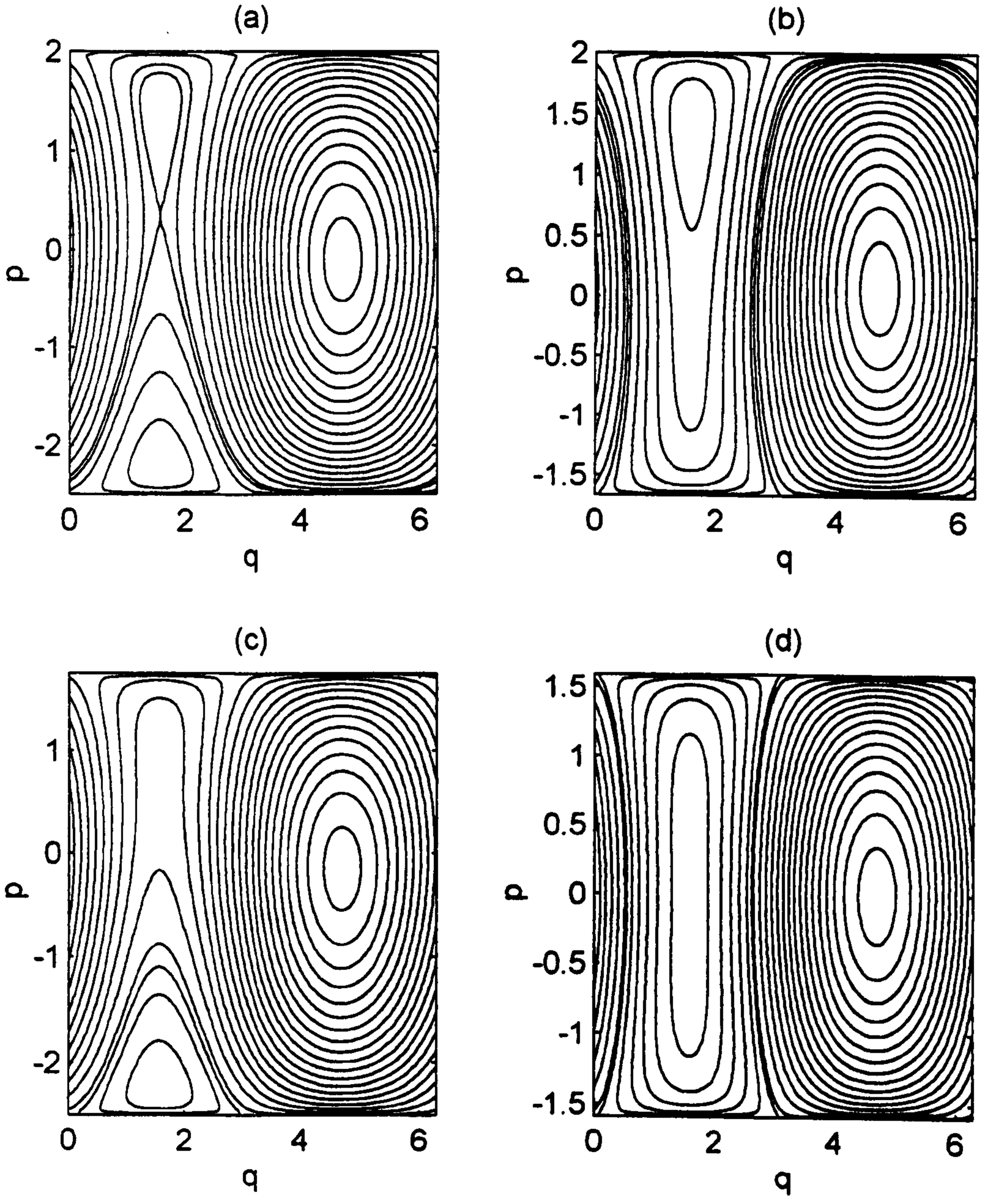

Figure 5.3: Particle phase space plots for self-consistent single-particle/field evolution: (a) $\Delta = 2$, $\mu = 0.2$ (region a); (b) $\Delta = 2$, $\mu = 0.3$ (region b/d); (c) $\Delta = 1.75$, $\mu = 0.2$ (region c/d); (d) $\Delta = 2^{2/3}$, $\mu = 2^{-5/3}$.

three different ranges:

- $0 < y < y_{min}(\Delta)$ defines the range of y within which a lower elliptic point may be found

- $y_{min}(\Delta) < y < y_{max}(\Delta)$ defines the range of y within which an hyperbolic point may be found

- $y_{min}(\Delta) < y < \infty$ defines the range of y within which an upper elliptic point may be found

For a given value of μ and Δ figure 5.2 determines the stationary points that will exist. The ranges of p within which these stationary points will lie is determined by the ranges of y from figure 5.4 and the substitution of these ranges and the value of μ into equation (5.21).

It will now be shown how the bounds on p i.e. $-1/2\mu \leq p \leq \Delta$ play a further role in the phase space topology. Recall that the lower bound on p results from the complete depletion of transverse electron energy and that the upper bound results when the electron has depleted all radiation field energy.

When $p = \Delta$ and $p = -1/2\mu$ the values of the Hamiltonian are $H = H_\Delta \equiv \Delta^2/2$ and $H = H_\mu \equiv 1/8\mu^2$ respectively. It will be seen that these two contours behave as separatrices in that they separate regions of phase space rotation and libration. Unlike true separatrices however neither passes through a stationary point.

Consider first the case where there is only one elliptic point at $q = \pi/2$ (regions (b), (c) and (d) of figure (5.2)). At $q = 0$ and π, the Hamiltonian has the value

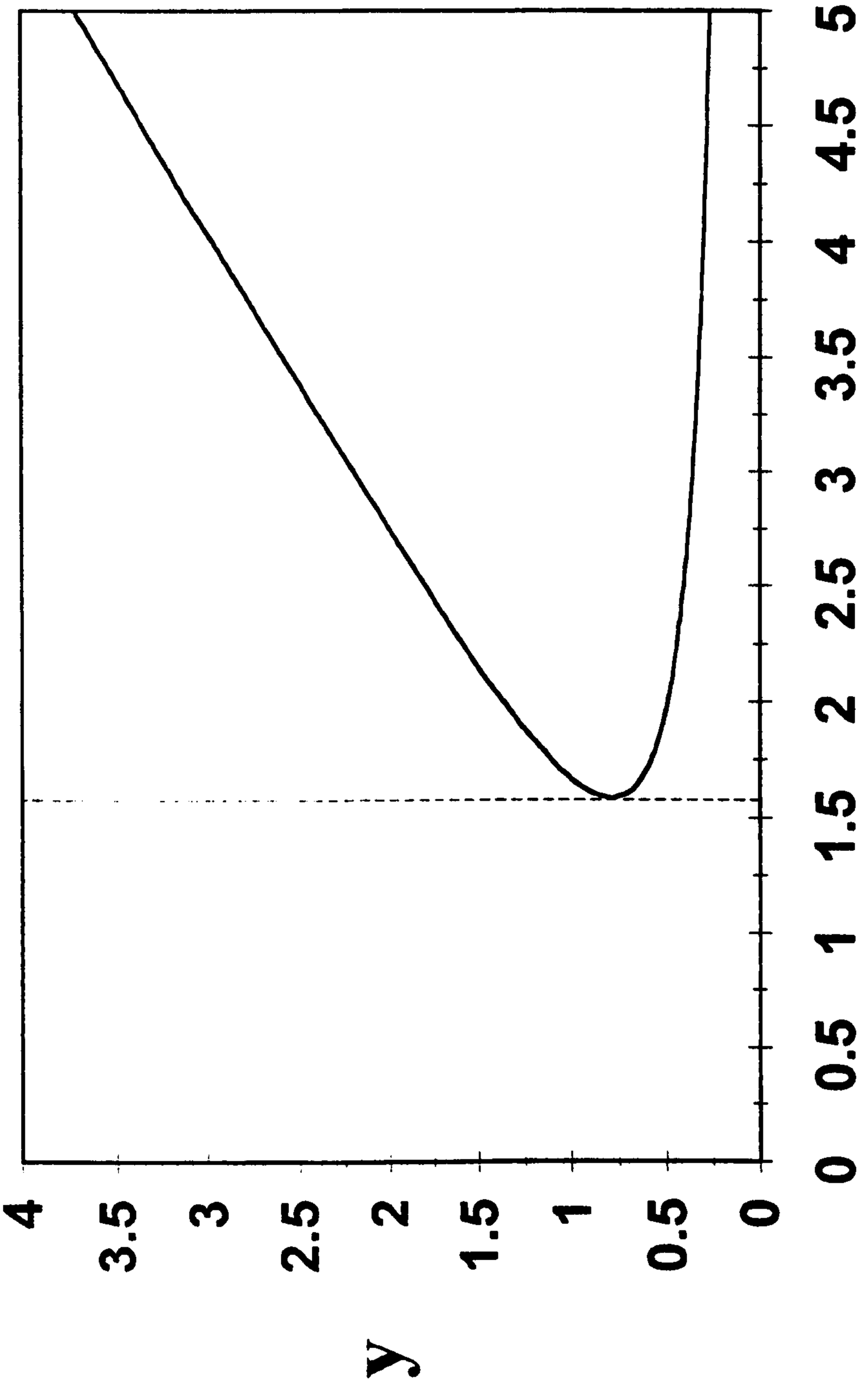

Figure 5.4: The ranges of y within which the stationary points at $q = \pi/2$ exist. The lower curve is $y_{min}(\Delta)$, the upper curve is $y_{max}(\Delta)$.

$H = p^2/2$ and so for $p = \Delta$, $H = H_\Delta$ and for $p = -1/2\mu$, $H = H_\mu$. Two distinct phase spaces result depending upon whether $H_\mu \gtrless H_\Delta$. Figure (5.5a) shows the contours H_μ and H_Δ for $H_\mu > H_\Delta$ and figure (5.5b) shows the same contours for $H_\mu < H_\Delta$. For $H_\mu > H_\Delta$ it is seen that the H_Δ and H_μ contours are similar in form except for the region $p \lesssim \Delta$. It appears that the H_μ contour 'attempts' to close at $q = 0$ and π in a similar way to the H_Δ contour. It cannot do this however as for these values of q, the value of p would be greater than its allowed maximum of Δ, and so the contour distorts to that shown in the figure. In a similar way when $H_\mu < H_\Delta$ the H_Δ contour cannot close at $q = 0$ and π as the value of p would be less than its allowed minimum of $p = -1/2\mu$ resulting in a similarly distorted contour.

By defining:

$$H_0 = 2\sqrt{\Delta}\sin q_0 \tag{5.24}$$

which specifies the contour on which the particle at $p = 0$ and $q = q_0$ will lie, it is possible to summarise the above results for the case where there is only one elliptic point at $q = \pi/2$ (regions (b),(c) and (d) of figure (5.2)):

For $H_\mu > H_\Delta$ then if

- $H_0 > H_\mu$, the particle will librate about $q = \pi/2$
- $H_0 < H_\Delta$, the particle will librate about $q = 3\pi/2$
- $H_\Delta < H_0 < H_\mu$, the particle will rotate with an average phase flow towards negative q

For $H_\mu < H_\Delta$ then if

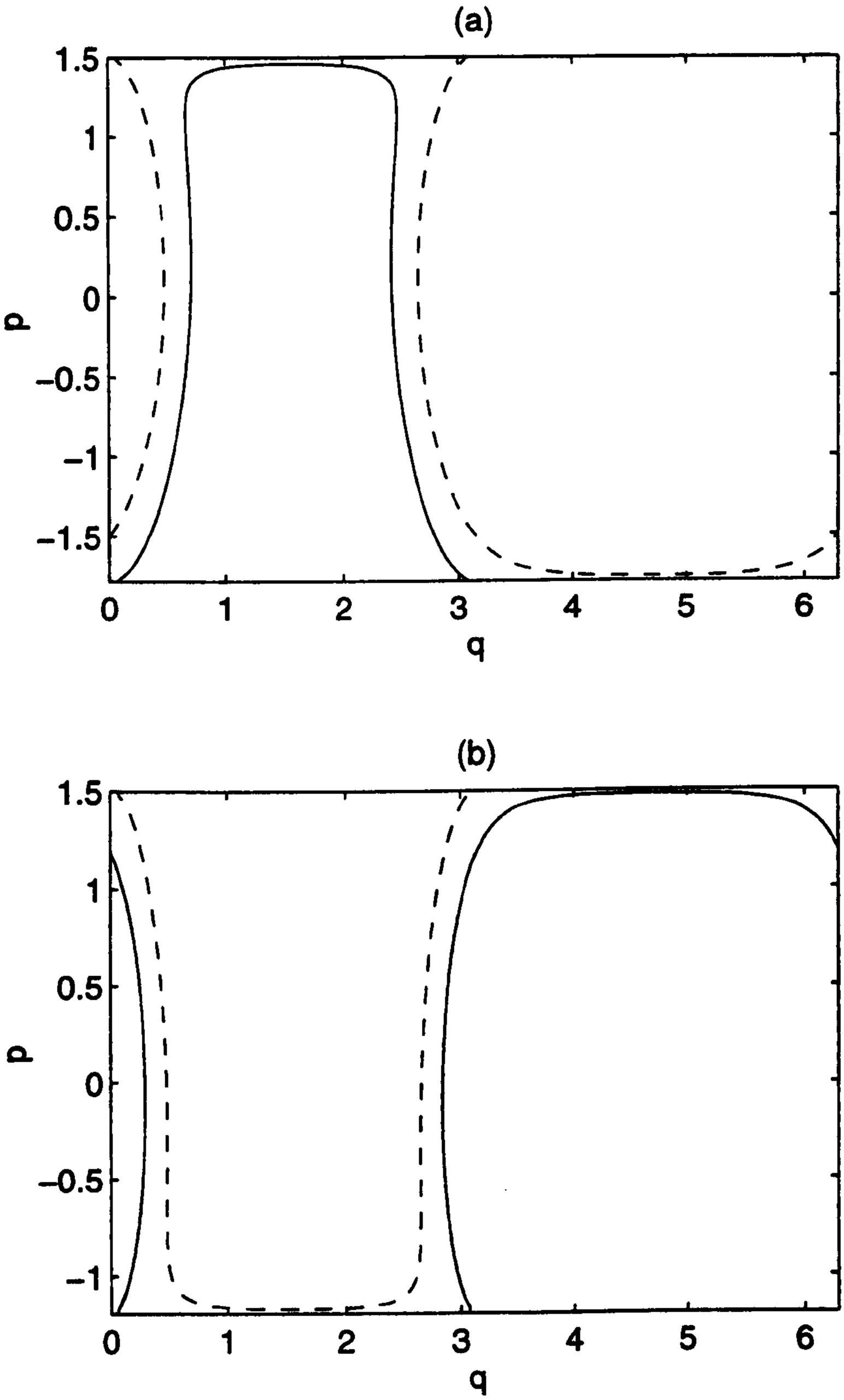

Figure 5.5: The contours H_μ (solid line) and H_Δ (dashed line): (a) $H_\mu > H_\Delta$; (b) $H_\mu < H_\Delta$.

- $H_0 > H_\Delta$, the particle will librate about $q = \pi/2$
- $H_0 < H_\mu$, the particle will librate about $q = 3\pi/2$
- $H_\mu < H_0 < H_\Delta$, the particle will rotate with an average phase flow towards positive q

For the special case of $H_\Delta = H_\mu$ then the phase space is symmetric about the line $p = 0$ and the particle will either librate about $q = \pi/2$ for $H_0 > H_\Delta$ or about $q = 3\pi/2$ for $H_0 < H_\Delta$. There will be no regions of phase flow rotation.

The presence of an hyperbolic point at $q = \pi/2$ (region (a) of figure (5.2)) results in a more featured phase space. The value of the Hamiltonian corresponding to the separatrix of the hyperbolic stationary point is defined as

$$H_h = \frac{{p_h}^2}{2} + 2\sqrt{1 + 2\mu p_h}\sqrt{\Delta - p_h} \tag{5.25}$$

where p_h is the p co-ordinate of the hyperbolic point i.e. $(\pi/2, p_h)$. This is found from the roots of the quartic (5.22).

There are six possible relative values for H_h, H_μ and H_Δ (neglecting equalities). The phase spaces of these three contours are shown in figures 5.6 (a..f) for the six relative values:

(a) $H_h < H_\Delta < H_\mu$, (b) $H_h < H_\mu < H_\Delta$, (c) $H_\Delta < H_h < H_\mu$,
(d) $H_\mu < H_h < H_\Delta$, (e) $H_\Delta < H_\mu < H_h$, (f) $H_\mu < H_\Delta < H_h$.

Some features to note from these figures are that if $H_\mu < H_\Delta$ then the phase flow of rotational orbits *accessible* (as the particle can only move on contours which cross $p = 0$) to the particle will have on average an increasing q. Conversely

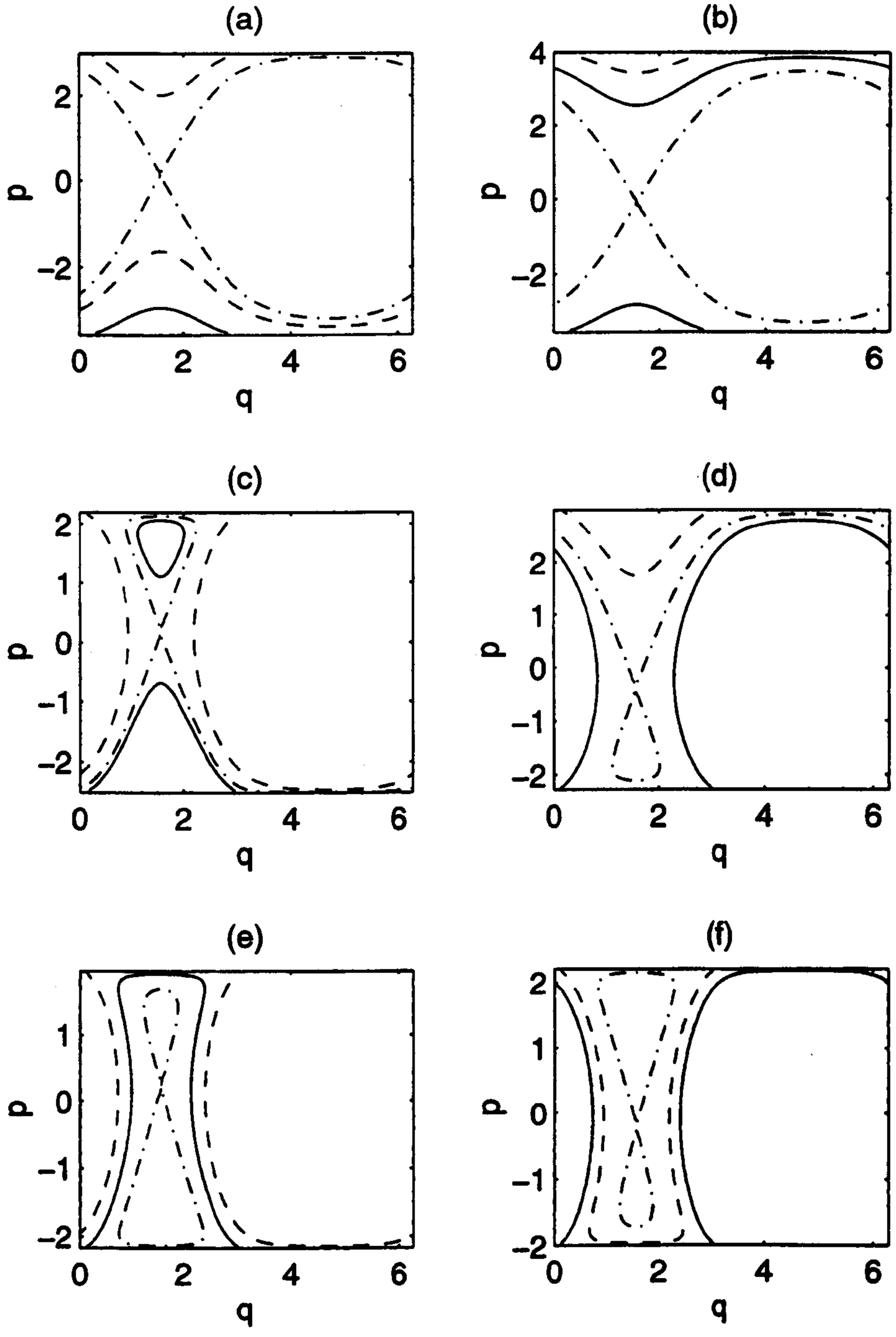

Figure 5.6: The contours H_μ (solid line), H_Δ (dashed line) and $H = H_h$ (dot-dash line): (a) $H_h < H_\Delta < H_\mu$, (b) $H_h < H_\mu < H_\Delta$, (c) $H_\Delta < H_h < H_\mu$, (d) $H_\mu < H_h < H_\Delta$, (e) $H_\Delta < H_\mu < H_h$, (f) $H_\mu < H_\Delta < H_h$.

if $H_\mu > H_\Delta$ then the phase flow of rotational orbits will have on average a decreasing q. Also note that if $H_h > H_\Delta$ then the upper orbit of the seperatrix of the hyperbolic point will be homoclinic, and if $H_h > H_\mu$ then the lower orbit of the seperatrix of the hyperbolic point will be homoclinic. Otherwise seperatrix orbits of the hyperbolic point are heteroclinic.

5.1.4 Complete Transverse Energy Depletion for Self-Consistent Particle-Field Evolution

It can be seen from the analysis of the previous section that if $H_0 = H_\mu$, then it is possible for the particle to attain a value of $p = -1/2\mu$ i.e. complete depletion of its perpendicular momentum. For this value of H_0, the value of q_0 is from (5.24)

$$q_0 = \sin^{-1}\left(\frac{1}{16\mu^2\sqrt{\Delta}}\right) \tag{5.26}$$

For $16\mu^2\sqrt{\Delta} > 1$, the region of interest is $0 \leq q_0 \leq \pi/2$, as for these values of q_0 the particle will initially lose energy. The contour approaches $p = -1/2\mu$ at $q = 0$ so $0 \leq q \leq \pi/2$ at all times. The analysis which follows will yield an expression for the interaction length required for the particle to exhaust all of its perpendicular energy.

Firstly, equations (5.18) and (5.20) for H and $\dot{p}$ will be restated. As in the last section, the analysis is performed for the case of a particle interacting self-consistently with the field :

$$H = \frac{p^2}{2} + 2\sqrt{1+2\mu p}\sqrt{\Delta - p}\sin q \tag{5.27}$$

$$\dot{p} = -2\sqrt{1+2\mu p}\sqrt{\Delta - p}\cos q \tag{5.28}$$

From (5.27),

$$\sin q = \frac{2H - p^2}{4\sqrt{1+2\mu p}\sqrt{\Delta - p}} \tag{5.29}$$

Now

$$\cos q = \sqrt{1 - \sin^2 q} \tag{5.30}$$

where the positive root applicable to the region of interest $0 \leq q \leq \pi/2$ has been taken. Substituting (5.29) into (5.30) gives

$$\cos q = \frac{\sqrt{16(1+2\mu p)(\Delta - p) - (2H - p^2)^2}}{4\sqrt{1+2\mu p}\sqrt{\Delta - p}} \tag{5.31}$$

Substituting for $\cos q$ into (5.28) gives

$$\frac{dp}{d\bar{z}} = -\frac{1}{2}\sqrt{16(1+2\mu p)(\Delta - p) - (2H - p^2)^2} \tag{5.32}$$

This is a general differential equation for p in the interval $0 \leq q \leq \pi/2$ in terms of the control parameters Δ, μ and H.

It is now possible to separate variables and by specifying that $H = H_\mu$, $p(\bar{z} = 0) = 0$ and $p(\bar{z} = L) = -1/2\mu$, an expression for L, the scaled interaction length required for complete transverse energy depletion of the particle, is obtained:

$$L = -2\int_0^{-1/2\mu} \frac{dp}{\sqrt{Q(p)}} \tag{5.33}$$

$$\text{where: } Q(p) = (1/2\mu + p)(32\mu(\Delta - p) - (1/2\mu + p)(1/2\mu - p)^2) \tag{5.34}$$

This integral can be reduced to an elliptic integral using standard transformations, the precise transformation depending on the roots of $Q(p)$, which is a quartic polynomial in p. From (5.34), it is seen that $p = -1/2\mu$ is always a root of $Q(p)$. In addition, from (5.31) it is clear that any roots of $Q(p)$ are also zeros of $\cos q$, i.e. values of p at which the contour H_μ intersects $q = \pi/2$ or $3\pi/2$. This limits the number of cases to be considered to just two :

(i) $Q(p)$ has two real roots $\alpha_2 < 0 \leq \alpha_1$ and two complex roots $b + ic$ and $b - ic$, where $c > 0$.

(ii) $Q(p)$ has four real roots $\alpha_4 < 0 \leq \alpha_3 < \alpha_2 < \alpha_1$.

In both cases, $p = -1/2\mu$ must be the smallest real root as paths with $p < -1/2\mu$ are not physical.

Case (i): $Q(p)$ has two real roots and two complex roots

As $p = -1/2\mu$ is always a root of $Q(p)$, this case implies that there is one other value of p at which the contour H_μ intersects $q = \pi/2$ or $3\pi/2$. Examples of these are shown in figures 5.5 (a and b) and 5.6 (a,d,e and f). The transformation of the integral (5.33) in this case involves the variables [76] :

$$\tan \phi/2 = \sqrt{\frac{\cos\theta_1}{\cos\theta_2}\frac{\alpha_1 - p}{p - \alpha_2}} \tag{5.35}$$

$$k = \sin\frac{\theta_1 - \theta_2}{2} \tag{5.36}$$

$$D = -\frac{\cos\theta_1 \cos\theta_2}{c}$$

$$\tan\theta_1 = \frac{\alpha_1 - b}{c} \tag{5.37}$$

$$\tan\theta_2 = \frac{\alpha_2 - b}{c} \quad , \theta_1, \theta_2 \text{ acute} \tag{5.38}$$

where: $\alpha_2(= -1/2\mu) < 0 \leq \alpha_1$ are the real roots and $b+ic$, $b-ic$ are the complex roots. The transformed integral then becomes

$$L = -2D \int_{\phi_0}^{\pi} \frac{d\phi}{\sqrt{1 - k^2 \sin^2\phi}} \tag{5.39}$$

Splitting this integral into two over the limits $[\phi_0, 0]$ and $[0, \pi]$, where $\phi_0 = \phi(\bar{z} = 0)$, and using the relation:

$$F(k, \pi) = 2F(k, \pi/2) = 2K(k) \tag{5.40}$$

where $F(k,\phi)$ is an incomplete elliptic integral of the first kind and $K(k)$ is a complete elliptic integral of the first kind, yields the result:

$$L = \frac{2\cos\theta_1\cos\theta_2}{c}\left(2K(k) - F(k,\phi_0)\right) \tag{5.41}$$

$$\text{where } \tan\phi_0/2 = \sqrt{\frac{\cos\theta_1}{\cos\theta_2}\frac{\alpha_1}{(-\alpha_2)}} \tag{5.42}$$

and the definitions of k, θ_1 and θ_2 are given in (5.36), (5.37) and (5.38) respectively.

Case(ii): $Q(p)$ has three positive real roots and one negative real root

As $p = -1/2\mu$ is always a root of $Q(p)$, this implies that there are 3 other values of p at which the contour H_μ intersects $q = \pi/2$ and $3\pi/2$. Examples of these are shown in figure 5.6(b and c). Here only the case where $H_\mu > H_\Delta$ is considered (figure 5.6(c)) otherwise the contour H_μ which intersects $p = -1/2\mu$ does not intersect the line $p = 0$ making it inaccessible to the particle. The transformation for this case involves the variables [76] :

$$\sin^2\phi = \left(\frac{\alpha_1-\alpha_3}{\alpha_3-\alpha_4}\right)\left(\frac{p-\alpha_4}{\alpha_1-p}\right) \tag{5.43}$$

$$k = \sqrt{\left(\frac{\alpha_3-\alpha_4}{\alpha_1-\alpha_3}\right)\left(\frac{\alpha_1-\alpha_2}{\alpha_2-\alpha_4}\right)} \tag{5.44}$$

$$D = \frac{2}{\sqrt{(\alpha_1-\alpha_3)(\alpha_2-\alpha_4)}}$$

where: $\alpha_4(=-1/2\mu) < 0 \leq \alpha_3 < \alpha_2 < \alpha_1$ are the four real roots of $Q(p)$. As before, the limits of the transformed integral are found by substituting the limits of the original integral into (5.43) which leads to

$$L = -2D\int_{\phi_0}^{0}\frac{d\phi}{\sqrt{1-k^2\sin^2\phi}} \tag{5.45}$$

Rearranging this equation yields the result

$$L = \frac{4}{\sqrt{(\alpha_1 - \alpha_3)(\alpha_2 - \alpha_4)}} F(k, \phi_0) \tag{5.46}$$

$$\text{where } \phi_0 = \sin^{-1} \sqrt{\frac{-\alpha_4}{\alpha_1} \frac{(\alpha_1 - \alpha_3)}{(\alpha_1 - \alpha_2)}} \tag{5.47}$$

5.1.5 Conclusions

The dynamics of a CRM within the limits $k_\perp r_L \ll 1$ and $\rho \ll 1$ have been analysed using a fully Hamiltonian method for two specific resonant cases: no field evolution and self-consistent field evolution with a single particle.

In the case of no field evolution, it was found that the size of the depletion parameter, μ relative to a critical value μ_c significantly changes the topology of the phase space around $q = \pi/2$. This description will be valid for a CRM oscillator operating in a high-Q cylindrical cavity where the electromagnetic field profile is fixed.

In the case of self-consistent field evolution with a single particle, a map of the parameter space (Δ, μ) was constructed and regions of this map associated with specific characteristics of the corresponding phase space (q, p). The results of this analysis in the limit of $\mu = 0$ concur with those from similar studies of the high gain Compton FEL. The effect of the bounds on the transverse electron energy on the topology of the phase space was also investigated. Finally, an analytical expression in terms of elliptic integrals for the interaction length required to deplete all of a single particle's transverse energy was obtained. These investigations may be of use in describing the evolution of both electrons and field in a pre-bunched electon beam configuration.

5.2 A Landau-Ginzburg Equation for the CRM

5.2.1 Introduction

The linear and nonlinear evolution of the interaction between a beam of relativistic electrons gyrating in a uniform magnetic field and a TE_{mn} or TM_{mn} cylindrical waveguide mode is described by the system of equations (3.167..3.169), when the recoil of the electrons is small ($\rho \ll 1$) and $k_\perp r_L \ll 1$. In the linear regime, these equations have been used to derive a dispersion relation, the roots of which determine growth of the electromagnetic field in the linear regime (see section 4.2.1). Analysis of the nonlinear regime however has up to now required a numerical integration of $2N+2$ coupled equations describing the evolution of the phases and energies of $N \gg 1$ electrons together with the evolution of the complex electromagnetic field amplitude. The aim of this section is to show that the evolution of the interaction can be approximated far into the nonlinear regime by a set of only three complex equations and that these equations can be further used to derive a Landau-Ginzburg equation which describes the evolution of the electromagnetic field up to saturation. This Landau-Ginzburg equation has the useful property of having a full analytical solution.

5.2.2 A Collective Variable Description of the CRM

The method of collective variables was successfully used to analyse the CRM interaction in the linear regime. In this section, it will be shown that this method may be generalised to describe the nonlinear regime also. The starting point of

the analysis is the set of $2N+2$ equations (3.167..3.169), which describe the CRM interaction when $\rho \ll 1$:

$$\frac{d\phi_j}{d\bar{z}} = \bar{p}_j - i\frac{\mu}{\sqrt{1+2\mu(\bar{p}_j-\delta)}}\left(\bar{A}e^{i\phi_j} - c.c.\right) \tag{5.48}$$

$$\frac{d\bar{p}_j}{d\bar{z}} = -\sqrt{1+2\mu(\bar{p}_j-\delta)}\left(\bar{A}e^{i\phi_j} + c.c.\right) \tag{5.49}$$

$$\frac{d\bar{A}}{d\bar{z}} = \left\langle \sqrt{1+2\mu(\bar{p}-\delta)}e^{-i\phi}\right\rangle \tag{5.50}$$

Using the variables originally defined in (4.1..4.3) i.e.

$$\phi' = \phi - \delta\bar{z} \quad , \quad p' = \bar{p} - \delta \quad , \quad A' = \bar{A}e^{i\delta\bar{z}}$$

the equations (5.48..5.50) can be written in the more compact form

$$\frac{d\phi'_j}{d\bar{z}} = p'_j - i\frac{\mu}{\sqrt{1+2\mu p'_j}}(A'e^{i\phi'_j} - c.c.) \tag{5.51}$$

$$\frac{dp'_j}{d\bar{z}} = -\sqrt{1+2\mu p'_j}(A'e^{i\bar{\phi}_j} + c.c.) \tag{5.52}$$

$$\frac{dA'}{d\bar{z}} = \left\langle \sqrt{1+2\mu p'}\, e^{-i\phi'}\right\rangle + i\delta A' \tag{5.53}$$

As shown in section 3.4, the equations (5.51..5.53) have two constants of evolution :

$$\langle p'\rangle + |A'|^2 = |A'_0|^2 \tag{5.54}$$

$$\frac{\langle p'^2\rangle}{2} - i(A'\left\langle \sqrt{1+2\mu p'}\, e^{i\phi'}\right\rangle - c.c.) - \delta|A'|^2 =$$

$$-i(A'_0\left\langle e^{i\phi'_0}\right\rangle - c.c.) - \delta|A'_0|^2 \tag{5.55}$$

which correspond to conservation of energy and the Hamiltonian of the system respectively.

This set of equations can be further simplified by defining a complex variable

$$\mathcal{U}_j = \sqrt{1+2\mu p'_j}\, e^{i\phi'_j} \tag{5.56}$$

which enables the set of evolution equations (5.51..5.53) to be written as a set of two complex equations

$$\frac{d\mathcal{U}_j}{d\bar{z}} = \frac{i}{2\mu}\mathcal{U}_j\left(|\mathcal{U}_j|^2 - 1\right) - 2\mu A'^* \tag{5.57}$$

$$\frac{dA'}{d\bar{z}} = \langle \mathcal{U}^* \rangle + i\delta A'. \tag{5.58}$$

Defining the variables

$$b = \langle \mathcal{U}^* \rangle \quad , \quad \mathcal{P} = \langle |\mathcal{U}|^2 \mathcal{U}^* \rangle \tag{5.59}$$

it is easily shown using (5.57) that

$$\frac{db}{d\bar{z}} = -\frac{i}{2\mu}(\mathcal{P} - b) - 2\mu A' \tag{5.60}$$

$$\frac{d\mathcal{P}}{d\bar{z}} = -\frac{i}{2\mu}\langle \mathcal{U}^* |\mathcal{U}|^2 (|\mathcal{U}|^2 - 1)\rangle$$

$$-4\mu A' \langle |\mathcal{U}|^2 \rangle - 2\mu A'^* \langle \mathcal{U}^{*2} \rangle \tag{5.61}$$

The variables b and $\mathcal{P}$ are analogous to the 'bunching parameter' and 'energy modulation parameter' of FEL theory [77].

The last term in (5.61) is a second harmonic term, proportional to $\langle e^{-2i\phi'} \rangle$ and, as with [77], will be neglected from now on. In order to close the set of equations (5.58), (5.61) and (5.60), it is necessary to use the following ansatz

$$\langle (p' - \langle p' \rangle)^2 \mathcal{U}^* \rangle \approx \langle (p' - \langle p' \rangle)^2 \rangle \langle \mathcal{U}^* \rangle \tag{5.62}$$

which is exact if the p' have a Gaussian distribution. This can be rearranged to give

$$\langle p'^2 \mathcal{U}^* \rangle = \langle p'^2 \rangle \langle \mathcal{U}^* \rangle + 2\langle p' \mathcal{U}^* \rangle \langle p' \rangle - 2\langle p' \rangle^2 \langle \mathcal{U}^* \rangle \tag{5.63}$$

It can be seen that if $\mu = 0$ i.e. $\mathcal{U} = e^{i\phi'}$ then (5.62) reduces to the ansatz used in [77] to facilitate a collective variable description of the FEL. Using the

definition of $\mathcal{U}$, the constants of motion (5.54), (5.55) and ansatz (5.62) then it is possible to write $d\mathcal{P}/d\bar{z}$ in terms of b, $\mathcal{P}$ and A' only, so closing the system of equations (5.58), (5.60) and (5.61) to

$$\frac{db}{d\bar{z}} = -\frac{i}{2\mu}(\mathcal{P}-b) - 2\mu A' \tag{5.64}$$

$$\begin{aligned}\frac{d\mathcal{P}}{d\bar{z}} = & -\frac{i}{2\mu}(1-4\mu|A'|^2)(\mathcal{P}-b) + 4\mu(A'|b|^2 - A'^*b^2) \\ & + 4\mu i|A'|^4 b - 4\mu A' + 8\mu^2|A'|^2A' \\ & - 4\mu i\delta\left(|A'|^2 - |A'_0|^2\right)b - 4\mu(A'_0b_0^* - c.c)b\end{aligned} \tag{5.65}$$

$$\frac{dA'}{d\bar{z}} = b + i\delta A' \tag{5.66}$$

where $b_0 = b(\bar{z}=0)$ and $A'_0 = A'(\bar{z}=0)$. Figures 5.7(a) and 5.7(b) show how $|A'|^2$ varies with $\bar{z}$ from a numerical integration of the original equations (5.48..5.50) and from a numerical integration of the collective variable equations (5.64..5.66) respectively for the case where $\delta = 0$ and $\mu = 0.1$. Figures 5.8(a) and 5.8(b) show equivalent graphs to those in figure 5.7 for the case where $\delta = 0$ and $\mu = 0.8$. It can be seen that there is good agreement between these results through to saturation, justifying the use of (5.62) and the neglect of terms varying as $\langle e^{-2i\phi'}\rangle$.

5.2.3 Derivation of a Landau-Ginzburg equation

Successive differentiation of (5.66) and the use of (5.64) and (5.65) transforms the set of collective variable equations to a single third-order nonlinear differential equation describing the electromagnetic field evolution,

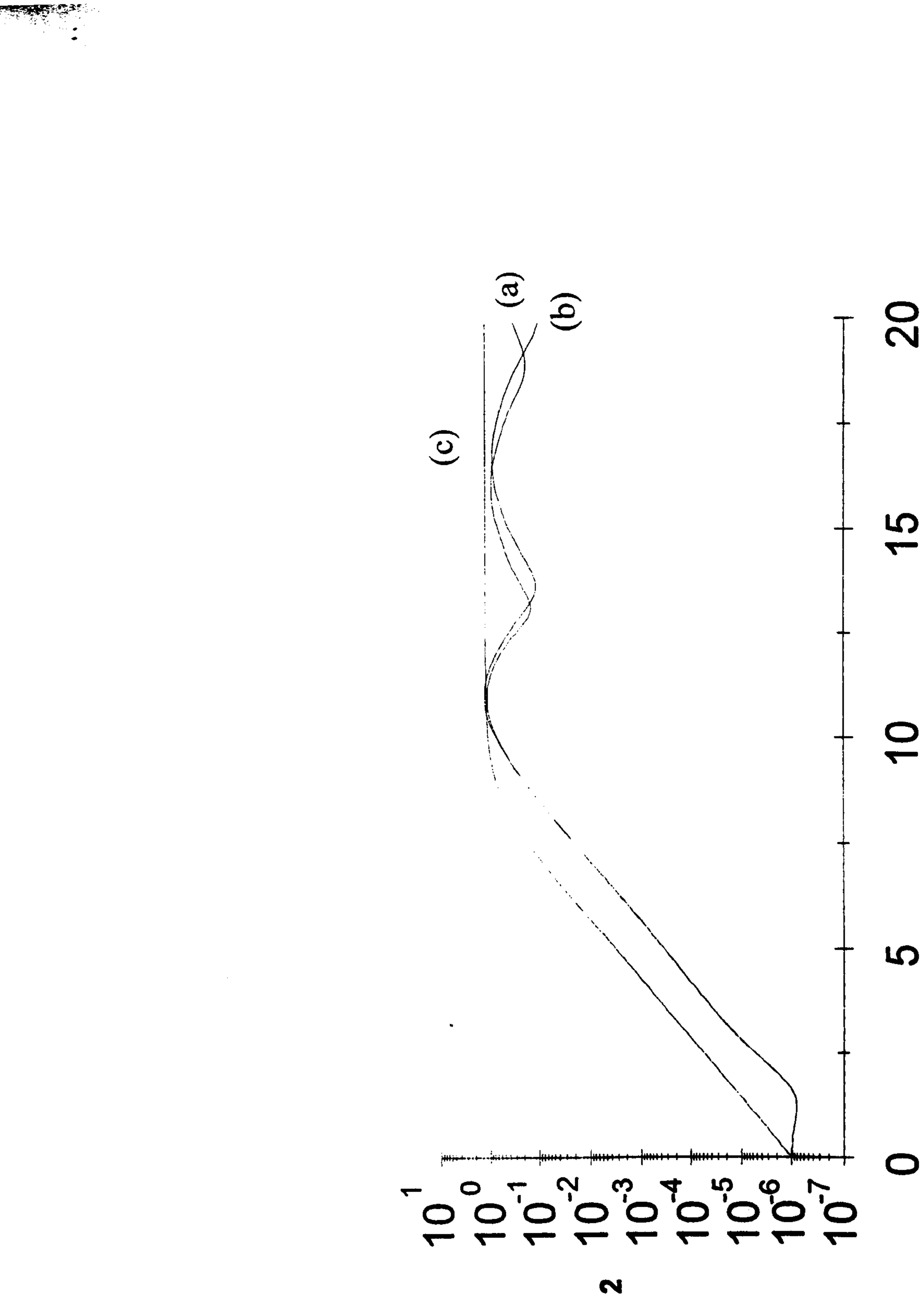

Figure 5.7: Plot of $|A'|^2$ vs $\bar{z}$ for $\delta = 0$ and $\mu = 0.1$. **(a) numerical solution of equations (5.48..5.50) (b) numerical solution of collective variable equations (5.64..5.66) (c) analytical solution of equation (5.74)**

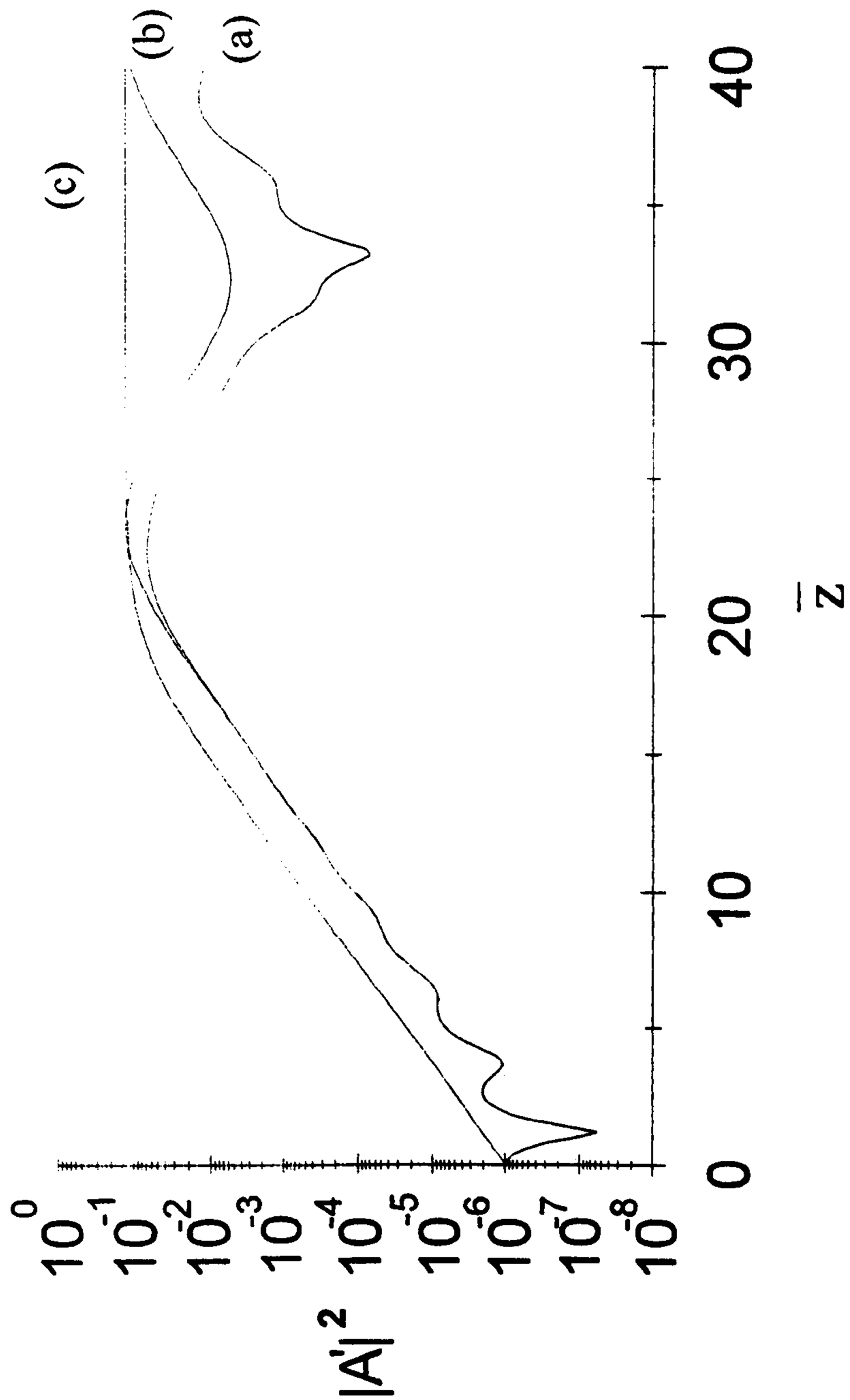

Figure 5.8: Plot of $|A'|^2$ vs $\bar{z}$ for $\delta = 0$ and $\mu = 0.8$. (a) numerical solution of equations (5.48..5.50) (b) numerical solution of collective variable equations (5.64..5.66) (c) analytical solution of equation (5.74)

$$\frac{d^3A'}{d\bar{z}^3} - i\delta\frac{d^2A'}{d\bar{z}^2} + 2\mu\frac{dA'}{d\bar{z}} - iA' = \tag{5.67}$$
$$- 2iA'\left|\frac{dA'}{d\bar{z}} - i\delta A'\right|^2 + 2iA'^*\left(\frac{dA'}{d\bar{z}} - i\delta A'\right)^2$$
$$+ 2i|A'|^2\frac{d^2A'}{d\bar{z}^2} + 2|A'|^4\left(\frac{dA'}{d\bar{z}} - i\delta A'\right) + 2i\delta^2|A'|^2A'.$$

It has been assumed that A'_0 is negligibly small and $b_0 = 0$. It will be shown here that this equation can be reduced to the form of a Landau-Ginzburg equation with complex coefficients. The methods used will be similar to those used in [78].

Neglecting all the nonlinear terms in (5.67) it is found that the field evolves as

$$A'(\bar{z}) \approx a\ exp(-ik\bar{z}) \tag{5.68}$$

where k is that complex root of the dispersion relation

$$k^3 + \delta k^2 - 2\mu k - 1 = 0 \tag{5.69}$$

such that $k = k_r + ik_i$ where $k_i > 0$. It is easily checked using the variable $\lambda = -k$ that this dispersion relation is identical to (4.42) which was obtained from a linear analysis of the full set of equations (3.151..3.155) in the limit $\rho \ll 1$.

Using (5.68) to evaluate the nonlinear terms in (5.67) and using the further assumption that the complex amplitude a is a slowly varying function of $\bar{z}$, an approximate evolution equation for a can be obtained [79]:

$$\frac{d^3a}{d\bar{z}^3} - i(3k+\delta)\frac{d^2a}{d\bar{z}^2} - (3k^2 + 2k\delta - 2\mu)\frac{da}{d\bar{z}} = \tag{5.70}$$
$$- 2i(k+\delta)(2k+k^*+\delta)a|a|^2e^{2k_iz} - 2i(k+\delta)a|a|^4e^{4k_iz}$$

Neglecting all derivatives of a higher than the first and considering only the cubic nonlinear term it is possible to write the equation for a as

$$\frac{da}{d\bar{z}} \approx -ce^{2k_i\bar{z}}a|a|^2 \tag{5.71}$$

where

$$c = c_r + ic_i = -2i\frac{(k+\delta)(2k+k^*+\delta)}{3k^2+2\delta k-2\mu} \tag{5.72}$$

This allows an equation for the original field variable A' to be written using (5.68) as

$$\frac{dA'}{d\bar{z}} = -ikA' - cA'|A'|^2 \tag{5.73}$$

which is a Landau-Ginzburg equation with complex coefficients and has the same form as the corresponding equations describing the saturation process and the phase transition in atomic lasers [80]. It can be shown from (5.73) that the corresponding equations for the scaled field intensity $I = |A'|^2$ and phase ξ where $A' = |A'|e^{i\xi}$ are

$$\frac{dI}{d\bar{z}} = 2I(k_i - c_rI) \tag{5.74}$$

$$\frac{d\xi}{d\bar{z}} = -k_r - c_iI. \tag{5.75}$$

From the form of (5.74) it is apparent that c_r is analogous to the self-saturation coefficient of atomic laser theory [80].

The method of solution of (5.74) will now be described. As (5.74) is a first order separable differential equation, it can be integrated directly to give

$$\bar{z} = \frac{1}{2c_r}\int_{I_0}^{I}\frac{dI}{I(k_i/c_r - I)} \tag{5.76}$$

where $I_0 = I(\bar{z} = 0)$. The integrand on the RHS can now be split using the method of partial fractions i.e.

$$\frac{1}{I\,(k_i/c_r - I)} = \frac{c_r}{k_i}\left(\frac{1}{I} - \frac{1}{(I - k_i/c_r)}\right)$$

which results in (5.76) becoming

$$\bar{z} = \frac{1}{2k_i}\ln\left(\frac{I}{I_0}\frac{(I_0 - k_i/c_r)}{(I - k_i/c_r)}\right).$$

This can be rearranged to give an expression for the scaled electromagnetic field intensity as a function of $\bar{z}$, allowing a direct substitution for I in (5.75) and integration resulting in an expression which describes the field phase evolution as a function of $\bar{z}$. The equations which describe the field intensity and phase evolution are

$$I(\bar{z}) = \frac{k_i I_0 e^{2k_i\bar{z}}}{(k_i - c_r I_0)(1 + \frac{c_r I_0}{(k_i - c_r I_0)}e^{2k_i\bar{z}})} \tag{5.77}$$

$$\xi(\bar{z}) = -k_r\bar{z} - \frac{c_i}{2c_r}\ln\left(1 + \frac{c_r I_0}{k_i}\left(e^{2k_i\bar{z}} - 1\right)\right) + \xi_0 \tag{5.78}$$

where $\xi_0 = \xi(\bar{z} = 0)$. It is clear that as $\bar{z} \to \infty$ then

$$I \to \frac{k_i}{c_r} \quad , \quad \frac{d\xi}{d\bar{z}} \to -k_r - \frac{k_i c_i}{c_r}. \tag{5.79}$$

The solution of (5.74) is shown in figures 5.7(c) and 5.8(c) for $\mu = 0.1$ and $\mu = 0.8$ respectively. Note that because the Landau-Ginzburg equation has only been used to model the evolution of the exponentially growing wave, its solution does not display the region of 'lethargy' at the beginning of the interaction, as this is caused by interference of the growing, decaying and oscillatory waves corresponding to the three roots of the dispersion relation (5.69). As discussed in section 4.2.1, this is most pronounced for cases of large μ for which the linear

growth rate of the amplified wave is significantly smaller than those where $\mu \approx 0$. Figure 5.9 shows the variation of the saturation intensity predicted by (5.79) with μ for the case of exact resonance ($\delta = 0$). This is therefore an *analytical* prediction of the effect of free energy depletion on the saturation intensity of a cyclotron resonance maser. The intensity at the first saturation peak is also plotted in figure 5.9 as calculated from a numerical solution of equations (5.48..5.50). Note that as $\mu \rightarrow 0$ the saturation intensity predicted by the analytical result (5.77) approaches 1.5. The linear instability threshold for μ of $(27/32)^{1/3} \approx 0.95$ can also be observed. The elegance of the Landau-Ginzburg model is evident given the simplicity of the equations and their excellent agreement of results with those from the full numerical integration of equations (5.48..5.50).

5.2.4 Conclusion

It has been shown that it is possible to describe the evolution of the electron and field dynamics of a low-efficiency cyclotron resonance maser up to saturation of the field amplitude using three complex collective variable equations. Using this description, it is possible to reduce the equation for the field evolution to a Landau-Ginzburg equation with complex coefficients. Analytical predictions of the effect of free energy depletion on the saturated field intensity show good agreement with corresponding numerical calculations. The Landau-Ginzburg form obtained here shows that the evolution of the electromagnetic field up to saturation in a cyclotron resonance maser can be described by the same equation used to model the field evolution in an atomic laser.

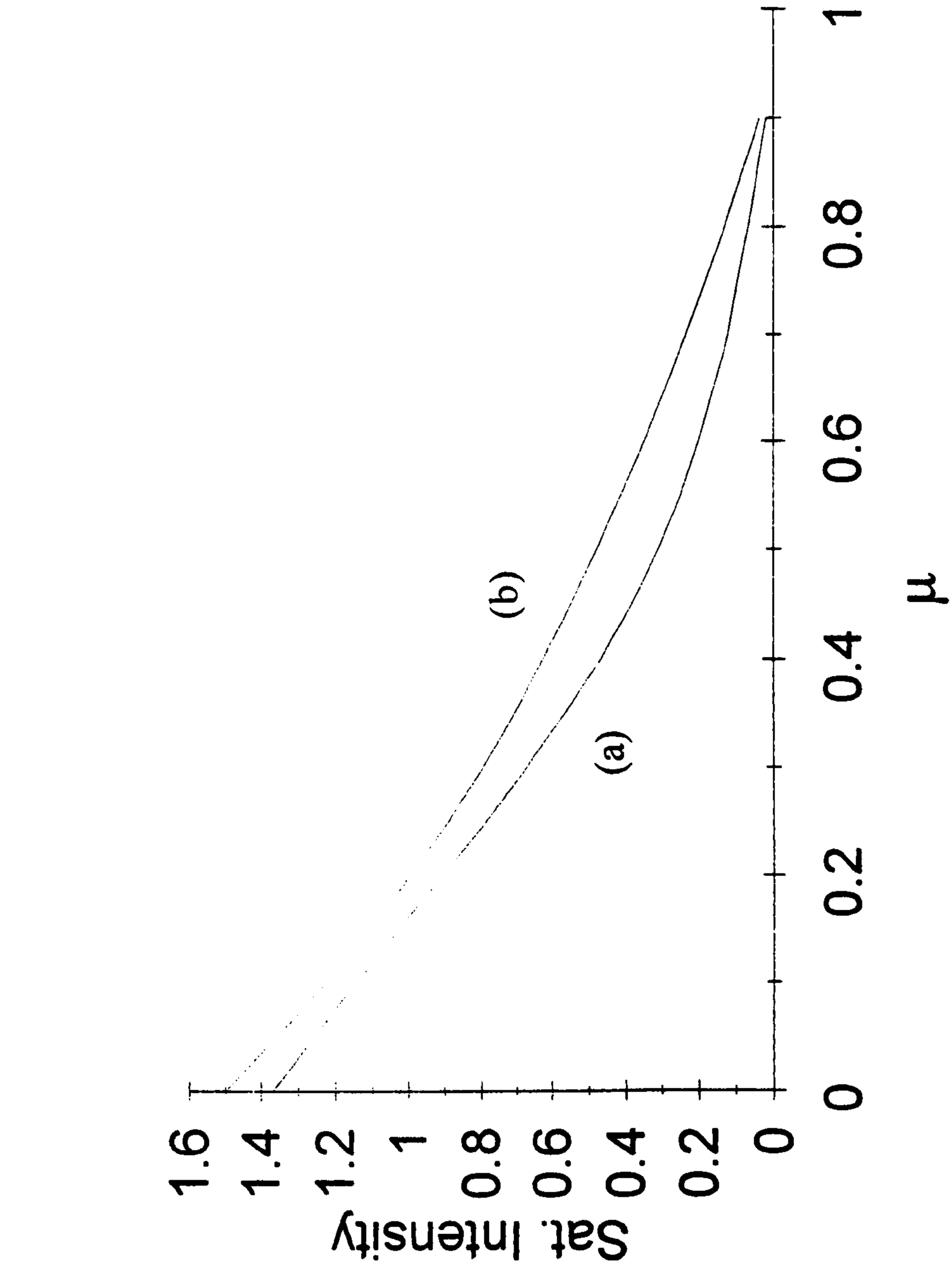

Figure 5.9: Plot of saturation intensity vs μ for $\delta = 0$. (a) numerical solution of equations (5.48.. 5.50) (b) analytical solution of equation (5.74) in the limit $\bar{z} \to \infty$

The results are remarkable from two points of view. Firstly, the simplicity of the Landau-Ginzburg equations when compared with the complicated set from which they were derived and secondly the similarity between atomic lasers and cyclotron resonance masers through the Landau-Ginzburg equation given the obvious differences between them.

Chapter 6

Superradiance in the CRM

6.1 Introduction

The previous chapters in this thesis have all been concerned with the evolution of the electromagnetic field in the steady-state regime, where the slowly varying envelope of the radiation is dependent on one variable only i.e. the spatial dimension z. This limit corresponds to the assumption of an infinitely long electron pulse of uniform density, so that one section of the electron beam, and hence radiation, evolves identically with all other sections as the interaction progresses. The relative slippage of the radiation pulse through the electron beam, which will occur when the axial velocity of the electrons and the group velocity of the radiation are not equal, is neglected, as in chapter 3. The radiation intensity in this regime was shown in chapter 3 to scale as $n_e^{4/3}$, where n_e is the electron density. This chapter is concerned with a quite different regime to that described above, the superradiant regime, in which the radiated intensity may be proportional to the *square* of the electron density. This regime will be shown to be due

to cooperative synchrotron emission and is critically dependent upon the effects of slippage.

Radiation intensities scaling as n_e^2 may also arise from coherent synchrotron radiation emitted by electrons which have been pre-bunched by an external source. The radiation fields emitted by these electrons sum up coherently to give the n_e^2 scaling. This is superradiance as defined by Dicke [81] i.e. spontaneous emission from a coherently prepared system. Strictly speaking, this chapter is concerned with a different phenomenon. Ideally, the electrons enter the beginning of the interaction in an unprepared state i.e. unbunched and with no input signal, so that the intensity of the (spontaneously) emitted radiation is initially proportional to n_e. On interacting with this radiation, the system evolves in such a way that the electrons emit radiation with an intensity proportional to n_e^2. This behaviour is a self-organizing phenomenon, whose atomic analogy has been called superfluorescence [82]. In this chapter, references will be made to 'superradiance' in this latter sense i.e. radiation intensity scaling as n_e^2 from a *self-bunched* system. This change of terminology from Dicke is historical in order to keep the same terminology as the same superradiant effect from FEL theory [83].

The essential difference between the superradiant regime and the usual steady-state regime is the effect of slippage. As the interaction progresses, the radiation slips ahead or behind the electron pulse by a distance L_s. If the length of this 'slippage region' is much less than the electron pulse length and the interaction started from a noiseless initial state (i.e. no electron 'shot noise' or noise over the radiation pulse), the radiation field amplitude will be approximately uniform

over the entire length of the pulse. This is the steady-state regime, as described in previous chapters, where the field evolution does not depend on the position in the electron pulse, but only on the (scaled) interaction length $\bar{z}$. However, it is now feasible using new types of cathode such as photocathodes [73] and field emission arrays [37, 74] that the opposite situation can occur, where the slippage length is greater than the length of the electron pulse. In this case, steady-state evolution cannot occur and slippage effects dominate the field evolution.

It is not sufficient however, to consider only the length of the slippage region and the electron pulse when deciding whether steady-state or superradiant emission is taking place. The gain must also be taken account of, so the electron pulse is defined as being 'short' or 'long' with respect to a 'co-operation length', defined as the slippage which occurs in one gain length. A gain length is defined as the distance over which the field intensity increases by a factor of $e^{\sqrt{3}/2}$ in the linear regime. This nomenclature is similar to that used in describing co-operative processes in atomic systems [84]. Note that even in the long-pulse limit there is always a region at the trailing/leading edge of the electron pulse, depending on whether the radiation group velocity is larger/smaller than the electron axial velocity, which will evolve as a short electron pulse because there is no radiation entering from one side of it and all emitted radiation propagates in the other direction (see figure 6.1). For positive slippage ($v_g > v_{||}$), this region will be at the rear of the electron pulse, whereas for negative slippage ($v_g < v_{||}$), it will be at the front of the electron pulse. The weak superradiant emission from this region of the electron pulse will be amplified as it propagates through the

remainder of the electron pulse, resulting in a spike of radiation with an intensity much greater than the steady-state saturation value. This phenomenon is termed 'strong' superradiance to distinguish it from the superradiance emitted by short electron pulses, which is termed 'weak' superradiance. The terms weak and strong are used to reflect the fact that the peak intensities are respectively smaller and greater than those of the steady-state regime.

Consider an observer in a frame travelling at the axial velocity of the electrons so that in this frame, the gyrating electrons have only transverse momentum. As the electrons are emitting spontaneously, the amount of radiation emitted in the backwards direction ($-\bar{z}$) will be approximately equal to that emitted in the forward direction. In order to neglect this backward wave interaction, it is necessary to impose the condition that the electrons are travelling at relativistic axial velocities with respect to the laboratory frame, so that on transforming to the laboratory frame, the intensity of the backward travelling radiation is negligible compared to the forward. This condition, coupled with the critical dependence on the relative slippage between the electrons and the radiation, suggest that the CARM is the type of CRM device which is most likely to give rise to superradiant phenomena (see figure 1.5).

6.1.1 Definition of Parameters

Consider an electron pulse and a radiation pulse envelope, travelling with velocities $v_{\|}$ and v_g respectively. After a time interval Δt, the difference between the distance travelled by the radiation pulse and the electron pulse, termed the

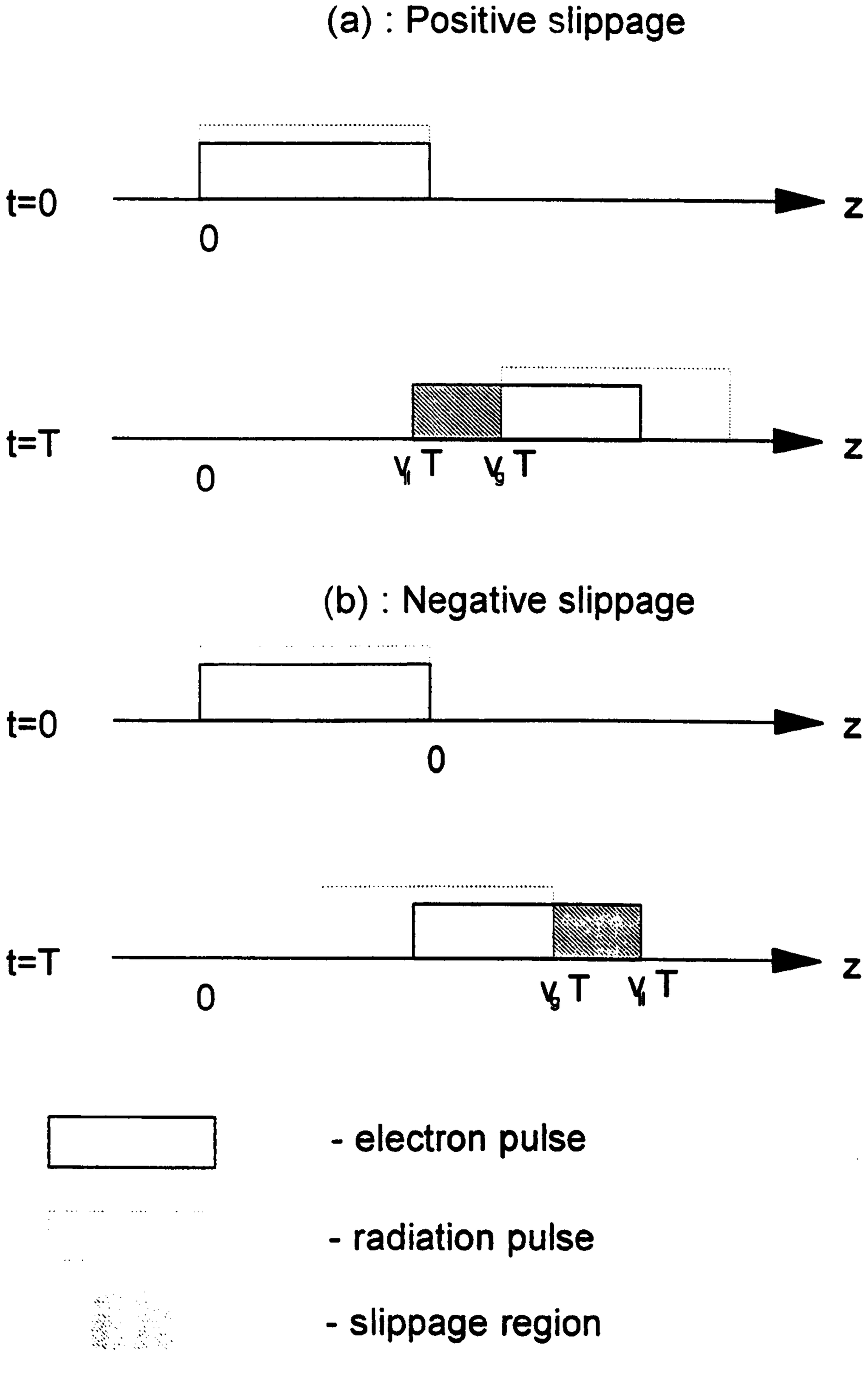

Figure 6.1: Diagram showing slippage regions when (a) $\beta < 1$ and (b) $\beta > 1$.

slippage length L_s, will be

$$L_s = \left(\frac{1-\beta}{\beta}\right) v_{\|} \Delta t \tag{6.1}$$

where

$$\beta = \frac{v_{\|}}{v_g}. \tag{6.2}$$

Note that if $\beta < 1$, $L_s > 0$ and the radiation pulse slips ahead of the electron pulse. Conversely, if $\beta > 1$, $L_s < 0$ and the radiation pulse slips behind the electron pulse. Consequently, the two cases are termed positive slippage and negative slippage respectively.

Using the resonance condition (3.41) and the dispersion relation for a cold waveguide mode (3.63), the factor $(1-\beta)/\beta$ can be rewritten as

$$\begin{aligned} \frac{1-\beta}{\beta} &= \frac{c^2 k_{\|}}{\omega v_{\|}} - 1 \\ &\approx \frac{k_{c0} k_{\|} c^2}{\omega^2} + \frac{k_{\|}^2 c^2}{\omega^2} - 1 \\ &= \frac{k_{c0} k_{\|} - k_{\perp}^2}{k_{\perp}^2 + k_{\|}^2} \end{aligned} \tag{6.3}$$

Using the variables X and α_c, defined as

$$X = \frac{k_{\perp}^2}{k_{\|} k_{c0}} \tag{6.4}$$

$$\alpha_c = \frac{k_{c0}^2}{k_{\perp}^2} \tag{6.5}$$

it is possible to write (6.3) as

$$\frac{1-\beta}{\beta} = \frac{k_{c0}}{k_{\|}} \frac{(1-X)}{(1+\alpha_c X^2)}. \tag{6.6}$$

Note that if $X = 1$, no slippage will occur between the electron pulse and the radiation pulse i.e. $v_{\|} = v_g$. From (6.1) and (6.6), when the electron pulse travels

a distance of one cyclotron wavelength or period $\lambda_{c0} = 2\pi/k_{c0}$, the slippage length will be

$$l_s = \frac{(1-X)}{(1+\alpha_c X^2)}\lambda_{\|} \tag{6.7}$$

If the interaction distance z is represented as N_c cyclotron periods i.e. $z = N_c\lambda_{c0}$ and the electron pulse length as N_b slippage lengths i.e. $L_b = N_b l_s$, the ratio of the slippage length to the electron pulse length, which will be termed the slippage parameter, is given by

$$S = \frac{N_c}{N_b} \tag{6.8}$$

Note that if $S > 1$, the radiation pulse will have slipped a distance greater than the entire electron pulse length and there will be no steady-state region.

In chapter 4, the linear solution for the electromagnetic field in the steady-state limit was found in (4.39) to evolve as

$$A \propto \exp\left(|\Im(\lambda_3(\rho,\mu))|\bar{z}\right) = \exp\left(\frac{k_\perp^2\rho}{k_{\|}}|\Im(\lambda_3(\rho,\mu))|z\right) \tag{6.9}$$

where $\lambda_3(\rho,\mu)$ is a complex root of the full dispersion relation (4.36). The gain length is therefore the value of z for which the argument of the exponential is $\sqrt{3}/2$ i.e.

$$L_g = \frac{k_{\|}}{k_\perp^2\rho} = \frac{\lambda_{\|}}{2\pi\rho X} \tag{6.10}$$

Note that the limits $\rho \to 0$, $\mu \to 0$ and $\delta \to 0$ have been taken in this expression, so that $|\Im(\lambda_3(\rho,\mu))| \to \sqrt{3}/2$. This is equivalent to neglecting the effect of variations in $\bar{u}_\perp$ and $\bar{u}_{\|}$. This assumption is reasonable even for significant values of ρ and μ because the parameters being defined in this section are concerned with electrons which are emitting *spontaneously*. i.e. those on the trailing edge

of the electron pulse when $\beta < 1$ and on the leading edge of the electron pulse when $\beta > 1$. The amount of radiation emitted from these electrons will be relatively small, when compared with the electrons in the body of the pulse which amplify the spontaneously emitted radiation, so $\bar{u}_\perp$ and $\bar{u}_\parallel$ will remain almost at their initial values. As the spontaneously emitted radiation slips over the other electrons and is amplified, the effects of depletion of either the transverse or axial momentum become more important. Therefore, just as the radiation intensity is uniform over the electron pulse length in the steady-state regime, but non-uniform in the superradiant regime, so the effects of momentum depletion are uniform over the electron pulse length in the steady-state regime, but non-uniform in the superradiant regime.

The slippage which occurs in one gain length is termed the cooperation length and will be defined as

$$\begin{aligned} L_c &= \left(\frac{1-\beta}{\beta}\right) L_g \\ &= \left(\frac{1-X}{1+\alpha_c X^2}\right) \frac{\lambda_\parallel}{2\pi\rho X} \end{aligned} \tag{6.11}$$

The co-operation length can be interpreted as the minimum distance between which electrons may interact cooperatively via the radiation field. The ratio of the cooperation length to the electron pulse length determines the importance of superradiant effects on the field evolution, so the 'superradiant parameter' K is defined as

$$K = \frac{L_c}{L_b} = \frac{1}{2\pi\rho X N_b} \tag{6.12}$$

where $L_b = N_b l_s$ has been used. Note that the superradiant parameter K can

also be interpreted as the slippage parameter S per unit gain i.e.

$$K = \frac{S}{G} \tag{6.13}$$

where G, the unsaturated gain, is the argument of the exponential in (6.9) i.e.

$$G = \frac{k_\perp^2 \rho}{k_\parallel} z$$

$$\Rightarrow G = 2\pi\rho X N_c \tag{6.14}$$

As we are only interested in the case of high gain i.e. $G > 1$, then (6.13) implies that $S = GK > K$. The definition of K means that the long pulse limit corresponds to $K \ll 1$ ($L_b \gg L_c$) and the short pulse limit corresponds to $K \gtrsim 1$ ($L_b \lesssim L_c$).

6.1.2 Dissipative Model of Weak Superradiance

The effect of the relative slippage between an electron pulse of length L_b and a radiation pulse can be shown without introducing a description involving partial differential equations using a simple dissipative model [85]. This model introduces a loss term into the wave equation, which represents radiation escaping from the electron pulse into vacuum and undergoing no further interaction. This loss term will be proportional to the rate of slippage (slippage per unit distance travelled by the electron pulse), which from (6.1) is $(1-\beta)/\beta$, and inversely proportional to the length of the electron pulse L_b. The unscaled wave equations for the TE and TM mode interactions (3.74) and (3.142) can therefore be generalised heuristically to include the effects of slippage i.e.

$$\frac{dF_s(z)}{dz} = -\frac{i\omega\mu_0 k_\perp D_{TE} J_{m-1}(k_\perp R_0)}{2k_\parallel} \left\langle \frac{u_\perp}{u_\parallel} e^{-i\phi} \right\rangle - k_l F_s(z) \tag{6.15}$$

$$\frac{dG_s(z)}{dz} = \frac{-\mu_0 I k_\perp \omega^2}{2c^2 k_{||} k_{c0} u_{||0}} \left(\frac{k_{||} c^2}{\omega} \gamma_0 - u_{||0} \right) \times$$
$$D_{TM} J_{m-1}(k_\perp R_0) \left\langle \frac{u_\perp}{u_{||}} e^{-i\phi} \right\rangle - k_l G_s(z) \qquad (6.16)$$

where

$$k_l = \frac{(1-\beta)}{\beta} \frac{1}{L_b}.$$

When the scaling procedures of sections 3.2.3 and 3.3.4 are followed, both (6.16) and (6.16) reduce to

$$\frac{d\bar{A}}{d\bar{z}} = \left\langle \frac{\bar{u}_\perp}{\bar{u}_{||}} e^{-i\phi} \right\rangle - \bar{k}_l \bar{A} \qquad (6.17)$$

where the scaled loss term is defined as

$$\bar{k}_l = \frac{(1-X)}{X(1+\alpha_c X^2)} \frac{\lambda_{||}}{2\pi\rho} \frac{1}{L_b}. \qquad (6.18)$$

It is sufficient for now to assume that any variations in the transverse and axial momentum of the electrons are very small i.e. $\bar{u}_\perp = \bar{u}_{||} \approx 1$. **The effects of significant variations in these quantities will be discussed in forthcoming sections. Rewriting the electron pulse length as** $L_b = N_b l_s$, **it can be seen on comparing (6.18) with (6.12) that** $\bar{k}_l$ **is equivalent to the superradiant parameter** K.

If the loss term is small, or more specifically, $1/\bar{k}_l \gg \bar{z}_f$, where $\bar{z}_f$ is the scaled interaction length of the amplifier, the radiation will remain inside the electron pulse for almost the whole interaction. This is the usual steady-state amplifier limit, which has been analysed in the previous chapters. In the opposite limit i.e. $1/\bar{k}_l \ll \bar{z}_f$ the radiation is rapidly escaping from the electron pulse. The effective interaction length between the electrons and the radiation is now $1/\bar{k}_l$, and in this case, the interaction 'switches off' with a decay constant for the field amplitude of $1/\bar{k}_l$. Equations (3.182..3.184) can be rewritten including the loss

term in the wave equation resulting in

$$\frac{d\phi_j}{d\bar{z}} = \bar{p}_j \tag{6.19}$$

$$\frac{d\bar{p}_j}{d\bar{z}} = -(\bar{A}e^{i\phi_j} + c.c.) \tag{6.20}$$

$$\frac{d\bar{A}}{d\bar{z}} = \langle e^{-i\phi} \rangle - \bar{k}_l \bar{A} \tag{6.21}$$

The electromagnetic field variables can be adiabatically eliminated by setting $d\bar{A}/d\bar{z} = 0$ in (6.21). The complex field amplitude can then be expressed as

$$\bar{A} = \frac{\langle e^{-i\phi} \rangle}{\bar{k}_l} \tag{6.22}$$

As the set of equations (6.19..6.21) have only one free parameter i.e. $\bar{k}_l$, then for a given value of $\bar{k}_l$, $\langle e^{-i\phi} \rangle$ will have the same value at saturation. This means that from (6.18),

$$|\bar{A}|^2 \propto \rho^2$$

so the unscaled radiation intensity at saturation, I_{sat}, varies as

$$I_{sat} \propto \rho^4 |\bar{A}|^2 \propto \rho^6 \propto n_e^2 \tag{6.23}$$

This scaling of the saturation intensity is therefore proportional to the square of the number of emitters as opposed to the $n_e^{4/3}$ dependence which was derived from the analysis of the steady-state evolution in section 3.4. The relation (6.23) is characteristic of a superradiant emission process.

If the set of equations (6.19..6.21) are linearised following the procedure of chapter 4 and the electromagnetic field is eliminated using (6.21), the equation describing the evolution of the linearised bunching parameter $b = -i\langle \phi_1' e^{-i\phi_0'} \rangle$ is

$$\frac{d^2 b}{d\bar{z}^2} = \frac{i}{\bar{k}_l} b$$

which has the solution

$$b = b_0 \exp\left(\frac{1+i}{\sqrt{2\bar{k}_l}}\bar{z}\right) \tag{6.24}$$

so the linear solution diverges on a length scale (with respect to $\bar{z}$) of $1/\lambda_s$ where

$$\lambda_s = \frac{1}{\sqrt{2\bar{k}_l}}. \tag{6.25}$$

It is now possible to state the conditions under which superradiant effects should be observed, that is, that the (scaled) length scales of the incoherent decay $1/\bar{k}_l$, the superradiant pulse $1/\lambda_s$ and the interaction length $\bar{z}_f$ should be ordered as follows:

$$\frac{1}{\bar{k}_l} \ll \frac{1}{\lambda_s} \ll \bar{z}_f \tag{6.26}$$

Using (6.18), it is possible to rewrite the above with respect to the length of the electron pulse i.e.

$$L_b \ll 2^{1/3} L_c \ll \left(\frac{k_{c0}}{k_{\|}} \frac{(1-X)}{(1+\alpha_c X^2)} z\right)^{2/3} \tag{6.27}$$

where L_c is the co-operation length as defined in (6.11). From the discussion in the introduction, these are therefore the conditions under which weak superradiance should occur.

6.2 Linear Theory

In this section, a linear analysis of the CRM interaction including the effect of the relative slippage between the electron pulse and the radiation envelope will show the existence of two distinct regions of the electron pulse within which the electromagnetic field evolves in a quite different manner. This analysis is based on a similar linear analysis of superradiant evolution in FELs [86].

In order to describe the CRM interaction for electron pulses, the ordinary differential equations (3.151..3.155) derived in chapter 3 must become partial differential equations. This is achieved by replacing $d/d\bar{z}$ by

$$\frac{d}{d\bar{z}} \equiv \frac{\partial}{\partial \bar{z}} + \frac{1}{\beta}\frac{\partial}{\partial \bar{t}} \quad \text{for electrons} \tag{6.28}$$

$$\frac{d}{d\bar{z}} \equiv \frac{\partial}{\partial \bar{z}} + \frac{\partial}{\partial \bar{t}} \quad \text{for radiation.} \tag{6.29}$$

where the scaled length and time variables are defined as

$$\bar{z} = \frac{k_\perp^2}{k_\parallel}\rho z \quad , \quad \bar{t} = \frac{k_\perp^2}{k_\parallel}\rho v_g t \tag{6.30}$$

so the generalised set of evolution equations describing the CRM interaction involving electron pulses is

$$\left(\frac{\partial}{\partial \bar{z}} + \frac{1}{\beta}\frac{\partial}{\partial \bar{t}}\right)\phi'_j = p'_j - i\frac{\mu}{\bar{u}_\perp \bar{u}_\parallel}(A'e^{i\phi'_j} - c.c.) \tag{6.31}$$

$$\left(\frac{\partial}{\partial \bar{z}} + \frac{1}{\beta}\frac{\partial}{\partial \bar{t}}\right)p'_j = (\rho(p'_j + \delta) - 1)\frac{\bar{u}_{\perp j}}{\bar{u}^2_{\parallel j}}(A'e^{i\phi'_j} + c.c.) \tag{6.32}$$

$$\left(\frac{\partial}{\partial \bar{z}} + \frac{1}{\beta}\frac{\partial}{\partial \bar{t}}\right)\bar{u}_{\perp j} = -\frac{\mu}{\bar{u}_{\parallel j}}(A'e^{i\phi'_j} + c.c.) \tag{6.33}$$

$$\left(\frac{\partial}{\partial \bar{z}} + \frac{1}{\beta}\frac{\partial}{\partial \bar{t}}\right)\bar{u}_{\parallel j} = -\rho\frac{\bar{u}_{\perp j}}{\bar{u}_{\parallel j}}(A'e^{i\phi'_j} + c.c.) \tag{6.34}$$

$$\left(\frac{\partial}{\partial \bar{z}} + \frac{\partial}{\partial \bar{t}}\right)A' = \left\langle \frac{\bar{u}_\perp}{\bar{u}_\parallel}e^{-i\phi'} \right\rangle + i\delta A' \tag{6.35}$$

where: $j = 1..N_e$, $\langle ... \rangle = \frac{1}{N_e}\sum_{j=1}^{N_e} ...$, $\phi' = \phi - \delta\bar{z}$, $p' = \bar{p} - \delta$, $A' = \bar{A}e^{i\delta \bar{z}}$ and $\beta = v_\parallel / v_g$. This set of equations will now be linearised using exactly the same methods which were employed for the case of steady-state evolution in chapter 4. Linearising the dependent variables about their values at equilibrium ($\bar{z} = 0$) and using the set of collective variables defined in (4.14..4.17), the set of linear equations can be written as

$$\left(\frac{\partial}{\partial \bar{z}} + \frac{1}{\beta}\frac{\partial}{\partial \bar{t}}\right)b = -iP - \mu A \tag{6.36}$$

$$\left(\frac{\partial}{\partial \bar{z}} + \frac{1}{\beta}\frac{\partial}{\partial \bar{t}}\right) P = (\rho\delta - 1)\mathcal{A} \tag{6.37}$$

$$\left(\frac{\partial}{\partial \bar{z}} + \frac{1}{\beta}\frac{\partial}{\partial \bar{t}}\right) U_{\perp} = -\mu\mathcal{A} \tag{6.38}$$

$$\left(\frac{\partial}{\partial \bar{z}} + \frac{1}{\beta}\frac{\partial}{\partial \bar{t}}\right) U_{\parallel} = -\rho\mathcal{A} \tag{6.39}$$

$$\left(\frac{\partial}{\partial \bar{z}} + \frac{\partial}{\partial \bar{t}}\right) \mathcal{A} = b + U_{\perp} - U_{\parallel} + i\delta\mathcal{A} \tag{6.40}$$

where, as in chapter 4, terms proportional to $\langle e^{-i2\phi_0} \rangle$ have been dropped and A_1' has been written simply as $\mathcal{A}$.

If the new independent variables $\bar{z}'$ and $\bar{t}'$ are defined as

$$\bar{z}' = \bar{z} \quad , \quad \bar{t}' = \bar{z} - \beta\bar{t} \tag{6.41}$$

then $\bar{t}'$ represents the position with respect to the rear of the electron pulse when $\beta < 1$ and the front of the electron pulse when $\beta > 1$ so

$$\frac{\partial}{\partial \bar{z}} = \frac{\partial}{\partial \bar{z}'} + \frac{\partial}{\partial \bar{t}'}$$

$$\frac{\partial}{\partial \bar{t}} = -\beta\frac{\partial}{\partial \bar{t}'}$$

and the set of linear equations (6.36..6.40) becomes

$$\frac{\partial b}{\partial \bar{z}'} = -iP - \mu\mathcal{A} \tag{6.42}$$

$$\frac{\partial P}{\partial \bar{z}'} = (\rho\delta - 1)\mathcal{A} \tag{6.43}$$

$$\frac{\partial U_{\perp}}{\partial \bar{z}'} = -\mu\mathcal{A} \tag{6.44}$$

$$\frac{\partial U_{\parallel}}{\partial \bar{z}'} = -\rho\mathcal{A} \tag{6.45}$$

$$\left(\frac{\partial}{\partial \bar{z}'} + (1-\beta)\frac{\partial}{\partial \bar{t}'}\right) \mathcal{A}. = b + U_{\perp} - U_{\parallel} + i\delta\mathcal{A} \tag{6.46}$$

The boundary conditions are assumed to be

$$\mathcal{A}(\bar{z}' = 0, \bar{t}') = \mathcal{A}_0(\bar{t}') \tag{6.47}$$

$$b(\bar{z}'=0,\bar{t}') = b_0(\bar{t}') \tag{6.48}$$

$$P(\bar{z}'=0,\bar{t}') = U_\perp(\bar{z}'=0,\bar{t}') = U_\parallel(\bar{z}'=0,\bar{t}') = 0 \tag{6.49}$$

so (6.42..6.46) can be Laplace transformed using the standard Laplace transformation

$$\tilde{X}(s,\bar{t}') = \int_0^\infty X(\bar{z}',\bar{t}')e^{-s\bar{z}'}d\bar{z}' \tag{6.50}$$

resulting in

$$s\tilde{b} - b_0(\bar{t}') = -i\tilde{P} - \mu\tilde{\mathcal{A}} \tag{6.51}$$

$$s\tilde{P} = (\rho\delta - 1)\tilde{\mathcal{A}} \tag{6.52}$$

$$s\tilde{U}_\perp = -\mu\tilde{\mathcal{A}} \tag{6.53}$$

$$s\tilde{U}_\parallel = -\rho\tilde{\mathcal{A}} \tag{6.54}$$

$$s\tilde{\mathcal{A}} - \mathcal{A}_0(\bar{t}') + (1-\beta)\frac{d\tilde{\mathcal{A}}(s,\bar{t}')}{d\bar{t}'} = \tilde{b} + \tilde{U}_\perp - \tilde{U}_\parallel + i\delta\tilde{\mathcal{A}} \tag{6.55}$$

which can be reduced to a single equation in the transformed field amplitude $\tilde{\mathcal{A}}(s,\bar{t}')$:

$$\frac{d\tilde{\mathcal{A}}(s,\bar{t}')}{d\bar{t}'} - \frac{i\Delta(s)}{(1-\beta)s^2}\tilde{\mathcal{A}}(s,\bar{t}') = \frac{1}{1-\beta}\left(\frac{b_0(\bar{t}')}{s} + \mathcal{A}_0(\bar{t}')\right)$$

where

$$\Delta(s) = is^3 + \delta s^2 - i(\rho - 2\mu)s + 1 - \rho\delta.$$

The differential equation can be rewritten using (4.32) to give

$$\frac{d\tilde{\mathcal{A}}(\lambda,\bar{t}')}{d\bar{t}'} + \frac{i\Delta(\lambda)}{(1-\beta)\lambda^2}\tilde{\mathcal{A}}(\lambda,\bar{t}') = \frac{1}{1-\beta}\left(\mathcal{A}_0(\bar{t}') - \frac{ib_0(\bar{t}')}{\lambda}\right) \tag{6.56}$$

where

$$\Delta(\lambda) = \lambda^3 - \delta\lambda^2 + (\rho - 2\mu)\lambda + 1 - \rho\delta. \tag{6.57}$$

Equation (6.56) is a first order linear ordinary differential equation, which has the general solution

$$\tilde{A}(\lambda,\bar{t}') = \exp\left(-\frac{i\Delta(\lambda)\bar{t}'}{(1-\beta)\lambda^2}\right)\times \qquad (6.58)$$
$$\left[\int_0^{\bar{t}'}\exp\left(\frac{i\Delta(\lambda)\bar{t}''}{(1-\beta)\lambda^2}\right)\frac{1}{1-\beta}\left(\frac{\mathcal{A}_0(\bar{t}'')-ib_0(\bar{t}'')}{\lambda}\right)d\bar{t}''+C\right]$$

where C is an arbitrary constant whose value is fixed by the initial condition on $\bar{t}'$.

For simplicity, the case which will be considered here is that where there is no field excitation and constant bunching at $\bar{z}'=0$ i.e.

$$\mathcal{A}_0(\bar{t}')=0 \quad , \quad b_0(\bar{t}')=b_0 \qquad (6.59)$$

which makes the evaluation of (6.58) straightforward. The result is

$$\tilde{\mathcal{A}}(\lambda,\bar{t}') = -\frac{b_0\lambda}{\Delta(\lambda)}\left(1-\exp\left(-\frac{i\Delta(\lambda)\bar{t}'}{(1-\beta)\lambda^2}\right)\right)+C\exp\left(-\frac{i\Delta(\lambda)\bar{t}'}{(1-\beta)\lambda^2}\right). \qquad (6.60)$$

Note that when $\bar{t}'=0$, $\tilde{\mathcal{A}}(\lambda,0)=C$. Now $\mathcal{A}(\bar{z}',\bar{t}'=0)$ is a constant, so

$$\frac{\partial\mathcal{A}(\bar{z}',\bar{t}'=0)}{\partial\bar{z}'}=0.$$

Laplace transforming this relation results in

$$\begin{aligned} s\tilde{\mathcal{A}}(s,0)-\mathcal{A}(0,0) &= 0 \\ \Rightarrow \tilde{\mathcal{A}}(s,0)=\frac{\mathcal{A}(0,0)}{s} &= -i\frac{\mathcal{A}(0,0)}{\lambda} \end{aligned} \qquad (6.61)$$

so

$$C=-i\frac{\mathcal{A}(0,0)}{\lambda}=0 \qquad (6.62)$$

as $\mathcal{A}_0(0)=0$ was assumed in (6.59). The solution for the transformed electromagnetic field amplitude in (6.60) is therefore

$$\tilde{\mathcal{A}}(\lambda,\bar{t}') = -\frac{b_0\lambda}{\Delta(\lambda)}\left(1-\exp\left(-\frac{i\Delta(\lambda)\bar{t}'}{(1-\beta)\lambda^2}\right)\right) \qquad (6.63)$$

for the boundary conditions (6.59).

It is now possible to perform an inverse Laplace transform on (6.63), where the inverse Laplace transform is defined as

$$\begin{aligned} X(\bar{z}', \bar{t}') &= \frac{1}{2\pi i} \int_{\sigma - i\infty}^{\sigma + i\infty} \tilde{X}(s, \bar{t}') e^{s\bar{z}'} ds \\ &= \frac{1}{2\pi} \int_{-\infty - i\sigma}^{\infty - i\sigma} \tilde{X}(\lambda, \bar{t}') e^{i\lambda\bar{z}'} d\lambda \quad (\bar{z}' > 0) \end{aligned} \tag{6.64}$$

where the path of integration lies below all the singularities of the integrand in the complex plane. Applying this to (6.63) results in

$$\mathcal{A}(\bar{z}', \bar{t}') = -\frac{b_0}{2\pi} \int_{-\infty - i\sigma}^{\infty - i\sigma} \frac{\lambda e^{i\lambda\bar{z}'}}{\Delta(\lambda)} \left(1 - \exp\left(-\frac{i\Delta(\lambda)\bar{t}'}{\lambda^2(1-\beta)}\right)\right) d\lambda \tag{6.65}$$

If $\bar{z}'$ and $\bar{t}'$ are rewritten in terms of the original scaled variables $\bar{z}$ and $\bar{t}$, (6.65) can be rewritten as the sum of two terms i.e.

$$\mathcal{A}(\bar{z}, \bar{t}) = \mathcal{A}_1(\bar{z}) + \mathcal{A}_2(\bar{z}, \bar{t}). \tag{6.66}$$

The first term in (6.66) is space ($\bar{z}$) dependent only and is given by the residues of the three simple poles $\lambda_{1,2,3}$, which are the roots of the cubic equation

$$\Delta(\lambda) = \lambda^3 - \delta\lambda^2 + (\rho - 2\mu)\lambda + (1 - \rho\delta) = 0 \tag{6.67}$$

so $\mathcal{A}_1(\bar{z})$ is just the solution of the steady-state problem (4.37). $\mathcal{A}_1(\bar{z})$ will be renamed $\mathcal{A}_{SS}(\bar{z})$ from now on, where

$$\mathcal{A}_{SS}(\bar{z}) = -ib_0 \sum_{k=1}^{3} \frac{\lambda_k e^{i\lambda_k \bar{z}}}{(\lambda_k - \lambda_l)(\lambda_k - \lambda_m)} \quad (k \neq l \neq m). \tag{6.68}$$

The second term in (6.66) is both space ($\bar{z}$) and time ($\bar{t}$) dependent. From (6.65),it can be seen that $A_2(\bar{z}, \bar{t})$ is given by the residues of the same three simple poles

$\lambda_{1,2,3}$ *and* by the residue of the essential singularity at $\lambda = 0$. The expression for $\mathcal{A}_2(\bar{z}, \bar{t})$ is therefore

$$\mathcal{A}_2(\bar{z}, \bar{t}) = \frac{b_0}{2\pi} \int_{-\infty - i\sigma}^{\infty - i\sigma} \frac{\lambda}{\Delta(\lambda)} \exp\left(-\frac{i\Delta(\lambda)(\bar{z} - \beta\bar{t})}{(1-\beta)\lambda^2} + i\lambda\bar{z} \right) d\lambda \tag{6.69}$$

It is useful at this point to introduce the variables $\bar{z}_1$ and $\bar{z}_2$ where

$$\bar{z}_1 = \frac{1}{1-\beta}(\bar{z} - \beta\bar{t}) \tag{6.70}$$

$$\bar{z}_2 = \frac{\beta}{1-\beta}(\bar{t} - \bar{z}) \tag{6.71}$$

and

$$\bar{z} = \bar{z}_1 + \bar{z}_2 \tag{6.72}$$

Note that $\bar{z}_1$ and $\bar{z}_2$ have been normalised to the cooperation length i.e.

$$\bar{z}_1 = \frac{(z - v_\parallel t)}{\beta L_c} \tag{6.73}$$

$$\bar{z}_2 = \frac{(v_g t - z)}{L_c}. \tag{6.74}$$

The variables $\bar{z}_1$ and $\bar{z}_2$ allow the argument of the exponential in (6.69) to be rewritten as

$$-\frac{i\Delta(\lambda)\bar{t}'}{\lambda^2(1-\beta)} + i\lambda\bar{z}' = -\frac{i\Delta(\lambda)}{\lambda^2}\bar{z}_1 + i\lambda\bar{z} = -\frac{i\Delta(\lambda)}{\lambda^2}\bar{z}_1 + i\lambda\bar{z}_1 + i\lambda\bar{z}_2.$$

If the definition of $\Delta(\lambda)$ is used, this results in (6.69) becoming

$$\mathcal{A}_2(\bar{z}, \bar{t}) = \frac{b_0}{2\pi} \int_{-\infty - i\sigma}^{\infty - i\sigma} \frac{\lambda}{\Delta(\lambda)} \exp\left[i\left(\delta\bar{z}_1 - \frac{\rho - 2\mu}{\lambda}\bar{z}_1 - \frac{1 - \rho\delta}{\lambda^2} \right) \right] \exp(i\lambda\bar{z}_2) d\lambda. \tag{6.75}$$

Consider now the integral in (6.75) over the complex plane, which is shown schematically in figure 6.2. From the definition of the inverse Laplace transform (6.64), the line $\Im(\lambda) = -\sigma$ must lie below all the singularities of the integrand in

order for the integral to converge. If λ is split into real and imaginary parts, the term $\exp(i\lambda\bar{z}_2)$ in (6.75) becomes

$$\exp(i\lambda\bar{z}_2) = \exp(i\lambda_r\bar{z}_2)\exp(-\lambda_i\bar{z}_2) \tag{6.76}$$

where $\lambda_r = \Re(\lambda)$ and $\lambda_i = \Im(\lambda)$. There are therefore two possible paths which can be used to complete the contour over which the integral is performed, depending on whether $\bar{z}_2 > 0$ or $\bar{z}_2 < 0$. If $\bar{z}_2 < 0$, then it is necessary that $\lambda_i \to -\infty$ so that the contribution from the infinite semi-circular section used to close the path of integration tends to zero as the path radius tends to infinity i.e. path ABCA in figure 6.2. As this path does not enclose any singularities, the integral in (6.75) will be zero. The resultant field amplitude from (6.66) will therefore be

$$\mathcal{A}(\bar{z},\bar{t}) = \mathcal{A}_{SS}(\bar{z}) \text{ when } \bar{z}_2 < 0 \tag{6.77}$$

Conversely, if $\bar{z}_2 > 0$, then (6.76) suggests that $\lambda_i \to +\infty$ to ensure that the contribution from the infinite semi-circular section used to close the path tends to zero i.e. path ABDA in figure 6.2. This path encloses the three simple poles which are the roots of $\Delta(\lambda) = 0$ *and* the essential singularity at $\lambda = 0$. From (6.75) it can be seen that

$$\mathcal{A}_2(\bar{z}_1,\bar{z}_2) = -\mathcal{A}_{SS}(\bar{z}) + \mathcal{A}_{SR}(\bar{z}_1,\bar{z}_2) \text{ when } \bar{z}_2 > 0 \tag{6.78}$$

where $\mathcal{A}_{SR}$ arises from the essential singularity alone. The resultant electromagnetic field amplitude is therefore given by (6.66) to be

$$\mathcal{A}(\bar{z}_1,\bar{z}_2) = \mathcal{A}_{SR}(\bar{z}_1,\bar{z}_2) \text{ when } \bar{z}_2 > 0 \tag{6.79}$$

where

$$\mathcal{A}_{SR}(\bar{z}_1,\bar{z}_2) = \frac{b_0}{2\pi}e^{i\delta\bar{z}_1}\oint_\Gamma \frac{\lambda}{\Delta(\lambda)}\exp\left[-i\left(\frac{c_1\bar{z}_1}{\lambda}+\frac{c_0\bar{z}_1}{\lambda^2}-\lambda\bar{z}_2\right)\right]d\lambda \tag{6.80}$$

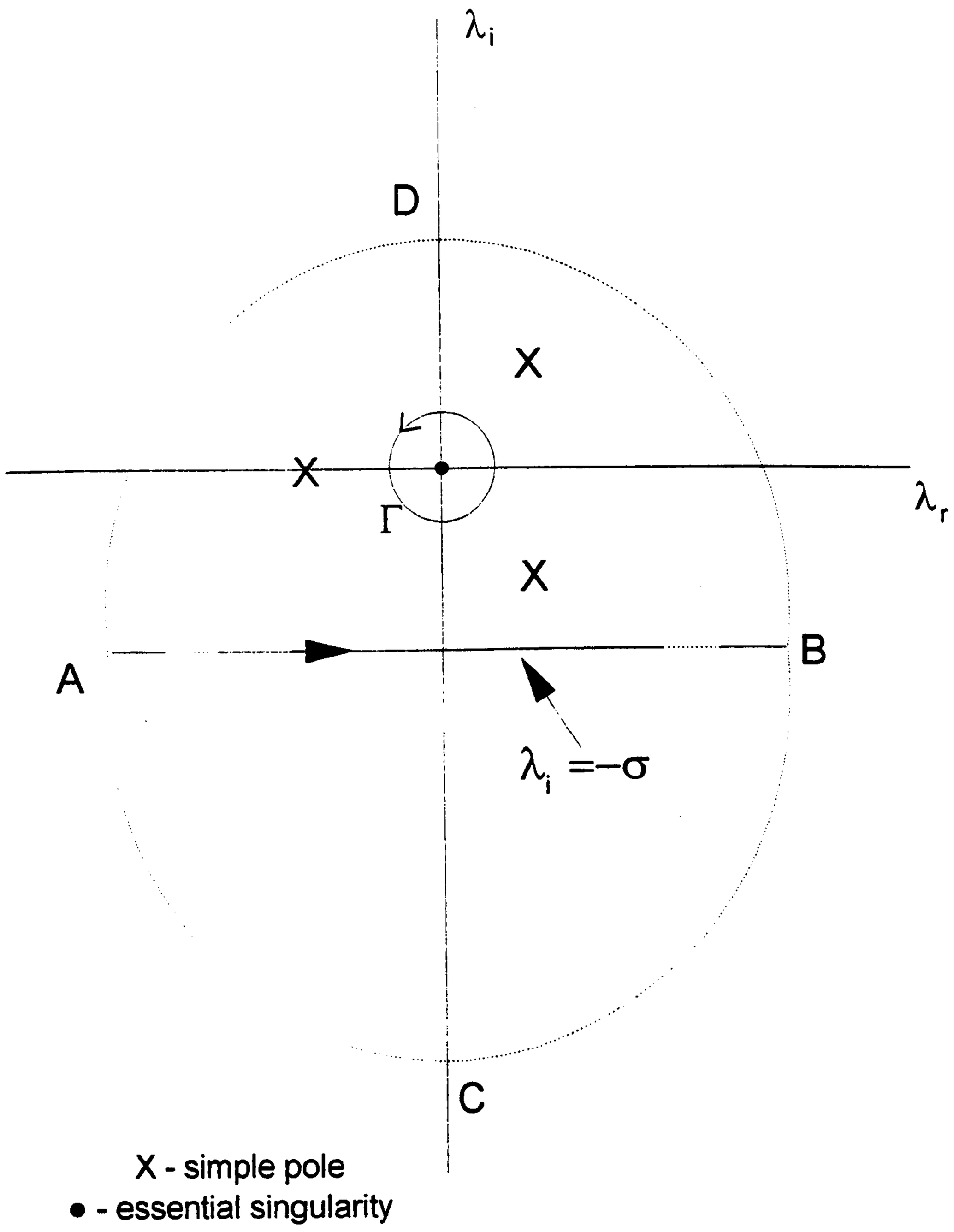

Figure 6.2: Schematic diagram of the complex plane showing singularities and possible paths of integration.

The contour Γ is a counterclockwise path which encloses the singularity at $\lambda = 0$ but does not enclose any of the simple poles, and the coefficients c_0 and c_1 have been defined as

$$c_0 = 1 - \rho\delta \quad , \quad c_1 = \rho - 2\mu \tag{6.81}$$

Equation (6.80) means that when $\bar{z}_1 > 0$ and $\bar{z}_2 > 0$, the electromagnetic field evolution is due to a different process from that which produces steady-state evolution i.e. due to superradiance. From the definitions of $\bar{z}_1$ and $\bar{z}_2$, it can be seen that the region where this process occurs is the slippage region, which is the part of the electron pulse which does not overlap with the original radiation pulse. The slippage region for the case of positive slippage ($\beta < 1$) and negative slippage ($\beta > 1$) is shown in figure 6.1.

In order to evaluate (6.80), the new variables x, ζ, $\bar{\Delta}$ and ϵ, defined as

$$x = (c_0 \bar{z}_1 \bar{z}_2^2)^{1/3} \tag{6.82}$$

$$\zeta = \left(\frac{\bar{z}_2}{\bar{z}_1}\frac{1}{c_0}\right)^{1/3} \lambda \tag{6.83}$$

$$\epsilon = c_1 \left(\frac{1}{c_0^2}\frac{\bar{z}_1}{\bar{z}_2}\right)^{1/3} \tag{6.84}$$

$$\bar{\Delta}(\zeta) = \frac{\bar{z}_2}{\bar{z}_1}\frac{1}{c_0}\Delta(\zeta) = \zeta^3 - \delta\left(\frac{\bar{z}_2}{\bar{z}_1}\frac{1}{c_0}\right)^{1/3}\zeta^2 + c_1\left(\frac{\bar{z}_2}{\bar{z}_1}\frac{1}{c_0}\right)^{2/3}\zeta + \frac{\bar{z}_2}{\bar{z}_1} \tag{6.85}$$

will be used. Equation (6.80) now becomes

$$\mathcal{A}_{SR}(\bar{z}_1, \bar{z}_2) = \frac{b_0}{2\pi} e^{i\delta\bar{z}_1} \left(\frac{\bar{z}_2}{\bar{z}_1}\frac{1}{c_0}\right)^{1/3} \oint_{\Gamma'} \frac{\zeta}{\bar{\Delta}(\zeta)} \exp\left[-ix\left(\frac{1}{\zeta^2} + \frac{\epsilon}{\zeta} - \zeta\right)\right] d\zeta \tag{6.86}$$

where Γ' encloses $\zeta = 0$ but does not enclose any of the simple poles. Each term in the integrand can now be expanded as a power series in ζ and simple poles

found. The exponential terms are expanded using

$$e^Z = \sum_{n=0}^{\infty} \frac{Z^n}{n!}$$

where Z is an arbitrary complex number. Therefore

$$\exp(ix\zeta) = \sum_{a=0}^{\infty} \frac{(ix)^a}{a!} \zeta^a$$

$$\exp\left(-\frac{ix}{\zeta^2}\right) = \sum_{b=0}^{\infty} \frac{(-ix)^b}{b!} \zeta^{-2b}$$

$$\exp\left(-\frac{i\varepsilon x}{\zeta}\right) = \sum_{c=0}^{\infty} \frac{(-i\varepsilon x)^c}{c!} \zeta^{-c}$$

so

$$\exp\left[-ix\left(\frac{1}{\zeta^2} + \frac{\varepsilon}{\zeta} - \zeta\right)\right] = \sum_{a=0}^{\infty}\sum_{b=0}^{\infty}\sum_{c=0}^{\infty} \frac{(-1)^{b+c}(ix)^{a+b+c}\varepsilon^c \zeta^{a-2b-c}}{a!\ b!\ c!} \tag{6.87}$$

Before expanding $1/\bar{\Delta}(\zeta)$in (6.86), it must be split up using the method of partial fractions i.e.

$$\frac{1}{\bar{\Delta}(\zeta)} = \frac{C_1}{(\zeta - \zeta_1)} + \frac{C_2}{(\zeta - \zeta_2)} + \frac{C_3}{(\zeta - \zeta_3)} \tag{6.88}$$

where $\zeta_{1,2,3}$ are the three roots of $\bar{\Delta}(\zeta) = 0$. The three constants C_1, C_2 and C_3 can be found by multiplying both sides of (6.88) by $\bar{\Delta}(\zeta)$. Rewriting (6.88) as

$$\frac{1}{\bar{\Delta}(\zeta)} = -\sum_{k=1}^{3} \frac{C_k}{\zeta_k} \frac{1}{(1 - \zeta/\zeta_k)}$$

it can be seen that the Laurent expansion

$$\frac{1}{1 - Z} = \sum_{n=0}^{\infty} Z^n \qquad (|Z| < 1) \tag{6.89}$$

will be useful. The condition $|Z| < 1$ or $|\zeta/\zeta_k| < 1\ \forall k$ is always satisfied because the contour of integration in (6.80) and (6.86) encloses the origin of the complex plane but does not enclose any of the simple poles at $\zeta = \zeta_{1,2,3}$. Therefore

$$\frac{1}{\bar{\Delta}(\zeta)} = -\sum_{d=0}^{\infty} \zeta^d \left(\frac{C_1}{\zeta_1^{d+1}} + \frac{C_2}{\zeta_2^{d+1}} + \frac{C_3}{\zeta_3^{d+1}}\right) \tag{6.90}$$

where

$$C_1 = \frac{1}{(\zeta_1 - \zeta_2)(\zeta_1 - \zeta_3)} \ , \ C_2 = \frac{1}{(\zeta_2 - \zeta_1)(\zeta_2 - \zeta_3)} \ , \ C_3 = \frac{1}{(\zeta_3 - \zeta_1)(\zeta_3 - \zeta_2)}. \tag{6.91}$$

Using (6.87) and (6.90) the full series expansion of the integrand is therefore

$$\frac{\zeta}{\bar{\Delta}(\zeta)} \exp\left[-ix\left(\frac{1}{\zeta^2} + \frac{\varepsilon}{\zeta} - \zeta\right)\right] = \tag{6.92}$$

$$-\sum_{a,b,c,d=0}^{\infty}\left(\frac{C_1}{\zeta_1^{d+1}} + \frac{C_2}{\zeta_2^{d+1}} + \frac{C_3}{\zeta_3^{d+1}}\right)\frac{(-1)^{b+c}(ix)^{a+b+c}\varepsilon^c\zeta^{a-2b-c+d+1}}{a!\ b!\ c!}$$

so the integral of (6.86) is just $2\pi i\times$ the coefficient of ζ^{-1} from (6.92). When the coefficient of ζ is -1, then from (6.92),

$$d = -a + 2b + c - 2 \quad (d \geq 0)$$

The coefficient of ζ^{-1} is therefore

$$\sum_{a=0}^{\infty}\sum_{b=0}^{\infty}\sum_{c=c_{min}}^{\infty} F(a,b,c)\frac{(-1)^{b+c+1}(ix)^{a+b+c}\varepsilon^c}{a!\ b!\ c!} \tag{6.93}$$

where

$$F(a,b,c) = \sum_{k,l,m=1}^{3}\frac{1}{(\zeta_k - \zeta_l)(\zeta_k - \zeta_m)}\frac{1}{\zeta_k^{-a+2b+c-1}} \quad (k \neq l \neq m) \tag{6.94}$$

and

$$c_{min} = \begin{cases} 0 & \text{if } a - 2b + 2 < 0 \\ a - 2b + 2 & \text{otherwise} \end{cases}$$

The linear solution for the complex electromagnetic field amplitude in the slippage region ($\bar{z}_1 > 0$ and $\bar{z}_2 > 0$) is therefore

$$\mathcal{A}_{SR}(\bar{z}_1, \bar{z}_2) = ib_0\left(\frac{\bar{z}_2}{\bar{z}_1}\frac{1}{c_0}\right)^{\frac{1}{3}} e^{i\delta\bar{z}_1}$$
$$\times\sum_{a=0}^{\infty}\sum_{b=0}^{\infty}\sum_{c=c_{min}}^{\infty} F(a,b,c)\frac{(-1)^{b+c+1}(ix)^{a+b+c}\varepsilon^c}{a!\ b!\ c!} \tag{6.95}$$

It is not a simple matter to extract physical information from the series solution for $\mathcal{A}_{SR}$. This is more easily accomplished using an asymptotic solution, obtained by approximating the contour integral (6.86) using the saddle-point method [87]. The expression (6.86) can be rewritten in the form

$$\mathcal{A}_{SR}(x) = \kappa \oint_{\Gamma'} X(\zeta) \exp\left(x f(\zeta)\right) d\zeta \tag{6.96}$$

where

$$\kappa = \frac{b_0}{2\pi} e^{i\delta \bar{z}_1} \left(\frac{\bar{z}_2}{\bar{z}_1}\frac{1}{c_0}\right)^{1/3} \tag{6.97}$$

$$X(\zeta) = \frac{\zeta}{\bar{\Delta}(\zeta)} \tag{6.98}$$

$$f(\zeta) = i\left(\zeta - \frac{1}{\zeta^2} - \frac{\varepsilon}{\zeta}\right). \tag{6.99}$$

The integral (6.96) can be approximated in the limit of large $|x|$. Physically, this limit means that the region of the electron pulse under observation is far behind the radiation pulse emitted at $\bar{z} = 0$. The approximation involves continuously deforming the contour of integration so that the only significant contribution to the integral comes from the regions of the complex plane near the points which satisfy $f'(\zeta) = 0$. It can be shown that these points are neither maxima nor minima of $f(\zeta)$ but saddle-points [87]. Expressing ζ and $f(\zeta)$ as

$$\zeta = \zeta_r + i\zeta_i \quad , \quad f(\zeta) = f_r(\zeta_r, \zeta_i) + i f_i(\zeta_r, \zeta_i)$$

then the exponential function in the integrand of (6.96) can be written as

$$\exp\left(x f(\zeta)\right) = e^{ix f_i} e^{x f_r}$$

which except for x and f_i constant is a rapidly oscillating function which averages to zero along sections of the path Γ' where f_i is varying. The integrand will be large when f_r is algebraically large.

At least two curves of constant f_r may be drawn through a saddle point. In the sectors between these curves, f_r will be alternately greater and less than at the saddle point itself. In order to keep large values of f_r in as short a section of the path as possible, the path should avoid the sectors where where f_r is greater than at the saddle point and keep to the sectors where f_r is less than at the saddle point as much as possible i.e. the path taken should be the path of steepest ascent and descent through the saddle point. It can be shown that this path is that along which f_i is constant [87]. If ζ_s is a saddle-point, $f(\zeta)$ can be expanded in the form

$$f(\zeta) = f(\zeta_s) + \frac{1}{2}(\zeta - \zeta_s)^2 f''(\zeta_s) + \ldots$$

and the direction of the path will be such that $(z - z_s)^2 f''(\zeta_s)$ is real and negative. The integral (6.96) can now be reduced to [87]

$$\mathcal{A}_{SR}(x) \approx \sqrt{\frac{2\pi}{x f''(\zeta_s)}} \kappa X(\zeta_s) \exp\left(x f(\zeta_s)\right) \tag{6.100}$$

The saddle point around which the dominant contribution occurs, ζ_s, is the root of $f'(\zeta) = 0$ such that the product $\Re\left(f(\zeta)\right)x$ is positive, so that (6.100) is an exponentially growing function.

From the definition of $f(\zeta)$ in (6.99), it is easily found that

$$f'(\zeta) = i\left(1 + \frac{2}{\zeta^3} + \frac{\varepsilon}{\zeta^2}\right)$$

so the three saddle points are the roots of

$$\zeta^3 + \varepsilon\zeta + 2 = 0. \tag{6.101}$$

From (6.99) and (6.100) it is clear that for the superradiant intensity $|\mathcal{A}_{SR}|^2$ to undergo exponential growth, the saddle point ζ_s must be complex. The condition

for ζ_s to be complex can be obtained from (6.101) and is found to be

$$\varepsilon > -3 \tag{6.102}$$

which is equivalent to

$$\frac{(\rho - 2\mu)^3}{(1-\rho\delta)^2}\frac{\bar{z}_1}{\bar{z}_2} > -27. \tag{6.103}$$

Note that as well as being dependent on the parameters ρ, μ and δ, the threshold condition (6.103) is dependent on $\bar{z}_1$ and $\bar{z}_2$ i.e. whether or not the system is linearly unstable is dependent on the position in the electron pulse.

6.2.1 Superradiant Evolution When $\rho \to 0$ and $\mu \to 0$.

When the condition (6.102) is satisfied, the three stationary points correspond to a growing exponential term, a decaying exponential term and an oscillatory term. For large x, the growing exponential term will dominate the other two. When $\rho \to 0$ and $\mu \to 0$, then $\varepsilon \to 0$, so that the threshold condition for ζ_s to be complex is satisfied for all values of $\bar{z}_1, \bar{z}_2 > 0$ and $x \to (\bar{z}_1\bar{z}_2^2)^{1/3}$. From (6.101), and the definition of $f(\zeta)$, (6.99), the exponentially growing term corresponds to $\zeta_s = 2^{1/3}\exp(-i\pi/3)$. The linear solution for the complex field amplitude can now be approximated for large x as

$$\mathcal{A}_{SR} \approx \frac{b_0\bar{z}_1}{x^{3/2}Q(\bar{z}_1,\bar{z}_2)\sqrt{3\pi}}\exp(i\delta\bar{z}_1)\exp\left(\frac{3}{2}(\sqrt{3}+i)\frac{x}{2^{2/3}} - \frac{i\pi}{4}\right) \tag{6.104}$$

where

$$Q(\bar{z}_1,\bar{z}_2) = 1 + \delta\left(\frac{2\bar{z}_1}{\bar{z}_2}\right)^{2/3}\exp\left(\frac{i\pi}{3}\right) - \frac{2\bar{z}_1}{\bar{z}_2} \tag{6.105}$$

so the exponential growth rate of the electromagnetic field amplitude in the superradiant regime when $\rho \to 0$ and $\mu \to 0$ is

$$\begin{aligned} g_{SR} &= \frac{3\sqrt{3}}{2^{5/3}} x \\ &= \frac{3\sqrt{3}}{2^{5/3}} \frac{k_\perp^2 \rho}{k_\parallel} \frac{\beta^{2/3}}{(1-\beta)} (z - v_\parallel t)^{1/3} (v_g t - z)^{2/3}. \end{aligned} \tag{6.106}$$

Note that this is also the asymptotic growth rate of the instability when $c_1 = 0$, even if $\rho \not\ll 1$ and $\mu \not\ll 1$. It is immediately noticeable that the growth rate of the superradiant signal does not depend upon the detuning δ, contrary to the case of the steady-state signal $\mathcal{A}_{SS}$. This is a consequence of the different natures of the singularities of the inverse Laplace transform integral in the steady-state region ($\bar{\Delta}(\lambda) = 0$) and in the slippage region ($\lambda = 0$). A diagram of the electromagnetic field evolution is shown in figure 6.3 for a case of positive slippage ($\beta < 1$) and a fixed $\bar{z} < 1/K$. The field intensity is plotted against $\bar{z}_1$. It can be seen from this figure that there are two distinct regions of evolution, labelled (a) and (b), in the area occupied by the electrons i.e. $0 \leq \bar{z}_1 \leq 1/K$. In region (a), $\bar{z} < \bar{z}_1 < 1/K$, the field intensity is independent of the position in the pulse ($\bar{z}_1$) and is just that due to the steady-state evolution of the field i.e. the field amplitude is a function of $\bar{z}$ only, which is constant in this case. In region (b), $0 < \bar{z}_1 < \bar{z}$ or $\bar{z}_1 > 0$ and $\bar{z}_2 > 0$, so this is the slippage region, as $\bar{z}_1 = \bar{z}$ is the point in the electron pulse reached by the radiation emitted by the tail of that pulse at the beginning of the interaction. The field amplitude evolution in this region is described by (6.104) and is not uniform over the electron pulse due to the slippage effects. Region (c), where $1/K < \bar{z}_1 < \bar{z} + 1/K$, shows the radiation escaping from the front of the electron pulse into vacuum. This radiation no longer undergoes any interaction

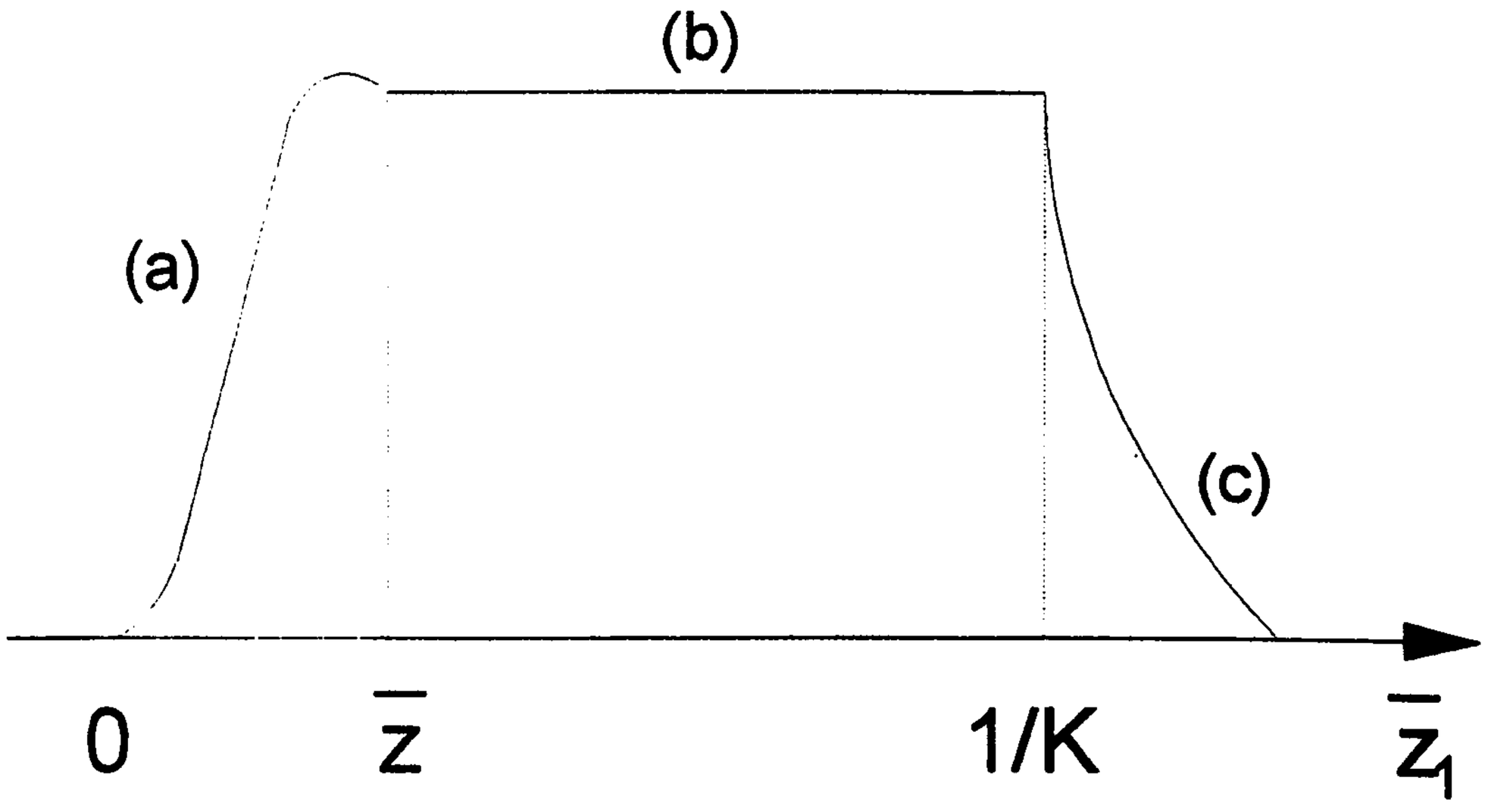

Figure 6.3: Plot of $|\mathcal{A}|^2$ against $\bar{z}_1$ when $S < 1$.

with the electrons, and is a record of the steady-state evolution. Figure 6.4 shows a case where the slippage parameter $S > 1$. This means that the initial radiation pulse has slipped over the entire electron pulse. It can be seen from this figure that there is now no steady-state region. If $\beta > 1$, then these figures would again be obtained with the only difference being that the relative positions of the different regions would be reversed, as the slippage region would occur at the front of the electron pulse and the radiation would escape from the electron pulse tail.

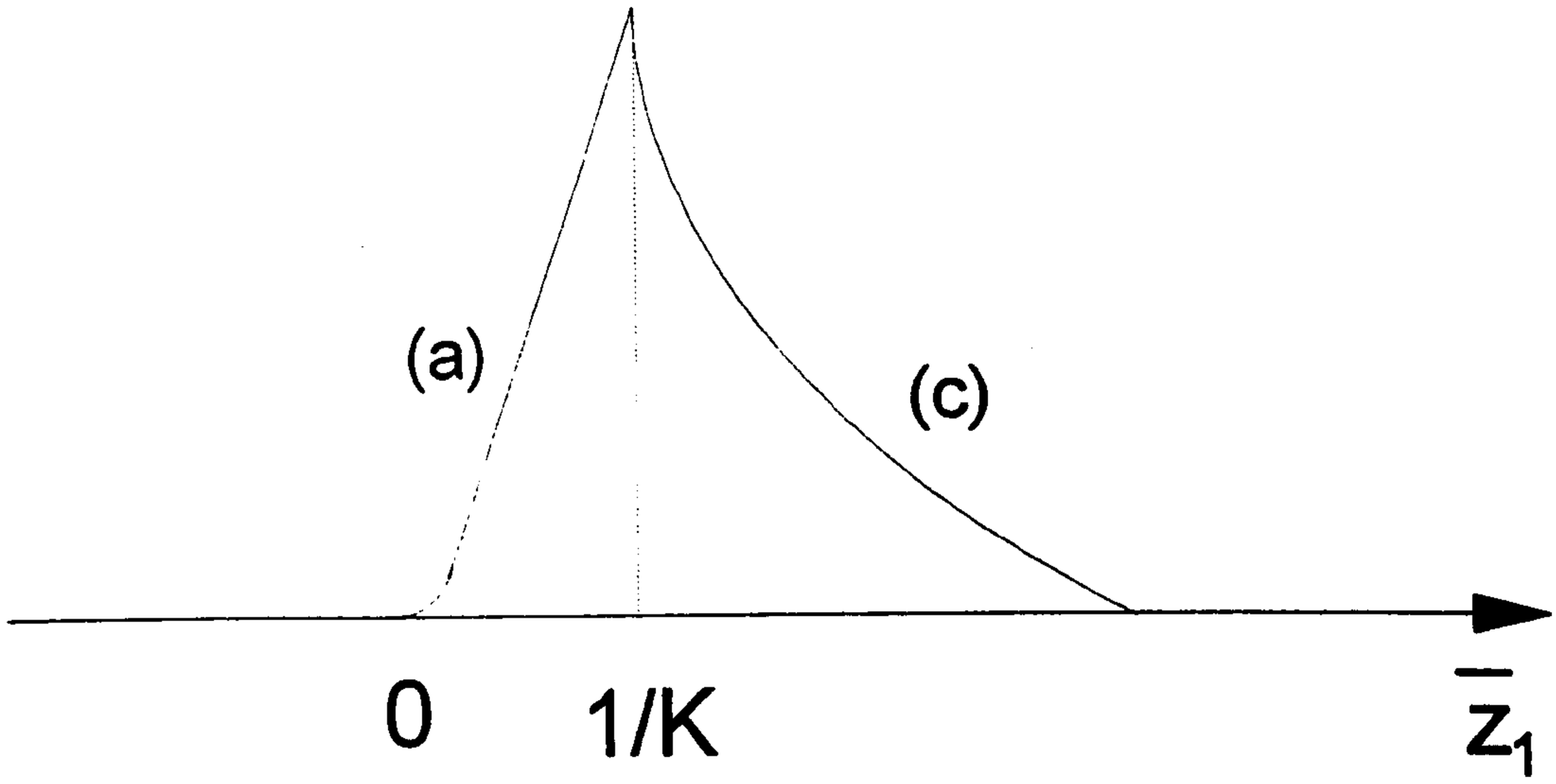

Figure 6.4: Plot of $|\mathcal{A}|^2$ against $\bar{z}_1$ when $S > 1$.

6.2.2 The Effect of Free Energy Depletion on Superradiant Phenomena

In this section, the effect of depletion of the transverse momentum of the electron pulse on the superradiant evolution of the electromagnetic field will be studied. It is sufficient that we consider the limit $\rho \to 0$ in order to analyse these effects. In this limit, the parameter ε becomes

$$\varepsilon \to -2\mu \left(\frac{\bar{z}_1}{\bar{z}_2}\right)^{1/3}$$

and the threshold condition for the electromagnetic field intensity to asymptotically undergo exponential gain, given in (6.102), reduces to

$$\frac{\bar{z}_2}{\bar{z}_1} > \frac{8\mu^3}{27} \tag{6.107}$$

which can be rewritten in terms of $\bar{z}_1$ and $\bar{z}$ using (6.72)

$$\bar{z}_1 < \frac{\bar{z}}{1 + \left(\frac{2\mu}{3}\right)^3} \tag{6.108}$$

Consider a fixed point in the interaction i.e. constant $\bar{z}$ and the growth rate of the superradiant instability at different points in the electron pulse. The case of positive slippage will be assumed for simplicity. The inequality (6.108) suggests that the system is always unstable at the trailing edge of the electron pulse ($\bar{z}_1 = 0$) but that points in the pulse with $\bar{z}_1 > 0$ are closer to the instability threshold. If $\bar{z}_1$ is increased further, the instability will eventually disappear when the condition (6.108) is no longer satisfied. Physically, this can be explained as follows : as there is no radiation entering the rear of the electron pulse, the electrons there are emitting spontaneously, and no significant depletion of their transverse momentum occurs. In contrast, electrons further forward in the electron pulse interact with and amplify radiation which was emitted from those electrons behind them in the pulse and undergo significant depletion of their transverse momentum, consequently reducing the growth rate of the radiation field amplitude. In section 6.3, this effect will be seen to be important for long electron pulses, where strong superradiance can occur.

6.2.3 Superradiant Evolution When $\rho \ll 1$:

Relaxing the limit on ρ imposed in the previous two sections, it can be seen from (6.82) that the case where

$$c_0 = 0 \Rightarrow \rho\delta = 1$$

requires a slightly different set of variables to be used, as x has been defined as being proportional to c_0. The condition $\rho\delta = 1$ was shown in chapters 3 and 4 to be that for which autoresonance occurred. The following analysis will therefore enable an expression to be found describing the superradiant evolution of the electromagnetic field amplitude when autoresonance occurs.

The starting point of the analysis will be (6.80), which when $c_0 = 0$ becomes

$$\mathcal{A}_{SR}(\bar{z}_1, \bar{z}_2) = \frac{b_0}{2\pi} e^{i\delta\bar{z}_1} \oint_\Gamma \frac{\lambda}{\Delta_a(\lambda)} \exp\left[-ix\left(\frac{c_1\bar{z}_1}{\lambda} - \lambda\bar{z}_2\right)\right] d\lambda \tag{6.109}$$

where $\Delta_a(\lambda) = \lambda^2 - (1/\rho)\lambda + c_1$. Defining the new set of variables

$$\zeta_a = \sqrt{\frac{c_1\bar{z}_1}{\bar{z}_2}}\lambda \tag{6.110}$$

$$x_a = \sqrt{c_1\bar{z}_1\bar{z}_2} \tag{6.111}$$

$$\bar{\Delta}_a(\zeta_a) = \frac{\bar{z}_2}{c_1\bar{z}_1}\Delta_a(\lambda) \tag{6.112}$$

the expression (6.109) becomes

$$\mathcal{A}_{SR}(\bar{z}_1, \bar{z}_2) = \frac{b_0}{2\pi} e^{i\delta\bar{z}_1} \frac{c_1\bar{z}_1}{\bar{z}_2} c_1\bar{z}_1 \oint_\Gamma \frac{\lambda}{\bar{\Delta}_a(\zeta_a)} \exp\left[-ix_a f_a(\zeta_c)\right] d\zeta_c \tag{6.113}$$

where

$$f_a(\zeta_c) = \frac{1}{\zeta_a} - \zeta_a.$$

The integral in (6.113) can be evaluated as before using the saddle-point method, where the saddle points are those which satisfy $f_a'(\zeta_a) = 0$, which in this case are $\zeta_a = \pm i$. The value which corresponds to exponential growth of the field amplitude is $\zeta_a = -i$, so using only this value, the exponential growth rate of the electromagnetic field amplitude at autoresonance, g_a, is shown to be

$$g_a = 2x_a = 2\left((\rho - 2\mu)\bar{z}_1\bar{z}_2\right)^{1/2} \tag{6.114}$$

with the necessary condition that $\rho > 2\mu$. Note that this growth rate is proportional to $\bar{z}_1^{1/2}\bar{z}_2^{1/2}$, whereas the growth rate of the instability when $c_0 \neq 0$ is proportional to $\bar{z}_1^{1/3}\bar{z}_2^{2/3}$.

A critical difference between this instability and that of sections 6.2.1 and 6.2.2 is that when autoresonance occurs ($\rho\delta = 1$), and free-energy depletion effects are small, the bunching does not evolve at all (see (6.36) and (6.37)), at least in the linear regime, but stays fixed at its initial value. Amplification of the spontaneous radiation is due to the depletion of the axial momentum of the electron beam.

6.3 Nonlinear Theory

This section is concerned with the nonlinear evolution of superradiance. In order to study this regime, it is necessary to use a set of partial differential equations (PDEs) which are a generalisation of the ordinary differential equations used in the analysis of the steady-state regime. Such a set of equations is shown in (6.31..6.35) but it is possible to write this set in terms of $\bar{z}_1$ and $\bar{z}_2$ using (6.72) and the fact that $\bar{z}_1$ and $\bar{z}_2$ are the characteristics for the electrons and the radiation respectively. This means that

$$\frac{\partial}{d\bar{z}} + \frac{1}{\beta}\frac{\partial}{\partial\bar{t}} \rightarrow \frac{\partial}{\partial\bar{z}_2}$$

$$\frac{\partial}{d\bar{z}} + \frac{\partial}{\partial\bar{t}} \rightarrow \frac{\partial}{\partial\bar{z}_1}$$

so the set of coupled PDEs which will be used in the nonlinear analysis of superradiance is

$$\frac{\partial}{\partial\bar{z}_2}\phi_j'(\bar{z}_1,\bar{z}_2) \;=\; p_j' \qquad (6.115)$$

$$- \quad i\frac{\mu}{\bar{u}_{\perp j}(\bar{z}_1,\bar{z}_2)\bar{u}_{\|j}(\bar{z}_1,\bar{z}_2)}(A'(\bar{z}_1,\bar{z}_2)e^{i\phi'_j(\bar{z}_1,\bar{z}_2)} - c.c.)$$

$$\frac{\partial}{\partial\bar{z}_2}p'_j(\bar{z}_1,\bar{z}_2) = (\rho(p'_j(\bar{z}_1,\bar{z}_2)+\delta)-1)\frac{\bar{u}_{\perp j}(\bar{z}_1,\bar{z}_2)}{\bar{u}^2_{\|j}(\bar{z}_1,\bar{z}_2)}$$

$$\times \quad (A'(\bar{z}_1,\bar{z}_2)e^{i\phi'_j(\bar{z}_1,\bar{z}_2)} + c.c.) \tag{6.116}$$

$$\frac{\partial}{\partial\bar{z}_2}\bar{u}_{\perp j}(\bar{z}_1,\bar{z}_2) = -\frac{\mu}{\bar{u}_{\|j}(\bar{z}_1,\bar{z}_2)}(A'(\bar{z}_1,\bar{z}_2)e^{i\phi'_j(\bar{z}_1,\bar{z}_2)} + c.c.) \tag{6.117}$$

$$\frac{\partial}{\partial\bar{z}_2}\bar{u}_{\|j}(\bar{z}_1,\bar{z}_2) = -\rho\frac{\bar{u}_{\perp j}(\bar{z}_1,\bar{z}_2)}{\bar{u}_{\|j}(\bar{z}_1,\bar{z}_2)}(A'(\bar{z}_1,\bar{z}_2)e^{i\phi'_j(\bar{z}_1,\bar{z}_2)} + c.c.) \tag{6.118}$$

$$\frac{\partial}{\partial\bar{z}_1}A'(\bar{z}_1,\bar{z}_2) = \left\langle\frac{\bar{u}_{\perp}(\bar{z}_1,\bar{z}_2)}{\bar{u}_{\|}(\bar{z}_1,\bar{z}_2)}e^{-i\phi(\bar{z}_1,\bar{z}_2)}\right\rangle + i\delta A'(\bar{z}_1,\bar{z}_2) \tag{6.119}$$

6.3.1 Self-similar Solution for Weak Superradiance

Recalling the expression for the superradiant field amplitude in the linear regime when $\rho \to 0$ and $\mu \to 0$, which from (6.104) is

$$\mathcal{A}_{SR} \approx \frac{b_0\bar{z}_1}{x^{3/2}Q(\bar{z}_1,\bar{z}_2)\sqrt{3\pi}}\exp(i\delta\bar{z}_1)\exp\left(\frac{3}{2}(\sqrt{3}+i)\frac{x}{2^{2/3}} - \frac{i\pi}{4}\right)$$

it is possible to extend the results of the linear analysis in the short pulse limit using the following ansatz on the electron and field variables [90] :

$$A' = \bar{z}_1\exp(i\delta\bar{z}_1)A'_1(y) \tag{6.120}$$

$$\phi'_j = \phi'_{1j}(y) - \delta\bar{z}_1 \tag{6.121}$$

$$p'_j = \sqrt{\bar{z}_1}p'_{1j}(y) \tag{6.122}$$

The partial differential equations (6.115..6.119), which reduce in the limit $\rho \to 0$ to

$$\frac{\partial}{\partial\bar{z}_2}\phi'_j(\bar{z}_1,\bar{z}_2) = p'_j(\bar{z}_1,\bar{z}_2) - i\frac{\mu}{\bar{u}_{\perp j}(\bar{z}_1,\bar{z}_2)}(A'(\bar{z}_1,\bar{z}_2)e^{i\phi'_j(\bar{z}_1,\bar{z}_2)} - c.c.) \tag{6.123}$$

$$\frac{\partial}{\partial\bar{z}_2}p'_j(\bar{z}_1,\bar{z}_2) = -\bar{u}_{\perp j}(\bar{z}_1,\bar{z}_2)(A'(\bar{z}_1,\bar{z}_2)e^{i\phi'_j(\bar{z}_1,\bar{z}_2)} + c.c.) \tag{6.124}$$

$$\frac{\partial}{\partial\bar{z}_2}\bar{u}_{\perp j}(\bar{z}_1,\bar{z}_2) = -\mu(A'(\bar{z}_1,\bar{z}_2)e^{i\phi'_j(\bar{z}_1,\bar{z}_2)} + c.c.) \tag{6.125}$$

$$\frac{\partial}{\partial \bar{z}_1} A'(\bar{z}_1, \bar{z}_2) \;=\; \left\langle \bar{u}_\perp(\bar{z}_1, \bar{z}_2) e^{-i\phi(\bar{z}_1, \bar{z}_2)} \right\rangle + i\delta A'(\bar{z}_1, \bar{z}_2) \tag{6.126}$$

can be rewritten in terms of the new independent variables

$$\bar{z}'_1 \;=\; \bar{z}_1 \tag{6.127}$$

$$y \;=\; x^{3/2} = \sqrt{\bar{z}_1}\bar{z}_2 \tag{6.128}$$

as a set of *ordinary* differential equations i.e.

$$\frac{d\phi'_{1j}}{dy} \;=\; p'_{1j}$$

$$-i\frac{\mu\sqrt{\bar{z}'_1}}{\bar{u}_\perp}\left(A'_1 e^{i\phi'_{1j}} - c.c.\right) \tag{6.129}$$

$$\frac{dp'_{1j}}{dy} \;=\; -\bar{u}_\perp\left(A'_1 e^{i\phi'_{1j}} + c.c.\right) \tag{6.130}$$

$$\frac{d\bar{u}_{\perp j}}{dy} \;=\; -\mu\sqrt{\bar{z}'_1}\left(A'_1 e^{i\phi'_{1j}} + c.c.\right) \tag{6.131}$$

$$\frac{y}{2}\frac{dA'_1}{dy} + A_1 \;=\; \left\langle \bar{u}_\perp e^{-i\phi'_1} \right\rangle . \tag{6.132}$$

Note that the free energy depletion terms are proportional to $\mu\sqrt{\bar{z}'_1}$, so they can be made negligible either by imposing the condition that $\mu \to 0$ as in the case of steady-state evolution *or* by making $\bar{z}_1 \to 0$ i.e. observing a point near the rear of the electron pulse. This is further evidence that free-energy depletion effects are not uniform over the extent of the electron pulse.

Figure 6.5 shows a plot of $|A'_1(y)|^2$ against y for several values of μ as calculated from (6.129..6.132) when $\bar{z}'_1 = 1/K$ (the front of the electron pulse) and $b_0 = 0.01$. The detrimental effect of the free energy depletion terms on the radiation amplification can be clearly seen.

It is therefore possible to obtain a condition for free energy depletion effects to be negligible over the entire electron pulse during a superradiant process by

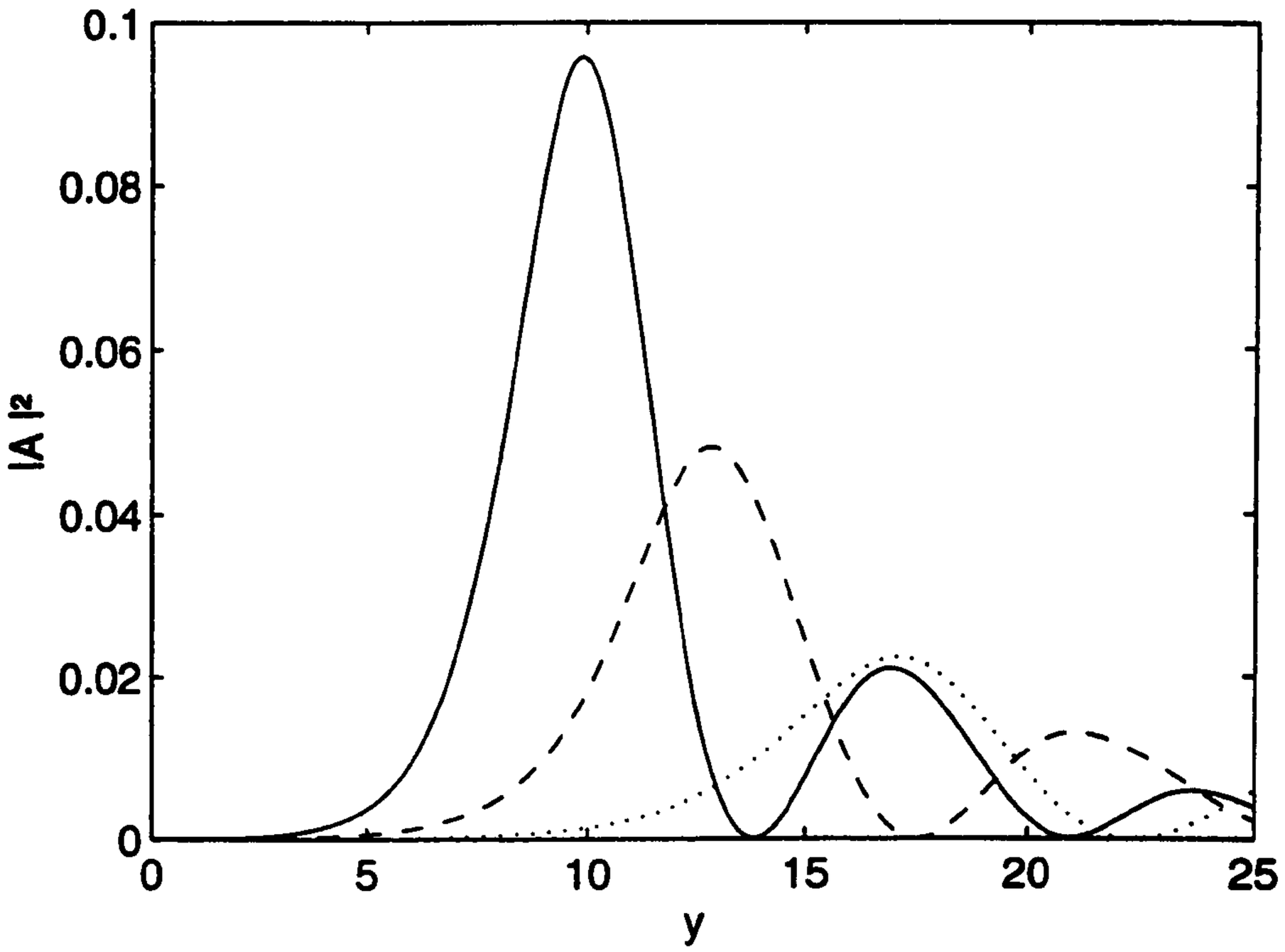

Figure 6.5: Plot of $|A_1'(y)|^2$ against y when $\bar{z}_1' = 1/K = 0.5$, $b_0 = 0.01$ and **(a)**$\mu = 0.01$ (solid line), (b)$\mu = 0.5$ (dashed line), (c)$\mu = 1$ (dotted line).

imposing the condition that they be negligible at the leading edge of the pulse i.e. when $\bar{z}_1' = 1/K$. This implies $\mu/\sqrt{K} \ll 1$ or

$$K \gg \mu^2. \tag{6.133}$$

It will be shown that when this condition is satisfied, the resulting equations describe a superradiant process where radiated intensities are proportional to the square of the electron density and arise from spontaneous emission.

Consider equations (6.129..6.132) in the limit $\mu\sqrt{\bar{z}_1} \ll 1$ i.e.

$$\frac{d\phi_{1j}'}{dy} = p_{1j}' \tag{6.134}$$

$$\frac{dp_{1j}'}{dy} = -\left(A_1' e^{i\phi_{1j}'} + \text{c.c.}\right) \tag{6.135}$$

$$\frac{y}{2}\frac{dA_1'}{dy} + A_1 = \left\langle e^{-i\phi_1'} \right\rangle. \tag{6.136}$$

Note that by defining the variable $w = y^2$, (6.136) can be written as

$$\frac{d}{dw}(A_1' w) = \left\langle e^{-i\phi_1'} \right\rangle \equiv b_1$$

so that by integration,

$$A_1' = \frac{1}{w}\int_0^w b_1(w')\, dw' \equiv \bar{b}_1 \tag{6.137}$$

where $\bar{b}_1$ is the average of the bunching parameter with respect to w.

The solution of (6.134..6.136) will not depend on $\bar{z}_1$ and δ, but only on the initial conditions $A_1'(0) = \left\langle e^{-i\phi_1'(0)} \right\rangle$ and $p_{1j}' = 0$. The independence of $A_1'(y)$ from $\bar{z}_1'$ and δ, has two important consequences. First, the scaling $|A'| = \bar{z}_1'|A_1'|$ implies that $|A'|^2 \propto \rho^2$ from (6.70). This was shown in section 6.2 to imply that the unscaled field intensity varied as

$$I_{sat} \propto n_e^2$$

signifying superradiant emission.

Second, the phase factor $\exp(i\delta\bar{z}_1)$ in (6.120) forces the signal to oscillate at the spontaneous frequency $\omega_s = \frac{\omega_c}{\gamma} + k_{||}v_{||}$, regardless of the assumed frequency ω. In fact, following the chain of field variable transformations, the unscaled electric field, E, varies as

$$E \propto E_0 \exp(i\omega t) \propto A' \exp(i\omega t - i\delta\bar{z}) \propto A_1' \exp[(i\omega t - i\delta\bar{z}_2)$$

where (6.72) and (6.120) have been used. Now

$$\delta\bar{z}_2 = (\omega - \omega_s)\left(t - \frac{z}{v_g}\right)\frac{1}{1-\beta}$$

so if $\beta \ll 1$, the radiation phase is proportional to $\exp(i\omega_s t)$. Hence the factor $\exp(i\delta\bar{z}_1)$ shifts the carrier frequency of the signal from ω to the spontaneous

frequency ω_s. The solution of (6.134..6.136) therefore describes a superradiant process, with intensity scaling as n_e^2 and with the frequency ω_s of spontaneous emission. The situation for $\beta \not\ll 1$ is not so straightforward as the waveguide plays a greater role in the interaction.

6.3.2 Modelling Superradiant Effects in the Nonlinear Regime

In this section, the computer code used to numerically solve the coupled nonlinear PDEs (6.115..6.119) will be described. This code is a modified version of one originally used to model slippage effects in FELs which was written by Dr B.W.J. McNeil [88, 89]. At present, this code can only be used to model positive slippage effects. The use of this code is sufficient to prove the principles of the nonlinear evolution of a superradiant CRM instability. The construction of a code to model nonlinear superradiant effects specific to a CRM is an area of future work.

The code models the interaction of an electron pulse and a radiation pulse by discretizing the pulses into intervals of width equal to the slippage length per cyclotron period, l_s, as defined in (6.7). If the spatial width of each interval is equivalent to a change in ϕ of 2π for the electrons, then each interval can evolve independently i.e. the average in (6.119) is taken only over the electrons in one interval. The relative slippage between the electrons and the wave can then be represented by shifting the radiation intervals with respect to the electron intervals.

Representing the interaction distance z as

$$z = N_c \lambda_{c0}$$

the scaled interaction distance $\bar{z}$ can then be written as

$$\bar{z} = 2\pi\rho X N_c \tag{6.138}$$

so the change in $\bar{z}$ over one cyclotron period will be

$$\Delta\bar{z} = 2\pi\rho X \tag{6.139}$$

Furthermore, as $\bar{z} = \bar{z}_1 + \bar{z}_2$, $\bar{z}_1$ and $\bar{z}_2$ change by steps of $2\pi\rho X$ per cyclotron period along the characteristics $\bar{z}_2 = \text{constant}$ and $\bar{z}_1 = \text{constant}$ respectively, as

$$\Delta\bar{z}_1 = \Delta\bar{z} = 2\pi\rho X \quad \text{for } \bar{z}_2 = \text{constant}$$

$$\Delta\bar{z}_2 = \Delta\bar{z} = 2\pi\rho X \quad \text{for } \bar{z}_1 = \text{constant}$$

The characteristics $\bar{z}_1 = \text{constant}$ and $\bar{z}_2 = \text{constant}$ correspond to $\Delta z = v_{||}\Delta t$ and $\Delta z = v_g \Delta t$ respectively.

From the definitions of $\bar{z}_1$ and $\bar{z}_2$, (6.70) and (6.71), it is noticeable that if $t = \text{constant}$, then $\Delta\bar{z}_1 = \Delta\bar{z}_2 = 2\pi\rho X$ corresponds to a 'static' distance of $\Delta z = \beta l_s$ along the electron pulse and $\Delta z = l_s$ along the radiation pulse. Hence for $\beta \approx 1$, the 'natural' unit length in which to discretize both the electron pulse and the radiation pulse is $2\pi\rho X$ i.e. l_s.

Consider the phase change caused by a change of $2\pi\rho X$ in $\bar{z}_1$ for constant t i.e. a 'static' change of $\Delta z = \beta l_s$ along the electron pulse. Neglecting slowly varying terms, the phase of the electron with respect to the wave can be expressed as

$$\phi \approx \omega t - \phi_g - k_{||} z. \tag{6.140}$$

where ϕ_g is the electron gyro-angle. As the electrons are propagating in the z direction, it is convenient to express the electron gyro-angle as

$$\phi_g \approx k_{c0} z \tag{6.141}$$

so the change in the electron phase is given by

$$\Delta\phi = \omega\Delta t - (k_{c0} + k_{||})\Delta z. \tag{6.142}$$

If $\Delta t = 0$ and $\Delta z = \beta l_s$ then

$$\Delta\phi = (k_{c0} + k_{||})\beta l_s = (k_{c0} + k_{||})\left(\frac{1 - X}{1 + \alpha_c X^2}\right)\frac{2\pi}{k_{||}} \tag{6.143}$$

where (6.7) has been used. This means that for $|\Delta\phi| = 2\pi$, the condition

$$1 - X = 1 \tag{6.144}$$

must be satisfied i.e. the condition $|\Delta\phi| = 2\pi$ can only hold if $X \to 0$, which corresponds to the limit of free space or $v_g = c$. In a waveguide, this condition cannot be satisfied exactly, so interpolation is necessary, as the electrons in one interval of the electron pulse will be interacting with two separate intervals of the radiation pulse. As the code used to produce the numerical results of this section was originally written for a free-space FEL, no such interpolation is performed. Unfortunately, although the interpolation is unnecessary for cases where $X \ll 1$, such values of X mean that the gain per cyclotron period $2\pi\rho X$ is very small ($\rho \ll 1$ is also assumed for the calculations of this section). In order to simulate high-gain ($G > 1$), it is therefore necessary to integrate over a very large number of cyclotron periods and use a very large number of intervals for both the electron

and light pulses. The amount of computer memory required for such an integration is therefore extremely large, and outwith the capabilities of the system on which the code was run. The results produced from numerical integration were therefore produced using values of X large enough that the computer memory limitations allowed the code to be run. With regard to this, these results should be considered as an approximation to the results which would be obtained if the proper interpolation techniques were used. They are included to illustrate the principles of radiation evolution including slippage effects rather than accurately predict, for example, peak radiation intensities.

The partial differential equations are integrated with step size $\Delta\bar{z}_1 = \Delta\bar{z}_2 = 2\pi\rho X$ per cyclotron period, repeated through N_c cyclotron periods, so that the total integration interval is $2\pi\rho X N_c$ i.e. the total unsaturated gain when $\mu \rightarrow 0$ and $\rho \rightarrow 0$. After each integration step, the electron pulse is allowed to slip behind the radiation pulse by one slippage length l_s so that at the end of the integration, the total slippage length will be $L_s = N_c l_s$.

In section 3.4.4, some difficulties of integrating the steady-state equations (3.151..3.155) when significant depletion of the axial momenta of the electrons occurred were discussed. As the partial differential equations (6.115..6.117) are directly related to the steady-state equations, it is obvious that similar problems can also occur in the numerical integration of (6.115..6.118). To avoid these difficulties, the results presented in this section will be for cases where $\rho \ll 1$.

6.3.3 Weak Superradiance

The code described in section 6.3.2 was used to integrate the equations (6.115..6.119) for the case of weak superradiance, where short electron pulses are used i.e. $L_b \lesssim L_c$, so $K \gtrsim 1$. A typical graph showing the scaled radiated intensity $|A'|^2$ plotted against $\bar{z}$ for fixed $\bar{z}_1 = 1/K$ is shown in figure 6.6 for $\rho = 0.01$ and several values of μ. It can be seen that the emitted radiation consists of a large superradiant pulse followed by a number of substantially smaller pulses, similar to a nonlinear ringing effect. The shape and relative size of the pulses are similar to those of figure 6.5 which were calculated using (6.129..6.132). Similar to the steady-state regime, it can be seen that increasing μ has a detrimental effect on the amplification of the radiation. The peak intensity of the first pulse and the value of $\bar{z}$ at which it occurred have been plotted against ρ and μ in figures 6.7 and 6.8 for values of G such that the superradiant parameter K lies in the range $1 \leq K \leq 10$.

The superradiant scaling $|A'|^2_{sat} \propto \rho^2$ can be seen in figure 6.7 for $\mu \rightarrow 0$, as the gradient of the $|A'|^2_{sat}$ vs ρ plot is ≈ 2 on a logarithmic scale. However, when μ is significant this scaling occurs only for very small values of ρ i.e. for large values of K. This supports the use of (6.133) as the condition under which free-energy depletion effects may be neglected. When both ρ and μ are significant, the scaling of the peak intensity begins to 'level off' towards the steady-state case where $|A'|^2_{sat} =$ constant. This can be explained by considering the effects of slippage on saturation. As the electrons in the slippage region of the electron pulse are interacting with spontaneously emitted radiation of low amplitude, they

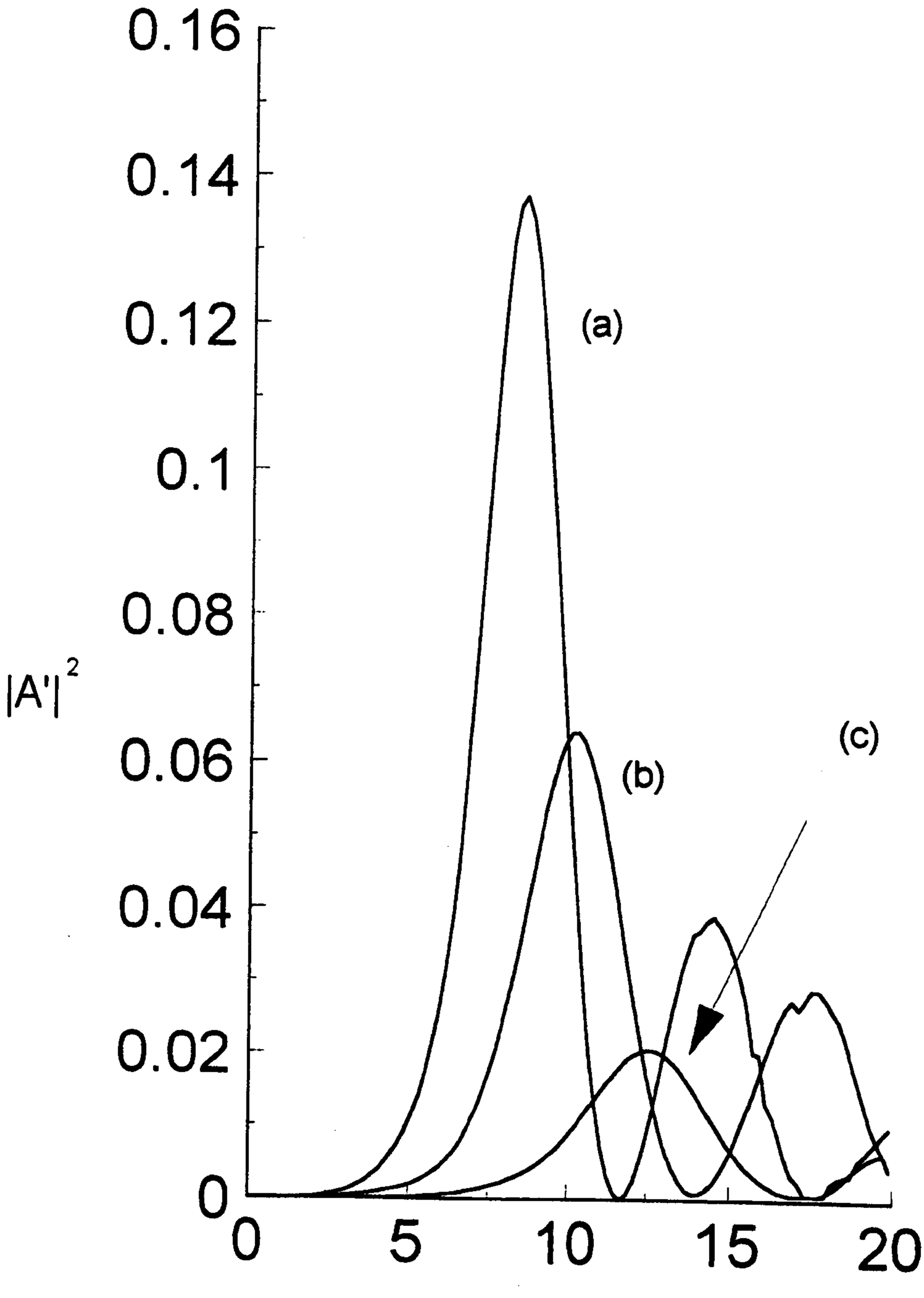

Figure 6.6: Plot of $|A'|^2$ against $\bar{z}$ for $\bar{z}_1 = 1/K$, $\rho = 0.001$, $X = 0.16$ and (a) $\mu = 0.01$. (b) $\mu = 0.5$ (c) $\mu = 1$.

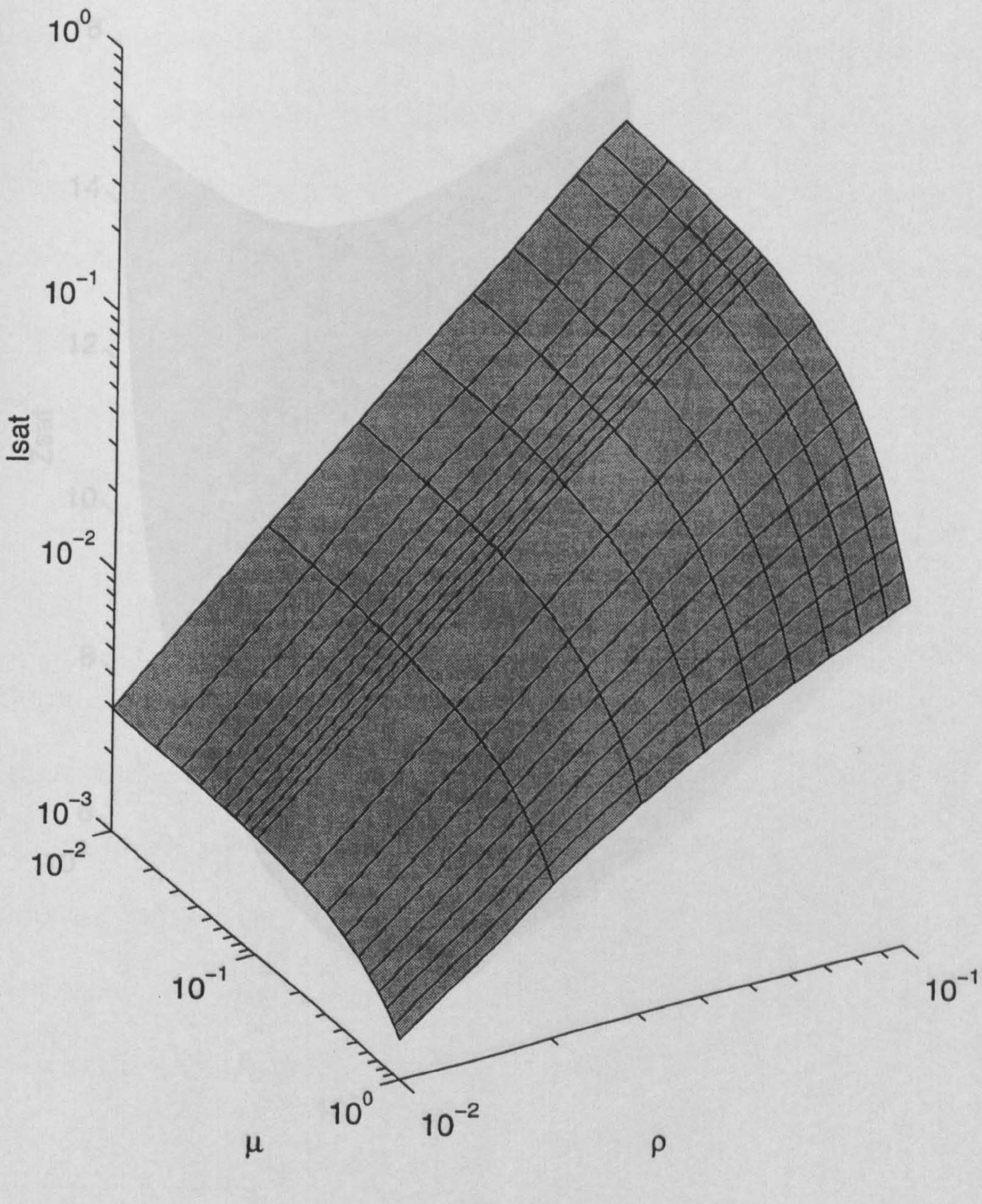

Figure 6.7: Plot of peak scaled intensity against ρ and μ for $1 < K < 10$.

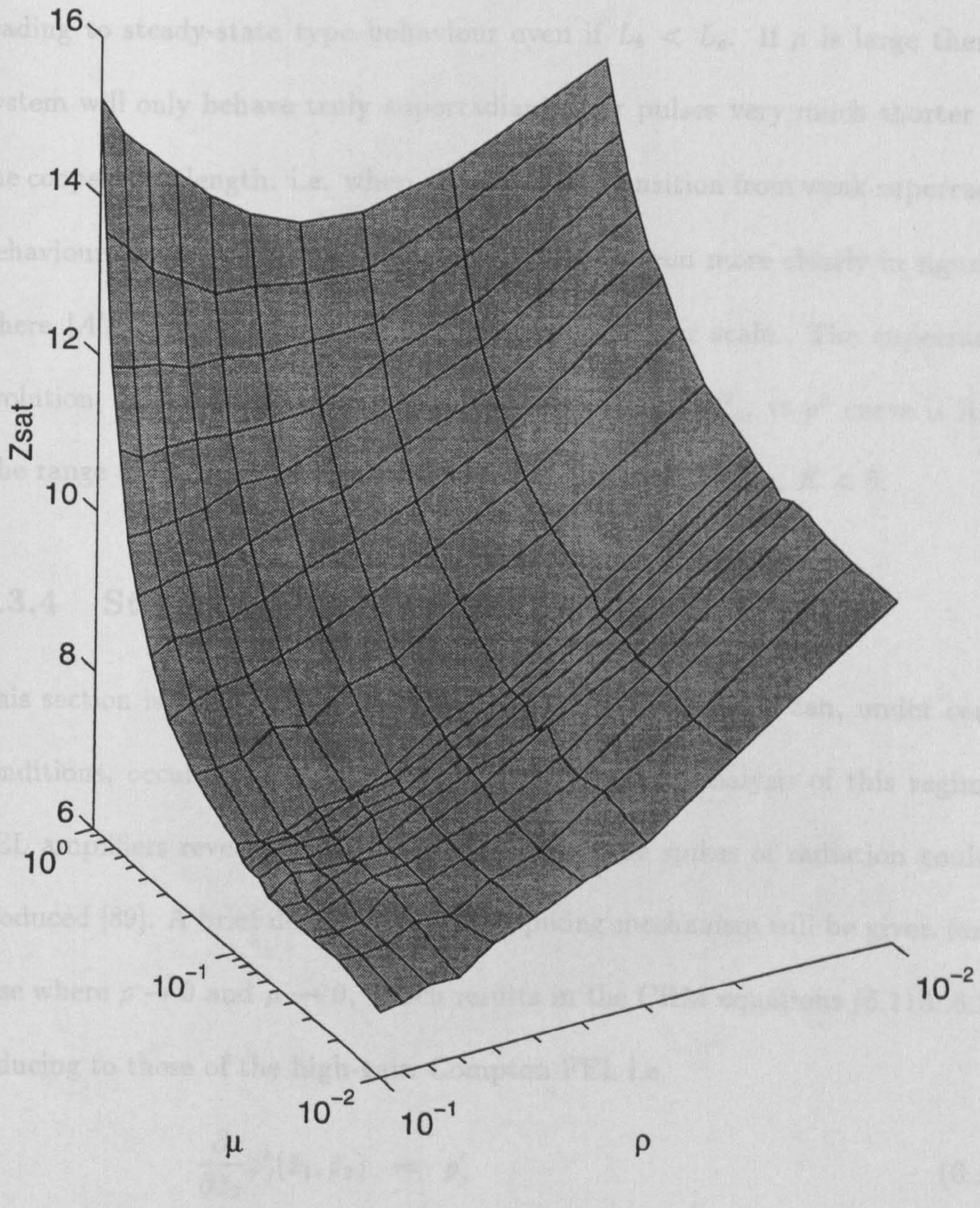

Figure 6.8: Plot of position of the scaled intensity peak $\bar{z}_{sat}$ against ρ and μ for $1 < K < 10$.

will not undergo saturation effects, and will emit continuously. For large values of μ however, saturation effects due to free energy depletion begin to occur at much smaller values of the field amplitude, i.e. closer to the rear of the electron pulse, leading to steady-state type behaviour even if $L_b < L_c$. If μ is large then the system will only behave truly superradiantly for pulses very much shorter than the cooperation length. i.e. when $K \gg 1$. The transition from weak superradiant behaviour to steady-state type behaviour can be seen more clearly in figure 6.9 where $|A'|^2_{sat}$ is plotted against ρ^2 and μ on a linear scale. The superradiant evolution, where $|A'|^2_{sat} \propto \rho^2$ can be seen where the $|A'|^2_{sat}$ vs ρ^2 curve is linear. The range of the superradiant parameter in this case is $0.5 < K < 5$.

6.3.4 Strong Superradiance

This section is concerned with superradiant processes which can, under certain conditions, occur in long electron pulses. Numerical analysis of this regime in FEL amplifiers revealed that very large amplitude spikes of radiation could be produced [89]. A brief description of the spiking mechanism will be given for the case where $\rho \to 0$ and $\mu \to 0$, which results in the CRM equations (6.115..6.119) reducing to those of the high-gain Compton FEL i.e.

$$\frac{\partial}{\partial \bar{z}_2}\phi'_j(\bar{z}_1, \bar{z}_2) = p'_j \tag{6.145}$$

$$\frac{\partial}{\partial \bar{z}_2}p'_j(\bar{z}_1, \bar{z}_2) = -(A'(\bar{z}_1, \bar{z}_2)e^{i\phi'_j(\bar{z}_1, \bar{z}_2)} + c.c.) \tag{6.146}$$

$$\frac{\partial}{\partial \bar{z}_1}A'(\bar{z}_1, \bar{z}_2) = \left\langle e^{-i\phi'(\bar{z}_1, \bar{z}_2)} \right\rangle + i\delta A'(\bar{z}_1, \bar{z}_2) \tag{6.147}$$

The effect of free energy depletion effects on the generation of radiation spikes will then be demonstrated by relaxing the limit on μ. For simplicity, the case of

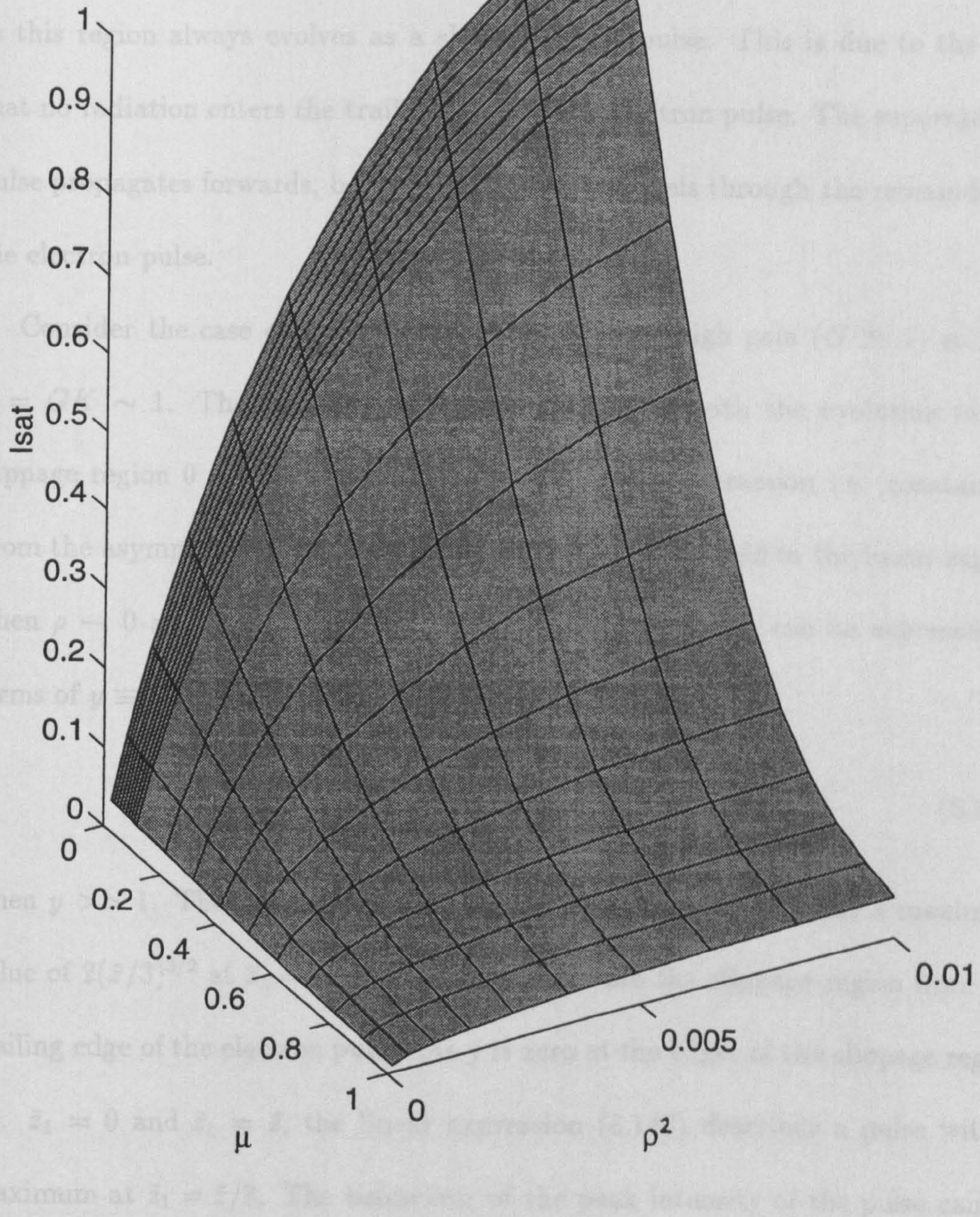

Figure 6.9: Plot of peak scaled intensity against ρ^2 and μ for $0.5 < K < 5$.

positive slippage will again be assumed.

The spiking behaviour is thought to be due to the amplification of the superradiant pulse which originates in the rear of the electron pulse , $0 < z - v_{||}t < L_b$, as this region always evolves as a short electron pulse. This is due to the fact that no radiation enters the trailing edge of the electron pulse. The superradiant pulse propagates forwards, being amplified as it travels through the remainder of the electron pulse.

Consider the case of a long pulse ($K \ll 1$) and high gain ($G \gg 1$) so that $S = GK \sim 1$. The following analysis is concerned with the evolution in the slippage region $0 < \bar{z}_1 < \bar{z}$ for a fixed point in the interaction i.e. constant $\bar{z}$. From the asymptotic expression for the electromagnetic field in the linear regime when $\rho \rightarrow 0$ and $\mu \rightarrow 0$, (6.104), the scaled field intensity can be expressed in terms of $y \equiv x^{3/2} = \sqrt{\bar{z}_1}(\bar{z} - \bar{z}_1)$ as

$$|\mathcal{A}_{SR}|^2 \propto \exp\left[3\sqrt{3}\left(\frac{y}{2}\right)^{3/2}\right] \tag{6.148}$$

when $y >> 1$. The variable y as a function of $\bar{z}_1$ for a fixed $\bar{z}$ has a maximum value of $2(\bar{z}/3)^{3/2}$ at $\bar{z}_1 = \bar{z}/3$ i.e. at one third into the slippage region from the trailing edge of the electron pulse. As y is zero at the edges of the slippage region i.e. $\bar{z}_1 = 0$ and $\bar{z}_1 = \bar{z}$, the linear expression (6.148) describes a pulse with a maximum at $\bar{z}_1 = \bar{z}/3$. The behaviour of the peak intensity of the pulse can be found by substituting $\bar{z}_1 = \bar{z}/3$ in (6.104). The result is

$$|\mathcal{A}_{SR}|^2_{peak} = \frac{|b_0|^2}{4\pi\bar{z}\delta^2}\exp(\sqrt{3}\bar{z}) \tag{6.149}$$

so the superradiant pulse grows exponentially in amplitude as it propagates

through the electron pulse. The asymptotic expression above loses its validity at resonance ($\delta = 0$).

An example of strong superradiance is shown in figure 6.10 which shows the scaled intensity of the radiation pulse plotted in a 'window' which travels at the group velocity of the radiation. For the case of positive slippage, the electron pulse travels backwards in this window. The radiation evolution is plotted for different points in the interaction ($N_c \equiv z/\lambda_{c0}$ is the number of cyclotron periods travelled). The position of the electron pulse is denoted by the dashed line. The horizontal axis in the figure is marked in units of $2\pi\rho X$. As the interaction progresses, the three regions of field evolution shown schematically in figure 6.3 can be clearly seen: the region of superradiant evolution at the rear of the electron pulse, the flat steady-state region and the region in front of the electron pulse, where the radiation has escaped into vacuum. The build-up of the superradiant spike to intensities much larger than that of steady-state region is clearly visible.

If the limit on μ is now relaxed, the set of equations used to describe the system is (6.123..6.126). For the part of the pulse where $\bar{z}_1 \ll 1/\mu^2$, the free energy depletion terms will be negligible and a superradiant pulse will be generated, as was shown above. However, as the pulse propagates throught the electron pulse, the free energy depletion terms become significant, and disrupt the amplification of the radiation.

This disruption of the amplification can be demonstrated using the same parameters as those used to create the graph in figure 6.10 but for a different value of μ. Figures 6.11 and 6.12 show the field evolution when $\mu = 0.5$ and $\mu = 1$ re-

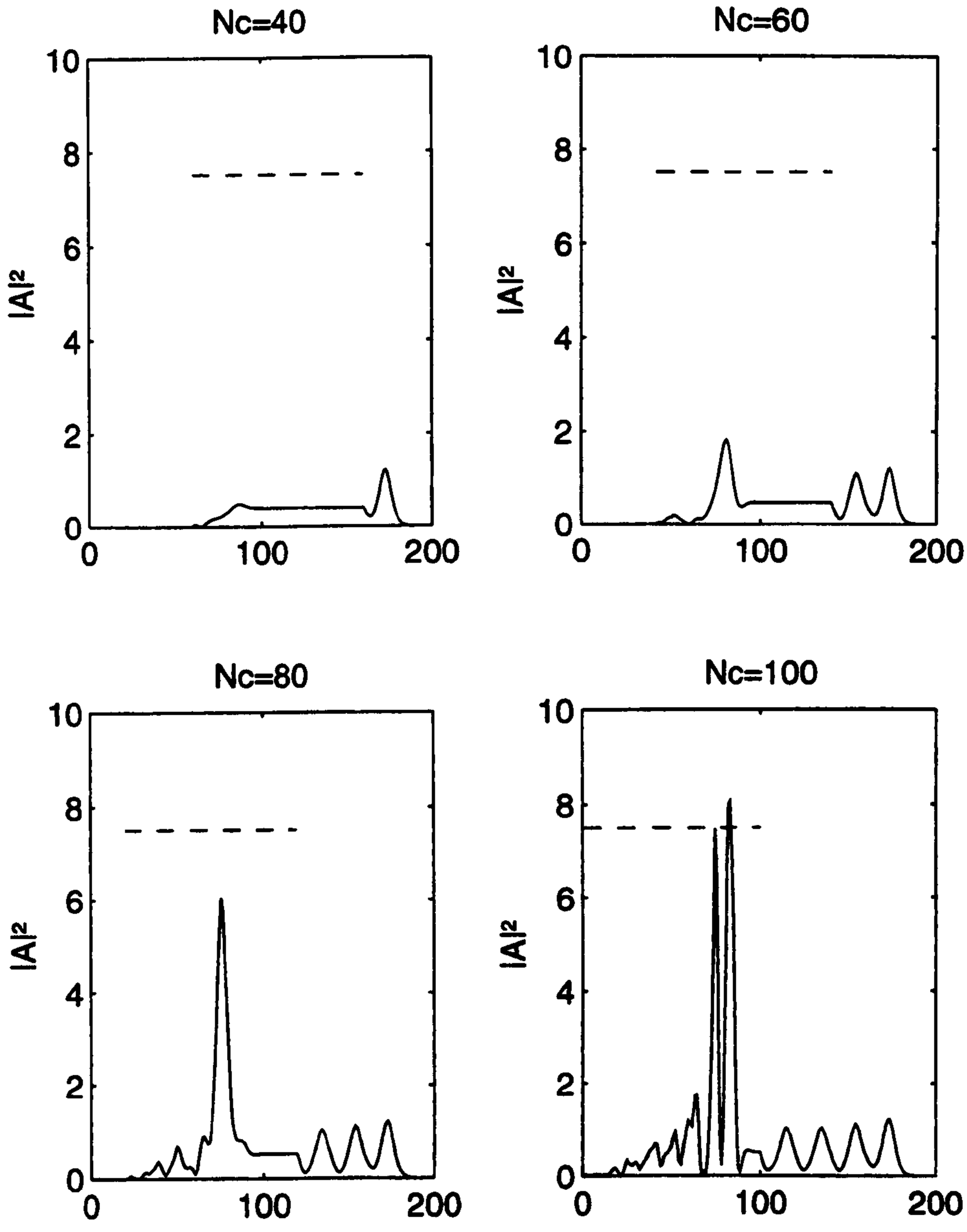

Figure 6.10: Plot of $|A'|^2$ for $\rho = 0.0636$, $X = 0.63$, $\mu = 0.001$, $\delta = 0$, $K = 0.039$, $G = 25.5$ and (a) $N_c = 40$, (b)$N_c = 60$, (c)$N_c = 80$, (d)$N_c = 100$.

spectively. As expected, the increased significance of free energy depletion effects has a strong effect on the peak intensity of the radiation spikes. When $\mu = 0.5$, and $N_c = 100$ the intensity of the superradiant spike is roughly the same as the steady-state intensity, but the spike is still growing at this stage, whereas the steady-state region has saturated long before. More conclusive however is the case where $\mu = 1$, shown in figure 6.12. For this value of μ, the steady-state region of the pulse cannot undergo exponential growth as $\mu < 0.95$ for steady-state instability when $\delta = 0$ and $\rho \ll 1$. However, the superradiant evolution at the rear of the electron pulse is still unstable, giving rise to a very 'clean' spike of radiation. The amplitude of this spike is still far less than that when $\mu \ll 1$. The effect of free energy depletion on strong superradiance is therefore to reduce the peak intensity of the spikes of intense electromagnetic radiation, but by increasing μ to a value outside the instability threshold for the steady-state region, the superradiant evolution can be made to grow without the simultaneous growth of the steady-state region.

6.4 Conclusions

It has been shown in this chapter that in addition to the usual steady-state interaction in a CRM, where the radiation intensity is only dependent on the distance through the interaction region, there is another type of interaction which can occur if the relative slippage between the electron pulse and the radiation pulse is significant. It was shown that this interaction involves a non-uniform distribution of the radiation field over the electron pulse. The effect of this is for

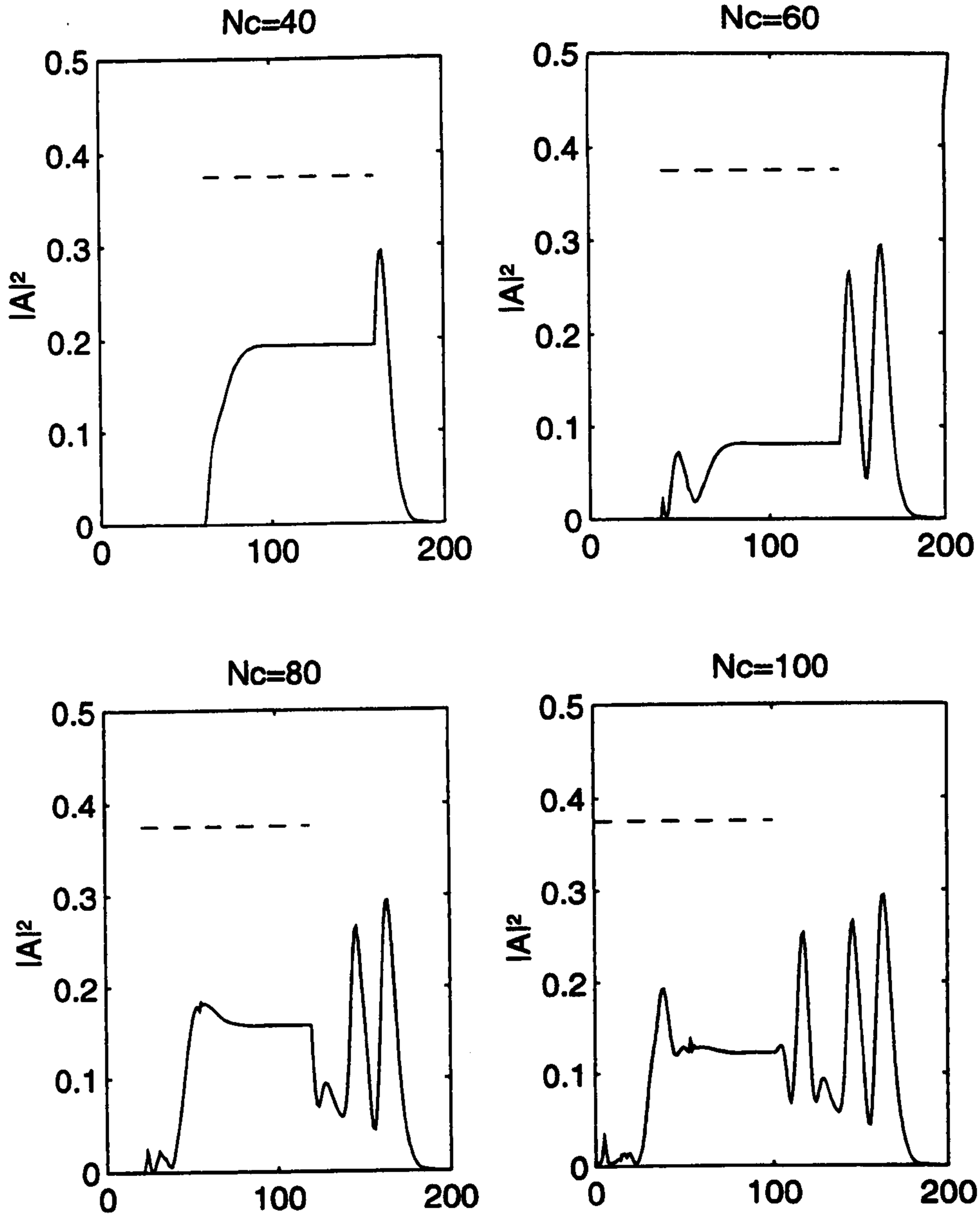

Figure 6.11: Scaled intensity vs $\bar{z}_1$ for the same case as in figure 6.10 but with $\mu = 0.5$.

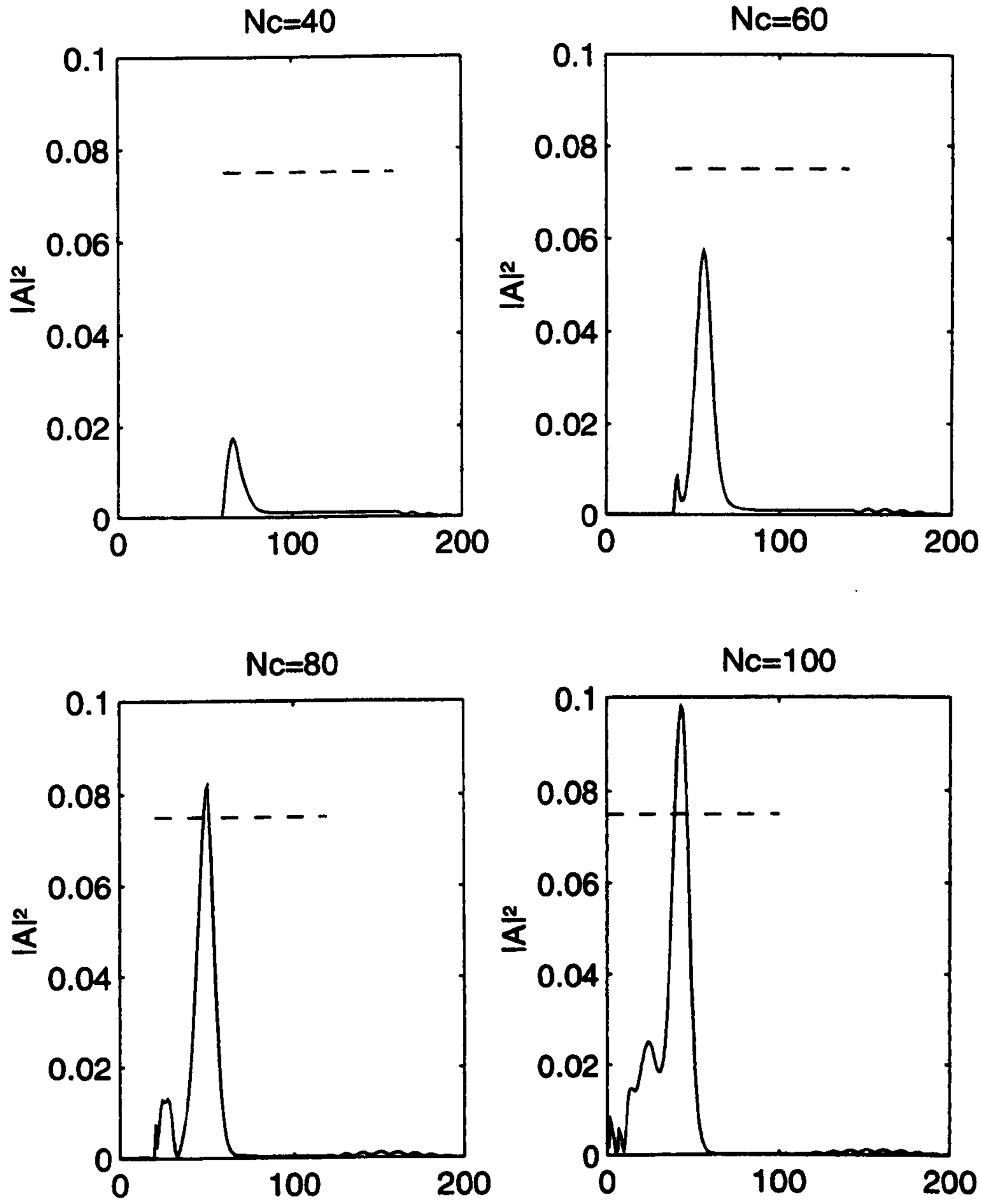

Figure 6.12: Scaled intensity vs $\bar{z}_1$ for the same case as in figure 6.10 but with $\mu = 1$.

the radiation to evolve superradiantly, so that peak intensities scale as the square of the electron density, n_e, as opposed to the steady-state scaling of $n_e^{4/3}$. The analysis carried out in this chapter was specific to the case of a beam of electrons travelling at relativistic electron velocities. This condition and the critical role of slippage imply that the type of device which is most likely to give rise to superradiant phenomena is most likely to be a CARM.

The concept of the cooperation length was introduced using a simple but effective dissipative model, which demonstrated the conditions under which one would expect to observe superadiant phenomena. A rigorous linear analysis then produced general expressions for the rate of growth of the electromagnetic field, shown to be proportional to $(\bar{z}_1\bar{z}_2^2)^{1/3}$. It was also shown that free-energy depletion effects gave rise to a threshold condition for instability, similar to the case of steady-state evolution. A crucial difference between the threshold condition for superradiant instability and that for steady-state instability was that the superradiant instability threshold was dependent on the position in the electron pulse. This implies that free-energy depletion effects are non-uniform over the extent of the electron pulse.

Superradiant evolution was also shown to occur when the condition for exact autoresonance was satisfied. The special features of this instability were that it required $\rho > 2\mu$ and the spatial growth rate was proportional to $(\bar{z}_1\bar{z}_2)^{1/2}$. The radiation amplification mechanism for this autoresonant superradiance was found to be due to depletion of the axial momentum of the electron beam, as opposed to a bunching in phase.

Using a computer code, the nonlinear evolution of superradiance in the CRM was studied for the case of positive slippage under the condition $\rho \ll 1$. It was found that there there were two superradiant regimes: weak superradiance, which involved short electron pulses and produced low radiation intensities , and strong superradiance, which involved long electron pulses and large radiation intensities. The effect of free energy depletion on both these regimes was studied. For the case of weak superradiance, it was shown that the partial differential equations used to analyse the nonlinear regime of the interaction could be reduced to a set of self-similar ordinary differential equations. A result of this reduction was a general condition for the neglect of free energy depletion effects when analysing weak superradiance i.e. $K \gg \mu^2$. For the case of strong superradiance, it was found that when free energy depletion effects were negligible, large intensity radiation spikes were produced in the slippage region of the electron pulse, due to amplification of the superradiant pulse originating at the trailing edge of the electron pulse as it propagated through the remainder of the pulse. The inclusion of free energy depletion effects caused the intensity of the spikes to be decreased, but the trailing region of the electron pulse was found to always emit superradiantly, even if free-energy depletion effects were so large that the steady-state region underwent no significant evolution.

Chapter 7

Conclusions and Future Work

7.1 Conclusions

The theoretical studies described in this thesis have produced a series of new and significant results in the field of CRM theory. The most significant of these results are described below :

7.1.1 Universally Scaled Evolution Equations

It was shown in chapter 3 that it is possible to derive from first principles a set of universally scaled evolution equations which describe the linear and nonlinear evolution of the CRM interaction between a beam of relativistic electrons and a single TE or TM waveguide mode. The universal scaling was found to simplify both the analysis of the interaction and the interpretation of the results produced. The number of free parameters involved in the universally scaled set was just three : ρ, the fundamental CRM parameter, ν, the free energy parameter and

δ, the detuning between the electrons and the wave. The parameters ρ and ν were combined to form the depletion parameter, μ. Using this universally scaled set of equations, the CRM interaction was studied far into the nonlinear regime over a wide range of the parameter space for the case of steady-state evolution of the radiation field, where the relative slippage between the radiation and the electrons is negligible.

Among the results obtained from the universally scaled equations was an identification of the different saturation mechanisms and the conditions under which they occur: phase trapping, due to electrons bunching to an optimum level in phase before de-bunching, was shown to occur when $\rho \ll 1$ and $\mu \ll 1$ and free energy depletion, due to the effect of depletion of the transverse momentum of the electron beam was shown to occur when $\mu \not\ll 1$.

In the limiting case where $\rho \ll 1$ and $\mu \ll 1$, the evolution equations were shown to reduce to a set where no free parameters are present which also describes the interactions which occur in a number of other beam-wave devices such as the high-gain Comption FEL, the Cerenkov maser and the Smith Purcell laser.

The form of the universally scaled equations enabled the identification of the condition for exact autoresonance to occur i.e. $\rho\delta = 1$. The concept of autoresonance and the effect it has on the electron and field evolution was analysed and discussed.

7.1.2 Steady State Linear Theory

Using a rigorous linear analysis, the linear growth of the instability was studied using a linearised set of universally scaled evolution equations, chapter 4. The method of collective variables, which has not previously been applied to CRM-type devices, was used to derive a dispersion relation which determines the linear behaviour of the system. Using this dispersion relation, a threshold condition for linear instability to occur was derived. Above this threshold, an expression for the growth rate of the electromagnetic field was found and compared with the results of other linear theories.

The linear growth of the instability was found to consist of two distinct regimes : the low-gain regime, where the 'partial waves' which correspond to the roots of the dispersion relation interfere, and the high-gain regime, where the amplitude of the electromagnetic field grows exponentially. In the low-gain regime, it was found that Madey's relations between the stimulated emission (gain), spontaneous emission and the energy spread of the electrons, originally derived for the FEL, could be reproduced.

Using the linear analysis, it was also possible to identify the different bunching mechanisms responsible for wave amplification and the condition for autoresonance to occur. The condition for instability to occur at exact autoresonance was derived and the resulting growth rate of the instability was evaluated.

7.1.3 Hamiltonian Theory of the CRM

In section 5.1, it was shown that it is possible to state the equations of motion for the electrons *and* the electromagnetic field in a CRM as a system of Hamilton's equations when the recoil of the electrons is negligible i.e. $\rho \ll 1$. This enabled an analysis of the CRM interaction in the steady-state limit in terms of phase space. This phase space analysis was performed for two particular cases :

1. the case where the evolution of the field is negligible, similar to that in a low-gain CRM high-Q oscillator close to saturation.

2. the case where the field evolution evolves self-consistently with a single particle, similar to the interaction involving a perfectly pre-bunched electron beam and a waveguide mode. The relevance of this case to experiments lies in the development of new cathodes capable of generating very short electron pulses at high repetition rates.

For both cases, the evolution of the phase space with the variation of parameters such as μ and the initial field intensity was studied.

7.1.4 A Landau-Ginzburg Equation for the CRM

In section 5.2, it was shown that another feature of the universally scaled equations when $\rho \ll 1$ is that it is possible to describe the linear and nonlinear evolution of the electromagnetic field using collective variables which are a generalisation of those variables used in the linear analysis of the interaction in chapter 4. This was shown to greatly reduce the number of equations to be solved, resulting

in a description of the linear and nonlinear regime of the CRM interaction using three complex equations. These equations describe the interaction in a similar way to those used to describe the polarisation, population difference and field amplitude and phase in atomic laser theory.

Using this collective variable description, it was then shown that it is possible to approximately describe the evolution of the electromagnetic field up to saturation by an analytically solveable Landau-Ginzburg equation. This allows quantities such as saturation intensities, which usually have to be evaluated via the numerical solution of a large set of coupled differential equations, to be evaluated analytically. In addition, it demonstrates that the evolution of the electromagnetic field up to saturation in a cyclotron resonance maser amplifier can be described by the same equation used to model the field evolution in an atomic laser.

7.1.5 Superradiance in the CRM

It was shown in chapter 6 that in addition to the usual steady-state interaction in a CRM, where the radiation intensity is only dependent on the distance through the interaction region, there is another type of interaction which can occur if the relative slippage between the electron pulse and the radiation pulse is significant. Under certain conditions, this slippage can cause the radiation to evolve superradiantly, so that peak intensities scale as the square of the electron density, n_e, as opposed to the steady-state scaling of $n_e^{4/3}$.

The conditions under which one would expect to observe superradiant phe-

nomena were deduced using a dissipative model. It was found using this model that the length of the electron pulse relative to a cooperation length determined the importance of superradiant effects in the field evolution.

A rigorous linear analysis produced general expressions for the rate of growth of the electromagnetic field. It was shown that free-energy depletion effects gave rise to a threshold condition for instability, similar to the case of steady-state evolution. A crucial difference between the threshold condition for superradiant instability and that for steady-state instability was that the superradiant instability threshold was dependent on the position in the electron pulse. This implies that free-energy depletion effects are non-uniform over the extent of the electron pulse. A superradiant instability was also shown to occur when the condition for exact autoresonance was satisfied. The radiation amplification mechanism for this autoresonant superradiance was found to be due to depletion of the axial momentum of the electron beam, as opposed to a bunching in phase.

The nonlinear evolution of superradiance in the CRM was studied using a computer code for the case of positive slippage under the condition $\rho \ll 1$. It was found that there there were two superradiant regimes: weak superradiance, which involved short electron pulses and produced low radiation intensities , and strong superradiance, which involved long electron pulses and large radiation intensities. For the case of weak superradiance, it was shown that the partial differential equations used to analyse the nonlinear regime of the interaction could be reduced to a set of self-similar ordinary differential equations. A result of this reduction was a general condition for the neglect of free energy depletion effects when

analysing weak superradiance i.e. $K \gg \mu^2$. For the case of strong superradiance, it was found that when free energy depletion effects were negligible, large intensity radiation spikes were produced in the slippage region of the electron pulse, due to amplification of the superradiant pulse originating at the trailing edge of the electron pulse as it propagated through the remainder of the pulse. The inclusion of free energy depletion effects caused the intensity of these spikes to be reduced. It was shown that growth of a superradiant spike occurred even when the value of μ was so large that steady-state instability could not occur.

It can be seen from these summaries that the aim of the thesis, to find and study novel aspects of CRM theory, has been achieved.

7.2 Future Work

Given the accomplishments of this thesis, summarised in the previous section, the main areas of future work will be as follows :

1. The extension of the range of validity of the universally scaled evolution equations, via the relaxation of some of the approximations used in their derivation in chapter 3. This would enable analysis of the CRM interaction involving cyclotron harmonics, non-uniformity of the waveguide mode across an electron gyro-orbit, multiple waveguide modes and large beam density effects. The last two in this list are interconnected due to the fact that large beam-density effects give rise to the simultaneous excitation of TE and TM waveguide modes.

2. The extension of the Hamiltonian theory described in section 5.1 to include a description of the CRM interaction in terms of action-angle variables. The use of action angle variables makes it simple to identify the frequency of any periodic motion without finding a complete solution to the motion of the system. This will be relevant to the type of oscillations which the electrons perform after saturation.

   Other areas of the Hamiltonian analysis which are open to further investigation include the derivation of a Hamiltonian valid when $\rho \not\ll 1$, and a thorough investigation of the many-particle Hamiltonian, particularly with regard to the transition from ordered motion to chaotic motion and its behaviour in different regions of parameter space. Another situation of interest, also possibly leading to chaos would be the self-consistent evolution of two or more waveguide modes with a single particle.

3. The extension of the analytical description of the CRM interaction to include the simultaneous nonlinear evolution of all three partial waves, as opposed to just the exponentially growing partial wave. This, coupled with the inclusion of higher order nonlinearities, could provide interesting results with regard to the saturation of the CRM instability.

   An analytical description of the nonlinear evolution of the interaction when $\rho \not\ll 1$ would also be of interest.

4. Further investigation of superradiant instabilities in CRM-type interactions, particularly in the nonlinear regime. It has already been mentioned in chapter 6 that although the modified FEL code used in the analysis of the

nonlinear evolution of superradiance was extremely useful, in order to accurately model slippage effects in a waveguide, interpolation techniques are required. Similar to the case of steady-state evolution, it should be possible to extend the analysis of superradiant effects to include the effect of multiple waveguide modes. As different waveguide modes have different group velocities however, the relative slippage of the electron beam with respect to each mode is not equal. The analysis of section 6.3 would therefore require modification.

In addition to improvements in the numerical simulation of superradiant effects, it should be possible to approximate analytically the evolution of a superradiant pulse and the effects of free-energy depletion on it for the case of weak superradiance, as was achieved for the case of steady-state evolution. Such an analytical description has already been found for superradiant evolution in atomic systems and FELs [90].

With the construction of a CARM oscillator at Strathclyde University, an exciting area of research would be the extension of the analysis of chapter 6 to describe the interaction which would occur in a CRM oscillator. This would be invaluable in determining the optimum conditions under which superradiant radiation evolution could be observed experimentally. No superradiant evolution, as defined here, has been identified experimentally in any form of electron beam device to date.

Publications

1. 'Universally Scaled Cyclotron Resonance Maser Equations', B. W. J. M^{c}Neil, G. R. M. Robb and A. D. R. Phelps, J. Phys. D: Appl. Phys., Vol. 27, p. 1092, 1994.

2. 'Landau-Ginzburg Equation for the Cyclotron Resonance Maser', G. R. M. Robb, Phys. Rev. E, Vol. 50, p. 3345, 1994.

3. 'Universally Scaled Equations for Gyrotron and CARM Amplifiers', B. W. J. M^{c}Neil, G. R. M. Robb and A. D. R. Phelps, Proc. 18th Int. Conf. Infrared and Millimeter Waves, SPIE 2104, p. 396, 1993.

4. 'A Hamiltonian Theory of the Gyrotron and CARM', B. W. J. M^{c}Neil, G. R. M. Robb and A. D. R. Phelps, Millimeter and Submillimeter Waves, SPIE 2211, p. 479, 1994.

5. 'A Novel Scaling of the Gyrotron/CARM Equations of Evolution', B. W. J. M^{c}Neil, G. R. M. Robb and A. D. R. Phelps, EUROEM94 Symposium on Electromagnetic Field Environments and Consequences, Bordeaux, France, 1994.

6. 'Superradiance Due to Pulse Propagation in CRM-Type Devices', G. R. M. Robb, B. W. J. M^{c}Neil and A. D. R. Phelps, 19th International Conference on Infrared and Millimeter Waves, Sendai, Japan, JSAP No. AP941228, p. 155-156, 1994.

Bibliography

[1] 'Classical Electrodynamics', J. D. Jackson, Wiley, New York, 1975.

[2] 'Spontaneous and Stimulated Emission From Quasi-Free Electrons', A. Friedman, A. Gover, G. Kurizki, S. Ruschin and A. Yariv, Rev. Mod. Phys., Vol. 60, p. 471, 1988.

[3] 'Backward Wave Oscillations in an Unloaded Waveguide', R. H. Pantell, Proc. IRE, Vol. 47, p. 1146, 1959.

[4] 'The Cyclotron Resonance Backward Wave Oscillator', K. K. Chow, R. H. Pantell, Proc. IEE, Vol. 48, p. 1865, 1960.

[5] 'Tuneable Source of Millimetre and Submillimetre Radiation', I. B. Bott, Proc. IEEE , Vol. 52, p. 330, 1964.

[6] 'A Powerful Source of Millimetre Radiation', I. B. Bott, Phys. Letts. Vol., 14, p. 330, 1965.

[7] 'Research on Electronic Interaction with the Fields of Mirror Resonators', J. Feinstein, Proc. Int. Cong. Microwave Tubes, 5th, 1964.

[8] 'Interaction Between Electron Fluxes and Electromagnetic Waves In Waveguides', A. V. Gaponov, Izv. VUZ. Radiofizika, Vol. 2, p. 450, 1959.

[9] 'Strong Submillimeter Radiation From Intense Relativistic Electron Beams', V. L. Granatstein, M. Herndon, R. K. Parker, S. P. Schlesinger, IEEE Trans. Microwave Theory Tech., Vol. MTT-22, p. 1000, 1974.

[10] 'Application of Intense Relativistic Electron Beams to Microwave Generation', Y. Carmel and J. Nation, J. Appl. Phys., Vol. 44, p. 5268, 1973.

[11] 'Coherent Synchrotron Radiation From an Intense Relativistic Electon Beam', V. L. Granatstein, M. Herndon, R. K. Parker, S. P. Schlesinger, IEEE J. Quantum Electron., Vol. 10, p. 651, 1974.

[12] 'Gigawatt Microwave Emission From an Intense Relativistic Electron Beam', V. L. Granatstein, M. Herndon, P. Sprangle, Y. Carmel and J. A. Nation, Plasma Physics, Vol. 17, p. 23, 1975.

[13] 'Experimental Investigation of a High Current Relativistic Cyclotron Maser', N. S. Ginzburg, Soviet Physics: Tech. Phys., Vol. 24, p. 218, 1979.

[14] 'An Electron Cyclotron Maser for Nano-second Megawatt Pulses', Frank, J. Phys. D:Appl. Phys., Vol. 15, p. 41, 1982.

[15] 'Stimulated Cyclotron Radiation of Millimetre Wavelengths From a High Power Relativistic Electron Beam', S. N. Voronkov, V. I. Krementsov, P. S. Strelkov and A. K. Shkvarunets, Soviet Physics: Tech. Phys., Vol. 27, p. 106, 1982.

[16] 'High Voltage Ka-Band Gyrotron Experiment', S. H. Gold, A. W. Fliflet, W. M. Manheimer, W. M. Black, V. L. Granatstein, A. K. Kinkead, D. L. Hardesty and M. Sucy, IEEE Trans. on Plasma Sci., Vol. PS-13, p. 374, 1985.

[17] 'Operation Of a Tunable Gyrotron at the Second Harmonic of the Electron Cyclotron Frequency', G. F. Brand, P. W. Fekete, K. D. Hong, K. J. Moore and T. Idehara, Int. J. Electron., Vol. 68, p. 1099, 1990.

[18] 'Submillimeter Wave Generation by Second Harmonic Operation Of Tunable Gyrotrons', K. D. Hong, G. F. Brand, P. W. Fekete and T. Idehara, Int. J. Infrared and Millimeter Waves, Vol. 13, p. 215, 1992.

[19] 'Relativistic Gyrotrons and Cyclotron Autoresonance Masers', V. L. Bratman, N. S. Ginzburg, G. S. Nusinovich, M. I. Petelin and P. S. Strelkov, Int. J. Electron., vol. 51, p. 541, 1981.

[20] 'Experimental Study of a 28GHz High-Power Long-Pulse Cyclotron Autoresonance Maser Oscillator', S. Alberti, B. G. Danly, G. Gulotta, E. Giguet, T. Kimura, W. L. Menninger, J. L. Rullier and R. J. Temkin, Phys. Rev. Lett., Vol. 71, p. 2018, 1993.

[21] 'Cyclotron Autoresonance Maser With High Doppler Frequency Up-Conversion', V. L. Bratman, G. G. Denisov, M. M. Ofitserov, S. V. Samsonov, O. V. Arkipov, V. I. Kazacha, A. K. Krasnykh, E. A. Perelstein and A. V. Zamrij, Int. J. Infrared Millimeter Waves, Vol. 13, p. 1857, 1992.

[22] 'High-Frequency Gyrotrons and Their Application to Tokamak Plasma Heating', K. E. Kreischer and R. J. Temkin, in Infrared and Millimeter Waves, Vol. 7, ed. K. J. Button, Academic Press, 1983.

[23] 'Applications For Gyrotrons in Fusion Research', A. Riviere, Int. J. Electron., Vol. 61, p. 693-695, 1986.

[24] 'Material Processing and Plasma Chemistry by Use of High Power Radiation of Gyrotrons', Y. Bykov, Proc. Course and Workshop on High Power Microwave Generation and Applications, Int. School of Plasma Physics, Varenna, 1991.

[25] 'Gyrotron Oscillators : Their Principles and Practice', ed. C. J. Edgecombe, Taylor & Francis, London, 1993.

[26] 'High-Power Microwave Sources', eds. V. L. Granatstein and I. Alexeff, Artech House, 1987.

[27] 'Microwave Tubes', A. S. Gilmour, Artech House, 1986.

[28] 'The Gyrotron', V. A. Flyagin, A. V. Gaponov, M. I. Petelin and V. K. Yulpatov, IEEE Trans. Microwave Theory Tech., Vol. MTT-25, p. 514, 1977.

[29] 'The Electron Cyclotron Maser-An Historical Survey', J. L. Hirshfield and V. L. Granatstein, IEEE Trans. Microwave Theory Tech., Vol. MTT-25, p. 522, 1977.

[30] 'Current Status and Prospects of Gyrotron Development', M. Thumm, ITG-Fachberichte 120, Elektronenröhren und Vakuumelektronik, Garmisch Partenkirchen, VDE-Verlag GmbH, p. 63, 1992.

[31] 'Review of Quasi-Optical Gyrotron Development', A. W. Fliflet, T. A. Hargreaves, R. P. Fischer, W. M. Manheimer, P. Sprangle, J. Fusion Energy, Vol. 9, p. 31, 1990.

[32] 'Electron Cyclotron Maser Emission From Pulsed Electron Beams', A. D. R. Phelps and T. Garvey, J. Phys. D: Appl. Phys., Vol. 19, p. 2051, 1986.

[33] 'Pulsed mm-Wave Electron Cyclotron Maser Experiments', S. N. Spark, Ph.D. Thesis, University of Strathclyde, 1988.

[34] 'Tuneable 35-200GHz, High Power Gyrotron', S. N. Spark, A. D. R. Phelps, Int. J. Infrared and Millimeter Waves, Vol. 12, p. 855, 1991.

[35] 'Comparitive Study of Gyrotrons Based on Thermionic and Cold Cathodes', A. W. Cross, S. N. Spark, K. Ronald, A. D. R. Phelps and W. He, 18th International Conference on Infrared and Millimeter Waves, Colchester, UK, Proceedings of the International Society for Optical Engineering, SPIE, Vol. 2104, p. 448,1993.

[36] 'Electron Cyclotron Maser Experiments Using Cold and Thermionic Cathodes', A. W. Cross, Ph.D. Thesis, University of Strathclyde, 1993.

[37] 'Field Emission Array Experiments Relevant to Cold Gyrotron Cathodes', M. Garven, A. D. R. Phelps, S. N. Spark, D. F. Howell and N. Cade, Vacuum, Vol. 45, p. 513, 1994.

[38] 'Novel Gyrotron Experiments Employing a Field Emission Array Cathode', M. Garven, Ph.D. Thesis, University of Strathclyde, 1994.

[39] '100Hz PRF CARM Experiment', S. J. Cooke, S. N. Spark, W. He and A. D. R. Phelps, 18th International Conference on Infrared and Millimeter Waves, Colchester, UK, Proceedings of the International Society for Optical Engineering, SPIE, Vol. 2104, p. 462,1993.

[40] 'Radiation Transfer and the Possibility of Negative Absorption in Radio Astronomy', R. Q. Twiss, Austr. J. Phys., Vol. 11, p. 564, 1958.

[41] 'Stimulated Emission of Radiation by Relativistic Electrons in a Magnetic Field', J. Schneider, Phys. Rev. Lett. , Vol. 2, p. 504, 1959.

[42] 'Quantum Mechanics', Volume 1, C. Cohen-Tannoudji, B. Diu and F. Laloë, Wiley, New York, 1977.

[43] 'Diamagnetism of Metals', L. Landau, Z. Physik, vol. 64, p. 629, 1930.

[44] 'Travelling Wave Tubes', J. R. Pierce, Van Nostrand Reinhold Co, 1950.

[45] 'Simple Macroscopic Theory of Cyclotron Maser Instabilities', Y. Y. Lau, IEEE Trans. Electron Devices, Vol. ED-29, p. 320, 1982.

[46] 'A Unified Theory of the Diocotron, Cyclotron Maser, and Negative Mass Instabilities', Y. Y. Lau, IEEE Trans. Electron Devices, Vol. ED-31, p. 329, 1984.

[47] 'A Unified Theory of Gyrotron and Peniotron Interactions', C. N. Lashmore-Davies, Phys. Fluids. B, Vol. 4, p. 1047, 1992.

[48] 'The Small-Signal Theory of the Cyclotron Maser and Other Gyrotron-Type Devices', G. Dohler and D. Gallacher, IEEE Trans. Electron Devices, Vol. 35, p. 1730, 1988.

[49] 'Theory of Microwave Emission by Velocity-Space Instabilities of an Intense Relativistic Electron Beam', E. Ott and W. M. Manheimer, IEEE Trans. Plasma Sci., Vol. PS-1, p. 1, 1975.

[50] 'Comparative Study of the Axial and Azimuthal Bunching Mechanisms in Electromagnetic Cyclotron Instabilities', K. R. Chu, J. L. Hirshfield, Phys. Fluids, Vol. 21, p. 461, 1978.

[51] 'The Linear and Self-Consistent Nonlinear Theory of the Electron Cyclotron Maser Instability', P. Sprangle and A. T. Drobot, IEEE Trans. Microwave Theory Tech., vol. MTT-25, p. 528, 1977.

[52] 'General Formula of the Energy-Transfer Rate in Gyrotron, Cyclotron-Autoresonance-Maser and Nonwiggler-Free-Electron-Laser Oscillators', S. C. Zhang, Phys. Rev. A, Vol. 45, p. 1177, 1992.

[53] 'Theory of Electron Cyclotron Maser Interaction in a Cavity at the Harmonic Frequencies', K. R. Chu, Phys. Fluids, Vol. 21, p. 2354, 1978.

[54] 'A Kinetic Theory for Electron Cyclotron Maser Interaction in a Waveguide : Coupling Between a Transverse Electric Mode and a Transverse Magnetic Mode', R. A. Schill, S. R. Seshadri, Phys. Fluids B, Vol. 2, p. 2818, 1990.

[55] 'A Kinetic Theory for Electron Cyclotron Maser Interaction in a Waveguide : Mode Coupling Among All Supported Waveguide Modes', R. A. Schill, Phys. Fluids B, Vol. 2, p. 2798, 1990.

[56] 'Theory and Simulation of the Gyrotron Travelling Wave Tube Amplifier Operating at Cycloton Harmonics', K. R. Chu, A. T. Drobot, H. Z. Szu and P. Sprangle, IEEE Trans. Microwave Tech., Vol. MTT-28, p. 313, 1980.

[57] 'Self-consistent Large Signal Theory of the Gyrotron Travelling Wave Tube Amplifier', A. K. Ganguly and S. Ahn, Int. J. Electron., Vol. 53, p. 641, 1982.

[58] 'CARM Amplifier Theory and Simulation', C. Chen, B. G. Danly, J. A. Davies, W. L. Menninger, J. S. Wurtele and G. Zhang, Nucl. Instr. and Meth. in Phys. Res. A, Vol. 304, p. 593, 1991.

[59] 'Linear and Nonlinear Theory of the Doppler-Shifted Cyclotron Resonance Maser Based on TE and TM Waveguide Modes', A. W. Fliflet, Int. J. Electron., Vol. 61, p. 1049, 1986.

[60] 'Mode Interaction in Gyrotrons', G. S. Nusinovich, Int. J. Electron., Vol. 51, p. 457, 1981.

[61] 'Multimode Oscillation and Mode Competition in High-Frequency Gyrotrons', K. E. Kreischer, R. J. Temkin, H. R. Fetterman and W. J. Mulligan, IEEE Trans. Microwave Theory Tech., Vol. MTT-32, p. 481, 1984.

[62] 'Parametric Instabilites in Gyro-Devices at Cyclotron Harmonics', G. S. Nusinovich, Int. J. Electron., Vol. 72, p. 795, 1992.

[63] 'Handbook Of Mathematical Functions', M. Abramowitz and I. A. Stegun, Dover, 1970.

[64] 'Collective Instabilities and High-Gain Regime in a Free Electron Laser', R. Bonifacio, C. Pellegrini and L. Narducci, Optics Comm., Vol. 50, p. 373, 1984.

[65] 'Theory of Guided Electromagnetic Waves', R. A. Waldron, Van Nostrand Reinhold Co, London, 1969.

[66] 'Collective Instability of a Free Electron Laser Including Space Charge and Harmonics', J. B. Murphy, C. Pellegrini and R. Bonifacio, Optics Comm., Vol. 53, p. 197, 1985.

[67] 'A Free Electron Laser in a Uniform Magnetic Field.', S. K. Ride, W. B. Colson, Appl. Phys. Vol. 20, p. 41, 1979.

[68] 'Theory of a Nonwiggler Collective FEL an a Uniform Magnetic Field', A. Fruchtman and L. Friedland, IEEE J. Quant. Electron., Vol. QE-19, p. 327, 1983.

[69] 'Common Properties of Free Electron Lasers', V. L. Bratman, N. S. Ginzburg and M. I. Petelin, Optics Comm., Vol. 30, p. 409, 1979.

[70] 'Analysis of the Sideband Instability in the Free Electron Laser', J. N. Elgin, Phys. Rev. A, Vol. 43, p. 2514, 1991 (and references therein).

[71] 'Generalized Gain-Spread Relation and Optical Guiding Effect in High-Gain Free Electron Laser Amplifiers', R. Bonifacio, F. Casagrande and L. De Salvo Souza, Optics Comm., Vol. 58, p. 259, 1986 (and references therein).

[72] 'Relationship Between Mean Radiated Energy and Spontaneous Power Spectrum in a Free Electron Laser', J. M. J. Madey, Nuovo Cimento B, Vol. 50, p. 64, 1979.

[73] Selection of papers in Proc. 12th Int. Conf. Free Electron Lasers, Nucl. Inst. Meth. Phys. Res. A304, 1991.

[74] 'Vacuum Microelectronic Array Gyrotron Cathode Experiments', M. Garven, S. N. Spark, A. D. R. Phelps, N. Cade, Proc. 18th Int. Conf. Infrared and Millimeter Waves, SPIE 2104, p452, 1993.

[75] 'The Self-Consistent Pendulum Picture of the Free Electron Laser Revised and the Instability Threshold for Exponential Gain', F. Casagrande, R. Bonifacio and A. Airoldi, Nucl. Inst. Meth. Phys. Res. A304, p. 439, 1991.

[76] 'Higher Transcendental Functions', A. Erdélyi, W. Magnus, F. Oberhettinger, F. G. Tricomi, Volume 2, M^{c}Graw–Hill, London, 1953.

[77] 'A Collective Variable Description of the FEL', R. Bonifacio, F. Casagrande and L. De Salvo Souza, Phys. Rev. A, Vol. 33, p. 2836, 1986.

[78] 'A Landau-Ginzburg Equation for the High-Gain Compton FEL', R. Bonifacio, C. Maroli and A. Dragan, Optics Comm., Vol. 76, p. 353, 1990.

[79] 'Three-Mode Treatment of a High-Gain Steady-State Free-Electron Laser', C. Maroli, N. Sterpi, M. Vasconi and R. Bonifacio, Phys. Rev. A, Vol. 44, p. 5206, 1991.

[80] 'Laser Physics', M. Sargent, M. O. Scully and W. E. Lamb, Addison-Wesley, 1974.

[81] 'Coherence in Spontaneous Radiation Processes', R. H. Dicke, Phys. Rev., Vol. 93, p. 99, 1954.

[82] 'Dissipative Systems in Quantum Optics', ed. R. Bonifacio, Springer, Berlin, 1982.

[83] 'Physics of the High-Gain FEL and Superradiance', R. Bonifacio, F. Casagrande, G. Cerchioni, L. De Salo Souza, P. Pierini and N. Piovella, La Rivista del Nuovo Cimento, Vol. 13, no. 9, 1990.

[84] 'Optical Resonance and Two-Level Atoms', L. H. Allen and J. H. Eberly, Wiley, New York, 1975.

[85] 'Classical and Quantum Treatment of Amplifier and Superradiant Free-Electron Laser Dynamics', R. Bonifacio and F. Casagrande, J. Opt. Soc. Am. B, Vol. 2, p. 250, 1985.

[86] 'Slippage and Superradiance in the High-Gain FEL : Linear Theory', R. Bonifacio, C. Maroli and N. Piovella, Optics Comm., Vol. 68, p. 369, 1988.

[87] 'Some Mathematical Methods of Physics', G. Goertzel and N. Tralli, McGraw-Hill, New York, 1960.

[88] Private Communication, B. W. J. McNeil.

[89] 'Superradiance in the High-Gain Free-Electron Laser', R. Bonifacio, B. W. J. McNeil and P. Pierini, Phys. Rev. A, Vol. 40, p. 4467, 1989.

[90] 'A Hyperbolic Secant Solution for the Superradiance in Free Electron Lasers', N. Piovella, Optics Comm., Vol. 83, p. 92, 1991.

SOME PARTS
EXCLUDED
UNDER
INSTRUCTION
FROM THE
UNIVERSITY